Optimal Operation of Energy Hubs in the Context of Smart Grids

by

Mohammad Chehreghani Bozchalui

A thesis
presented to the University of Waterloo
in fulfillment of the
thesis requirement for the degree of
Doctor of Philosophy
in
Electrical and Computer Engineering

Waterloo, Ontario, Canada, 2011

I hereby declare that I am the sole author of this thesis. This is a true copy of the thesis, including any required final revisions, as accepted by my examiners.

I understand that my thesis may be made electronically available to the public.

Abstract

With the rapid growth of energy demand and consequently growth in supply, increasing energy costs, and environmental concerns, there is a critical need to find new ways to make better use of existing energy systems and resources and decelerate the demand growth towards a sustainable energy system. All of these facts are leading to the proposal of novel approaches to optimize the utilization of energy in different sectors to reduce the customer's total energy costs, demand and greenhouse gas (GHG) emissions while taking into account the end-user preferences.

Utilities have implemented Demand Side Management (DSM) and Demand Response (DR) programs to better manage their network, offer better services to their customers, handle the increase in electricity demand, and at the same time increase system reliability and reduce environmental impacts. Smart Grid developments such as information technology, communication infrastructure and smart meters improve the effectiveness and capability of Energy Management Systems (EMSs) and facilitate the development of automated operational decision-making structures for energy systems, thus assisting DSM and DR programs to reach their full potential. The literature review indicates that whereas significant work has been done in DSM and DR in utilities, these works have mostly focused on direct load control of particular loads, and there is a lack of a general framework to consider all types of energy hubs in an integrated Energy Hub Management System (EHMS). In this context, mathematical modeling of energy systems for EMSs, which is the main concern of the present work, plays a critical role.

This research proposes mathematical optimization models of energy hubs which can be readily incorporated into EHMS in the context of Smart Grids. The energy hub could be a single or multi-carrier energy system in residential, commercial, agricultural and/or industrial sectors. Therefore, mathematical models for energy hubs in residential, commercial, and agricultural sectors have been developed and are presented and discussed in this thesis.

In the residential sector, this research presents mathematical optimization models of residential energy hubs which can be readily incorporated into automated decision making technologies in Smart Grids, and can be solved efficiently in a real-time frame to optimally control all major residential energy loads, storage and production components while properly considering the customer preferences and comfort levels. Mathematical models for major household demand, i.e., fridge, freezer, dishwasher, washer and dryer, stove, water heater, hot tub, and pool pumps, are formulated. Also, mathematical models of other components of a residential energy system including lighting, heating, and air-conditioning

are developed, and generic models for solar PV panels and energy storage/generation devices are proposed. The developed mathematical models result in a Mixed Integer Linear Programming (MILP) optimization problem, whose objective is to minimize demand, total costs of electricity and gas, emissions and peak load over the scheduling horizon while considering end-user preferences. The application of this model to a real household are shown to result in savings of up to 20% on energy costs and 50% on peak demand, while maintaining the household owner?s desired comfort levels.

In the commercial sector, mathematical optimization models of produce storage facilities to optimize the operation of their energy systems are proposed. In the storage facilities, climate control of the storage rooms consumes considerable energy; thus, a mathematical model of storage facilities appropriate for their optimal operation is developed, so that it can be implemented as a supervisory control in existing climate controllers. The proposed model incorporates weather forecasts, electricity price information, and the end-user preferences to optimally operate existing climate control systems in storage facilities. The objective is to minimize total energy costs and demand charges while considering important parameters of storage facilities; in particular, inside temperature and humidity should be kept within acceptable ranges. Effects of uncertainty in electricity price and weather forecast on optimal operation of the storage facilities are studied via Monte-Carlo simulations. The presented simulation results show the effectiveness of the proposed model to reduce total energy costs while maintaining required operational constraints.

In the agricultural sector, this work presents mathematical optimization models of greenhouses to optimize the operation of their energy systems. In greenhouses, artificial lighting, CO_2 production, and climate control consume considerable energy; thus, a mathematical model of greenhouses appropriate for their optimal operation is developed, so that it can be implemented as a supervisory control in existing greenhouse controllers. The proposed model incorporates weather forecasts, electricity price information, and the end-user preferences to optimally operate existing control systems in greenhouses. The objective is to minimize total energy costs and demand charges while considering important parameters of greenhouses; in particular, inside temperature and humidity, CO_2 concentration, and lighting levels should be kept within acceptable ranges. Effects of uncertainty in electricity price and weather forecast on optimal operation of the storage facilities are studied via Monte-Carlo simulations and robust optimization approach. The presented simulation results show the effectiveness of the proposed model to reduce total energy costs while maintaining required operational constraints.

Acknowledgements

I would like to express my sincere gratitude to my supervisors Professor Claudio A. Canizares and Professor Kankar Bhattacharya for their invaluable trust, support, guidance and patience during the course of my PhD studies at the University of Waterloo. Their professionalism, thoughtful guidance and invaluable suggestions have helped me walk through various stages of my studies, while their passion and extraordinary dedication to work have always inspired me and encouraged me to work harder.

My appreciation extends to my Ph.D. committee for their valuable comments and inputs: Professor Daniel Kirschen from the University of Washington; Professor Ian H. Rowlands form the Department of Environment and Resource Studies at the University of Waterloo; and Professor Ehab El-Saadany and Dr. Ramadan El-Shatshat from the Department of Electrical and Computer Engineering at the University of Waterloo.

My warmest thanks and endless appreciations to my family for their years of unconditional support, encouragement, and true love. Nothing would have been possible without your devotion.

Over the years of my PhD studies, I have had the priceless opportunity of making many new friends in our lab; Hemant, Tarek, Mansour, Ismael, Victor, Ehsan, Isha, Nafeesa, Wajid, Juan, Daniel, Mariano, Behnam, Amr, Abdullah, Mehrdad, Indrajit and many others. I thank all my friends and colleagues in the Electricity Market Simulation and Optimization Lab for making our lab such a friendly and pleasant place to work in. I additionally would like to especially thank Rafael Avalos-Munoz, Hossein Haghighat, and my dear friend Amirhossein Hajimiragha for their kindness and all the little precious things I have learned from them.

I also like to thank my friends and colleagues in the Energy Hub Management Systems project, especially Sumit, Ahsan, Hussin, Gord, Greg, and Brian for their inputs and support during my PhD research.

I gratefully acknowledge the funding and support provided by the Energy Hub Management Systems project partners, including Ontario Centres of Excellence (OCE), Hydro One Networks Inc., Ontario Power Authority (OPA), and Energent Inc., to carry out this research. I also acknowledge partial support of Mathematics of Information Technology and Complex Systems (MITACS) during first year of my PhD studies.

Dedication

This thesis is dedicated to my family who have supported me all the way in my life.

Contents

List of Tables

List of Figures

List of Abbreviations

AC	Air Conditioning
ACS	Automated Control Systems
AMI	Advanced Metering Infrastructure
AMPL	A Modeling Language for Mathematical Programming
B2G	Building-to-Grid
BAS	Building Automation Systems
B& B	Branch and Bound method
CDM	Conservation and Demand Management
CFL	Compact Fluorescent Lamp
DER	Distributed Energy Resources
DG	Distributed Generation
DLC	Direct Load Control
CPP	Critical Peak Pricing
DR	Demand Response
DSM	Demand Side Management
EIS	Energy Information System
EHMS	Energy Hub Management System
EMS	Energy Management Systems
FLC	Fuzzy Logic Controller
FPGA	Field Programmable Gate Array
FRP	Fixed Rate Price
GA	Genetic Algorithm
GHG	Greenhouse Gas emissions
H2G	Home-to-Grid
HAN	Home-Area-Network
HAS	Home Automation Systems
HEM	Home Energy Management
HID	High Intensity Discharge
HOEP	Hourly Ontario Electricity Price
HVAC	Heating, Ventilation and Air Conditioning
I2G	Industry-to-Grid
IB	Incentive Based
IL	Illumination Level
ILC	Interruptible Load Control

IP	Integer Programming
IT	Information Technology
LM	Load Management
LP	Linear Programming
LPN	Large Positive Number
LR	Lagrangian Relaxation
MILP	Mixed Integer Linear Programming
MIQP	Mixed Integer Quadratic Programming
MPC	Model Predictive Control
NLP	Non-Linear Programming
NN	Neural Networks
PB	Price Based
pdf	Probability density function
PI	Proportional-Integral
PID	Proportional-Integral-Derivative
PLC	Programmable Logic Controller
PP	Polynomial Programming
RHOC	Receding Horizon Optimal Control
RLT	Reformulation-Linearization Techniques
RTP	Real Time Pricing
SCADA	Supervisory Control and Data Acquisition
TOU	Time of Use

Chapter 1

Introduction

1.1 Motivation

Energy, and in particular electricity, is one of the most important factors which affect the economic growth of any country. Traditionally, adequate and secure energy provision requires expansion of the transmission and generation capacity of the power system to supply the required demand. For example, Ontario's power system capacity needs to double by 2030, which includes replacing about 80% of the current generating facilities as they retire over time, and expanding the system to meet the demand growth. Building new facilities for expansion of the generation and transmission capacity of the network is not only very expensive, but there are also a variety of environmental issues to be considered.Currently, power plants are responsible for nearly 40% of the U.S. carbon footprint [1], and there is a need for new generation capacity to meet the rapid demand growth. In this context, finding new ways to make better use of electricity resources and slow the demand growth is vital.

Smart Grids are envisioned to support large penetrations of distributed demand-side resources coupled with system-wide Demand Response (DR) driven by economic and reliability signals, and utilities are looking at Demand Side Management (DSM) and DR services to better manage their networks [2, 3]. DR programs induce customers with payment incentives to reduce loads during periods of critical grid conditions or periods of high energy costs; in other words, DSM and DR programs reward both utilities and customers for a smarter energy use. Significant work has been done in the past to manage the energy consumption. Thus, Load Management (LM), Conservation and Demand Management (CDM), DSM, and DR programs have been implemented and promoted by utilities and

governments to reduce the demand or modulate the load shape in order to achieve a better match between the customers' demand and the utilities' current and planned resources in generation, transmission and distribution (e.g., [4, 5, 6]).

To date, large industrial and commercial customers have been the most active participants in DSM and DR programs because of their potential to achieve large peak load and energy consumption reductions upon direct request of the utility operator. Residential and small commercial and agricultural customers have traditionally participated less in DSM and DR activities mainly because of their individually smaller contributions to the system peak load and energy consumptions. On the other hand, the energy consumption contribution from residential and commercial customers in developed countries has been between 20% to 40% of total energy consumption in recent years [7]. Figure 1.1 depicts total energy consumption of the USA by sector in 2009, showing that the share of residential and commercial sectors in total energy consumption is more than 40%. The important role of these two sectors in the future energy demand can be further highlighted using the observed and projected growth rate of electricity consumptions in various sectors, as illustrated in Figure 1.2, showing higher growth rates in these sectors compared to the industrial sector. All these facts suggest that residential and commercial sectors are important resources for DR and DSM programs, and thus exploring new opportunities to better manage energy requirements in these sectors to reduce their demand and carbon footprint is relevant and timely.

To have an effective participation and considerable load reduction potential of small residential and commercial customers in DSM and DR programs, a large number of these customers need to be involved in such programs. Therefore, since the required hardware and communications infrastructure for these large number of geographically distributed small customers have been one of the main barriers in integration of these customers in the past, the role of DSM and DR programs in the residential and commercial sectors will be significant and these programs should reach their full potential with the development of Smart Grids. Hence, the main focus of the current work is on developing appropriate methods to enable residential, commercial and agricultural customers to better manage their energy utilization and reduce energy consumption and Greenhouse Gas (GHG) emissions, and thus facilitating the integration of these customers into Smart Grids.

Recently, deregulation of the power sector, increased competition, growing demand for energy, environmental concerns, and new technologies has rendered Energy Management Systems (EMSs) more attractive, and even an essential feature for both small and large loads. Information technology and a new generation of energy meters, typically referred to as "Smart Meters", which not only provide energy consumption readings but can also provide additional information on usage and have two-way communication capabilities, are

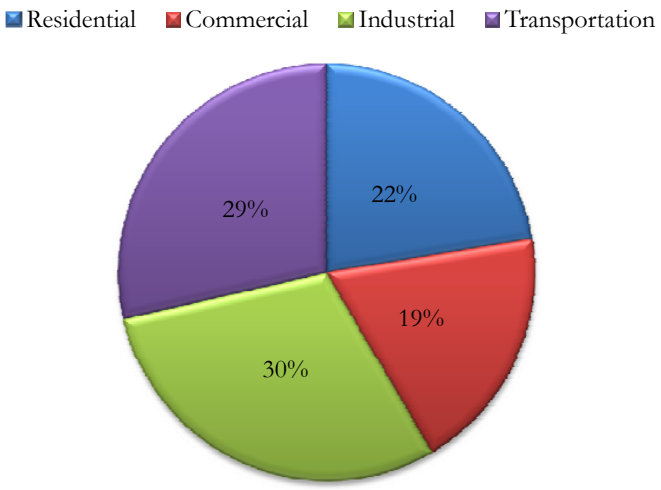

Figure 1.1: Total energy consumption of the USA by sector in 2009 [8].

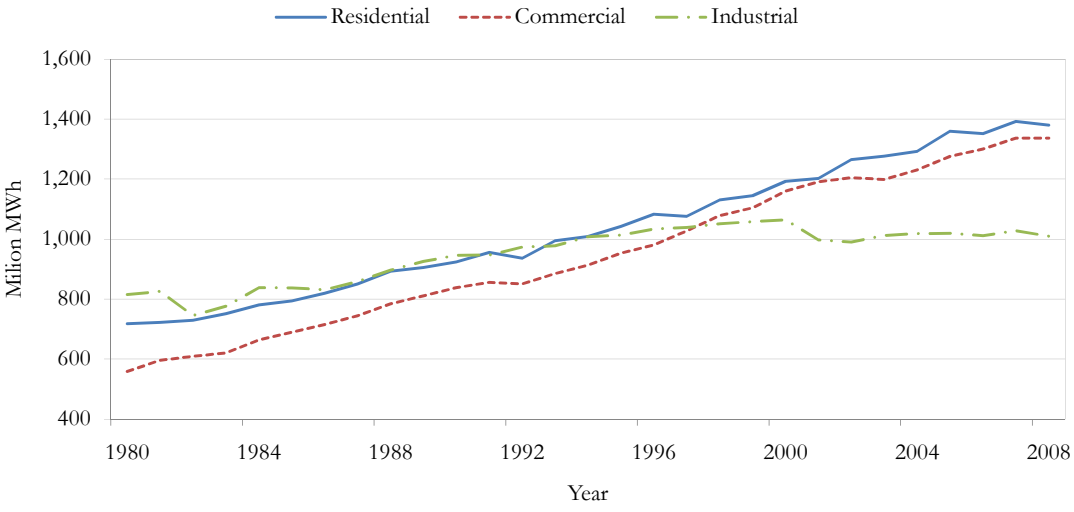

Figure 1.2: Total electricity consumptions of the USA by sector in the last three decades [8].

two key developments that improve the effectiveness and capability of EMSs. With these developments, both utilities and customers can have access to two-way communication infrastructures, control devices, and visual interfaces that allow them to send, retrieve, visualize, process and/or control their energy needs. All these technologies are referred to as Advanced Metering Infrastructure (AMI) [9]. Availability of AMI in "Smart Grids" make automated operational decision making structures feasible in energy systems, presenting a significant potential to improve performance and effectiveness of DSM and DR programs in order to get more customers involved in these programs to reduce energy consumption and carbon footprint. In this context, mathematical modeling for these customers to generate optimal operation decisions, which is the main concern of the present work, plays a critical role.

1.2 Literature Review

In this section the relevant research papers and developments pertaining to the topics of DSM and DR applications by sector, optimization modeling, and the Smart Grid are briefly discussed.

1.2.1 Residential Sector

Most of the existing DSM and DR programs in the residential sector focus on energy efficiency, dynamic pricing, and load control activities. Reported researches in the literature on the effects of dynamic pricing on residential customers indicates that there is no straightforward relationship between behaviour of the customer and implemented programs [10, 11, 12, 13, 14]. The authors in [10] states that dynamic pricing can provide substantial net benefits to residential customers as their price elasticities are significantly higher than other sectors. Effect of dynamic pricing on residential electricity bills is studied in [11], reporting significant reduction in the average monthly costs and reducing the on-peak load by half using Time-of-Use (TOU) pricing. Results of a field experiment to study the effect of Real-Time Pricing (RTP) on households are reported in [12], stating that residential customers are significantly price elastic and that customers responded by conserving energy during peak hours, but remarkably did not increase average consumption during off-peak times; thus, it is suggested to look at residential RTP as a peak energy conservation program, instead of a mechanism to shift consumption from peak to off-peak.

In [13], the authors analyze the demand response from residential electricity customers to a demand charge tariff in a Norwegian grid company. In addition to energy consumptions

cost, the tariff charges the maximum hourly peak consumption in each of the winter months, and the customers did not receive any information on their continuous consumption or any reminders when the tariff is in effect. The results indicate average demand reductions of up to 5%, with a maximum reduction of 12%. It is suggested that the reductions could have been even higher if customers had received more information on their continuous consumption levels, and in which periods they were charged if their consumption became too high. The authors in [14] present experiences from a pilot study focusing on daily DR from households, utilizing smart metering, remote load control, electricity pricing based on the hourly spot price combined with a time of day network tariff, and a token provided to the customers when reducing consumption during peak hours. The pilot study aimed to achieve daily load shifting from electrical boilers fir space heating and standard electric water heaters, and to explore customer acceptance and study the impact on load curves of hourly tariffs and automatic load control schemes.

Dynamic pricing by itself is not a sufficient measure to encourage residential customers to achieve DSM and DR objectives. This is mainly because of the fact that in these programs customers themselves need to analyze external information, re-schedule and control the appliances. Therefore, automating these processes might increase the success of DSM and DR programs in the residential sector. Thus, various works are reported in the literature on Direct Load Control (DLC) of residential loads, e.g., Air Conditioning (AC) [14, 15, 16, 17, 18, 19, 20, 21], space heating and water heater [14, 20, 21, 22, 23, 24], and pool pumps [20]. Most of these DLCs are implemented to achieve peak demand reduction.

A DLC technique for AC loads that incorporates an estimate of the comfort level is proposed in [15]. Some of the objectives of the controller are to reduce conflicts between operation of AC units and the DLC program, arrange the DLC schedule for all AC units, and minimize the "payback load effect", which is the amount of energy not consumed because of DLC action but will be consumed as the DLC time elapses. In [16], an approach based on multi-pass dynamic programming is proposed for the dispatch of AC DLC. The proposed method is applied to determine the required amount of load to be controlled at each time stage in order to maximize cost savings and peak load reduction. In [17, 18], the authors present physically based electrical load models of AC loads to be implemented in DLC programs, and in [19] a DLC program for AC units using a duty-cycle approach implementation is proposed to reduce peak load.

A linear programming model to optimize the amount of system peak load reduction through scheduling of control periods in commercial, residential, or industrial LM programs is presented in [20]. The optimization model determines the optimal schedule of load control to minimize system peak demand. The input variables include energy payback information, forecasted uncontrolled load pattern for a critical day, and limits on available

load which can be controlled for each program. The residential program comprises four components: pool pump, AC shed, AC cycle, and water heater control. In a research project conducted by ETH Zurich and other partners [21], only appliances with a storage capacity for thermal energy (cooling and heating household appliances) are considered to unify active management of appliances and major household loads in a single system. The proposed control strategy is based on a one-time-step prediction of the overall power consumption of a large cluster of appliances (several hundred appliances) using stochastic properties of the cluster.

In [22], an analytical model of water heaters is developed using linear and dynamic optimization models to generate the schedules of water heating loads in LM programs. The authors in [23] propose a multi-objective optimization model for remote load control strategies of a group of electric water heaters. The model attempts to minimize peak demand, maximize profits resulting from energy sales and maximize quality of service. In [24], a multi-criteria approach to the problem of space heating under a time varying price of electricity is proposed. In the developed dynamic goal programming model, the goals are minimizing deviation from the ideal temperature, costs and energy consumption.

In DLC programs, usually the hardware is installed by a utility and a one-way communication link is used to send load control signals to the customer. Existing DLC programs are two types: the utility operator has the permission and access to turn appliances On and Off, or the utility operator send a signal to the customer to request the execution of a control action. The advantage of the fist type of DLC programs is that the utility operator has direct access to the loads and can reduce peak demand as needed. Although it seems that loads can be easily controlled in this type of DLC programs, customer's preferences and comfort levels might not always be considered. Also, it should be noted that disconnected loads have "payback load effect" which might lead to another peak in the system if the program is not managed properly. In the second type of DLC programs, the utility operator can't assess the status of the control action, and there is always a possibility that the customers do not execute the control action for some reason (e.g., preferring a higher comfort level).

A few works are reported in the literature on application of optimization methods and artificial intelligence to schedule energy consumption in residential sector [25, 26, 27, 28, 29, 30, 31]. A fuzzy logic based approach to DLC of AC loads to reduce peak load is presented in [25], where customers comfort levels are modeled by fuzzy sets. A real-time dynamic min-max optimization technique over a finite-time horizon is presented in [26] and applied to building Heating, Ventilation and Air Conditioning (HVAC) control that involves minimization of fixed horizon electric utility costs. A detailed dynamic model of the building HVAC system is presented, and the proposed model is applied to the peak

demand control problem where electricity consumption and peak power usage in a building has to be controlled in response to real-time pricing. A particle swarm optimization based method is proposed in [27] for coordinated scheduling of available residential Distributed Energy Resources (DER) to maximize net benefits from smart home electrical energy services, and a method based on game theory is proposed in [28] for incentive-based energy consumption scheduling in the context of Smart Grids. In [29], an optimal and automatic residential load scheduling framework is presented, which attempts to achieve a trade-off between minimizing the electricity payment and minimizing waiting time for the operation of each appliance in households considering real-time pricing combined with block rates.

The authors in [30] present a Mixed Integer Linear Programming (MILP) optimization approach to analyze the influence of price signals on household power demand. It is assumed that all major appliances are switched On/Off manually, and that an automatic load management system for refrigerators and freezers is available. Mathematical models are developed for cooling devices by simply assuming a total cooling demand for a 24 hours time period. Finally, minimization of energy costs and maximization of comfort form the objective function of the optimization model. Individual preference curves are constructed out of the aggregated load curves of the individual appliances and the revealed preference of the household. The simulation results show a high potential to shave off peak load in a household and that price signals can be adequate instruments to control the temporal distribution of power demand in households.

The ongoing Demand Response Electrical Appliance Manager (DREAM) research project discussed in [31] proposes to use a controller, wireless technology, and a system of learning (both by machine and occupant) for automatically responding to electricity price signals to optimize the cost and thermal comfort. This controller also advises the user via a small traffic light on the appliance when to switch it On or Off in response to price signals from the utility, and suggests that other appliances in the house, such as electric water heaters and pool pumps can be stopped during high price time and activated again later to respond to price signals from the utility.

Note that in the above review, most of the existent works in the residential sector do not properly take into account end-users' preferences and comfort level; are designed for one particular objective (e.g., peak demand reduction or energy consumption minimization); only consider particular appliances/devices (e.g., HVAC and water heaters); and/or are not appropriate for real-time applications. With the advent of Smart Grid developments, improved computational techniques and tools, availability of AMI, EMS, and two-way communication infrastructure in Smart Grids, it is feasible to combine the advantages of the above mentioned methods to achieve advanced DSM and DR programs for residential customers. Thus, this thesis proposes mathematical optimization models of

residential energy hubs which can be readily incorporated into automated decision making technologies, such as Home Automation Systems (HAS) and EMSs, in the context of Smart Grids. These models can be solved efficiently in a real-time frame to optimally control all major residential energy loads, storage and production components while properly considering the customer preferences and comfort level, and hence can facilitate the integration of residential customers into Smart Grids.

1.2.2 Commercial Sector

Energy systems of commercial facilities usually comprise multi-carrier energy systems such as electricity, natural gas, gasoline, and thermal energy. Lighting, heating, cooling, and refrigeration are some examples of energy consuming activities within commercial facilities. Some of these activities are required to be carried out at a specific time regardless of other factors such as energy price. However, energy consumption can be optimized to reduce peak load and total energy costs while taking into account the operational constraints of associated devices and processes. An LM program implemented by Florida Power & Light directed to commercial and industrial loads is discussed in [20]. The participated loads in this program agree to have their peak load controlled for various periods of time in return for lower electric rates; the control period can run from 30 min. to up to 4 hrs. In [32], the authors present a DSM strategy and system for small to medium size electricity customers such as commercial buildings and institutions. The system is implemented on a university campus, where the loads, particularly air conditioners, are controlled using relays that periodically switch off during high demand periods. Each load is connected to a device that "talks" to them using a PLC protocol, and are controlled automatically from an EMS.

In in [33], load curves of some institutional and industrial are investigated to identify possible DSM solutions to reduce peak load, and remote switching systems are suggested for major loads. In [34], an agent based system for energy management in commercial buildings using different computational intelligence techniques (including fuzzy systems, Neural Networks (NN), and Genetic Algorithm (GA)) is proposed to minimize energy demand.

HVAC and refrigeration systems of commercial buildings consume considerable energy. One of the most common facilities that can be found in various sub-sectors of commercial and agricultural sectors is storage facilities. Many works are reported in the literature for optimization of HVAC systems in commercial sector (e.g., [35, 36, 37]). Comprehensive overviews of advanced control strategies and the existing methods for supervisory and optimal control of building HVAC and refrigeration systems are presented in [38] and [39].

A daily energy management formulation and the corresponding solution methodology for HVAC systems to minimize the energy and demand costs through control of HVAC units is presented in [40]. The methodology is an optimization based approach that combines Lagrangian Relaxation (LR), NN, stochastic dynamic programming, and heuristics to predict system dynamics and loads to optimize the set points.

It is observed that most of the existing works have focused on optimizing operation of HVAC systems as an individual system, but not as a part of the energy system of a commercial energy hub. Thus, this work concentrates on optimal operation of HVAC systems as an integral part of commercial energy hubs in Smart Grids. Also, since significant research is reported in the literature on HVAC control systems, the current research focuses on climate control of produce storage facilities as an example of a large number of similar storage rooms in commercial energy hubs. This is mainly because of duplicability of the research for similar facilities, and the unique potential of storage facilities for incorporation into DSM and DR programs.

Various methods are reported in the literature for the purpose of direct climate control in storage facilities. Prediction of climate conditions in produce storage facilities are studied and reported in the literature, for example in [41], [42], and [43]. Detailed physical models of storage facilities are also presented in [41, 42, 44, 45]. The potential of Receding Horizon Optimal Control (RHOC) for climate control in storage facilities for produces is demonstrated in [44] and [46]. A method based on Model Predictive Control (MPC) is proposed in [47] for temperature and humidity control of storage rooms. In [48], a fuzzy controller for fruit storage using NN and GA is developed, and in [49] the application of fuzzy logic in automated control of climate for potato stores is studied and implemented.

Large computation burden of optimal controls is mentioned as a barrier in [46] for direct real-time implementation of optimal control methods in climate control applications. MPC-type controllers are based on a mathematical model and can then be applied to a variety of simple to complex models; however, solving a complex model model is computationally expensive and may not be appropriate for real-time applications. Finally, the implementation of fuzzy logic based controllers implies tuning of many parameters for each case, which normally is a heuristic and time taking task; hence, this is not practically feasible.

In the current literature, there is a lack of a general framework that can be used to optimize intelligently and automatically a commercial energy system based on comprehensive internal and external information such as forecasted weather conditions, energy price forecast, and other associated variables. Therefore, this thesis proposes a mathematical model of storage facilities appropriate for optimal operation purposes based on approxi-

mate physical models of produce storage facilities and climate conditions predictions, so that it can be implemented as a supervisory real-time control in existing climate control systems. The proposed supervisory control in conjunction with current existing climate controllers would allow coordinated optimal operation of multiple produce storage facilities in a single site, while considering the user-defined preferences, thus facilitating the integration of commercial customers into Smart Grids.

1.2.3 Agricultural Sector

Energy systems of agricultural sector customers are usually multi-carrier energy systems consisting of electricity, natural gas, hot water, wood, and bio-fuels [50, 51, 52]. In the USA, poultry farms, dairy farms and greenhouses are some of the major energy consuming customers in the agricultural sector, where electricity consumption is about 16% of the total energy consumptions [52]. The potential for DR participation in greenhouses is much higher than farms because of the nature of activities that take place in these places. Most of the DSM programs in farms are focused on energy efficiency programs to reduce total energy consumption by installing more energy efficient technologies and the reduction of energy losses [53, 54, 55]. Thus, this thesis focuses on the optimal operation of energy systems of greenhouses in the agricultural sector in the context of Smart Grids.

All growing phases of crops can be modified by the control of temperature, humidity, light, and CO_2 in a greenhouse [56]. Thus, climate control is one of the most important factors in growing high quality horticultural produce. Increasing energy costs and environmental concerns have lead to more efficient and responsible energy consumption in greenhouses. The following approaches presented in the literature for climate control in greenhouses and are discussed next: Feedback controllers [57, 58, 59]; optimal control [56, 60, 61]; robust control [62, 63]; NN [62, 64, 65]; Fuzzy Logic Controller (FLC) [66, 67, 68, 69]; MPC [70, 71, 72, 73, 74, 75] and hierarchical control [60, 76, 77].

In [57], a nonlinear feedback technique is presented for climate control of greenhouses. The work considers the fact that temperature and humidity are highly coupled through nonlinear thermodynamic laws, and propose a feedback-feedforward approach to system decoupling for climate control of greenhouses. The authors in [58] use Proportional–Integral (PI) based controllers for temperature and humidity control of greenhouses, as most commercial solutions include this kind of gain controllers. A PI–puls control design for CO_2 enrichment systems is discussed in [59] to be used instead of existing control algorithms based on classically derived two- or three-term control laws with manually tuned parameters.

Optimal control of greenhouse climate using genetic algorithms in presented in [61]. A robust adaptive control method using NN for greenhouse climate control is proposed in [62], and [63] presents a robust adaptive control for greenhouse climate control. Black box models based on NN are applied in [64] to predict temperature and relative humidity in a greenhouse. In [65], an optimal CO_2 control in a greenhouse is modeled using NNs by predicting separately the temperature and CO_2 concentration.

In [66], an intelligent indoor environment control and EMS for greenhouses based on FLC is proposed and simulated in a Matlab Simulink environment. A fuzzy greenhouse climate control system implemented on a Field Programmable Gate Array (FPGA) is presented in [67], where inside temperature and relative humidity are controlled based on fuzzy rules. Two basic and optimized FLCs with a significant number of inputs and outputs are presented in [68] to minimize the production costs in greenhouses. The authors in [69] present a hierarchical collaborative structure to split fuzzy modeling of inside greenhouse air temperature and humidity into fuzzy sub-models to organize the information of the fuzzy system.

A real-time implementation of MPC-based optimal control of greenhouse air temperature control is reported in [70], where energy savings and better performance is achieved compared to an adaptive Proportional-Integral-Derivative (PID) controller. MPCs using particle swarm optimization for greenhouse climate control is presented in [71], and the authors in [72] present an MPC based on particle swarm optimization for minimization of energy costs. Another MPC based method for diurnal temperature control of greenhouses is presented in [73], and an MPC of greenhouse to reduce energy and water consumption is proposed in [74]. A web-based application of dynamic modeling and simulation of a greenhouse environment is presented in [75] to be used as an educational tool.

A hierarchical scheme based on time-scale decomposition for greenhouse climate control is presented in [60]. The slow subproblem (related to crop growth) is solved off-line and its solution is fed to an online fast subproblem (greenhouse dynamics including crop evapotranspiration and photosynthesis). A very detailed model of both subproblems is presented, and two pathways is foreseen to achieve a practical online controller: first, use the output trajectories as set points to low level controllers; and second, repeatedly solving an RHOC problem on the basis of the same goal function as used in the slow subproblem but over a shorter horizon. A PID based hierarchical control for greenhouses is proposed in [76], and an adaptive hierarchical control of greenhouse crop production based on generalized predictive control is proposed in [77] with the objective of maximizing profits.

Some works are reported in the literature on greenhouse climate control with energy cost minimization, mostly focusing on minimization of CO_2 and heating costs (e.g.,[61],

[66], [72], [74], and [78]). In [78], the authors address the issue of optimal light integral and CO_2 concentration combinations for lettuce in ventilated greenhouses, showing that savings can be achieved by coordinated operation of these systems.

Existing methods for energy management in greenhouses only focus on climate control of greenhouses, and thus fail to fully optimize total energy utilization in such multi-carrier agricultural facility. This is mainly due to a lack of a general optimization framework based on comprehensive internal and external information such as weather and energy price forecast, and other associated variables. Thus, this thesis proposes a mathematical model of greenhouses appropriate for optimal operation purposes of this multi-carrier energy hub, so that it can be implemented as at supervisory real-time control in existing greenhouse controllers. The objective is to minimize total energy costs and demand charges while important parameters of greenhouses, i.e., inside temperature and humidity, CO_2 concentration, and lighting levels are kept within acceptable ranges. The proposed supervisory control in conjunction with current existing climate controllers would allow coordinated optimal operation of greenhouse while considering the user-defined preferences, thus facilitating the integration of these agricultural customers into Smart Grids.

1.2.4 Smart Grids

Traditional power systems are vertically integrated structures in which power plants at the top of the hierarchy ensure power delivery to customers' loads at the bottom of the hierarchy. In these systems intelligence is only applied locally by protection systems and by central controls through Supervisory Control and Data Acquisition (SCADA) systems. New developments in practical methods, tools, and technologies based on advances in the fields of computation, control, and communications are allowing power grids to operate in more intelligent, secure, distributed, and fast ways [79].

Power circuit topology, communication infrastructure (e.g., Wide-Area Network (WAN) and Home-Area Network (HAN)), and Information Technology (IT) (e.g., enterprise services, geographic information systems, and data management) are the foundation of Smart Grids. In this context, applications and devices such as substation automation, smart meters, meter data management, distribution automation, and energy management systems are being deployed by utilities [80]. These will allow the integration of Distributed Generation (DG), energy storage, micro grids, and DR into Smart Grids.

The U.S. Department of Energy states: "Think of the Smart Grid as the internet brought to our electric system. Devices such as wind turbines, plug-in hybrid electric

vehicles and solar arrays are not part of the Smart Grid. Rather, the Smart Grid encompasses the technology that enables us to integrate, interface with and intelligently control these innovations and others" [81]. KEMA defines the Smart Grid as: "The Smart Grid is the networked application of digital technology to the energy delivery and consumption segments of the utility industry. More specifically, it incorporates advanced applications and the use of DER, communications, information management, and automated control technologies to modernize, optimize, and transform the electric power infrastructure. The Smart Grid vision seeks to bring together these technologies to make the grid self-healing, more reliable, safer, and more efficient, as well as to use intelligent meters and devices to empower customers to use electricity more efficiently. It also seeks to contribute to a sustainable future with improvements to national security, economic growth, and climate change" [82].

Based on the above definitions, it is envisioned that the Smart Grid of the future will support large penetration of distributed demand-side resources coupled with system-wide DR driven by economic and reliability signals. Currently, many DR programs being offered by utilities in North America to residential, commercial and industrial customers, and initiatives such as NIST/Gridwise Architecture Council efforts to define Home-to-Grid (H2G), Building-to-Grid (B2G), and Industry-to-Grid (I2G) interoperability requirements, as well as standards for HANs, will enable more integration of DR and demand-side resources into Smart Grids [83]. Availability of smart meters, two-way communication infrastructure, IT, and computational tools are the basic requirements to enable the research presented in this thesis to optimally operate energy hubs in Smart Grids.

1.2.5 Energy Hub Management Systems

The energy hub is a novel concept recently developed in the context of integrated energy systems with multiple energy carriers. *Hub* is defined as a center of activity; hence *energy hub* is any location where energy system activities, namely, energy production, conversion, storage, and consumption of different energy carriers take place [84, 85, 86, 87]. Thus, the authors in [84] and [85] propose the energy hub as a generalization or extension of a network node in an electric power system which exchanges power with the surrounding systems, primary energy sources, loads, and other components via multi-energy input and output ports.

The energy hub is not limited in size and can range from a single household energy system to an entire city energy system. Since the focus of the research is on the demand side, energy hubs are categorized in this thesis into four major sectors based on their "type" of energy consumption [88]:

- Residential (e.g., single detached houses).
- Commercial and institutional (e.g., produce storage facilities, retail stores, shopping malls, schools, hospitals).
- Agricultural (e.g., greenhouses).
- Industrial (e.g., paper mills).

In any electric energy system, the customers' objective is to minimize their energy cost, whereas utilities are not only concerned about the cost, but also other issues such as load shape, peak load, quality of service, etc. In the context of energy hubs, a two-tier hierarchical scheme is used in this thesis in order to distinguish between the different objectives of the customers and the utility. Therefore, at the lower level, i.e., micro hub level, the objective is to optimize the energy consumption from the customer's point of view, whereas at the macro hub level, i.e., a group of micro hubs controlled and scheduled together (e.g., a group of detached house micro hubs), the objective is to optimize the energy consumption from the utility point of view. Figure 1.3 shows the overall picture of the macro hub and micro hub interaction in an overall Energy Hub Management System (EHMS), and the associated data and information exchanges between them.

As seen in Figure 1.3, a typical residential macro hub comprises several micro hubs which communicate with the macro hub with regard to their energy usage and control decisions. The micro hubs are at the residential household level and the macro hub can be thought of as a group of residential micro hubs. This figure also shows the three other categories of the macro hubs, namely, commercial and institutional, agricultural, and industrial. In these macro hubs, there may or may not exist multiple micro hubs, but all would have similar arrangements for data and information exchange.

In view of the above discussions, the main objective of this research is to develop mathematical models of micro hubs which can be readily incorporated into EHMS. These mathematical optimization models of individual energy hubs will empower them to effectively manage their energy demand, production and storage in real-time. Three major energy consumption sectors, namely, residential, commercial and agricultural, are considered in this thesis. Mathematical modeling of the macro hubs and industrial micro hubs are beyond the scope of this thesis.

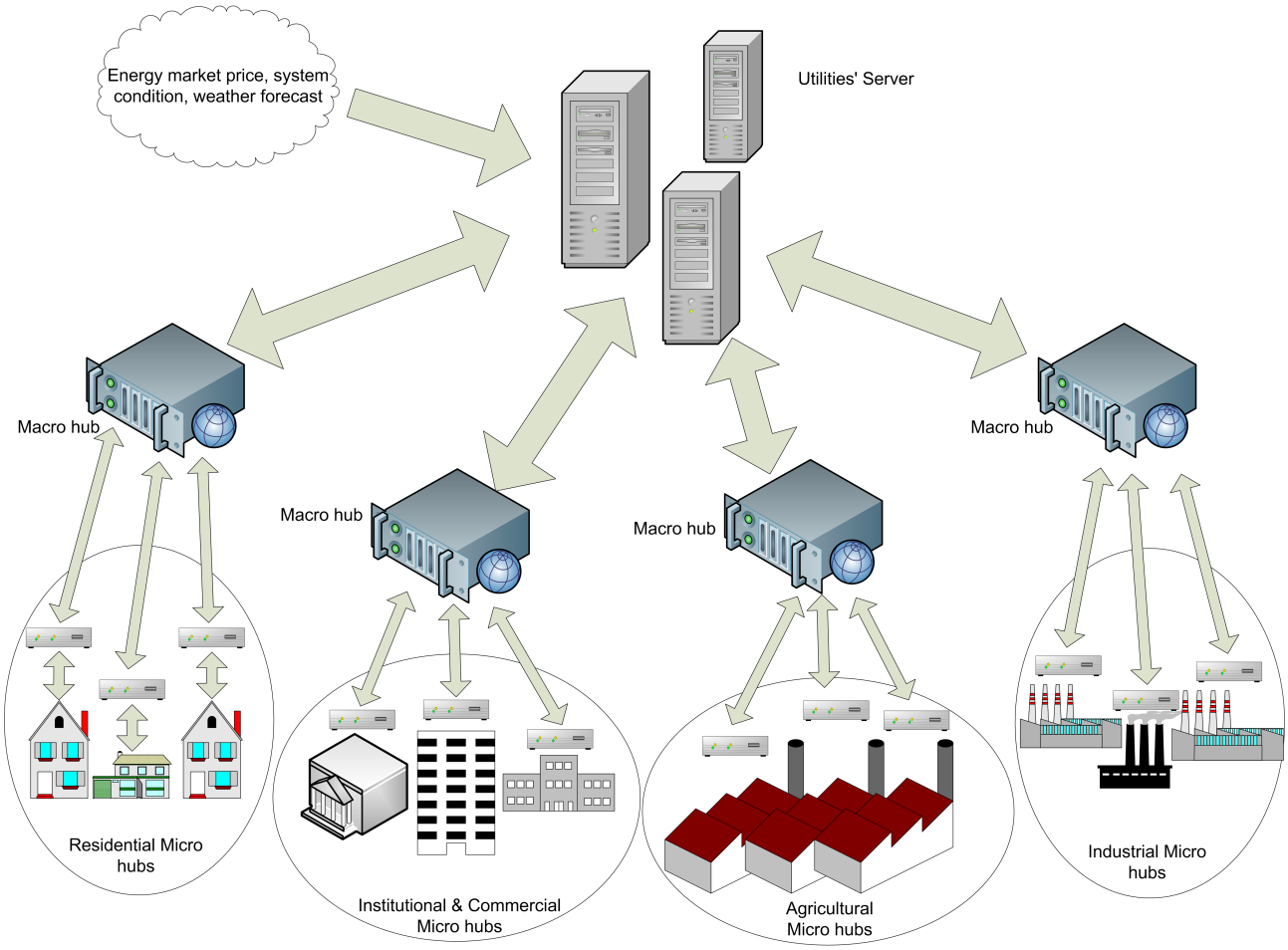

Figure 1.3: Overall picture of the EHMS.

1.3 Research Objectives

Based on the previous literature review and discussions, the followings are the main goals of the research presented in this thesis:

- Develop and apply mathematical models of residential energy hubs which can readily be integrated into automated decision making technologies, such as HASs and EMSs, in the context of Smart Grids. The proposed models are used to generate the optimal operational schedules for all major residential energy loads, storage and production components using a variety of information from the external environment to reduce total energy costs, energy demand, and emissions while considering the householder comfort and preferences. The proposed multi-period scheduling optimization models can be solved efficiently in real-time, and different objective functions such as minimization of demand, total cost of electricity and gas, emissions and peak load over the scheduling horizon are considered.

- Propose and apply a mathematical optimization model of produce storage facilities in the commercial sector to optimize the operation of their energy systems in the context of Smart Grids. The proposed model can be implemented as a real-time supervisory control in existing climate controllers, while incorporating weather forecasts, electricity price information, and end-user preferences to optimally operate existing climate control systems in storage facilities. The objective is to minimize total energy costs and demand charges while considering important parameters of storage facilities, i.e., inside temperature and humidity should be kept within acceptable ranges.

- Develop and apply mathematical models for optimal operation of greenhouses in the agricultural sector to optimize their operation to reduce total energy costs and CO_2 emissions. These models consider humidity, temperature, and CO_2 concentration characteristics of the climate control systems of greenhouses, as well as lighting systems which consume large amounts of electricity in greenhouses. Also, study the effects of uncertainty in electricity price and weather forecasts on optimal operation of greenhouses, and develop a robust optimization model to consider electricity price forecast errors in generating optimal operation of greenhouses.

1.4 Thesis Outline

The reminder of the thesis is organized as follows:

- Chapter 2 presents a review of the main background topics, concepts, and tools relevant to this research. First, a background review on DSM and DR programs is provided, and DSM objectives, strategies, approaches and its role in Smart Grids is explained. Then, the state-of-the-art in EMSs in residential, commercial, and agricultural sectors is presented and discussed. An overview of mathematical programming including (LP) and MILP problems, robust optimization, and some relevant solution methods are also discussed. Finally, relevant information on energy pricing and an estimation model of CO_2 emissions are presented.

- Chapter 3 presents the proposed residential energy hub optimization model. First the modeling approach is explained, followed by the formulation of mathematical models of typical residential energy hub components. Finally, some results of applying the proposed models to an actual household are presented and discussed.

- Chapter 4 presents the proposed optimization model for optimal operation of produce storage facilities in commercial energy hubs. In this chapter, first the proposed supervisory operation strategy is explained. Then, the proposed mathematical models of the storage facilities are provided, and some simulation results, including Monte-Carlo simulations, are presented and discussed for a realistic storage facility. Finally, a solution procedure for real-time implementation of the proposed model for optimal operation of storage facilities and relevant simulation results are presented.

- Chapter 5 presents the proposed greenhouse energy hub optimization mode for the agricultural sector. The proposed supervisory operation strategy for optimal operation of greenhouses is explained, and the proposed mathematical model is presented. Then, numerical results of the proposed models are presented and discussed for a realistic greenhouse, including Monte-Carlo simulations to study uncertainty in electricity price and weather forecasts. Finally, a robust optimization model for optimal operation of greenhouses considering uncertainties in electricity price is proposed and simulation results are presented.

- Chapter 6 presents the main conclusions and contributions of the research presented in this thesis, and identifies directions for future research.

Chapter 2

Background Review

2.1 Introduction

This chapter presents a background review of the main concepts and tools relevant to the research presented in this thesis. First, DSM and DR programs and their objectives, strategies, approaches and their role in Smart Grids are discussed in Section 2.2. This is followed in Section 2.3 by a review of the state-of-the-art in EMSs in residential, commercial, and agricultural sectors. A brief review of mathematical programming and their solution methods and tools, which are particularly relevant to this research, are presented in Section 2.4. Finally, relevant information on energy pricing and an estimation model of CO_2 emissions are discussed in Section 2.5.

2.2 Demand Side Management and Demand Response

DSM is a broad term that includes strategic load growth, energy conservation, energy efficiency, and DR programs. Strategic load growth refers to programs designed to increase load levels through electrification in a strategic fashion; energy conservation refers to any actions that result in less energy consumption, usually by making behavioral choices or changes; and energy efficiency refers to programs that are aimed at reducing the energy used by specific end-use devices and systems, typically without affecting the services provided [89]. These programs reduce overall electricity consumption by substituting with more energy efficient technologies in existing systems to produce the same level of end-

use services (e.g., high-efficiency appliances, efficient lighting programs, efficient building design, and advanced electric motor drives).

DR is related to energy price, with the U.S. Department of Energy defining it as: "changes in electricity usage by end-use customers from their normal consumption patterns in response to changes in the price of electricity over time, or to incentive payments designed to induce lower electricity use at times of high wholesale market prices or when system reliability is jeopardized" [90]. DR programs lead to less electricity consumption when prices are high, which change the customers' consumption pattern and thus modifies the load shapes of the utilities. DR costs and benefits for various stockholders have been investigated in the literature, as for example in [91], [92], [93], [94], and [95]. Benefits for participating customers would be incentive payments and bill savings, while increased grid reliability, better market performance, and deferred infrastructure costs are the expected system wide benefits of DR programs. DR programs can be classified as Incentive Based (IB) and Price Based (PB) programs [96]. IB programs include LM programs and market based programs such as demand side biding and capacity market. PB programs are based on dynamic pricing schemes such as TOU, RTP, and Critical Peak Pricing (CPP).

LM includes DLC and Interruptible Load Control (ILC). DLC usually involves residential customers and refers to program activities that can interrupt a customer load (individual appliances or equipment) via direct control by the utility system operator. ILC usually involves commercial and industrial customers and refers to program activities that can interrupt customer load at times of peak load by direct control of the utility operator or by action of the customer at the request of the system operator in accordance with contractual provisions [8]. The objective of all these activities is to modify the load shape of the system.

There are three load shape modification objectives in DR programs [97, 98, 99]: peak clipping, valley filling, and load shifting. These objectives, when combined with strategic conservation, strategic load growth and flexible load shaping, comprise the set of techniques for DSM programs. Figure 2.1 shows the DSM strategies and objectives. In "restructured" power systems, energy efficiency and dynamic energy management terminologies are commonly being used to refer to strategic conservation and flexible load shape, respectively. These programs emphasize improving the efficient and effective use of energy. Consequently, implementations in the restructured systems tend to target DR and energy efficiency objectives rather than strategic load growth [98].

The following describes energy efficiency and load shape modification objectives in DR programs [99, 100, 101]:

- Peak Clipping: To lower energy usage during periods of peak demand (e.g., with a

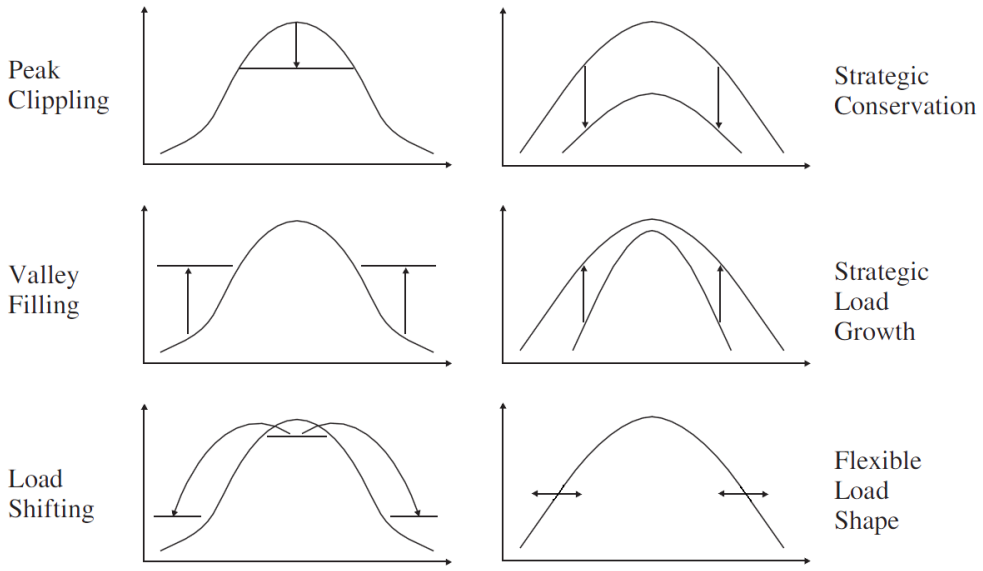

Figure 2.1: DSM strategies and objectives [97].

water heater DLC program).

- Valley Filling: To encourage customers to use off-peak energy technologies. This strategy is important for the utility to improve its overall load factor.
- Load Shifting: To convince customers to shift their demand (such as space heating and water heating storage systems) to hours when the price is low in a peak-pricing scheme, and to reward them for shifting demand to off-peak hours or penalize them for usage during peak hours. Notice that the main goal of load shifting is not to reduce energy consumption in the long-term, but to reduce peak load in the short term without affecting the comfort of the users.
- Strategic Conservation (Energy Efficiency): To lower customers' electricity costs by using energy efficient technologies (e.g., with high-efficiency appliances and Compact Fluorescent Lamp (CFL) lighting replacement program).
- Flexible Load Shape (Dynamic Energy Management): To easily redistribute to and alter customer power requirements at different times.

The earliest reported LM programs were implemented by U.S. utilities in the 1960's, and were directed to control residential customer's appliances. Utilities had understood the benefit of successful DLC and LM programs by the mid 1970's; however, there were also concerns about the customers not tolerating the expected inconveniences. A collection of early technical articles are organized in [102]. Since then, and over the past decades, DSM activities in the U.S. (and to a large extent in Canada) have been characterized by five waves of programs [103]:

1. The first wave took place from the mid to late 1970s, with the focus of the associated DSM activities on designing and implementing energy conservation and load management programs.

2. The second wave took place during the 1980s. During the first part of this decade, there was a focus on achieving a comprehensive set of load shape objectives, including energy conservation, load management and strategic electrification, where the latter means expanding the uses of electricity to achieve other objectives such as economic development. A series of cost-effectiveness tests were developed to ensure that programs would reflect the often-conflicting perspectives of the utility, its customers and society. Some experiments were carried out with RT pricing.

3. The third wave came in the early 1990s. It was brought on by new regulatory mechanisms for implementing DSM programs, with a new focus on measuring the environmental benefits of DSM programs.

4. The fourth wave came in the late 1990s. Regulators were concerned that DSM expenditures were on the decline; thus, they instituted a "public goods charge" to cover DSM expenditures.

5. The fifth wave began in the year 2000, and was triggered by price spikes in wholesale power markets. In this phase, there was widespread interest in implementing pricing reforms rather than relying on traditional DSM programs. In particular, there was interest in dynamic pricing.

DSM has become more relevant following the Kyoto accord, which have led many countries to review their DSM activities after the "liberalization" of the electricity sector [104]. DSM has become important because of it's capability to reduce energy consumption and peak demand, thus lessening required primary resources and decreasing produced GHG emissions in most cases. With the advent of Smart Grids technologies such as AMI and an improved communications infrastructure in the power grids, Smart Grids are envisioned to

support system-wide DR driven by economic and reliability signals. Consequently, a new wave of DSM has begun with more emphasis on environmental issues, GHG emissions, power system reliability, energy efficiency and reduction of energy consumption and costs. The new wave can be considered a sixth wave of DSM, or advanced DSM as part of Smart Grids. Many of the previously published concepts are applicable in the new wave of advanced DSM. In particular, modern DSM approaches are similar to the traditional ones, but with different technologies.[98]

2.2.1 Approaches

A relatively comprehensive description of each of the following alternatives for DSM programs is presented in [99, 105]:

- End-use equipment control:
  - AC of residential and commercial customers: remote control cycling, local controller, thermostat control, remote on-off control.
  - AC of commercial and industrial chillers: water column temperature control, remote control cycling, capacity reduction.
  - Water heaters of residential and commercial customers: remote On/Off control, timers.
  - Pumps: timers, remote On/Off control.
  - Heating: alternate source heating, remote On/Off control, remote cycling, smart thermostat.
  - Multiple loads: equipment interlock, demand limiter, energy management system, demand controller, peak alert, timers.
  - Processing Loads: interlocks, alternate source, pre-arranged sequence of remote control.
- Utility equipment control: voltage reduction, feeder control, power factor control.
- Energy storage: cold storage, heat storage, storage water heater, waste heat utilization.
- Incentive rates: time differentiated, interruptible, load control contracts, spot pricing, rebates and incentives, special programs.

- Dispersed Generation: wind, solar thermal, solar photovoltaic, fuel cells, standby generators, cogeneration, small hydro.
- Performance improvement of equipment and systems: high energy efficiency ratio equipment, heat pumps, buildings, process, economizer, utility system improvements.
- Demand side bidding: direct participation of customers offering load reductions.

The research presented in this thesis concentrates on the end-use equipment control approach based on recent developments in Smart Grid technologies (such as AMI, two-way communication infrastructure, and EMSs), to achieve DSM and DR objectives as well as customers energy cost and GHG emission reductions.

2.3 Energy Management Systems

2.3.1 Residential Sector

Figure 2.2 presents an overview of the residential energy hub which includes various appliances, energy storage systems (e.g., batteries, Electric Vehicles (EVs)), and energy production systems (e.g., solar photovoltaic, wind power). HAS and Home Energy Management (HEM) systems are used in residential buildings to integrate and automate a number of activities in households [106, 107, 108, 109, 110, 111, 112]. Turning lights on and off, setting thermostat up and down, covering windows, controlling audio/video equipment and activating security systems are some examples of the tasks usually performed by HASs. Most of these tasks are executed automatically to increase the comfort of the household owner. These systems can usually be configured and controlled by computers, smartphones and through the internet, so that the end-user programs the HAS to automatically adjust the room temperature based on the seasons, time of day and outside temperature. Dimmers, timers, motion sensors, and occupancy sensors are used to turn lights off automatically when rooms are unoccupied. Plug-in modules for On/Off control of lighting, and appliances with two-way communication capability are being controlled by a central controller. Z-Wave, X10, Wi-Fi, and ZigBee are common communication protocols for HAS [113, 114].

In general, there is a lack of intelligent decision making core to optimally operate household energy requirements. The current research proposes an intelligent decision making core based on the mathematical model of the residential energy systems to be integrated in HAS, HEM, and EMSs.

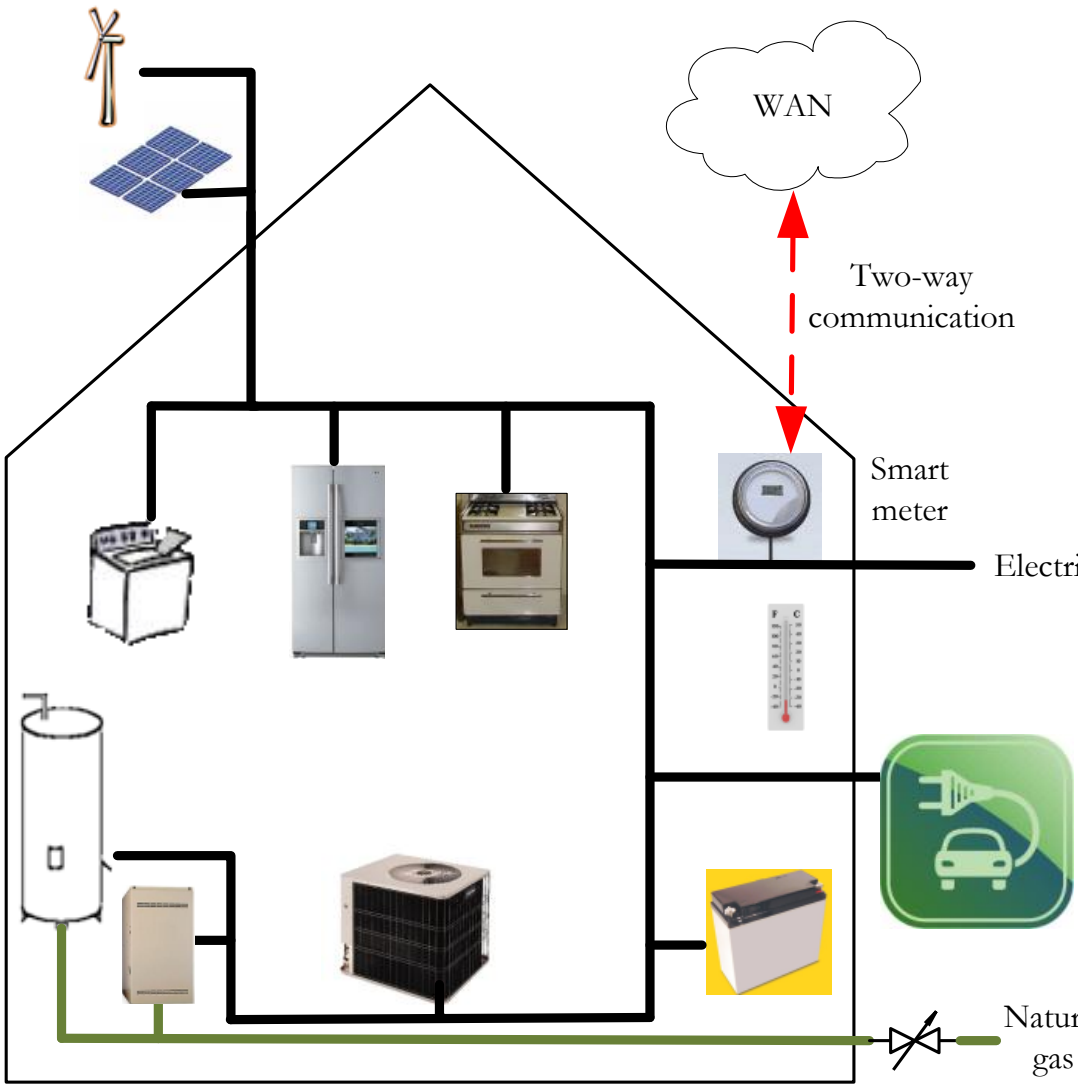

Figure 2.2: Residential energy hub.

2.3.2 Commercial Sector

There are EMSs and climate control systems in large commercial facilities to maintain good control of temperature, humidity, comfort and overall operation of energy system efficiently. Two main requirements of any climate control systems are to provide satisfactory indoor climate condition and minimize the overall energy consumption [39]. Building Automation Systems (BASs) enable monitoring and control of commercial building systems, and Energy Information Systems (EISs) are also commonly used in commercial facilities to integrate a large variety of data from sensor networks, meters, and databases to calculate some key figures of energy utilization. This information can be compared across similar facilities to provide an insight on energy efficiency of the facility. BACnet, and ZigBee are common communication standards for BASs and EIS [115, 116].

The objective in the indoor climate control of commercial storage facilities, in which this thesis focuses, is to keep the internal parameters (e.g., inside temperature and humidity) within pre-defined ranges. These parameters are affected by external parameters such as the stored produce and outdoor weather conditions. Most storage facilities take advantage of natural and forced air flows, in addition to mechanical heating and cooling systems, to control the inside climate. Air ventilations do not consume much energy, and in some weather conditions it might be necessary to utilize more energy consuming heating or cooling systems to maintain the internal parameters within the desired ranges. Figure 2.3 depicts the layout of climate control system of a storage facility; mixture of outdoor and inside air is circulated through the fans, the air flow is controlled by the fans capacity and the position of hatches in the air mixer, and humidifiers and dehumidifiers are used to control the humidity of the storage space.

Figure 2.4 presents a schematic diagram of typical climate control systems in storage facilities. Feedback based controllers dedicated to monitor and control inside temperature and relative humidity using direct measurements are common in existing climate control systems of storage facilities [117]. The main features of such feedback controllers are boolean logics to determine the use of ventilation and mechanical heating and cooling systems, and PID controllers to control the hatch positions. In these systems the objective is to decrease/increase the inside temperature to its set point value and avoid dropping below a lower limit or exceeding an upper limit by activating either cooling or heating devices in response to temperature variations. Usually, the feedback controllers use constant temperature set points for different times. These set points depend on the type of crop and are usually in the range of 4–8 °C, but in practice the actual inside temperature varies over a wider range.

In general, there is a lack of a general framework that can be used to optimize op-

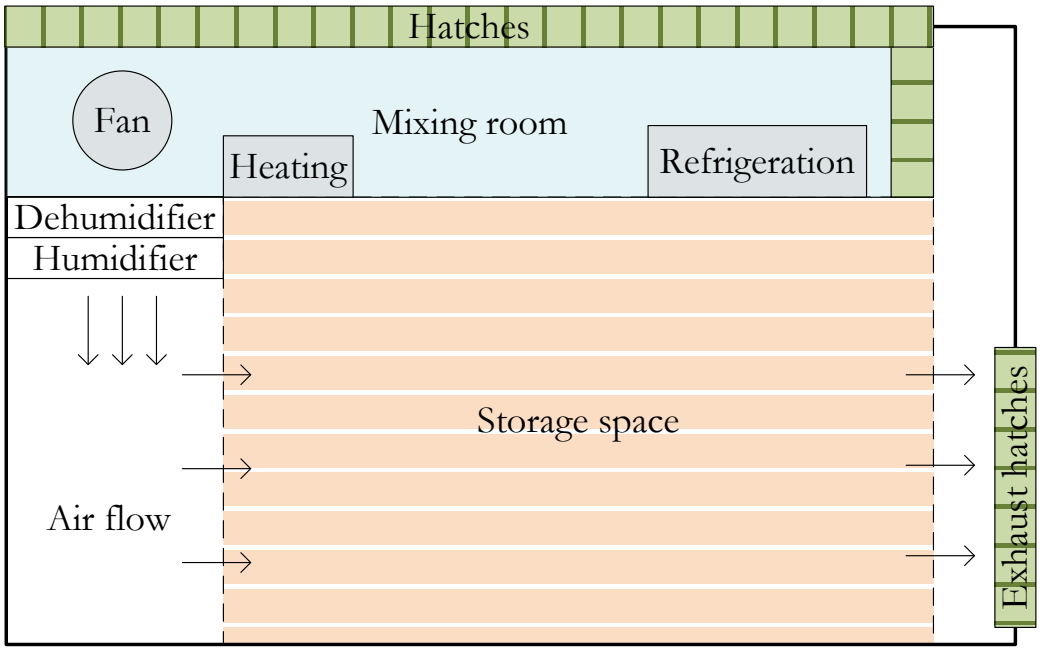

Figure 2.3: Typical layout of a storage facility.

eration of climate control systems of storage facilities based on comprehensive internal and external information such as forecasted weather conditions, energy price forecast, and other associated variables. In this thesis, a supervisory real-time control appropriate for optimal operation of storage facilities is proposed based on a mathematical model of storage facilities and predictions of climate conditions. The proposed supervisory control in conjunction with current existing climate controllers would allow coordinated optimal operation of multiple produce storage facilities in a single site, thus facilitating the integration of these commercial customers into Smart Grids.

2.3.3 Agricultural Sector

Figure 2.5 shows an overview of a greenhouse energy system. Climate control of greenhouses is a multi-variable problem, since the optimum coordination between heating, ventilation, fogging, supplementary lighting, and CO_2 demand in greenhouse needs to be addressed. Operational constraints of physical devices such as maximum window opening, flow rate of fans, rate of fogging system, and temperature of hot water tubes are the limiting features which need to be considered in these control systems. Also, pre-defined ranges for controlled

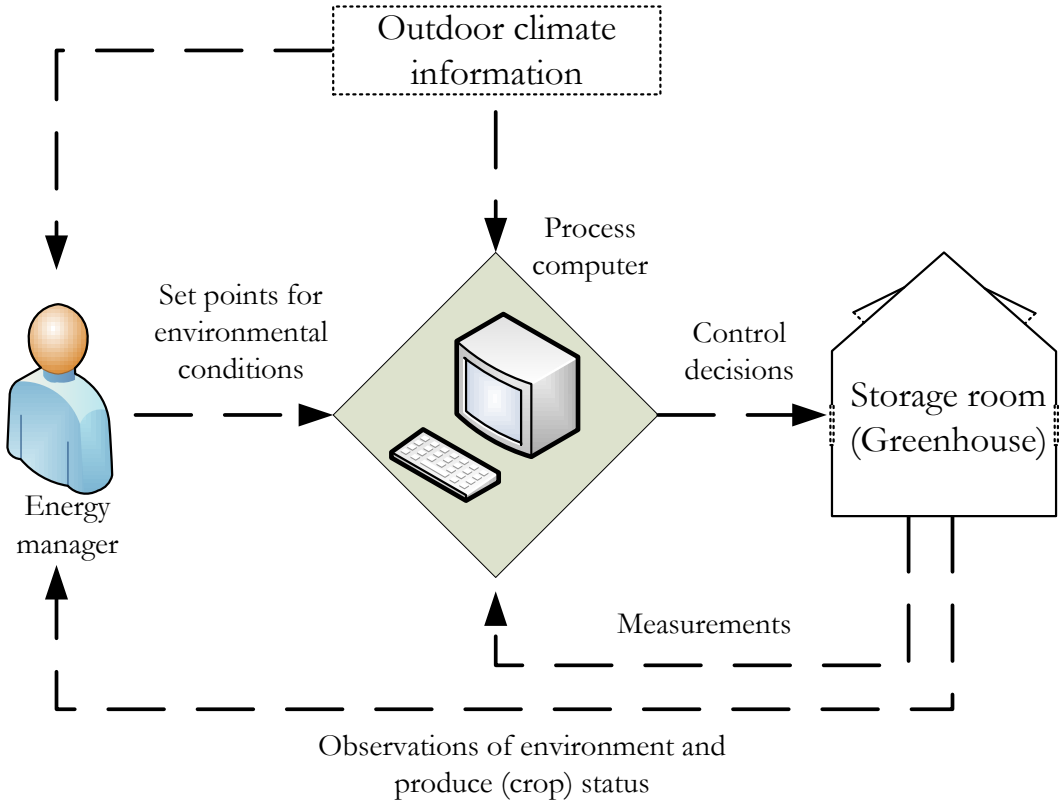

Figure 2.4: Schematic diagram of a typical climate control system in storage facilities and greenhouses.

variables should be chosen properly considering the physical limits of devices and related physical and thermodynamic laws (e.g., saturation bounds enforced by saturation law [57]).

In greenhouses, CO_2 enrichment is usually used to decrease the amount of supplemental lighting, as it is a much less expensive process. However, it is economically prohibitive to maintain elevated CO_2 concentrations inside the greenhouse during periods of high ventilation rates [78]. Transpiration of a crop can be controlled by manipulating the temperature and ventilation rate of the greenhouse [118], and photosynthesis is a function of irradiance, temperature and CO_2 concentration [119]. It should be noted that the greenhouse layout and available equipment, as well as the crop type grown in the greenhouse affects the climate control strategy and model.

Automated Control Systems (ACSs) in most greenhouses consist of central computers, sensors and a data acquisition system connected through communication protocols such as RS-232 and ModBus [120, 121]. These ACSs coordinate and integrate the control of greenhouse equipment and systems such as heaters, coolers, motors for windows opening and closing, pumps and irrigation systems in real time. Some ACSs deal with variables such as temperature, humidity, and CO_2 separately, whereas others consider associated interactions.

A typical climate control system in a greenhouses is depicted in Figure 2.4. Currently, major control algorithms in ACS work on logical On-Off and PID based controllers. These algorithms use climate control settings which usually include daily or multi-day schedules in which temperature and humidity targets can be defined for a number of periods in a day. The goal is to keep a given variable (e.g. temperature, relative humidity and CO_2 concentration) within a predefined range or to follow pre-defined set points. Greenhouses usually have weather stations that provide information on temperature, relative humidity, radiation, and wind speed to be used for their real-time climate control.

Existing methods for greenhouse management only focus on climate control, and thus fail to fully optimize total energy utilization in such multi-carrier agricultural facilities. Thus, this thesis proposes a supervisory control framework based on a mathematical model of greenhouses and using internal and external information such as weather and energy price forecasts for optimal operation of greenhouses. The proposed supervisory control in conjunction with current existing climate controllers would minimize total energy costs and demand charges while important parameters of greenhouses, i.e., inside temperature and humidity, CO_2 concentration, and lighting levels, are kept within acceptable ranges. The proposed technology would facilitate the integration of these agricultural multi-carrier energy hubs into Smart Grids.

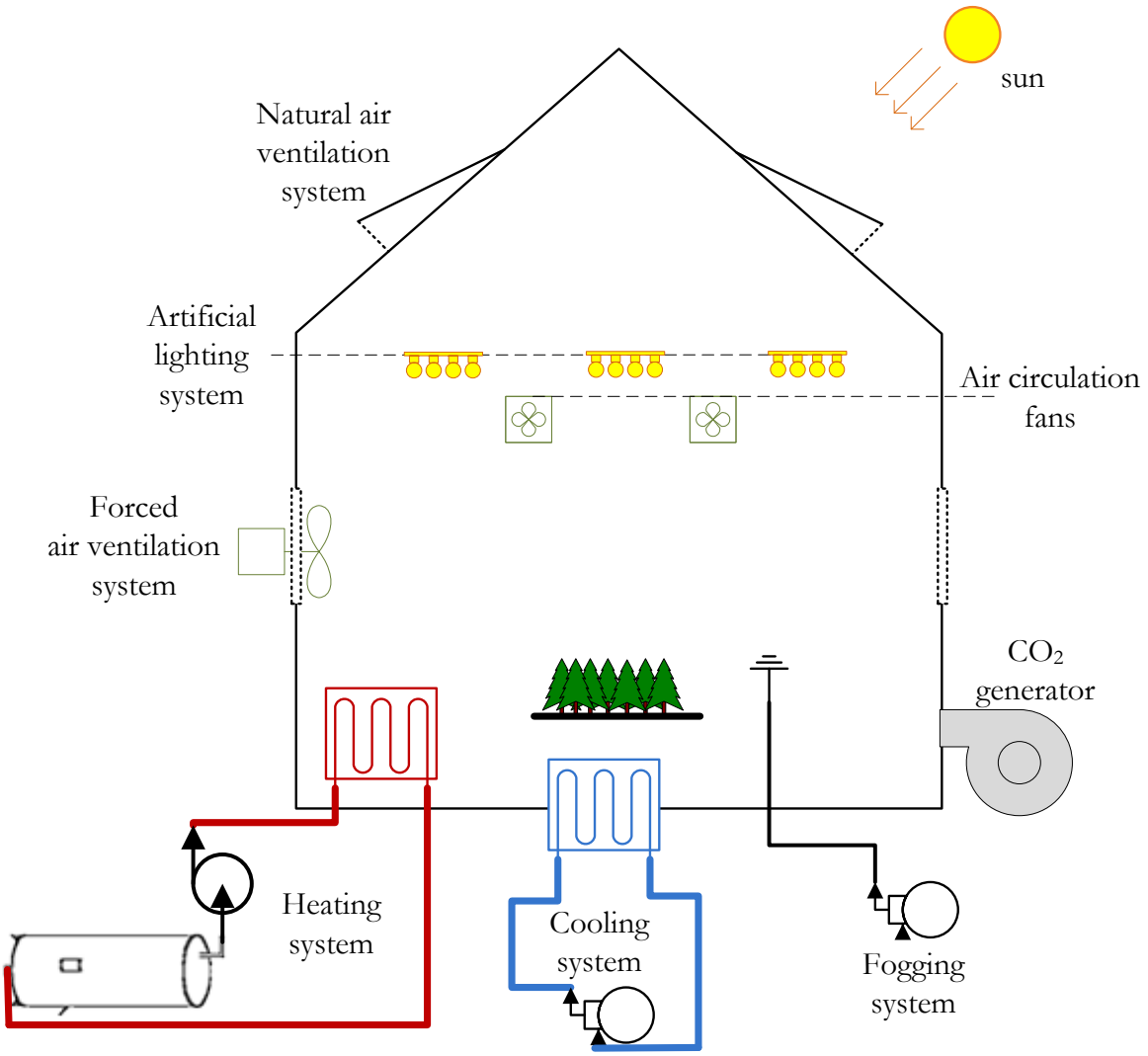

Figure 2.5: Greenhouse energy system.

2.4 Mathematical Programming

Mathematical optimization problems refer to finding the minimum or maximum of an objective function subject to a set of constraints. Without any loss of generality, an optimization problem can be defined as a minimization problem since the maximum of a function can be found by seeking the minimum of the negative of the same function. The set of values of the variables which result in the minimum objective function value is called the optimal solution. For any specific objective function there may be local and global optimal solutions. There are different methods to find optimal values of different type of optimization problems which are also known as mathematical programming techniques.

Mathematical optimization can be applied to many kinds of engineering problems including optimal control, optimal scheduling, optimal planning, and optimal decision making. Solving a real world problem using mathematical programming requires, first, problem identification; second, modeling of the problem; and, third, finding or developing an appropriate algorithm to solve the mathematical problem.

Mathematical optimization problems are usually stated by the objective function, decision variables, and constraints as follows:

$$\begin{aligned} \min \quad & f(\mathbf{x}) \\ \text{s.t.} \quad & g_k(\mathbf{x}) = 0, \quad \forall k = 1, \cdots, p \\ & h_j(\mathbf{x}) \geq 0, \quad \forall j = 1, \cdots, m \end{aligned} \tag{2.1}$$

where $\mathbf{x}$ is an n-dimensional vector of decision variables, $f(\mathbf{x})$ is the objective function, and $h_j(\mathbf{x})$ and $g_k(\mathbf{x})$ are inequality and equality constraints, respectively. Depending on the nature of formulation, different classes of mathematical programming techniques have been defined. For example, if the objective function and constraints, i.e., $f(\mathbf{x})$, $h_j(\mathbf{x})$, and $g_k(\mathbf{x})$, are all linear, and the decision variables x_i are continuous real-valued, the mathematical problem is referred to as an LP problem. If at least one of the $f(\mathbf{x})$, $h_j(\mathbf{x})$, and $g_k(\mathbf{x})$ is non-linear and x_i are continuous real-valued, the problem is referred to as a Non-Linear Programming (NLP) problem. An MILP problem is an LP problem in which some of x_is are integer or binary-valued.

There are different types of optimization problems and there is no single method universally accepted for solving all optimization problems efficiently. Depending on the type of the problem, various methods have been developed to solve different types of optimization problems. Solution methods for LP, NLP, and MILP problems are different, and a specific method that works well for NLP problems may not be the best choice for LP problems. Among the several techniques available for solving LP problems, the simplex

and interior-point algorithms are the most commonly used solution methods. Also, for solving Integer Programming (IP) and MILP problems, the cutting plane algorithm and the Branch-and-Bound (B&B) algorithm are popular [122].

Most of the energy hubs and related systems studied in this thesis are non-linear in nature, and expectedly, the mathematical models of these systems are either NLP or MINLP problems. Hence, developing models that capture the main characteristics of these systems for energy management applications in real time is challenging. Novel mathematical techniques are employed in this thesis to accurately simplify the mathematical models of the considered energy systems, so that the developed models can be solved efficiently in real time. Nonlinear terms and constraints in the developed problems are substituted by either exact linear equivalents or linear relaxations to convert the NLP and MINLP problems to LP and MILP problems, respectively.

2.4.1 Linear Programming

LP problems with continuous variables can be mathematically stated in the following general form:

$$\begin{aligned} \min \quad & \mathbf{c}^T\mathbf{x} \\ \text{s.t.} \quad & \mathbf{A}\mathbf{x} \leq \mathbf{b} \\ & \mathbf{l} \leq \mathbf{x} \leq \mathbf{u} \end{aligned} \tag{2.2}$$

where $\mathbf{x}$ is an n-dimensional decision vector, $\mathbf{l}$ and $\mathbf{u}$ are lower and upper bounds of $\mathbf{x}$, $\mathbf{A}$ is an $m \times n$ matrix, $\mathbf{c}$ and $\mathbf{b}$ are n and m-dimensional known parameter column vectors, respectively.

The simplex and interior-point algorithms are the most common methods to solve LP problems. An interior-point algorithm solves LP problems by generating a sequence of interior points from an initial interior point, whereas the simplex method changes the LP constraints (inequalities) to equations and then solves the problem by matrix manipulation.

2.4.2 Mixed Integer Linear Programming

The general form of MILP is as follows:

$$\begin{aligned} \min \quad & f(\mathbf{x}, \mathbf{y}) = \mathbf{c}^T\mathbf{x} + \mathbf{d}^T \\ \text{s.t.} \quad & \mathbf{A}\mathbf{x} + \mathbf{B}\mathbf{y} = \mathbf{b} \\ & \mathbf{x} \geq 0, \qquad x \in \mathbb{Z} \\ & \mathbf{y} \geq 0 \end{aligned} \tag{2.3}$$

where $\mathbf{x}$ is an n-dimensional decision vector restricted to be nonnegative and integer, $\mathbf{y}$ is a s-dimensional vector of nonnegative continuous variables, $\mathbf{c}$ is an n-dimensional vector, $\mathbf{d}$ is a s-dimensional vector, $\mathbf{b}$ is an m-dimensional vector, $\mathbf{A}$ is an $m \times n$ matrix, and $\mathbf{B}$ is an $m \times s$ matrix.

MILP problems are much harder to solve than LP problems and the B&B method is the most commonly used algorithm to solve this type of problems. In IP problems, when the number of integer variables is small it might be possible to calculate all of the possible combinations of variable values to select the solution whose objective function has the smallest value. When the number of variables increase, however, the number of required calculations increase exponentially; hence, an exhaustive enumeration this method is not practical for problems with large number of variables. Nevertheless, this idea can be used in an "intelligent" way in which not all of the possible combinations need to be calculated as is the case of the B&B method. This method works based on different techniques for reducing the number of required calculations (e.g., progressive separation and evaluation, strategic partitioning and search tree) [122].

2.4.3 Reformulation-Linearization Technique

Reformulation-Linearization Techniques (RLT) are relaxation techniques that can be used to produce tight polyhedral outer approximations or LP relaxations for an underlying non-linear, non-convex Polynomial Programming (PP) problem. The relaxation provides a tight lower bound on a minimization problem [123], [124]. In the RLT procedure, nonlinear implied constraints are generated by taking the products of bounding terms of the decision variables up to a suitable order, and also possibly products of other defining constraints of the problem. The resulting problem is subsequently linearized by variable substitutions, one for each nonlinear term appearing in the problem, including both the objective function and the constraints. This automatically creates outer linearizations that approximate the closure of the convex hull of the feasible region Ω.

Assume s and x are continuous variables bounded by $\underline{s} \leq s \leq \overline{s}$ and $\underline{x} \leq x \leq \overline{x}$, respectively. An LP relaxation for the nonlinear model can be formed by substituting second-order terms such as $s \cdot x$ with a new variable $\mu_{s,x}$ and a set of constraints, which are known as *RLT bound-factor product constraints*. Since s and x are bounded, the following relational constraints are valid:

$$(s - \underline{s})(x - \underline{x}) \geq 0 \tag{2.4a}$$
$$(s - \underline{s})(\overline{x} - x) \geq 0 \tag{2.4b}$$
$$(\overline{s} - s)(x - \underline{x}) \geq 0 \tag{2.4c}$$
$$(\overline{s} - s)(\overline{x} - x) \geq 0 \tag{2.4d}$$

By substituting $\mu_{s,x}(t) = s \cdot x$ in (2.4a)-(2.4d), the following *RLT bound-factor product constraints* for $\mu_{s,x}$ can be found:

$$\underline{s} \cdot x + \underline{x} \cdot s - \mu_{s,x} \leq \underline{s} \cdot \underline{x} \tag{2.5a}$$
$$\overline{s} \cdot x + \underline{x} \cdot s - \mu_{s,x} \geq \overline{s} \cdot \underline{x} \tag{2.5b}$$
$$\underline{s} \cdot x + \overline{x} \cdot s - \mu_{s,x} \geq \underline{s} \cdot \overline{x} \tag{2.5c}$$
$$\overline{s} \cdot x + \overline{x} \cdot s - \mu_{s,x} \leq \overline{s} \cdot \overline{x} \tag{2.5d}$$

By substituting the second-order term $s \cdot x$ with $\mu_{s,x}$ in the objective function and other constraints of the model, the order of the PP problem is reduced, in this case from second-order to a linear model. Similarly, the same approach can be applied to reduce third-order PP problems to second-order problems with the corresponding RLT constraints to finally obtain an LP relaxation problem of the model. The optimal solution to this LP relaxation provides a lower bound for the original problem.

2.4.4 Robust Optimization

Stochastic programming and robust optimization are the two methods that have been proposed in the literature to deal with data uncertainty in optimization problems [125, 126]. To address data uncertainty in stochastic programming, several scenarios for the data occurring with different probabilities are assumed which results in significantly increase in size of the resulted optimization model as a function of the number of scenarios. Also, exact distribution of the uncertain data is needed to run a large number of simulations to capture the characteristics of these distributions, which is rarely satisfied in practice. On the other hand, robust optimization approach, in which the problem is solved against the worst instances that might arise by a min-max objective, has attracted much attentions

in the literature [126]. The degree of conservatism of the solution can be controlled via a parameter usually called the "budget of uncertainty", and the generated optimal solutions are robust within the upper and lower bounds of the confidence intervals. This method is appropriate for real-time applications, has less computational burden as compared to stochastic programming methods, and provides effective results for the purpose of optimal operation compared to Monte-Carlo simulations.

Consider the following general MILP model:

$$\begin{aligned} \min \quad & \mathbf{c}^T\mathbf{x} \\ \text{s.t.} \quad & \mathbf{A}\mathbf{x} \leq \mathbf{b} \\ & \mathbf{l} \leq \mathbf{x} \leq \mathbf{u} \\ & x_i \in \mathbb{Z}_k, \qquad i = 1, \cdots, k \end{aligned} \tag{2.6}$$

where uncertainty is assumed to affect only the objective function coefficients. This means each entry c_j, $j \in N$ takes values in $[c_j, c_j + d_j]$, where d_j represents the deviations from the nominal cost coefficient c_j. Let $J_0 = \{j | d_j > 0\}$. By introducing Γ_0, the "budget of uncertainty", that takes values in the interval $[0, |J_0|]$, the robust counterpart of problem (2.6) is as follows:

$$\begin{aligned} \min \quad & \mathbf{c}^T\mathbf{x} + \max_{\{S_0 | S_0 \subseteq J_0, |S_0| \leq \Gamma_0\}} \left\{ \sum_{j \in S_0} d_j |x_j| \right\} \\ \text{s.t.} \quad & \mathbf{A}\mathbf{x} \leq \mathbf{b} \\ & \mathbf{l} \leq \mathbf{x} \leq \mathbf{u} \\ & x_i \in \mathbb{Z}_k, \qquad i = 1, \cdots, k \end{aligned} \tag{2.7}$$

The parameter Γ_0 controls the level of robustness in the objective. If $\Gamma_0 = 0$, the model completely ignores the influence of the price uncertainty, while if $\Gamma_0 = J_0$, all possible price deviations are considered, which results in the most conservative solution.

It is proved in [126] that (2.7) has an equivalent RMILP formulation as follows:

$$\begin{aligned}
\min \quad & \mathbf{c}^T\mathbf{x} + z_0\Gamma_0 + \sum_{j\in J_0} p_j & & \\
\text{s.t.} \quad & \mathbf{A}\mathbf{x} \leq \mathbf{b} & & \\
& \mathbf{l} \leq \mathbf{x} \leq \mathbf{u} & & \\
& x_i \in \mathbb{Z}_k, & & i = 1, \cdots, k \\
& z_0 + p_j \geq d_j\, y_j & & \forall j \in J_0 \\
& z_0 \geq 0 & & \\
& p_j \geq 0 & & \\
& y_j \geq 0 & & \forall j \in J_0 \\
& -y_j \leq x_j \leq y_j & & \forall j
\end{aligned} \tag{2.8}$$

This formulation is obtained using duality properties and exact linear equivalent of the cost coefficient deviations constraints, where z_0 and p_0 are dual variables of the original problem used to take into account the bounds of cost coefficients and y_j is used to obtain linear expressions, as completely explained in [126].

2.4.5 Mathematical Programming Tools

In this research a variety of optimization problems are developed which need to be solved and studied, and therefore, an adequate mathematical programming language is needed. There are many solvers available which can deal with various types of optimization problems. In this research AMPL [127], a modeling language for mathematical programming, is used to implement the developed mathematical models of the energy hubs, and ILOG CPLEX [128], one of the most popular solvers for LP and MILP problems, is used to solve the developed MILP problems. CPLEX uses both the simplex and interior-point algorithms to solve LP problems, and the B&B algorithm to solve MILP problems. IPOPT [129], a popular solver based on interior point methods, is used to to solve the proposed NLP models.

Table 2.1: Summary of FRP tariffs in Ontario for 2009 [130].

Customers	Season	Electricity use	Price (cents/kWh)
Residential	Summer	Up to 600 kWh	5.7
		More than 600 kWh	6.6
	Winter	Up to 1000 kWh	5.7
		More than 1000 kWh	6.6
Non-residential	All seasons	Up to 750 kWh	5.7
		More than 750 kWh	6.6

2.5 Energy Pricing and Emissions

2.5.1 Electricity Pricing

Various dynamic pricing methods may be available to electricity customers in the residential sector. Fixed Rate Price (FRP), TOU, and RTP are three types of dynamic pricing currently in use in various utilities that are used in the current research. Additional charges to account for delivery, taxes, etc., are also considered in this thesis in the calculation of energy costs.

Fixed Rate Price

In the FRP there is a threshold that defines higher and lower electricity prices for customers. If the total electrical energy consumption per month is less than the threshold, then the customers pay the lower price as a flat rate; if it exceeds the threshold, they pay the higher price for each kilowatt hour. For example, in Ontario the threshold is currently set at 600 kWh per month in the summer and 1000 kWh per month in the winter for residential customers, and 750 kWh per month for non-residential customers. The difference in the threshold values recognizes that in the winter, Ontario's customers use more energy for lighting and indoor activities and that some houses use electric heating. Table 2.1 presents a summary of the FRP tariffs in Ontario [130]. These FRP tariffs, with some additional charges are used in this thesis to calculate electricity costs.

Table 2.2: Summary of the TOU pricing in Ontario for 2009 [130].

Day of the Week	Time	Time-of-Use	Price (cents/kWh)
Weekends & holidays	12:00 a.m. to 12:00 p.m.	Off-peak	4.2
Summer Weekdays	7:00 a.m. to 11:00 a.m.	Mid-peak	7.6
	11:00 a.m. to 5:00 p.m.	On-peak	9.1
	5:00 p.m. to 10:00 p.m.	Mid-peak	7.6
	10:00 p.m. to 7:00 a.m.	Off-peak	4.2
Winter Weekdays	7:00 a.m. to 11:00 a.m.	On-peak	9.3
	11:00 a.m. to 5:00 p.m.	Mid-peak	8
	5:00 p.m. to 8:00 p.m.	On-peak	9.3
	8:00 p.m. to 10:00 p.m.	Mid-peak	8
	10:00 p.m. to 7:00 a.m.	Off-peak	4.4

Time-of-Use

TOU pricing is the simplest form of dynamic pricing. The main objective of dynamic pricing programs is to encourage the reduction of energy consumption during peak-load hours. In TOU pricing, the electricity price per kWh varies for different times of the day. In Ontario, TOU pricing is currently based on three periods of energy use:

- On-peak, when demand for electricity is the highest.
- Mid-peak, when demand for electricity is moderate.
- Off-peak, when demand for electricity is the lowest.

The classification of On-peak, Mid-peak, and Off-peak periods vary by season and day of the week. Table 2.2 presents the TOU pricing for different periods in Ontario for 2009 [130]. TOU price is offered to customers equipped with smart meters.

Real Time Pricing

In this method of electricity pricing, the price varies continuously, directly reflecting the wholesale electricity market price and are posted hourly and/or day-ahead for pre-planning. This provides a direct link between the wholesale and retail energy markets and reflects

the changing supply/demand balance of the system to try to introduce customers price elasticity in the market. In Ontario the Hourly Ontario Electricity Price (HOEP) is the real-time price that applies only to large customers who participate in the wholesale electricity market [131]. The HOEP is used in this work for residential customers to study the effect of RTP pricing on the operation of residential energy hubs.

Peak Demand Charges

In addition to energy consumption costs, large electricity customers pay peak demand charges based on the maximum amount of power withdrawn during the billing period, usually averaged over 15-minute time periods and measured in kilowatts (kW). The demand charges during winter and summer in Ontario for 2009, respectively, \$7/month-kW and \$8/month-kW, are used in this thesis [132].

2.5.2 Natural Gas Pricing

Although there are highly competitive natural gas markets in North America, where market prices are determined by spot pricing and future contracts reflecting current and expected supply and demand conditions, natural gas rates for residential and commercial customers are usually FRP [133], [134]. These rates include transportation, storage and delivery charges beside the commodity charges. Since the focus of the current research is on the residential, commercial and agricultural sectors, FRPs including some additional charges are used in this thesis, with an equivalent price of 2.9 cents/kWh.

2.5.3 CO_2 Emissions

CO_2 emissions of the power system at each hour need to be forecasted in order to minimize carbon footprint of the customer. Coal and gas-fired generating units, which are the main sources of CO_2 emissions in the power sector, produce different amounts of CO_2. Therefore, power generation from coal and gas-fired generating units needs to be known in order to estimate the CO_2 emissions from the system.

Day-ahead Power Generation Forecast

The system operators do not typically provide power generation forecasts for power plants. Therefore, the power generation from coal and gas-fired generating units needs to be fore-

casted. Econometric time-series models are proposed in [135] to develop forecasts for power generation from coal and gas-fired generation units in Ontario. External inputs required by the forecasting model are as follows:

- A 24-hour ahead total system demand profile obtained from pre-dispatch data.
- Hourly total system demand for the past 14 days.
- Hourly cumulative generation from coal- and gas-fired units respectively, for the past 14 days.

Based on these, the following time-series forecasting model is used here to forecast the power generation from coal- and gas-fired power plants, separately:

$$\hat{Y}_{t,p} = \bar{Y}_{t,p} + B_t \left(\hat{X}_t - \bar{X}_t \right) \tag{2.9a}$$

$$\bar{X}_t = \frac{1}{n} \sum_{j=1}^{n} X_{j,t} \tag{2.9b}$$

$$\bar{Y}_{t,p} = \frac{1}{n} \sum_{j=1}^{n} Y_{j,t,p} \tag{2.9c}$$

$$B_t = \frac{\sum_{j=1}^{n} Y_{j,t} \left(X_{j,t} - X_{mean} \right)}{\sum_{j=1}^{n} \left(X_{j,t} - X_{mean} \right)^2} \tag{2.9d}$$

where

t	Index for hour of the day, $t \in \{1, \cdots, 24\}$,
j	Index for days, $j \in \{1, \cdots, 14\}$,
n	Number of observations corresponding to each hour i,
p	Index for coal or gas fired units,
$X_{j,t}$	Historical value of Ontario market demand at t^{th} hour of j^{th} day (MW),
$\hat{X}_t$	Day-ahead value of Ontario's market demand at t^{th} hour (MW),
$\bar{X}_t$	Mean of n demand observations corresponding to hour t (MW),
$\hat{Y}_{t,p}$	Forecasted value of generation from power plants (coal or gas) at t^{th} hour (MW),
$Y_{j,t,p}$	Historical value of power output from power plants (coal or gas) at t^{th} hour of j^{th} day (MW),
$\bar{Y}_{t,p}$	Mean of n generation output from coal/gas units at hour t (MW).

Day-ahead Emissions Profile

Separate rates of emissions for gas and coal fired units are used, and accordingly, the day-ahead emissions profile is calculated as follows:

$$em(t) = R_c \times P_c(t) + R_g \times P_g(t) \qquad \forall t \in \{1, \cdots, 24\} \tag{2.10}$$

where

$em(t)$	Forecasted CO_2 emissions at t^{th} hour in tonne/hr,
$P_c(t)$	Forecasted generation of coal-fired plants at t^{th} hour in MW,
$P_g(t)$	Forecasted generation of gas-fired plants at t^{th} hour in MW,
R_c	Rate of CO_2 emissions from coal-fired plants = 1.0201 tonne /MWh [136],
R_g	Rate of CO_2 emissions from gas-fired plants = 0.5148 tonne/MWh [136], [137].

The marginal cost of CO_2 emissions is calculated using the social cost of CO_2 emissions or marginal damage cost of climate change, as follows:

$$C_{em}(t) = \frac{em(t) \times scc}{\hat{X}(t)} \qquad \forall t \in \{1, \cdots, 24\} \tag{2.11}$$

where

$C_{em}(t)$	Marginal cost of CO_2 at hour t (cents/kWh),
scc	Social cost of carbon dioxide emissions ($100/tonne) [138],
$\hat{X}(t)$	Day-ahead forecast of electricity demand at hour t in kW.

This thesis adopts the above forecast model results [135] obtained for the Ontario system and the resulting emissions profile of Ontario as exogenous inputs to the research problems discussed and presented.

2.6 Summary

In this chapter, first a background review on DSM and DR programs, and their objectives, strategies, and approaches were presented. Then, the state-of-the-art in EMSs in residential, commercial, and agricultural sectors were discussed. A brief review of mathematical programming, including LP and MILP problems and their solution methods and tools, which are particularly relevant to this research, were presented next. Finally, information on energy pricing and calculation of CO_2 emission values were presented. The background material reviewed in this chapter form the basis for the development of appropriate models for optimal operation of energy hubs in the context of Smart Grids.

Chapter 3

Optimal Operation of Residential Energy Hubs

3.1 Introduction

This chapter presents and discusses the developed mathematical optimization model of residential energy hubs which can be readily incorporated into automated decision making technologies in Smart Grids. Mathematical models for major household demand, i.e., fridge, freezer, dishwasher, washer and dryer, stove, water heater, hot tub, and pool pumps, are formulated. Also, mathematical models of other components of a residential energy system including AC, heating, and lighting, are developed, and generic models for solar Photo-Voltaic (PV) panels and energy storage/generation devices are proposed. The developed mathematical models of these devices and components result in an MILP optimization model for the optimal operation scheduling of the residential energy hub. The optimization model objective is to minimize demand, total cost of electricity and gas, GHG emissions, and peak load over the scheduling horizon using information from the external environment (e.g., energy prices, weather forecasts), while properly taking into account end-user preferences and comfort levels. The proposed mathematical model can be solved efficiently in real time to optimally control major household demands and energy storage and production components. This mathematical model, in conjunction with a communication infrastructure and smart meters, as part of a Smart Grid, will allow optimal operation of residential energy hubs.

In Section 3.2 the modeling approach of the residential energy hubs is discussed. This is followed in Section 3.3 by the mathematical model of residential energy hubs, including

description and definition of the model identifiers, objective functions, and operational constraints associated with the components of the hub. Several case studies were conducted to examine the performance of the developed mathematical model for a realistic residential energy hub, of which the most relevant ones are presented in Section 3.4.

3.2 Modeling Approach

The first step in the mathematical modeling of a residential energy hub is to identify the components of the system, and define relations between these components in the hub. In a typical residential energy hub, three categories of components can be identified: energy consumption, energy storage, and energy production. Each of these components has its own specific behaviour, operational constraints, and parameter settings required for adequate operation. Recognizing the components (appliances) behaviour is very important in order to identify and define the decision variables and formulate the mathematical model constraints. In other words, the EHMS must know what kind of loads (appliances) are available in the energy hub in order to properly represent it in the model.

Major household appliances consume a large portion of a house total energy demand, and some of those can be scheduled without a major effect on customer comfort while reducing energy costs and emissions. Since residential customers have been used to flat rate prices, most household owners operate their devices without considering their effect on the external systems or CO_2 emissions. By taking advantage of smart meter developments under Smart Grid initiatives, introduction of TOU electricity pricing, raising environmental concerns, and other of Smart Grid technologies, it should be possible to positively affect the patterns of energy consumption in residential sector.

Currently, smart appliance controllers are available that allow the customer to enter daily, weekly, as well as seasonal schedules for various device operations. Also, the operation of appliances can be controlled in a house using home networking systems developed to enable remote appliance control [106, 108, 109, 110]. These systems usually comprise several dedicated controllers which communicate with a central appliance controller when plugged into any electric socket in the house, and allow On/Off control of appliances. The user can thus program different schedules and events and implement rule-based decision making within the central appliance controller. In this context, an intelligent decision-making core that would be an integral part of EMSs is proposed in this thesis to optimally operate residential sector energy hubs based on their mathematical model.

Figure 3.1 presents an overview of the proposed residential energy hub which includes

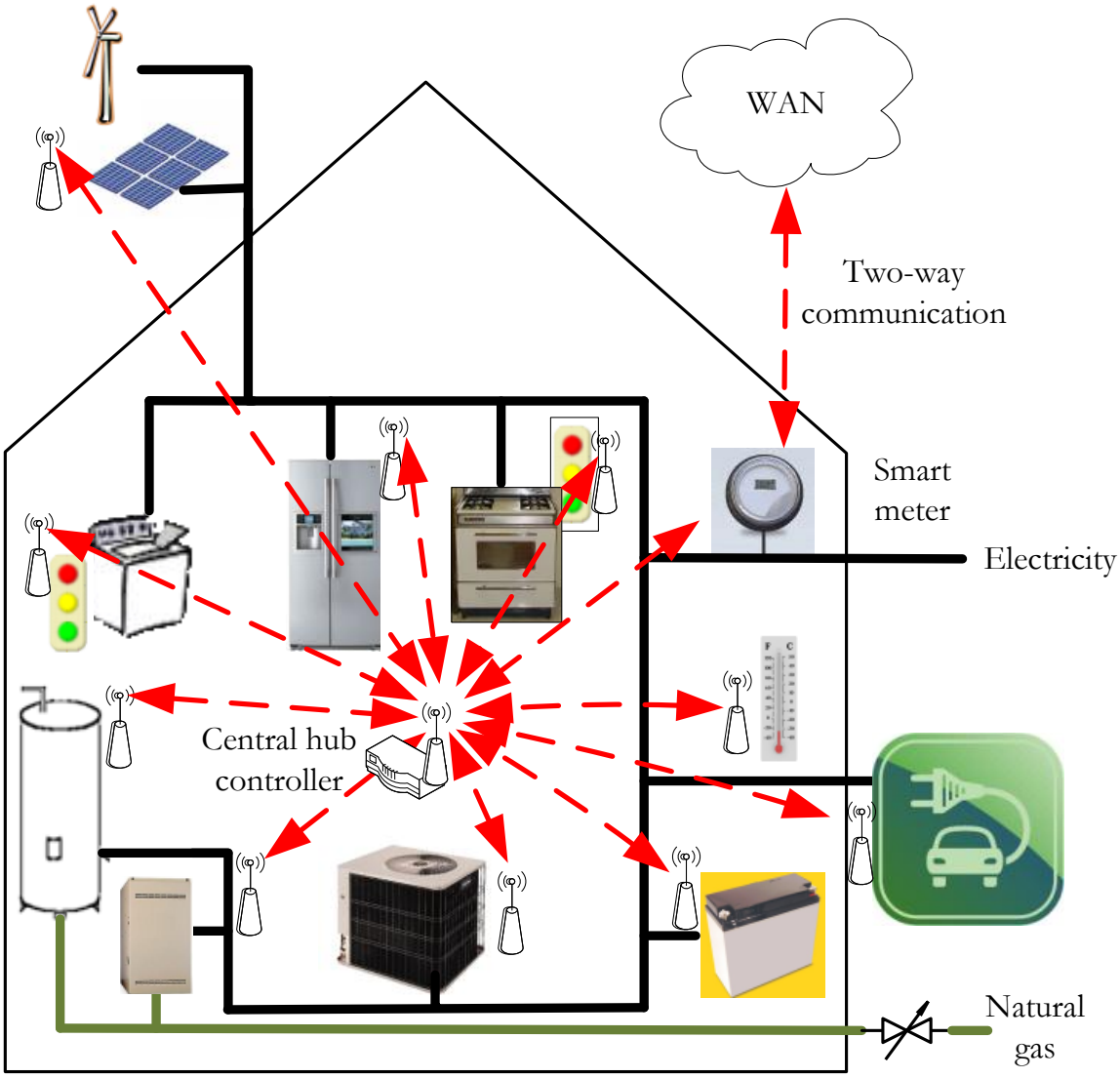

Figure 3.1: Configuration of the proposed residential energy hub.

various appliances, energy storage systems (e.g., batteries, EVs), energy production systems (e.g., solar photovoltaic, wind power), a smart meter and two-way communication links between these components. The proposed mathematical model and associated opti-

mization solver resides in the central hub controller.

A functional over-view of the central hub controller is presented in Figure 3.2. This controller uses the mathematical model of each component in the hub, parameter settings and external information as well as user preferences to generate the optimal operating decisions for all components in the energy hub over the scheduling horizon. The device database includes all the technical characteristics of the components (e.g., rated power, storage/production level). External information includes energy price information, weather forecast, solar radiation, and CO_2 emissions forecasts. Using this information, the optimization engine generates the optimal operating decisions for all components in the residential energy hub over the scheduling horizon.

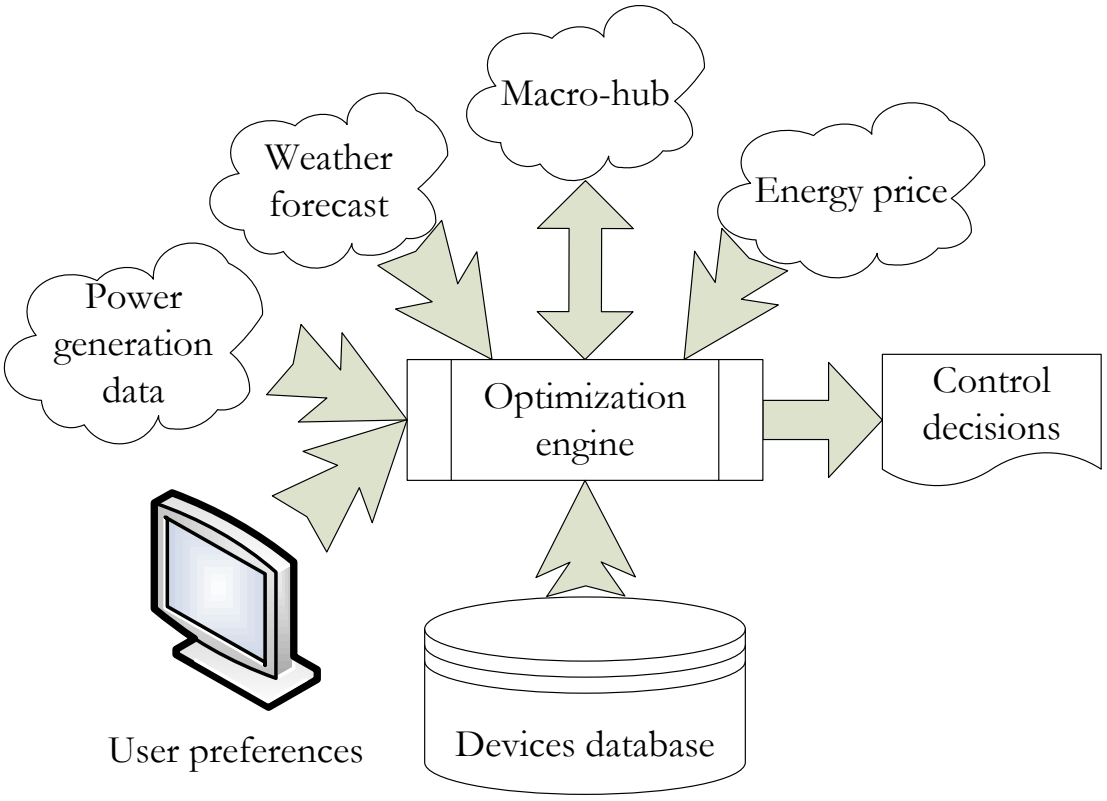

Figure 3.2: Functional overview of the central hub controller.

3.2.1 Customer Preferences

The operational models of the residential energy hub must give priority to customer's preferences, and be simple enough for successful implementation and easy interpretation of the results. The models should include normal behavior of the customer such as the desired room temperatures and the hours of operation of each device. Also, the maximum deviations from the nominal operation conditions that the customer is willing to accept for each device, such as maximum temperature deviations and the latest acceptable time to complete a task, should be incorporated.

3.2.2 Activity Level

In the residential sector, the occupancy of the house has a major effect on energy consumption patterns. Furthermore, energy consumption patterns differ in each house depending on the season, and the day such as weekdays and weekends. To consider the effect of household occupancy on energy consumption patterns, a new index termed as the *Activity Level* is proposed in this thesis for electrical appliances. This represents the hourly activity level of a house over the scheduling horizon.

To determine a reasonable value of the Activity Level of a residential energy hub, historical data of energy consumption provided by installed smart meters in each house can be used. Smart meters can provide a wealth of data, including energy consumed each hour or even in each fifteen minute interval. Therefore, the measured data of the previous weeks, months, and years can be used to predict the energy consumption on a particular day, and thus generate residential load profiles. For example, the authors in [139] propose the use of statistical methods to construct household load profiles on an hourly basis. Similarly, load models are developed using a linear regression and load patterns approach in [140], where the load profile is represented as the sum of daily-weekly components, outdoor temperature, and random variations. These load profiles can be modified to obtain the proposed Activity Level of a house on an hourly basis.

For example, Figure 3.3 shows an example of the Activity Level over a day for a single detached house; this is obtained from average hourly variations of energy consumption of the household on a summer day. In this figure, the Activity Level (y axis) is normalized with respect to the total energy consumption of the day, which is assumed to be 100%.

It should be noted that the Activity Level index has a different effect on each of the electrical appliances in the house. For example, the effect of the activity level on the fridge temperature is not the same as its effect on the room temperature. Thus, the effect of

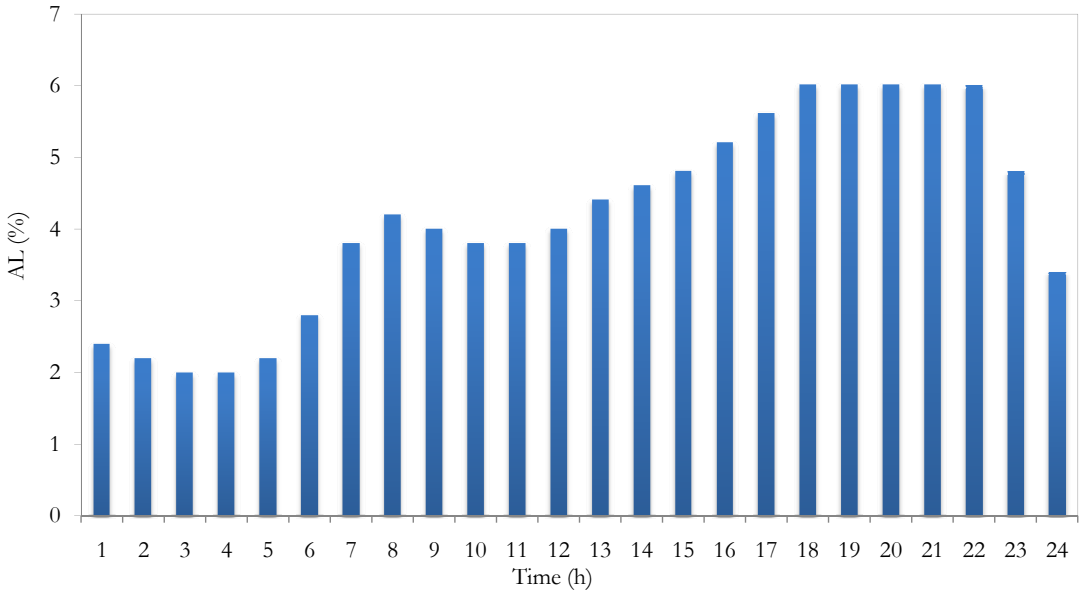

Figure 3.3: The activity level of a residential energy hub.

household activity on the fridge's energy consumption is modeled using an AL_{fr} index. Since, the minimal value of total energy consumption on a day usually occurs during time periods of inactivity inside the house, any load that is less than this base load will not contribute to the fridge activity. In the present work, it is assumed that the base load is 50% of the average hourly household energy consumption, resulting in the AL_{fr} index shown in Figure 3.4. It should be noted that the hot water demand on the water heater is modeled using a different activity index, as explained in Section 3.3.2.

3.2.3 Scheduling horizon

The scheduling horizon in the optimization models can vary from a few hours to days, depending on the type of energy hub and activities which take place in the hub. For example, in a residential energy hub the scheduling horizon could be set to 24 hours, with time intervals ranging from a few minutes to 1 hour. Without any loss of generality, in the present thesis, a 24 hour scheduling horizon with time intervals of 15 minutes is used, with the exception of the fridge for which a 7.5-minute interval used due to its thermodynamic characteristics.

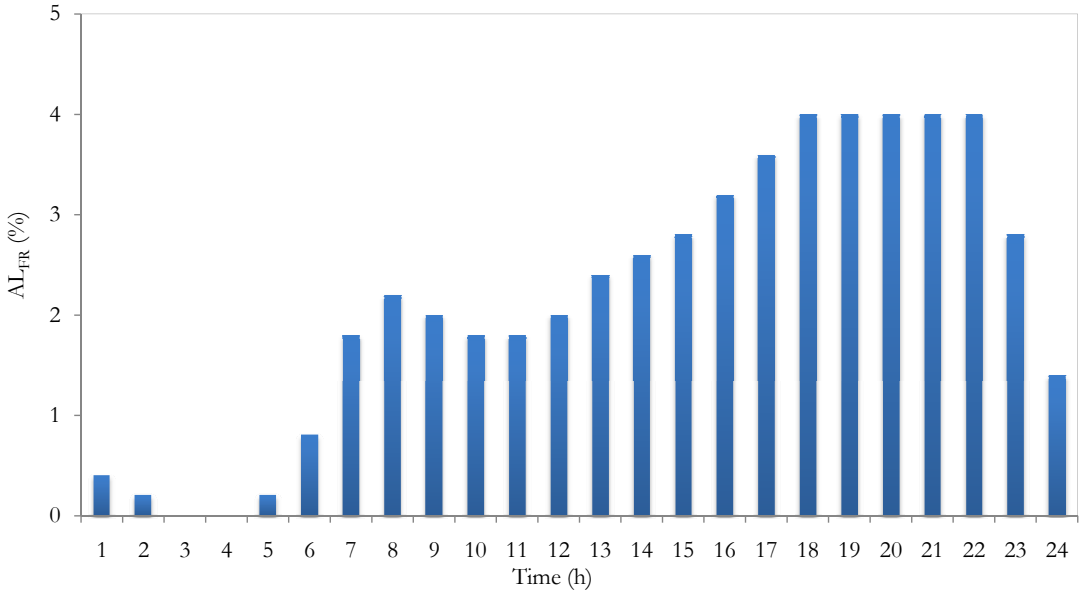

Figure 3.4: The activity level of the fridge obtained from Figure 3.3.

3.2.4 Other External Inputs

Outdoor weather conditions have major a impact on energy consumption of heating and cooling systems of a household. Heat transfer through walls and solar radiations are examples of the ways that outdoor conditions can affect indoor temperature. Nowadays, accurate weather forecasts are available every few hours for various time horizons. These forecasts are employed here to generate the optimal schedules.

3.3 Mathematical Model of Residential Energy Hubs

In this section, all the sets, variables, and parameters of the residential energy hub model are described first. Then, the objective function of the model and operational constraints associated with the components of the hub are explained in detail.

Table 3.1 summarizes the common indices, sets, variables, and parameters of the mathematical model. The first column in Table 3.1 indicates the corresponding notation, and the second column provides a brief description.

Table 3.1: Description and definition of the residential energy hub model identifiers.

Sets	**Description**
A	Set of devices; $A = \{ac, esd, dry, dw, fr, ht, il, pv, pmp, stv, twh, wh, wr\}$
T	Set of indices in scheduling horizon; $T = \{1 \dots 96\}$
T_i	$T_i \subseteq T$ is the set of periods in which device i may operate; $T_i = \{t \in T : et_i \leq t \leq lt_i\}$
Indices	**Description**
i	Index of devices (Appliances)
t	Index of time interval
z	Index of zones
Subscripts	**Description**
ac	Air conditioner
chd	Charger
dch	Discharge
esd	Energy storage device
dry	Dryer
dw	Dishwasher
fr	Fridge
in	Inside house
ht	Heating
li	Lighting
pv	Solar PV panel
pmp	Pool pump
stv	Stove

Continued on next page

Table 3.1 – continued from previous page

Subscripts	**Description**
twh	Tub Water Heater
wh	Water Heater
wr	Washer
Variables	**Description**
Dmd	Non-negative variable representing peak demand of the energy hub
$D_i(t)$	Binary variable denoting shut down of device i at time t: $D_i(t) = \begin{cases} 1 & \text{shutdown of device } i \text{ at time } t \\ 0 & \text{otherwise} \end{cases}$
$ESL_i(t)$	Energy storage level of device i at t
$L_z(t)$	Integer variable denoting illumination level produced by the lighting system of a given zone z in the house at time t
$S_i(t)$	State of device i at time t, binary; On/Off
$\theta_{in}(t)$	Inside temperature of the house at time t
$\theta_{fr}(t)$	Inside temperature of the fridge at time t
$\theta_{wh}(t)$	Water temperature at time t
$U_i(t)$	Binary variable denoting start up of device i at time t: $U_i(t) = \begin{cases} 1 & \text{startup of device } i \text{ at time } t \\ 0 & \text{otherwise} \end{cases}$
Parameters	**Description**
$AL(t)$	Activity Level at time t
$AL_{fr}(t)$	Activity Level of fridge at time t
α_i	Cooling/Warming effect of an On state of device i on corresponding variable (°C/interval)
β_i	Cooling/Warming effect of an Off state of device i on corresponding variable (°C /interval)
c_{dc}	Peak demand charges
$c_{ed}(t)$	Price of electricity demand at time t

Continued on next page

Table 3.1 – continued from previous page

Parameters	Description
$c_{es}(t)$	Price of electricity supply at time t
$c_{gd}(t)$	Price of gas demand at time t
$C_{em}(t)$	Marginal cost of CO_2 at hour t (cents/kWh)
$chd_i(t)$	Charged energy into device i at time interval t
dch_i	Discharged energy from device i during one time interval
$\Delta_{wr,dry}$	Maximum allowed time gap between operation of washer and dryer
$em(t)$	Forecasted CO_2 emissions at t^{th} hour in tonne/hr
et_i	Earliest operation time of device i
η_{esd}	Self-discharge rate of the esd and battery.
γ_i	Cooling/Warming effect of activity level on corresponding variable of device i ($^\circ$C/unit of activity level)
$HWU(t)$	Average hourly Hot Water Usage at time t
$il_z^{min}(t)$	Minimum required zonal illumination at time t
$il_z^{out}(t)$	Outdoor illumination level of a given zone in the house at time t
J	Objective function
lt_i	Latest operation time of device i
M	Large positive number
mu_i	Minimum Up time of device i)
md_i	Minimum Down time of device i
mso_i	Maximum Successive Operation time of device i
n	Number of observations corresponding to each hour i
$P^{max}(t)$	Allowed peak load of the energy hub at time t
P_i	Rated power of device i
$P_c(t)$	Forecasted generation of coal-fired plants at t^{th} hour in MW
$P_g(t)$	Forecasted generation of gas-fired plants at t^{th} hour in MW
Q_i	Heat rate of of device i
ρ_i	Effect of inside and outside temperature difference on the inside temperature corresponding to device i

Continued on next page

Table 3.1 – continued from previous page

Parameters	Description
R_c, R_g	Rate of CO_2 emissions from coal/gas-fired plants, respectively; 1.0201/0.5148 tonne/MWh [136]
rot_i	Required Operation Time of device i
scc	Social cost of carbon dioxide emissions \$100/tonne [138]
τ	Time interval duration
$\theta_{out}(t)$	Forecasted outdoor temperature at time interval t

The proposed general form of the optimization model for the residential energy hub is as follows:

$$\min \quad J = \text{Objective function} \tag{3.1a}$$

$$\text{s.t.} \quad \sum_{i \in A} P_i \, S_i(t) \leq P^{max}(t) \qquad \forall t \in T \tag{3.1b}$$

$$\text{Device } i \text{ operational constraints} \qquad \forall i \in A \tag{3.1c}$$

This model comprises three main parts: objective function, constraints on peak demand at each time interval, and operational constraints of the hub components. Constraint (3.1b) sets a cap on peak demand of the energy hub at each time interval, ensuring that maximum power consumption at a given time do not exceed a specified value. This peak power limit can be set (for example, as an external input from Macro-hub controller) in such a way that the utility can take advantage of peak-load reduction from each energy hub during peak-load hours. During the off-peak and mid-peak hours of the power system, this constraint could be relaxed. The objective function and devices operational constraints are explained in the next sub-sections.

3.3.1 Objective Functions

Depending on end-user choice, different objective functions can be adopted to solve the optimization problem. Thus, minimization of the customer's total energy costs, total energy consumption, peak load, emissions, and/or any combination of these over the scheduling horizon are considered in this chapter as possible objective functions for the optimization model.

Energy Costs

The customer's total energy costs over the scheduling horizon is given by:

$$J_1 = \sum_{t \in T} \left[\sum_{\substack{i \in A \\ i \notin \{li,esd,pv\}}} c_{ed}(t)\, P_i\, S_i(t) + \sum_{z \in li} c_{ed}(t)\, P_{li_z}\, L_z(t) - \sum_{i \in \{esd,pv\}} c_{es}(t)\, P_i\, S_i(t) + \sum_{i \in \{ht,wh\}} c_{gd}(t)\, Q_i\, S_i(t) \right] \tag{3.2}$$

The first two terms in this equation represent the cost of electricity consumption, the third term represents the revenue from selling stored/produced electricity to the power grid, and the last term represents the cost of gas consumption.

Energy Consumption

The total energy consumption of the hub over the scheduling horizon is given by:

$$J_2 = \sum_{t \in T} \left[\sum_{\substack{i \in A \\ i \notin \{li,esd,pv\}}} P_i\, S_i(t) + \sum_{z \in li} P_{li_z}\, L_z(t) - \sum_{i \in \{esd,pv\}} P_i\, S_i(t) + \sum_{i \in \{ht,wh\}} Q_i\, S_i(t) \right] \tag{3.3}$$

In this equation, the energy consumption of electrical devices are represented by the first two terms, and the electrical energy injected to the grid from stored/produced electricity is given by the third term; the last term represents the gas consumption. This objective allows to minimize operational hours of all devices and to maximize the operation of energy production/storage devices.

CO_2 Emissions Cost

The objective function is formulated using the hourly marginal cost of CO_2 as follows:

$$J_3 = \sum_{t\in T} \left[\sum_{\substack{i\in A \\ i\notin\{li,esd,pv\}}} C_{em}(t)\, P_i\, S_i(t) + \sum_{z\in li} C_{em}(t) P_{li_z}\, L_z(t) + \sum_{i\in\{ht,wh\}} scc\, R_g Q_i S_i(t) - \sum_{i\in\{esd,pv\}} C_{em}(t)\, P_i\, S_i(t) \right] \tag{3.4}$$

The first two terms in this equation represent the carbon footprint of the customer from the grid electricity usage, the third term depicts CO_2 emissions from gas consumption within the house, and the last term corresponds to the CO_2 reduction from injecting emission free electricity (from PV arrays) to the grid.

Peak Load

An objective function for minimization of peak demand charges can be adopted to reduce the peak load of the energy hub as follows:

$$J_4 = Dmd \cdot c_{dc} \tag{3.5}$$

where Dmd is a non-negative auxiliary variable used along with the following constraint to represent the peak demand of the energy hub:

$$Dmd \geq \sum_{\substack{i\in A \\ i\notin\{li,esd,pv\}}} P_i S_i(t) + \sum_{z\in li} P_{li_z} L_z(t) \qquad \forall t \in T \tag{3.6}$$

Since the assumed peak demand charge c_{dc} is a constant value, peak load of the energy hub is also minimized by minimization of J_4. which represents the peak demand charges.

Multi-Objective Optimization

In addition to the aforementioned individual objective functions, any combinations of these can also be used as an objective. In this work, the individual objective functions J_1, J_2, J_3, and J_4 are assigned weights to build an following objective function that simultaneously minimizes all of them:

$$J = \omega_1 J_1 + \omega_2 J_2 + \omega_3 J_3 + \omega_4 J_4 \tag{3.7}$$

where ω_1, ω_2, ω_3, and ω_4 are the weights attached to the customers' total energy cost, total energy consumption, total emissions cost, and peak demand charges, respectively.

3.3.2 Devices' Operational Constraints

Mathematical models of major household appliances, i.e., air-conditioning, heating system, water heater, pool pumps, fridge, dishwasher, washer and dryer, stove, energy storage/generation device, and PV solar array are presented next. These models represent the operational constraints of the residential energy hub devices and components.

Fridge

In order to model the operational aspects of a fridge for scheduling purposes, both the variable under control and operational constraints of the fridge should be considered. Thus, the model seeks to maintain the fridge temperature within a specified range, while taking into account technical aspects of the fridge operation as well as the customer preferences. The operational constraints of the fridge are as follows ($i = fr$):

$$S_i(t) = \begin{cases} 0 \text{ or } 1 & \text{if } t \in T_i \\ 0 & \text{if } t \notin T_i \end{cases} \tag{3.8a}$$

$$S_i(t=1) = \begin{cases} 1 & \text{if } \theta_{fr}(t=0) > \theta_{fr}^{max} \\ 0 & \text{if } \theta_{fr}(t=0) < \theta_{fr}^{min} \end{cases} \tag{3.8b}$$

$$\theta_{fr}^{min} \leq \theta_{fr}(t) \leq \theta_{fr}^{max} \qquad \forall t \in T_i \tag{3.8c}$$

$$\theta_{fr}(t) = \theta_{fr}(t-1) + \tau \left[\beta_{fr}\ AL_{fr}(t) - \alpha_{fr}\ S_i(t) + \gamma_{fr}\right] \qquad \forall t \in T \tag{3.8d}$$

The time period over which the fridge can be in operation is specified by (3.8a), where the customer defines the *et* and the *lt* of the fridge. Equation (3.8b) ensures that if the fridge temperature at $t = 0$ is more than the upper limit, as specified by the customer, the fridge state is On in the first time interval. Constraint (3.8c) ensures that the fridge temperature is within the customer's preferred range.

Equation (3.8d) relates the temperature of the fridge at time t to the temperature of the fridge at time $t-1$, the activity level of the fridge at time t, On/Off state of the fridge at time t, and its heat losses. The effect of the activity level on the fridge temperature is modeled using β_{fr}, so that when the household activity level increases there is more cooling demand on the fridge; this index is a measure of how many times the fridge door is opened and closed during a time interval, which affects the inside temperature in the fridge. The effect of the On state on fridge temperature reduction is represented by α_{fr}, and the warming effect of the Off state of the fridge is modeled by γ_{fr}. The latter represents the thermal leakage because of the temperature difference between inside the fridge and

the room. The parameters α_{fr}, β_{fr}, and γ_{fr} can be measured or estimated from simple performance tests as discussed in [141].

The above model, with different coefficients and parameter settings, can also be used to model a freezer in a household.

Air Conditioning and Heating

In addition to residential thermal loss, activity level of household, ambient temperature, and the maximum temperature deviation that the customer is willing to tolerate are included in modeling of AC and heating systems of a house. Operational constraints developed for modeling the heating system in a house are similar to the operational constraints of the AC. Therefore, the AC and heating system constraints are presented using a common set of equations, as follows ($i = \{ac, ht\}$):

$$S_i(t) = \begin{cases} 0 \text{ or } 1 & \text{if } t \in T_i, i \in \{ac, ht\} \\ 0 & \text{if } t \notin T_i, i \in \{ac, ht\} \end{cases} \tag{3.9a}$$

$$S_i(t=1) = \begin{cases} 1 & \text{if } \theta_{in}(t=0) > \theta_{in}^{max}, i = ac \\ 0 & \text{if } \theta_{in}(t=0) < \theta_{in}^{min}, i = ac \end{cases} \tag{3.9b}$$

$$S_i(t=1) = \begin{cases} 1 & \text{if } \theta_{in}(t=0) < \theta_{in}^{min}, i = ht \\ 0 & \text{if } \theta_{in}(t=0) > \theta_{in}^{max}, i = ht \end{cases} \tag{3.9c}$$

$$\theta_{in}^{min}(t) \leq \theta_{in}(t) \leq \theta_{in}^{max}(t) \qquad \forall t \in T_i, i \in \{ac, ht\} \tag{3.9d}$$

$$S_{ac}(t) + S_{ht}(t) \leq 1 \qquad \forall t \in T_i \tag{3.9e}$$

$$\theta_{in}(t) = \theta_{in}(t-1) + \tau \left[\beta_{ac}\ AL(t) - \alpha_{ac} S_i(t) + \rho_{ac}(\theta_{out}(t) - \theta_{in}(t))\right] \qquad \forall t \in T, i = ac \tag{3.9f}$$

$$\theta_{in}(t) = \theta_{in}(t-1) + \tau \left[\beta_{ht}\ AL(t) + \alpha_{ht} S_i(t) - \rho_{ht}(\theta_{in}(t) - \theta_{out}(t))\right] \qquad \forall t \in T, i = ht \tag{3.9g}$$

$$U_i(t) - D_i(t) = S_i(t) - S_i(t-1) \qquad \forall t \in T_i, i \in \{ac, ht\} \tag{3.9h}$$

$$U_i(t) + D_i(t) \leq 1 \qquad \forall t \in T_i, i \in ac, ht \tag{3.9i}$$

$$\sum_{k=t}^{t+mu_i} S_i(k) \geq mu_i - M(1 - U_i(t)) \qquad \forall t \in T_i, i \in \{ac, ht\} \tag{3.9j}$$

$$\sum_{k=t}^{t+md_i-1} S_i(k) \leq M(1 - D_i(t)) \qquad \forall t \in T_i, i \in \{ac, ht\} \tag{3.9k}$$

In this operational model, the time period over which the AC or the heating system can be in operation is specified by (3.9a), which is specified by the customer's et_i and lt_i settings. Equation (3.9b) ensures that if the indoor temperature at $t = 0$ is more than the upper limit, as specified by the customer, the AC state is On in the first time interval, and (3.9c) ensures that if the indoor temperature at $t = 0$ is less than the customer defined lower limit, the heating system state is On in the first time interval.

Constraint (3.9d) is included to maintain the indoor temperature within the customer preferred range, and (3.9e) ensures that the heating and AC do not operate simultaneously. Equations (3.9f) and (3.9g) represent the dynamics of indoor temperature for the AC and the heating system, respectively. These equations state that the indoor temperature at time t is a function of the indoor temperature at time $t-1$, household activity level at time t, On/Off state of the AC (heating system) at time t, and the outdoor and indoor temperature difference. The cooling (warming) effect of an On state of the AC (heating system) on indoor temperature is represented by α_{ac} (α_{ht}). The effect of the activity level on indoor temperature increase is modeled by β_{ac} (β_{ht}), and ρ_{ac} (ρ_{ht}) represents the effect of outdoor and indoor temperature differences on indoor temperature. Minimum up-time and minimum down-time requirements of the AC and the heating system operation are expressed by the linear set of constraints (3.9h)-(3.9k). This model captures the normal temperature and the maximum temperature deviation that the customer is willing to accept. From a technical point of view, residential thermal losses are modeled, and minimum up-time and minimum down-time specifications of the AC are considered to prevent frequent On/Off switching.

Water Heater

An average hourly hot water usage pattern can be considered for each individual house. In [142] a detailed model of residential hot water usage pattern in individual households is presented. The Building Energy Efficiency Standards of PG&E recommend an hourly schedule for average daily hot water usage of residential customers [143], where it is observed that there are significant variations in hot water consumption patterns between weekdays and weekends, recommending that these be respected in the schedules. Thus, this issue is considered in the present work in the development of models for water heaters. The procedure to calculate the hot water usage is explained in detail in [143]. Fig. 3.5 shows the average daily hot water usage patterns during weekdays and weekends as reported in [143]. There is a larger and earlier spike on weekdays' consumption patterns, whereas the spike occurs later and is significantly flatter on weekends.

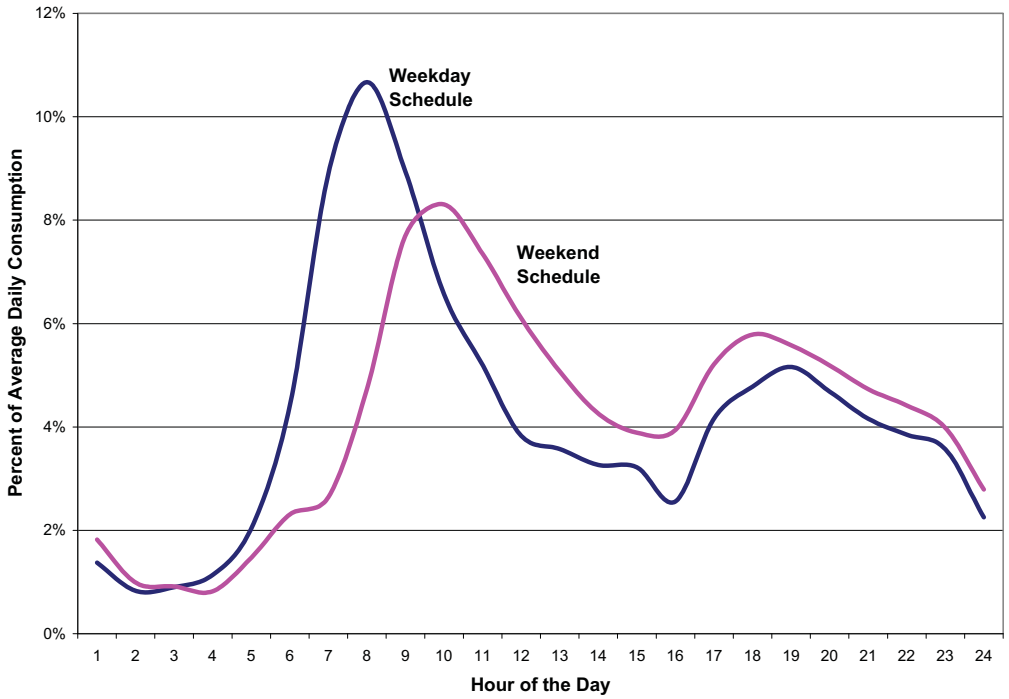

Figure 3.5: Average hourly hot water usage of an individual household [143].

The operational constraints of the water heater are represented by ($i = wh$):

$$S_i(t) = \begin{cases} 0 \text{ or } 1 & \text{if } t \in T_i, i = wh \\ 0 & \text{if } t \notin T_i, i = wh \end{cases} \tag{3.10a}$$

$$S_i(t=1) = \begin{cases} 1 & \text{if } \theta_{wh}(t=0) < \theta_{wh}^{min} \\ 0 & \text{if } \theta_{wh}(t=0) > \theta_{wh}^{max} \end{cases} \tag{3.10b}$$

$$\theta_{wh}^{min} \leq \theta_{wh}(t) \leq \theta_{wh}^{max} \qquad \forall t \in T_i \tag{3.10c}$$

$$\theta_{wh}(t) = \theta_{wh}(t-1) + \tau \left[\alpha_{wh} S_i(t) - \beta_{wh} HWU(t) - \gamma_{wh}\right] \qquad \forall t \in T \tag{3.10d}$$

Constraints (3.10a) to (3.10c) are similar to those of the fridge and AC model. Constraint (3.10d) states that water heater temperature at a time interval t is a function of the water temperature at the previous time interval, the average hot water usage, and the On/Off state of the water heater at time interval t. This model can be used for both electric and gas water heaters by slightly modifying the objective functions of the model.

Hot Tub Water Heater

The operational constraints of the water heater can also be used for a hot tub water heater. The only difference between these models is in their parameter settings such as average hot water usage, temperature settings, operational time, and associated coefficients that may have different values.

Dishwasher

Dishwasher, cloth washer, and dryer have a large peak load and consume considerable energy in a short time, therefore, the model proposed here are mainly based on shifting the operation of these appliances considering their operational constraints. The proposed operational model for the dishwasher is as follows ($i = dw$):

$$S_i(t) = \begin{cases} 0 \text{ or } 1 & \text{if } t \in T_i \\ 0 & \text{if } t \notin T_i \end{cases} \tag{3.11a}$$

$$U_i(t) - D_i(t) = S_i(t) - S_i(t-1) \qquad \forall t \in T_i \tag{3.11b}$$

$$U_i(t) + D_i(t) \leq 1 \qquad \forall t \in T_i \tag{3.11c}$$

$$\sum_{t \in T_i} S_i(k) = rot_i \qquad \forall t \in T_i \tag{3.11d}$$

$$\sum_{k=t}^{t+mso_i} S_i(k) \leq mso_i + M(1 - U_i(t)) \qquad \forall t \in T_i \tag{3.11e}$$

$$\sum_{k=t-mu+1}^{t} U_i(t) \leq S_i(t) \qquad \forall t \in [et_i + mu_i + 1, lt_i] \tag{3.11f}$$

$$\sum_{k=t-md+1}^{t} D_i(t) \leq 1 - S_i(t) \qquad \forall t \in [et_i + md_i + 1, lt_i] \tag{3.11g}$$

In this model, in addition to the time period over which the dishwasher can be in operation, which is specified by the customer's et and lt settings, additional constraints on the required operation time, maximum successive operation time, minimum up time, and minimum down time of the dishwasher are specified by the end-user, and modeled by (3.11d) to (3.11g), respectively.

Washer and Dryer

As mentioned, the operational models for washer and dryer are similar to the model of the dishwasher, and can be represented as follows ($i = \{wr, dry\}$):

$$S_i(t) = \begin{cases} 0 \text{ or } 1 & \text{if } t \in T_i \\ 0 & \text{if } t \notin T_i \end{cases} \tag{3.12a}$$

$$U_i(t) - D_i(t) = S_i(t) - S_i(t-1) \qquad \forall t \in T_i, i \in \{wr, dry\} \tag{3.12b}$$

$$U_i(t) + D_i(t) \leq 1 \qquad \forall t \in T_i, i \in \{wr, dry\} \tag{3.12c}$$

$$\sum_{t \in T_i} S_i(k) = rot_i \qquad \forall t \in T_i, i \in \{wr, dry\} \tag{3.12d}$$

$$\sum_{k=t}^{t+mso_i} S_i(k) \leq mso_i + M(1 - U_i(t)) \qquad \forall t \in [et_i, lt_i - mso_i], i \in \{wr, dry\} \tag{3.12e}$$

$$\sum_{k=t-mu+1}^{t} U_i(t) \leq S_i(t) \qquad \forall t \in [et_i + mu_i + 1, lt_i], i \in \{wr, dry\} \tag{3.12f}$$

$$\sum_{k=t-md+1}^{t} D_i(t) \leq 1 - S_i(t) \qquad \forall t \in [et_i + md_i + 1, lt_i], i \in \{wr, dry\} \tag{3.12g}$$

Constraints (3.11b) to (3.11g) are used to introduce the required operation time, maximum successive operation time, minimum up time, and minimum down time of the washer and dryer, as specified by the end-user.

The dryer operates usually after the washer completes its operation, but a large time gap between the operation of the two appliances is not typically acceptable. For example, customers most probably would not accept an operation schedule that runs the washer in the morning and the dryer in the afternoon, 12 hours later. Therefore, if the customer wants to coordinate the operation of the washer and the dryer, the following set of constraints needs to be considered:

$$U_{dry}(t) \leq \sum_{k=t-\Delta_{wr,dry}}^{t-mut_{wr}} U_{wr}(t-k) \qquad \forall t \in [et_i + \Delta_{wr,dry}, lt_{wr} - mut_{wr}] \tag{3.13a}$$

$$S_{dry}(t) + S_{wr}(t) \leq 1 \qquad \forall t \in T \tag{3.13b}$$

$$\sum_{t \in T_{dry}} U_{dry}(t) = \sum_{t \in T_{wr}} U_{wr}(t) \tag{3.13c}$$

Constraints (3.13a) to (3.13c) ensure that the dryer is scheduled after the washer without exceeding the maximum allowed time gap Δ_{wrdry}, within the scheduling horizon.

Stove

The operation of the stove depends on the household habits and hence direct control of the stove in not reasonable. Therefore, it is proposed to advise the customer on the "preferred" operation times of the stove. The proposed operational model of the stove is as follows ($i = stv$):

$$S_i(t) = \begin{cases} 0 \text{ or } 1 & \text{if } t \in T_i \\ 0 & \text{if } t \notin T_i \end{cases} \tag{3.14a}$$

$$U_i(t) \geq S_i(t) - S_i(t-1) \qquad \forall t \in T_i \tag{3.14b}$$

$$\sum_{t \in T_i} S_i(k) = rot_i \qquad \forall t \in T_i \tag{3.14c}$$

$$\sum_{k=t-mu+1}^{t} U_i(t) \leq S_i(t) \qquad \forall t \in [et_i + mu_i + 1, lt_i] \tag{3.14d}$$

$$\sum_{k=t}^{t+mso_i} S_i(k) \leq mso_i + M(1 - U_i(t)) \qquad \forall t \in T_i \tag{3.14e}$$

Here, the required operation time, minimum up time, and maximum successive operation time of the stove are parameter settings specified by the end-user, and are modeled by (3.14c), (3.14d) and (3.14e), respectively. For devices such as stove, dishwasher, washer, and dryer, if the end-user defines several operation windows, the operation of each device in each window can be modeled using a virtual device in the optimization model. For example, one might have to consider three virtual stoves in the optimization model to properly represent the customer defined operational windows, let's say for morning, afternoon, and overnight time periods. The optimal schedules of these virtual devices are then combined and reported to the end-user as operational schedule of a single device.

Pool pump

Pool pumps are used to maintain the quality of water in swimming pools by circulating the water through the filtering and chemical treatment systems. Therefore, by operating the pool pump for particular hours a day, the pumping system keeps the water relatively clean, and free of bacteria. The operational model of the pool pump is as follows ($i = pmp$):

$$S_i(t) = \begin{cases} 0 \text{ or } 1 & \text{if } t \in T_i \\ 0 & \text{if } t \notin T_i \end{cases} \tag{3.15a}$$

$$\sum_{t \in T_i} S_i(k) = rot_i \qquad \forall t \in T_i \qquad (3.15b)$$

$$U_i(t) \geq S_i(t) - S_i(t-1) \qquad \forall t \in T_i \qquad (3.15c)$$

$$\sum_{k=t-mu+1}^{t} U_i(t) \leq S_i(t) \qquad \forall t \in [et_i + mu_i + 1, lt_i] \qquad (3.15d)$$

$$\sum_{k=t-md+1}^{t} U_i(t) \leq 1 - S_i(t - md_i) \qquad \forall t \in [et_i + md_i + 1, lt_i] \qquad (3.15e)$$

$$\sum_{k=t}^{t+mso_i} S_i(k) \leq mso_i + M(1 - U_i(t)) \qquad \forall t \in T_i \qquad (3.15f)$$

Constraint (3.15b) ensures that the pool pump operates for the required time over the scheduling horizon; (3.15d) and (3.15e) model the minimum up-time and down-time requirements of the pool pump. To have an effective water circulation, it is important to distribute the water circulation periods within the scheduling horizon; therefore, (3.15f) ensures that the maximum number of successive operation time intervals of the pool pump is not more than a pre-set value.

Energy Storage Device

A modern household is expected to be equipped with some form of Energy Storage/production Device (ESD), such as batteries and EVs. To develop the model of the ESD for a residential hub, it is assumed that the amount of energy charged into the ESD at each time interval is known. The generic model of the ESD is given by ($i = esd$):

$$\begin{aligned} ESL_{esd}(t) = (1 - \eta_{esd}) ESL_{esd}(t-1) \\ + \tau \left[chd_{esd}(t) - S_i(t)\ dch_{esd} \right] \end{aligned} \qquad \forall t \in T \qquad (3.16a)$$

$$ESL_{esd}^{min} \leq ESL_{esd}(t) \leq ESL_{esd}^{max} \qquad \forall t \in T_i \qquad (3.16b)$$

$$U_i(t) \geq S_i(t) - S_i(t-1) \qquad \forall t \in T_i \qquad (3.16c)$$

$$\sum_{k=t-mu+1}^{t} U_i(t) \leq S_i(t) \qquad \forall t \in [et_i + mu_i + 1, lt_i] \qquad (3.16d)$$

$$\sum_{k=t-md+1}^{t} D_i(t) \leq 1 - S_i(t - md_i) \qquad \forall t \in [et_i + md_i + 1, lt_i] \qquad (3.16e)$$

where η_{esd} represents self-discharge rate of the ESD in percentage. Constraint (3.16a) relates the energy storage level of the ESD at time interval t to that at time $t-1$, self-discharge rate of the ESD, and the energy charge and discharge at time interval t. Constraint (3.16b) ensures that the energy storage level is never less than a specified minimum value. The minimum up-time and down-time requirements of the ESD are modeled by (3.16c)-(3.16e).

PV array

The solar PV array model presented and iscussed here is based on the model proposed in [141]. Figure 3.6 shows one possible way to connect a domestic PV electric power system to the grid. The DC/DC converter can be in two operational modes: the converter mode to charge the battery with a limited power as recommended by the battery manufacturer, and the inverter mode to discharge the stored energy back to the system. The discharge power rating is determined by the DC/DC converter power rating. The AC power generated by the DC/AC inverter can be consumed by the house appliances or injected to the utility grid in case of low electricity demand in the house.

The mathematical model of a PV system is modeled as follows ($i = pv$):

$$S_i(t) = \begin{cases} 0 \text{ or } 1 & \text{if } t \in T_i \\ 0 & \text{if } t \notin T_i \end{cases} \tag{3.17a}$$

$$chd_{pv}(t) = \begin{cases} P_{chd} & \text{if } P_{pv}(t) \geq P_{chd} \\ P_{pv} & \text{if } P_{pv} \leq P_{chd} \end{cases} \tag{3.17b}$$

$$\begin{aligned} &ESL_{pv}(t) = (1 - \eta_{pv}) ESL_{pv}(t-1) \\ &+ \tau \left[S_{pv,chd}(t) chd_{pv}(t) - S_{pv,dch}(t) dch_{pv} \right] \qquad \forall t \in T \end{aligned} \tag{3.17c}$$

$$ESL_{pv}^{min} \leq ESL_{pv}(t) \leq ESL_{pv}^{max} \qquad \forall t \in T_i \tag{3.17d}$$

$$S_{pv,dch}(t) + S_{pv,chd}(t) \leq 1 \qquad \forall t \in T \tag{3.17e}$$

Constraint (3.17b) simulates the constant current battery charger operation which is normally used to charge the PV system batteries. For simplicity, it is assumed that the battery voltage is constant during the discharging/charging operations; thus, a constant current battery charging is assumed to be a constant power charging process. Constraint (3.17c) shows the effect of the charge/discharge decisions on the battery storage level. Constraint (3.17d) is used to protect the battery against deep discharging and over charging, and (3.17e) reflects the fact that the converter does not operate in charge and discharge mode simultaneously. The conversion efficiency is assumed to be 100%.

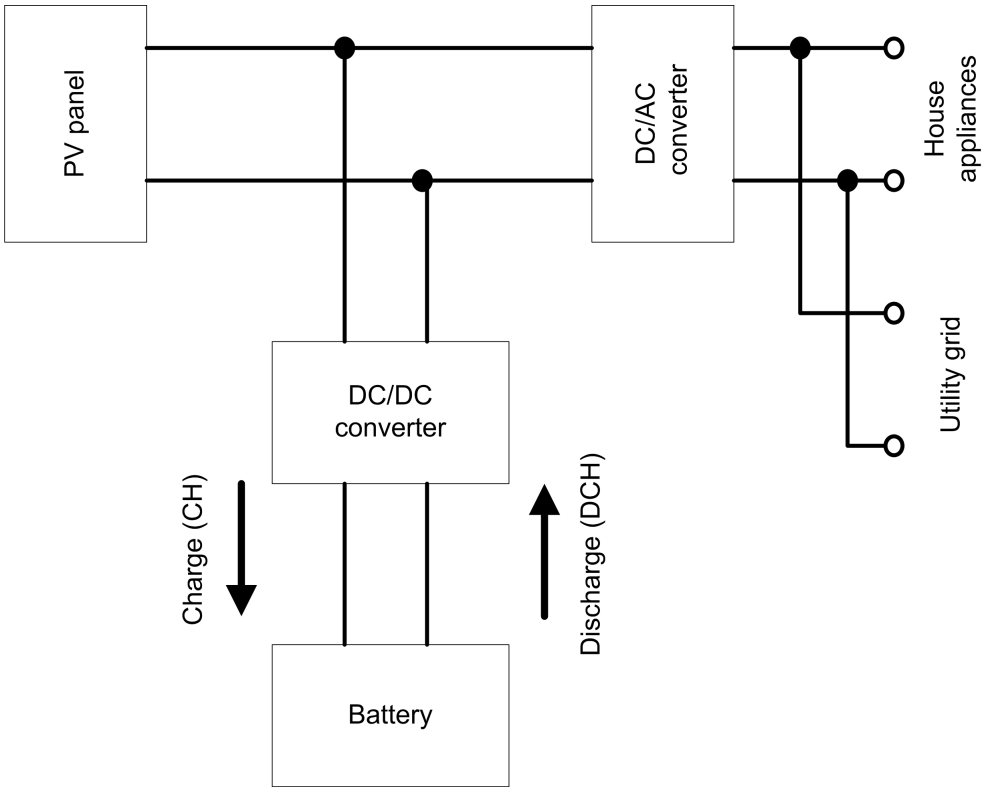

Figure 3.6: A typical domestic PV electric power system connection diagram [141].

Lighting

The lighting load of a house depends on the activity level and/or the house occupancy, and it is modeled using a illumination level index. It is assumed that the lighting load of the house can be divided into several zones and the minimum required illumination can be provided through the lighting system and outdoor illumination (sunshine). The following constraints represent the lighting load of a zone z in the house ($i = li$):

$$L_z(t) + L_z^{out}(t) \geq (1 + K_t)L_z^{min}(t) \qquad \forall t \in T_i \tag{3.18}$$

Constraint (3.18) ensures that the total zonal illumination (from the lighting system and outdoor sunshine) is more than a minimum required level. The effect of the house occupancy on the lighting load is considered in the minimum required illumination level for each zone, and it is assumed that residential customers tend to reduce illumination during peak-price hours. Thus, this "price elasticity" of the lighting load is modeled by a linear

function K_t, $0 \leq K_t \leq 1$, such that during peak hours K_t is equal to 0, which corresponds to the householder using the minimum required illumination; and during off-peak hours K_t is equal to 1, which means the household consumes more lighting than the minimum required illumination. The required illumination and the illumination from outdoor at time interval t are assumed to be exogenous inputs to the model. The effect of the house occupancy on the lighting load is considered in the minimum required illumination parameter.

3.4 Residential Energy Hub Simulations

This section is devoted to the presentation and discussion of some relevant simulation results of the developed mathematical models for residential energy hubs. Extensive studies were conducted in [135] and [141] to validate the developed mathematical model and to examine its performance for a residential energy hub. A few further case studies are carried out and presented in this thesis for a real residential customer in Ontario, Canada, with parameters and device ratings of the household properly chosen, and using realistic data inputs for outside temperatures, illumination levels, and solar PV panel generation. Table 3.2 presents a summary of the case studies presented and discussed in this chapter to further illustrate the capabilities and performance of the developed model.

3.4.1 Input Data and Parameter Settings

In order to carry out the model simulations for the residential energy hub, it is important to select appropriate model parameters which are close to those in the real world. For practical systems, most of these parameters need to be determined by proper estimation, appliance performance tests and customer preferences. The external inputs and data, and assumed parameter settings of the devices for the purpose of this study can be found in [135], and are provided in Appendix A for the sake of completeness.

3.4.2 Results and Discussion

In this section, the results obtained from the case studies are presented, and the performance of the developed model in each case is discussed.

Table 3.2: Summary of residential energy hub case studies.

Case	Objective function	Description
0	Maximization of comfort.	Maximize customer comfort such that the temperature deviation from the set points is minimized while all other user defined constraints on operation of the devices are met.
1	Minimization of total costs and peak demand.	Minimize total energy costs and peak demand of the household by assuming a peak demand charge for residential customers.
2	Minimization of total costs, energy consumption, and emissions.	The individual objective functions of minimizing total energy costs, energy consumption, and emissions are assigned weights to build a new objective function that simultaneously minimizes all of them. These weights are calculated by running the model with the individual objective functions, i.e., using J_1, J_2, and J_3 as individual objective function, which result in objective function values of $\$X$, Y kWh, and $\$Z$, respectively. Thus, in these simulations the weights are defined as follows: $\omega_1 = 1$, $\omega_2 = X/Y$, $\omega_3 = X/Z$, $\omega_4 = 0$.

Examples of Optimal Operational Schedules of Devices

The operational schedules of various devices generated in Case 0, Case 1, and Case 2 for a typical summer day are presented and discussed next for TOU pricing. In the results presented in this section, the upper and lower limits of each variable are shown by doted and dashed lines, respectively.

Case 0: Simulation results obtained from the model in Case 0 are depicted in Figure 3.7 and Figure 3.8. In this Case, stove, dishwasher, washer, and dryer are scheduled according to the user defined operation time windows, and lighting is operated to provide minimum required illumination levels at each hour according to the household preferences. Observe in Figure 3.8 that the inside house, water heater, and fridge temperatures track the user defined set points to maximize customers comfort, resulting in a 6 kW peak demand for the household at 9:45 pm.

Case 1: Figure 3.9 and Figure 3.10 present the simulation results obtained from the model in Case 1.The model generates optimal operational schedules to minimize peak demand of the energy hub in this case, as shown in Figure 3.9. Stove, dishwasher, washer, and dryer are optimally scheduled during the day, considering the user defined operation time windows, to reduce energy consumption and peak demand of the household. From the results presented in Figure 3.10, notice that the inside house, water heater, and fridge temperatures vary within the user defined upper and lower limits. Observe that the user defined inside temperature variation ranges are wider during working hours, when probably no one is present in the house, and narrower at other times. In this case, the peak demand of the household is 3.8 kW at 2:00 pm. which represents a 36% reduction with respect to Case 0.

Case 2: The optimal operational schedules generated by the model in Case 2 are depicted in Figure 3.11, and some of the resulting outputs are shown in Figure 3.12. In this case, the operation of AC, water heater, tub water heater, and fridge are optimally scheduled to maintain their inside temperatures within the user defined ranges, while reducing electricity costs, consumption, and CO_2 emissions. In this case, observe that the ESD is discharged mostly during TOU-summer on-peak hours (11:00 am to 5:00 pm), when the solar PV panel generation has the most impact on the reduction of CO_2 emissions. Notice that the operations of dishwasher, washer, and dryer are optimally scheduled during off-peak hours (after 10:00 pm), when both electricity price and CO_2 emissions of the grid are

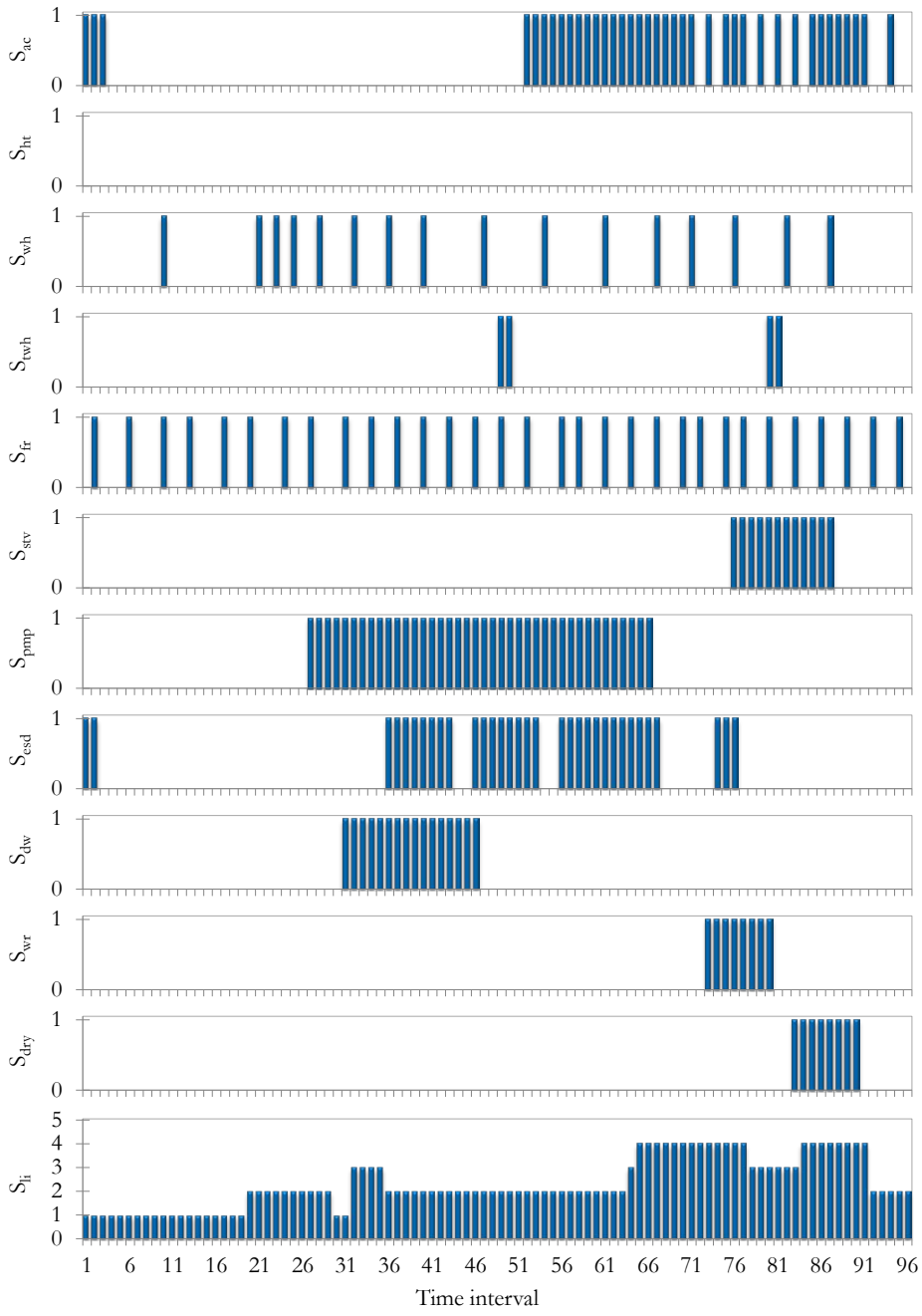

Figure 3.7: Optimal operational decisions of AC, heating, water heater, tub water heater, fridge, stove, pool pump, ESD, dishwasher, washer, dryer, and lighting, respectively, obtained from the model in Case 0 for a summer day.

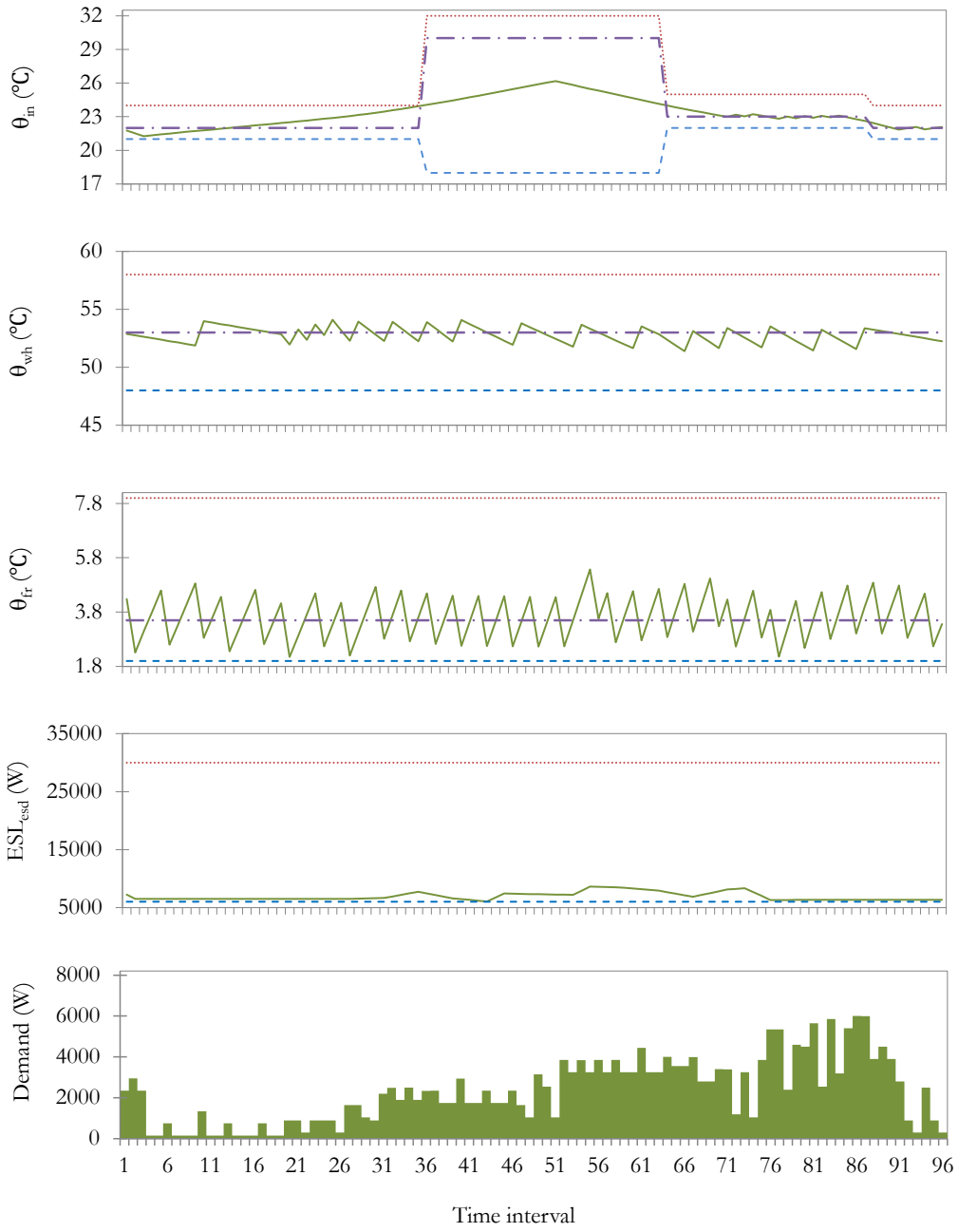

Figure 3.8: Inside house, water heater, and fridge temperatures settings and values, and energy storage level of the ESD and peak demand values, respectively, obtained from the model in Case 0 for a summer day.

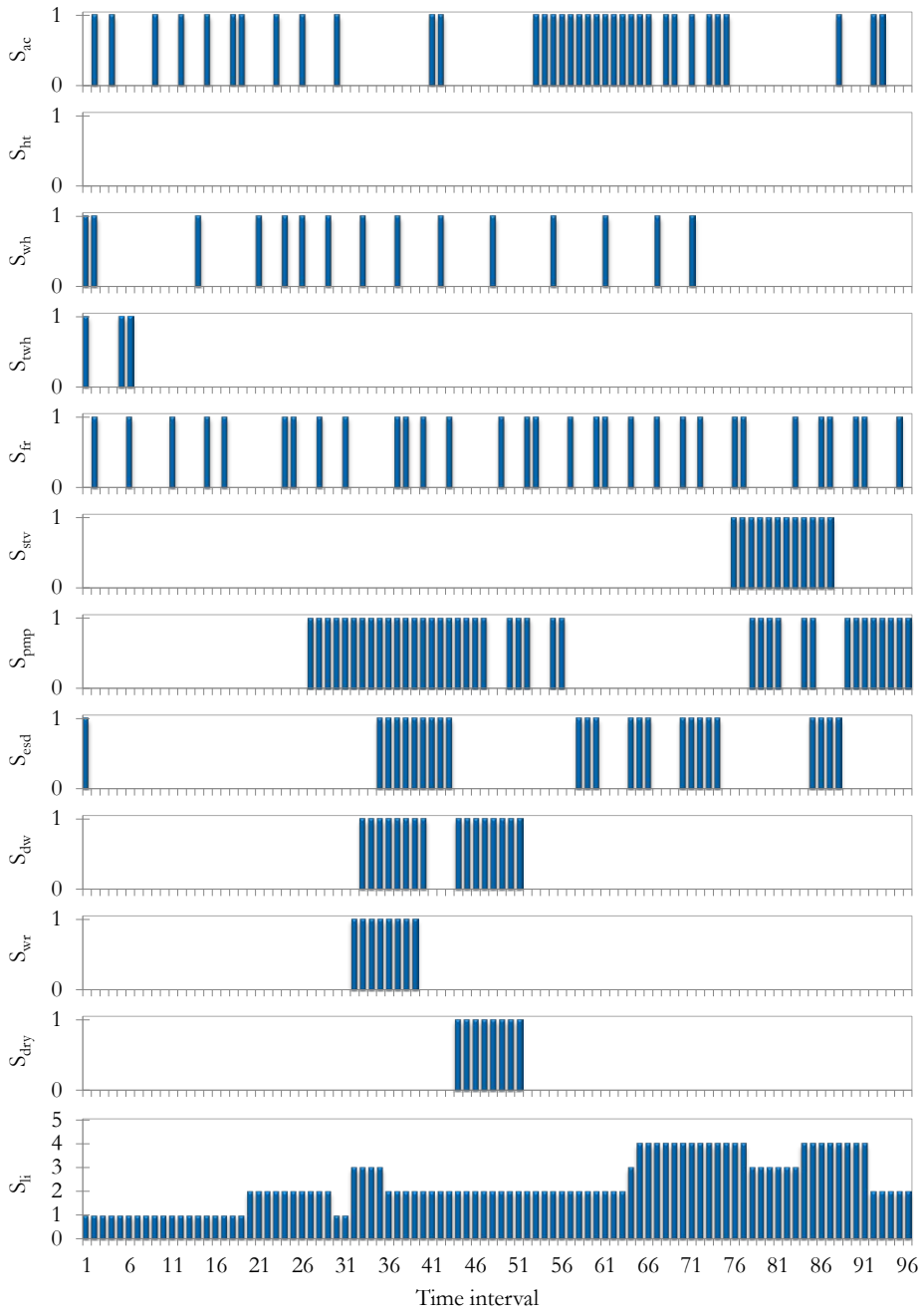

Figure 3.9: Optimal operational decisions of AC, heating, water heater, tub water heater, fridge, stove, pool pump, ESD, dishwasher, washer, dryer, and lighting, respectively, obtained from the model in Case 1 for a summer day.

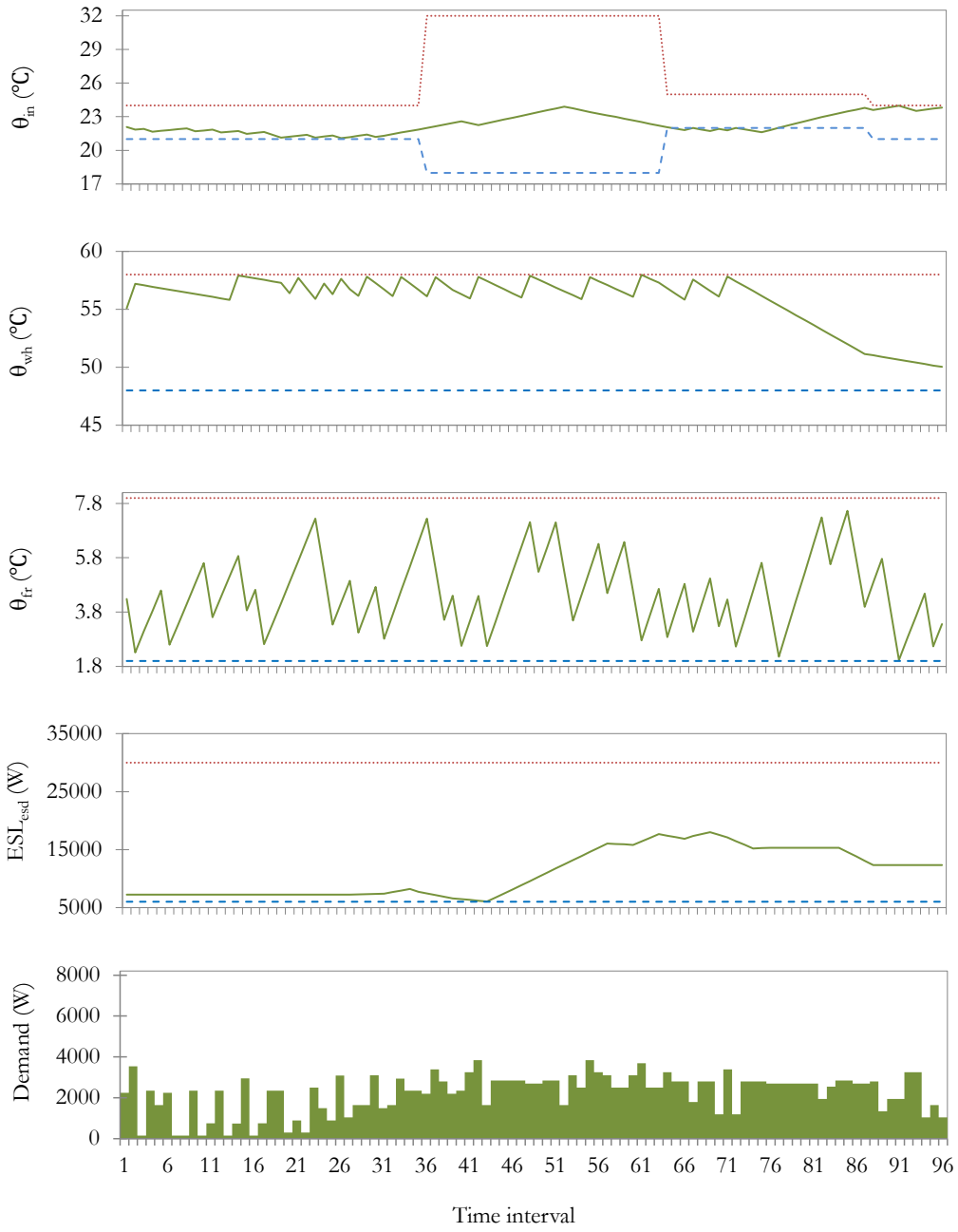

Figure 3.10: Inside house, water heater, and fridge temperatures settings and values, and energy storage level of the ESD and peak demand values, respectively, obtained from the model in Case 1 for a summer day.

low, considering that the operations of these devices are scheduled within the user defined earliest and latest operation time. Inside temperatures of house, water heater, hot-tub water heater, and fridge as well as the storage level of the ESD vary within the upper and lower limits. The electricity demand of the household, depicted in Figure 3.12, shows a peak demand of 8 kW at 10:30 pm, which represents a 33% increase with respect to Case 0.

Results Comparison

Table 3.3 presents a comparison of energy consumptions and energy costs of each individual device in all cases. Observe that both energy consumption and energy costs are lower for the AC in both Case 1 and Case 2, as compared to Case 0. The stove, dishwasher, washer, and dryer show no reduction in energy consumption, but, the energy costs for most of the devices are reduced in Case 2 due to the resulting differences in their operational schedules and TOU prices.

Table 3.4 presents a summary of the results, comparing energy costs and consumption, emissions, and peak demand of the household for all cases. In Case 1, the peak demand of the household is reduced significantly (more than 35%) compared to Case 0, while energy costs, energy consumption, and emissions are also less than in Case 0. In Case 2, the results show reductions of 13%, 6%, and 15% for total energy costs, energy consumption, and emissions, respectively, as compared to Case 0; and the peak demand of the household is 33% higher than in Case 0. Natural gas consumption and costs are slightly reduced in Case 1 and Case 2 compared to Case 0.

3.5 Implementation and Pilots

The developed mathematical models have been implemented and tested on a single board computer, showing that they can be solved efficiently for real-time applications. These models are being implemented in various pilot locations in Ontario to carry out field tests, monitor the performance of the provided system, and study the effectiveness of the models. Moreover, some experimental tests were performed to examine the validity and the accuracy of the developed model for the fridge [141].

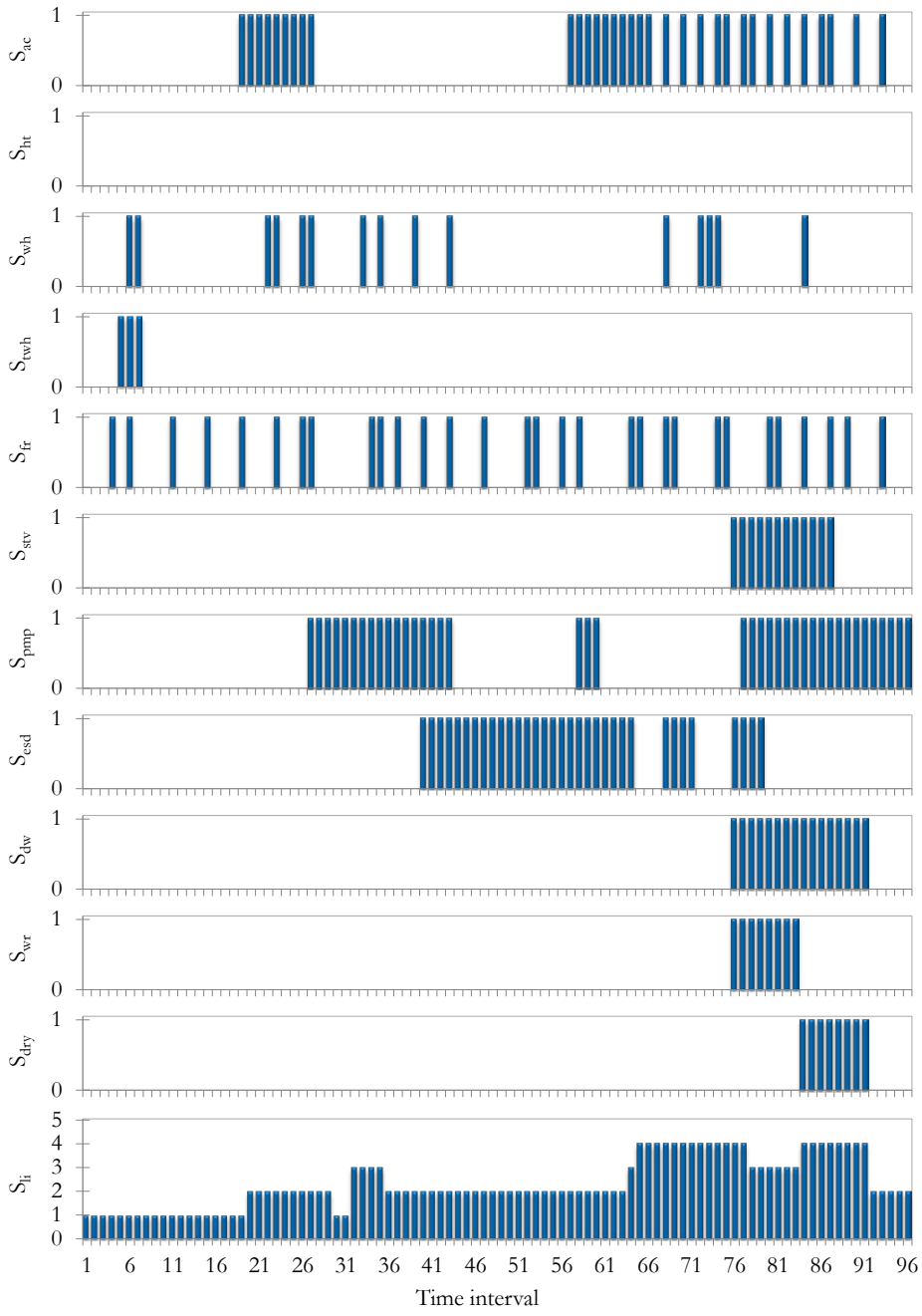

Figure 3.11: Optimal operational decisions of AC, heating, water heater, tub water heater, fridge, stove, pool pump, ESD, dishwasher, washer, dryer, and lighting, respectively, obtained from the model in Case 2 for a summer day.

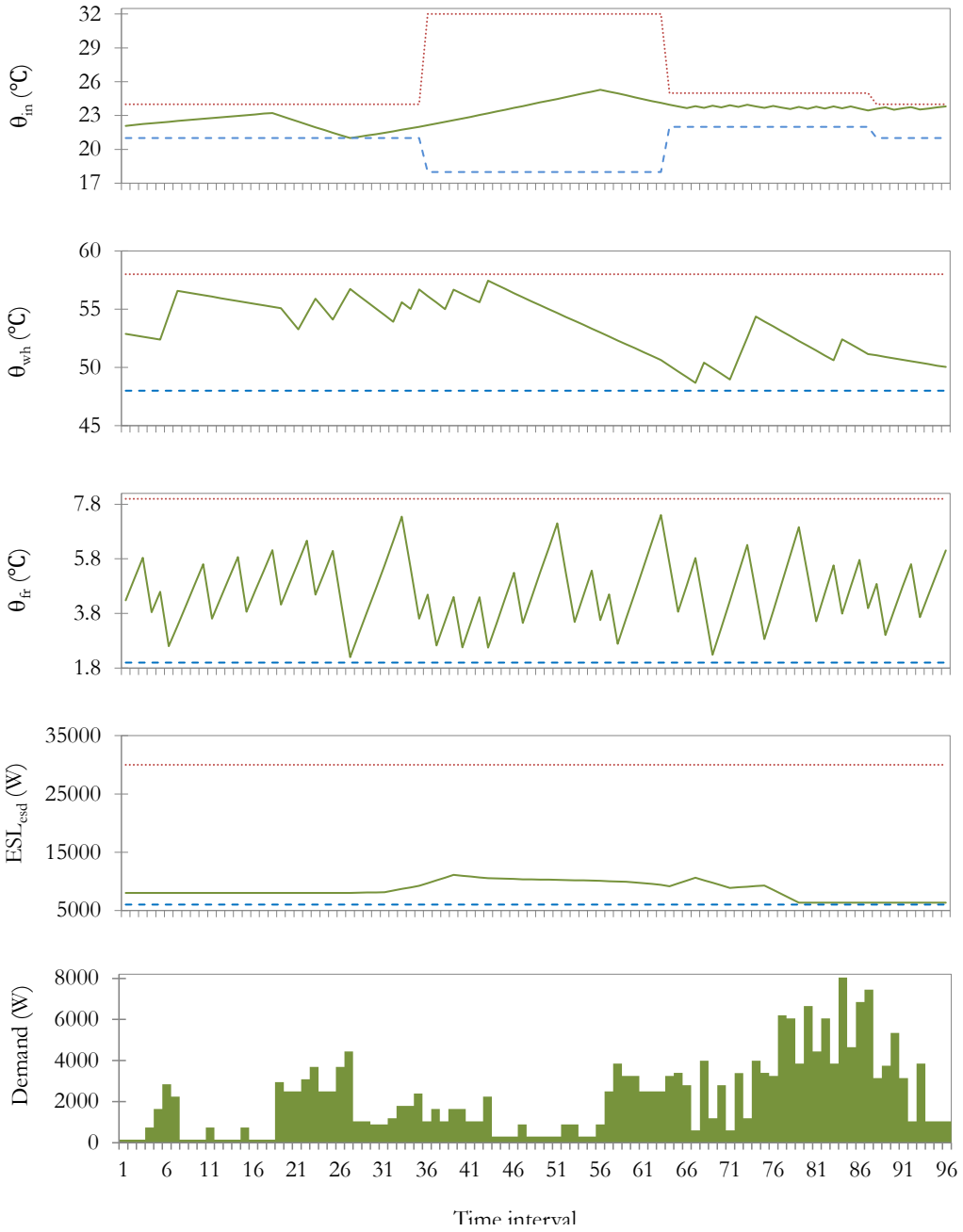

Figure 3.12: Inside house, water heater, and fridge temperatures settings and values, and energy storage level of the ESD and peak demand values, respectively, obtained from the model in Case 2 for a summer day.

Table 3.3: Results of all cases for individual devices using TOU for a summer day.

Device		Case 0		Case 1		Case 2	
		Energy consumption (kWh)	Energy cost ($)	Energy consumption (kWh)	Energy cost ($)	Energy consumption (kWh)	Energy cost ($)
Air Conditioner		20.90	0.15	19.25	0.14	18.15	0.12
Water heater	Electricity	2.38	0.25	2.23	0.23	2.23	0.22
	Gas	4.75	1.39	4.45	1.31	4.45	1.31
Fridge		4.65	0.48	4.65	0.48	4.50	0.46
Lighting		8.44	0.88	8.43	0.88	8.44	0.88
Stove		4.50	0.46	4.50	0.46	4.50	0.46
Dishwasher		2.80	0.33	2.80	0.34	2.80	0.27
Washer		0.90	0.10	0.90	0.10	0.90	0.10
Dryer		2.20	0.18	2.20	0.28	2.20	0.17
Tub Water heater		1.88	0.21	1.13	0.09	1.13	0.09
Pool pump		7.50	0.90	7.50	0.80	7.50	0.77

Table 3.4: Summary comparison of results in all cases using TOU for a summer day.

Item	Energy cost ($)	Energy consumption (kWh)	Gas cost ($)	Gas consumption (m^3)	ESD revenue ($)	ESD energy supply (kWh)	Emissions cost ($)	Emissions (kg)	Peak demand (W)
Case 0	6.08	56.14	1.39	4.75	19.85	24.75	0.48	4.81	5993
Case 1	5.72	53.59	1.31	4.45	15.04	18.75	0.45	4.50	3844
Case 2	5.28	52.34	1.31	4.45	19.85	24.75	0.40	4.08	8043

3.6 Summary

This chapter presented and discussed a novel mathematical model of residential energy hubs which can be readily integrated into HAS, HEM, and EMSs to increase their functionality and improve their effectiveness. The proposed optimization model ensures total energy costs and emissions reduction for customers while considering their preferences and comfort levels. Mathematical models of major household demands, i.e., fridge, freezer, dishwasher, washer and dryer, stove, water heater, hot tub, pool pumps, lighting, heating and air conditioning, and generic models for solar PV panels and energy generation/storage devices in a typical house were formulated. Based on these models, an MILP optimization problem for the optimal operation scheduling of residential energy hubs to minimize demand, total cost of electricity and gas, emissions and peak load of the hubs was developed. The developed model incorporates electricity and gas energy carriers, gives the priority to customers' preferences, and takes into account human comfort factors and CO_2 emissions, thus facilitating the integration of residential customers into Smart Grids.

The applications of the proposed models to a real household in Ontario, Canada, considering a number of simulation case studies, showed that savings of up to 20% on energy costs and 50% on peak demand can be achieved, while maintaining the household owner's desired comfort levels. The results of the various realistic simulations demonstrated that by choosing appropriate objective functions, the proposed mathematical model has the capability of generating optimal operational schedules of devices to minimize total energy costs, energy consumption and emissions, while taking into account the end-user preferences and comfort. The developed mathematical models have been implemented and tested on a single board computer, demonstrating that these models can be solved efficiently in real-time applications, and are being deployed in various pilot locations in Ontario to carryout field tests and study the performance of the provided technology.

Chapter 4

Optimal Operation of Commercial Energy Hubs: Produce Storage Facilities

4.1 Introduction

In this Chapter, a mathematical model for optimal operation of produce storage facilities is proposed that can be implemented as a supervisory real-time control in existing climate control systems. The developed model is based on approximate physical models of produce storage facilities and climate conditions predictions, and incorporates weather forecasts, electricity price information, and end-user preferences to optimally operate existing climate controllers. The objective is to minimize total energy costs and demand charges while considering operational constraints of devices and important parameters of storage facilities, i.e., inside temperature and humidity should be kept within acceptable ranges. The proposed supervisory control in conjunction with existing climate controllers would allow coordinated optimal operation of multiple produce storage facilities in a single site, thus facilitating the integration of these commercial customers into Smart Grids.

The reminder of the chapter is organized as follows: In Section 4.2 the proposed supervisory control strategy is described, and in Section 4.3, the developed mathematical model for the supervisory controller, discussing the objective functions and constraints, is presented. In Section 4.4 the most relevant results of various case studies including Monte-Carlo simulations are presented and discussed. Finally, in Section 4.5, a solution

procedure is proposed for real-time implementation of the developed mathematical model and numerical results are presented.

4.2 Proposed Supervisory Operation Strategy

The objective in indoor climate control of commercial storage facilities is to keep the internal parameters (e.g., inside temperature and humidity) within pre-defined ranges, while these are affected by external weather conditions and other parameters such as respiration and evaporation of stored produces. In order to achieve this, natural and forced air ventilation, mechanical heating and cooling systems, and humidifiers and dehumidifiers are employed in climate control systems of storage facilities. Nowadays, electricity price forecasts for RTP, and accurate weather forecasts for next few days, updated every few hours, are available. These forecasts are employed here to minimize energy consumption costs and demand charges associated with the operation of various devices controlled in storage facilities. Hence, a hierarchical operation strategy based on mathematical modeling of commercial produce storage facilities, that incorporates electricity price and weather forecasts, is proposed in this chapter for optimal operation of climate control systems of these storage facilities.

4.2.1 Hierarchical Operation Scheme

The architecture of the proposed scheme for optimal operation of the aforementioned climate control systems is presented in Figure 4.1. The feedback control system is shown in the lower part of the figure, and the proposed supervisory control, which generates set point inputs for the controller, is depicted above the existing controllers. The supervisory control uses the mathematical model of each component in the system, parameter settings, external information and user preferences to optimize the operation of the climate control system; outputs of the proposed optimization model are the required set points. The proposed supervisory control updates the set points every hour, while the feedback controller continuously monitors the parameters under control and tracks the target set points in real time. The supervisory control also monitors the system and re-runs the model in case of large discrepancies between the calculated and measured parameters.

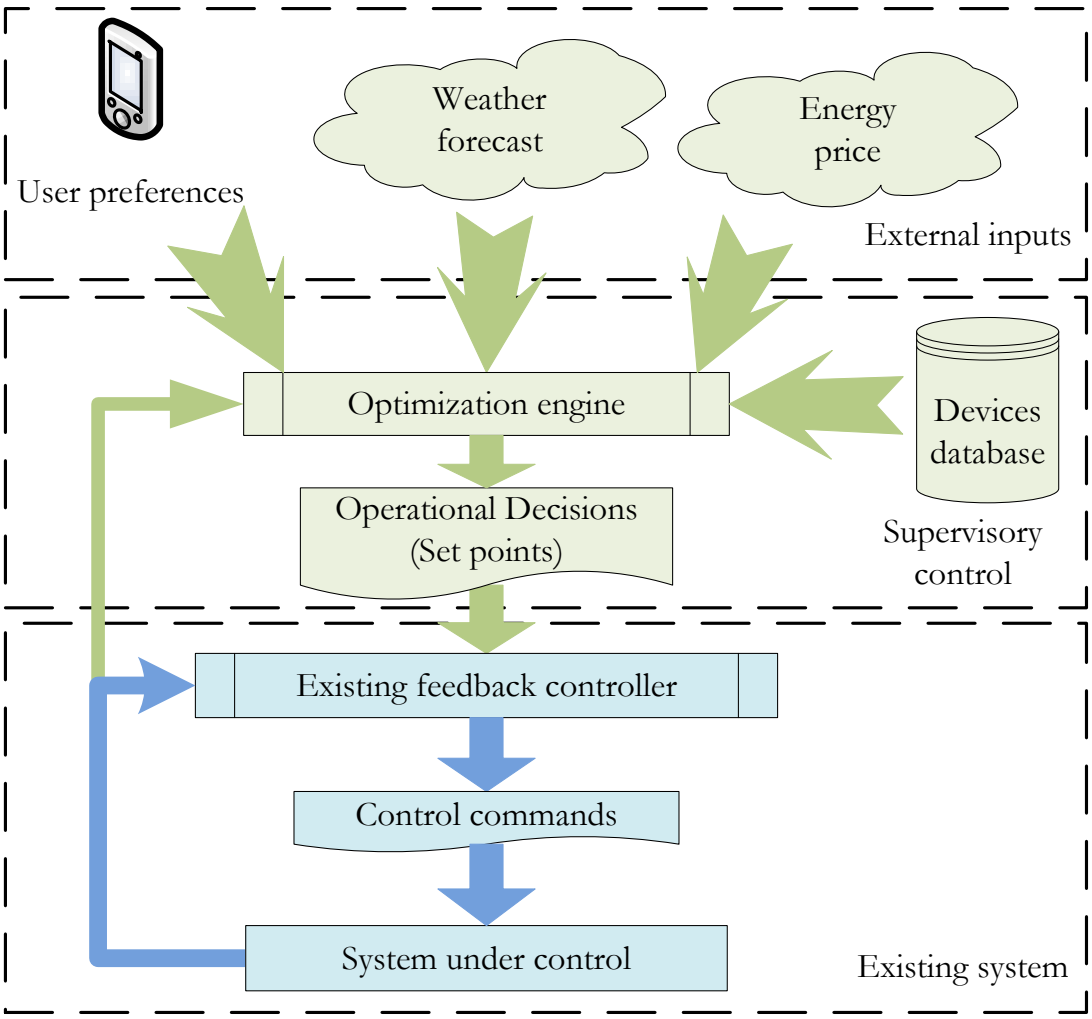

Figure 4.1: The proposed supervisory control and existing feedback control architecture of climate controllers in storage facilities.

4.2.2 Scheduling Horizon

The scheduling horizon in the optimization model can vary from a few hours to days, with the selection depending on the type of the activities which take place within, size of the storage facility, and the accuracy of weather and electricity price information. Without any loss of generality, a weekly scheduling horizon with time intervals of one hour are used in this work.

4.3 Mathematical Model

In this section, all the indices, sets, variables, and parameters of the proposed model for optimal operation of produce storage facilities are depicted in Table 4.1. The objective function of the model and the operational constraints associated with the components of the hub are explained next.

Table 4.1: Description and definition of the storage facilities model identifiers.

Sets	**Description**
A	Set of devices; $A = \{dh, fn, hu, ht, mx, pr, rf\}$
T	Set of indices in scheduling horizon; $T = \{1 \dots 168\}$
Indices	**Description**
i	Index of devices
t	Index of time interval
z	Index of zone
Subscripts	**Description**
a	Air
b	Bulk
dh	Dehumidifier
fn	Fan
hu	Humidifier
ht	Heating system
mx	Mixer
pr	Produce
rf	Refrigeration system
w	Water
Variables	**Description**
Dmd	Peak demand variable (kW)

Continued on next page

Table 4.1 – continued from previous page

Variables	**Description**
$\phi_z(t)$	Relative humidity of zone z at time t (%)
$\theta_z(t)$	Temperature of zone z at time t (°C)
$S_{i,z}(t)$	Operation state of device i of zone z at time t; $0 \leq S_{i,z}(t) \leq 1$
$w_z(t)$	Water content of air in zone z at time t (kg_w/kg_a)
$\widehat{w}_z(t)$	Saturated vapour concentration in zone z at time t (kg_w/kg_a)
Parameters	**Description**
A_{sp}	Specific surface area of produce (m^2_{pr}/m^3_b)
α_z	Thermal leakage of zone z ($kJ/(h\ °C)$)
β_z	Cooling effect of fan operation ($kJ/(h\ °C)$)
C_a	Specific heat of air, 1.006 ($kJ/(kg\ °C)$)
C_z	Total heat capacity of zone z ($kJ/\ °C$)
c_{dc}	Demand charge (\$/kW)
$c_{ed}(t)$	Electricity price at time t (\$/kWh)
ε	Porosity (m^3_a/m^3_b)
η_{rf}	Performance coefficient of the refrigeration system
γ_z	Cooling rate the refrigeration systems (kJ/h)
h_{ev}	Evaporation heat of water, 2270 (kJ/kg_w)
h_{re}	Respiration heat rate ($kJ/(kg_{pr}h)$)
J	Objective function of the optimization model
κ_z	Heat rate of the heating system (kJ/h)
k_{ev}	Evaporation coefficient ($kg_a/(m^2_{pr}\,h)$)
M_{pr}	Total weight of produce (kg)
m_w	Molar mass of water, 18.0153×10^{-3} (kg/mol)
μ_z	Effect of humidifier operation on water content of air in zone z ($kg_w/(kg_a\,h)$)
ν_z	Effect of dehumidifier operation on water content of air in zone z ($kg_w/(kg_a\,h)$)

Continued on next page

Table 4.1 – continued from previous page

Parameters	Description
N_T	Total number of intervals in scheduling horizon T
p_1	Constant, 100 (no dim.)
p_2	Constant, 1.7001 (Pa)
p_3	Constant, 7.7835 (Pa)
p_4	Constant, 1/17.0789 (K^{-1})
p_5	Constant, 0.6228 (kg_w/kg_a)
P_a	Actual water vapour pressure (Pa)
P_{atm}	Atmospheric air pressure (Pa)
P_{sat}	Saturated water vapour pressure (Pa)
P_i	Rated power of device i (W)
P_{par}	Partial vapour pressure (Pa)
$P_{tot}(t)$	Total demand of the storage facility at time t (kW)
$q_{m,z}(t)$	Miscellaneous heat loads like lights, and fans in zone z (kJ/h)
$q_{ev,z}(t)$	Evaporation heat at zone z (kJ/h)
$q_{re,z}(t)$	Respiration heat at zone z (kJ/h)
$q_{fn,z}(t)$	Thermal effect of circulated air flow through fans at zone z (kJ/h)
Q_z^{leak}	Air leakage from zone z (m^3/h)
Q_z^{max}	Maximum volumetric air flow rate of fans in zone z (m^3/h)
R	Ideal gas constant constant, 8.314472 $(J/(mol\,K))$
ρ_a	Density of air (kg/m^3)
ρ_b	Density of bulk (kg/m^3)
θ_0	Absolute temperature at 0 °C, 273.15 (K)
θ_{out}^{min}	Minimum acceptable outdoor temperature (°C)
θ_z^{set}	Inside temperature set point (°C)
θ_z^{min}	Minimum inside temperature in zone z (°C)
θ_z^{max}	Maximum inside temperature in zone z (°C)
$\theta_z^{l_0}$	Lower limit of average temperature in zone z (°C)

Continued on next page

Table 4.1 – continued from previous page

Parameters	Description
$\theta_z^{u_0}$	Upper limit of average temperature in zone z (°C)
τ	Length of time interval (h)
UA_z	Area integrated thermal resistance for heat transfer between ambient and inside air ($kJ/(h\ °C)$)
V_z	Volume of zone z (m^3)
V_a	Air volume per volume zone z (no dim.)
V_p	Produce volume per volume zone z (no dim.)
w_{hu}^{max}	Maximum water rate of humidifier (kg_w/h)
w_{dh}^{max}	Maximum rate of dehumidifier (kg_w/h)
ξ_z	Effect of operation of fans on water content of air in zone z (h^{-1})
ζ_z	Effect of air leakage on water content of air in zone z (h^{-1})

4.3.1 Objective Function

Depending on the end-user's choice, different objective functions can be adopted to solve the optimization problem. Thus, minimization of temperature deviations from their set points, energy costs, peak demand charges, and total costs including energy costs and demand charges over the scheduling horizon are considered in this work as possible objective functions for the optimization model.

Minimization of temperature deviations

To track the temperature settings closely, minimizing the sum of squares of the temperature variations from a given set point is considered as an objective function, as follows:

$$J_1 = \sum_{t \in T} \left(\theta_z(t) - \theta_z^{set}\right)^2 \tag{4.1}$$

This objective could be utilized for produces that require a fixed storage temperature, since some temperature "drift" is allowed in existing climate control systems.

Minimization of energy costs

This objective function represents the minimization of the customer's energy costs over the scheduling horizon:

$$J_2 = \sum_{t \in T} \sum_{i \in A} \tau c_{ed}(t)\, P_i\, S_i(t) \tag{4.2}$$

Minimization of peak demand charges

This objective seeks to reduce the demand charges as follows:

$$J_3 = c_{dc} \cdot Dmd \tag{4.3}$$

where Dmd is a non-negative variable used along with the following constraint to represent the peak demand of the storage facility over the scheduling horizon:

$$Dmd \geq \sum_{i \in A} P_i\, S_i(t) \qquad \forall t \in T \tag{4.4}$$

Minimization of total costs

In addition to the aforementioned individual objective functions, any combinations of these can also be used as an objective. For example, the objective function for minimization of total costs including energy costs and peak demand charges over the scheduling horizon can be represented as follows:

$$J_4 = J_2 + J_3 \tag{4.5}$$

Minimization of CO_2 emissions

The carbon footprint of the customer from the grid electricity usage is formulated using the hourly marginal cost of CO_2 as follows:

$$J_5 = \sum_{t \in T} \left[\sum_{i \in A} C_{em}(t)\, P_i\, S_i(t) \right] \tag{4.6}$$

4.3.2 Model Constraints

Mathematical models are developed in this section for inside temperature and humidity of produce storage facilities, which consider the technical and operational aspects of climate control systems. Inside humidity and temperature are affected by external parameters; for example, heat transfer through walls, operation of heating and cooling systems, and air ventilation can affect indoor climate. The products also produce heat due to respiration, with the product temperature determining the reaction rates, which affect the quality and weight loss of the product. Furthermore, inside humidity drives evaporation or condensation [47]. Thus, appropriate mathematical models are developed next to represent the storage facility temperature and humidity, and maintain these within a specified range.

Inside humidity

Various types of produces stored in storage facilities require to be kept within specific ranges of relative humidity to control their evaporation and condensation. Relative humidity of the storage facility is defined as:

$$\phi = \frac{P_{par}}{P_{sat}} 100\% \tag{4.7}$$

where, the saturated vapor pressure (P_{sat}) and the partial pressure (P_{par}) can be approximated by [144]:

$$P_{sat} = p_1 \left(-p_2 + p_3 e^{p_4 \theta}\right) \tag{4.8}$$

$$P_{par} = \frac{w P_{atm}}{p_5} \tag{4.9}$$

To model the humidity inside the storage facilities, the water content of air inside the storage facility needs to be modeled; this can be represented by the following constraint based on the moisture balance equation:

$$\begin{aligned} w_z(t) =& w_z(t-1) + \tau \left[\mu_z S_{fn,z}(t) S_{hu,z}(t)\right. \\ &+\zeta_z (w_{out}(t) - w_z(t)) \\ &-\nu_z S_{dh,z}(t) + w_{ev,z}(t) \\ &\left.+\xi_z S_{fn,z}(t) S_{mx,z}(t) \left(w_{out}(t) - w_z(t)\right)\right] \qquad \forall t \in T \end{aligned} \tag{4.10}$$

where the parameters μ_z, ζ_z, ν_z, and ξ_z can be calculated from name plate information, measurements or estimations from simple performance tests using the following formulas:

$$\zeta_z = Q_z^{leak}/(V_a V_z) \tag{4.11a}$$
$$\xi_z = Q_z^{max}/(V_a V_z) \tag{4.11b}$$
$$\mu_z = w_h^{max}/(\rho_a V_a V_z) \tag{4.11c}$$
$$\nu_z = w_{dh}^{max}/(\rho_a V_a V_z). \tag{4.11d}$$

Constraint (4.10) represents the water content in air inside the storage facility at time t as a function of its water content at time $t-1$; water produced because of evaporation; moisture loss through air leakage; and operation of fans, air mixers, humidifiers and dehumidifiers. The effect of evaporation on the water content of air is calculated using [41]:

$$w_{ev,z}(t) = \frac{k_{ev} A_{sp}}{\varepsilon \rho_a}(\widehat{w}_z(t) - w_z(t)) \tag{4.12}$$

where $\widehat{w}_z(t)$ is the saturated vapour concentration that can be calculated from approximate conversion of the ideal gas law:

$$\begin{aligned} P_a &= \frac{n_v}{V} R\,(\theta + \theta_0) \\ &= \frac{w \rho_a}{m_w} R\,(\theta + \theta_0) \end{aligned} \tag{4.13}$$

Thus, $\widehat{w}_z(t)$ is obtained from (4.13) as follows:

$$\begin{aligned} \widehat{w}_z(t) &= \frac{P_{sat}(t)}{\frac{R\rho_a}{m_w}(\theta_z(t) + \theta_0)} \\ &= \frac{p_1\left(-p_2 + p_3 e^{p_4 \theta_z(t)}\right)}{\frac{R\rho_a}{m_w}(\theta_z(t) + \theta_0)} \end{aligned} \tag{4.14}$$

Substituting (4.8) and (4.9) in (4.7), the following constraints ensures that relative humidity of inside air is within the range defined by a minimum and a maximum relative humidity:

$$w_z(t) \le \phi_z^{max} \frac{p_1 p_5}{P_{atm}}\left(-p_2 + p_3 e^{p_4 \theta_z(t)}\right) \qquad \forall t \in T \tag{4.15a}$$
$$w_z(t) \ge \phi_z^{min} \frac{p_1 p_5}{P_{atm}}\left(-p_2 + p_3 e^{p_4 \theta_z t}\right) \qquad \forall t \in T \tag{4.15b}$$

Inside temperature

Quasi steady-state thermal dynamics of the storage facility can be modeled using the following constraint based on the thermal balance equations:

$$\begin{aligned}\theta_z(t) =&\theta_z(t-1) + \frac{\tau}{C_z}\left[\kappa_z S_{ht,z}(t) + q_{m,z}(t)\right.\\ &-\gamma_z S_{rf,z}(t) + \alpha_z\left(\theta_{out}(t) - \theta_z(t)\right)\\ &\left.+q_{fn,z}(t) + q_{re,z}(t) - q_{ev,z}(t)\right] \qquad \forall t \in T \end{aligned} \tag{4.16}$$

This constraint states that the temperature of the storage space at time t is a function of its temperature at time $t-1$; miscellaneous heat of mechanical devices within the storage facility; heat loss through walls and air leakage; respiration and evaporation heats of the produce; and operation of fans, mixers, refrigeration and heating systems.

In (4.16), α_z accounts for the thermal leakage due to the difference between indoor and outdoor temperatures, and γ_z and κ_z represent the cooling and warming effect of an On state of the refrigeration and heating systems, respectively. These parameters can be calculated based on measurements or estimations from simple performance tests using the following formulas:

$$\alpha_z = UA_z + \rho_a c_a Q_z^{leak} \tag{4.17a}$$

$$\gamma_z = P_{rf}^{max}\eta_r \times 3600/1000 \tag{4.17b}$$

$$\kappa_z = P_{ht}^{max}\eta_{ht} \times 3600/1000 \tag{4.17c}$$

The thermal effect of circulated air through fans is calculated as follows: Exhaust hatches on the rear end of the storage facilities operate according to the opening position of the mixer hatches and the fans operation to keep the inside air pressure constant. This can be expressed as exhausting the same volume of air circulated into the storage facility through fans and mixer hatches via exhaust hatches. Therefore, the thermal effect of circulated air flow through fans can be written as follows:

$$\begin{aligned}q_{fn,z}(t) =&\beta_z S_{fn,z}(t)\left(S_{mx,z}(t)\theta_{out}(t) - (1 - S_{mx,z}(t))\theta_z(t)\right)\\ &-\beta_z S_{fn,t}(t)\left(S_{mx,z}(t)\theta_z(t)\right)\end{aligned} \tag{4.18}$$

The first and second terms in (4.18) represent the effects of intake and exhaust air of the storage facility, respectively, and can be re-written as follows:

$$q_{fn,z}(t) = \beta_z S_{fn,z}(t) S_{mx,z}(t)\left(\theta_{out}(t) - \theta_z(t)\right) \tag{4.19}$$

where β_z corresponds to the cooling effect of fan operation in conjunction with the opening status of the air mixer and the difference between inside and outdoor temperature, and can be estimated based on the following formula:

$$\beta_z = \rho_a c_a Q_z^{max} \tag{4.20}$$

Respiration and evaporation heats can be approximated at certain air temperature and pressure for different types of produces. For example, the followings are used in this thesis to represent the evaporation and respiration heats of potatoes, peaches, apples, and other similar produces [41]:

$$q_{ev,z}(t) = \frac{k_{ev} A_{sp} M_{pr} h_{ev}}{\rho_b} (\widehat{w}_z(t) - w_z(t)) \tag{4.21}$$

$$q_{re,z}(t) = h_{re} M_{pr,z} \tag{4.22}$$

The inside temperature of the storage facility, calculated by (4.16), must be kept within a range specified by a minimum and a maximum temperature, and the average inside temperature over the scheduling horizon must be within a tighter pre-defined temperature range. Thus, the following constraints are considered in the model to represent these requirements:

$$\theta_z^{min} \leq \theta_z(t) \leq \theta_z^{max} \qquad \forall t \in T \tag{4.23}$$

$$\theta_z^{l_0} \leq \sum_{t \in T} \theta_z(t)/N_T \leq \theta_z^{u_0} \tag{4.24}$$

Operational constraints of Devices

In a typical climate control system of storage facilities, the following categories of components can be identified: heating and refrigeration systems, humidifiers and dehumidifiers, and fans and air mixers. The logical relations and constraints for the operation of these devices need to be taken into account in the operation of climate control systems; thus, these operational constraints are modeled in the proposed optimization model as explained next.

Mechanical refrigeration and heating systems do not operate simultaneously, which is represented in the model by the following complementarity constraint:

$$0 \leq S_{rf,z}(t) \perp S_{ht,z}(t) \geq 0 \qquad \forall t \in T \tag{4.25}$$

Similarly, humidifiers and dehumidifiers do not operate simultaneously:

$$0 \leq S_{hu,z}(t) \perp S_{dh,z}(t) \geq 0 \qquad \forall t \in T \tag{4.26}$$

When the air mixer hatches are closed, the fans do not operate, which is represented here by the following constraint:

$$S_{fn,z}(t) \leq S_{mx,z}(t) \qquad \forall t \in T \tag{4.27}$$

When the outdoor temperature is less than a pre-specified value θ_{out}^{min}, the fans do not operate and circulate very cold air into the storage room, which can be modeled as follows:

$$\left(\theta_{out}(t) - \theta_{out}^{min}\right) S_{fn,z}(t) \geq 0 \qquad \forall t \in T \tag{4.28}$$

4.4 Numerical Results for Storage Facilities Model

Several case studies, of which the most relevant ones are presented in this section, are conducted to examine the performance of the developed mathematical model for optimal operation of climate control systems of storage facilities with single and multiple storage spaces. In these case studies, the mathematical model is run for a typical storage facility, where parameters and device ratings are suitably chosen and realistic data inputs for outside temperatures and humidity, electricity prices and demand charges are used. FRP, TOU and RTP tariffs for electricity and demand charges in Ontario–Canada are used to calculate total electricity costs. AMPL [127] is used to implement the developed mathematical models of the storage facility, and IPOPT [129], a popular solver based on interior point methods, is used to solve the developed NLP model.

4.4.1 Storage Facility Test Case

Information pertaining to an actual storage facility is taken from [145] and modified to carry out the simulations. The storage facility has a total capacity of 5000 metric tonnes, comprising six large storage bins, which can operate independently in pairs, thus resulting

in three separate climate control zones. The total volume of the storage facility and of each bin are 15510 m^3 and 1255 m^3, respectively. The rest of the storage facility's space comprise the loading areas and ventilation canals. Temperature and humidity of each pair of bins are controlled simultaneously through a distribution canal providing air ventilation for both bins. Three 3.7 kW fans provide 87,000 m^3/h air ventilation, and there is a humidifier system with a total capacity of 9.5 l/h. Mixing chambers are equipped with air intake hatches to adjust the ratio of fresh incoming and circulated air. Three 20 kW electrical heaters are installed to supplement heat or for drying incoming air when dehumidification is required. The cooling capacity of the refrigeration system is assumed to be 209 kW. All the input data used in these simulations can be found in Appendix B.

4.4.2 Simulation Scenarios

The following five case studies that illustrate the capabilities and performance of the developed model to optimally operate climate control systems of storage facilities are presented in this section:

- Case 0: A feasible solution is obtained for the model that meets all devices operating constraints and required inside temperature and humidity ranges. This case is considered here as *a* realistic "base case" to establish a reference for comparison purposes.
- Case 1: The optimization model minimizes inside temperature deviations from their set points for each zone while meeting the same required model constraints as in Case 0.
- Case 2: The optimization model minimizes total cost of energy consumption of all devices while meeting the same required model constraints as in Case 0.
- Case 3: The model minimizes peak demand charges of the storage facilities while meeting the same required model constraints as in Case 0.
- Case 4: The model minimizes total electricity costs of the storage facilities including electricity consumption costs and peak demand charges while meeting the same required model constraints as in Case 0.

4.4.3 Results and Discussions

The simulation results for Zone 2 in multi-zone operation (all Zones are optimized simultaneously) of the storage facility on a summer week using RTP are presented in Figure 4.2 to Figure 4.6. Figure 4.2 depicts the optimal operation decisions for all devices and the resulting inside temperatures and relative humidities obtained in Case 0. Observe that the model maintains the inside temperature and humidity within the pre-defined ranges by operating various devices.

Figure 4.3 presents the optimal solution obtained from minimizing temperature deviations from its set point (Case 1). In this case the model maintains the inside temperature very close to the set points and the inside humidity within the defined ranges by utilizing various devices. The optimal solution obtained from Case 2, minimizing energy costs, is presented in Figure 4.4; in this case, while the inside temperature and relative humidity vary within the pre-defined ranges, the cost reduction is achieved by operating the refrigeration system, dehumidifier, and fans during lower energy price periods.

Figure 4.5 depicts the optimal solution obtained in Case 3, where the model minimizes peak demand charges of the storage facility by coordinating the operation of various devices. The optimal solution obtained in Case 4 presented in Figure 4.6, shows that while the inside temperature and relative humidity vary within the pre-defined ranges, the model reduces total costs by operating the devices during lower energy price periods and by lowering the peak demand of the facility.

Figure 4.7 to Figure 4.11 present the demand of Zone 1, Zone 2, and Zone 3 and corresponding inside temperatures obtained from Case 0 to Case 4, respectively. Observe in Figure 4.7 for the base case (Case 0) that all the three zones' peak powers occur at the same time, resulting in high peak demand for the facility. In the minimization of temperature deviations (Case 1), depicted in Figure 4.8, the model operates the devices in each zone to minimize the inside temperatures deviations, resulting in a very high peak demand (294.3 kW) for the storage facility as compared to the base case. In Figure 4.9, representing the results of minimization of energy costs (Case 2), notice that the model operates the devices in each zone during low energy prices and keeps the inside temperatures and humidities within the predefined ranges. Although the model operates the devices of each zone during low energy price periods, peak demand of the storage facilities is higher in this case as compared to the base case.

In Case 3, depicted in Figure 4.10, the model changes the operation of the devices to minimize total peak demand of the storage facility while keeping the inside temperatures and humidities within the pre-defined ranges; thus, peak demand of the storage facility is

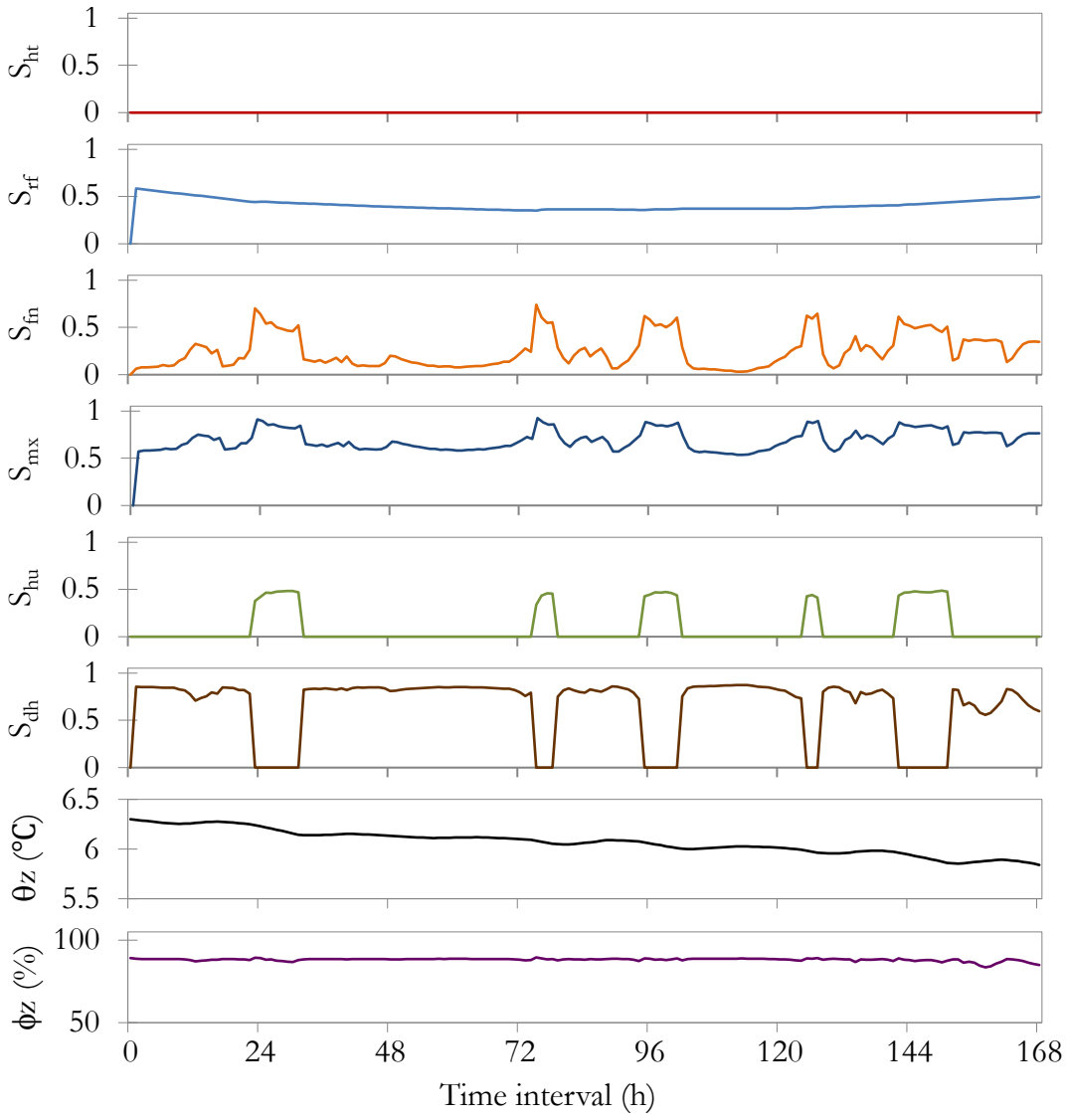

Figure 4.2: Zone 2 values of the decision variables for heating, refrigeration, fans, mixer, humidifier and dehumidifier, and resulting inside temperature and relative humidity, respectively, obtained from the storage facility model in multi-zone operation for the base case (Case 0) using RTP for a summer week.

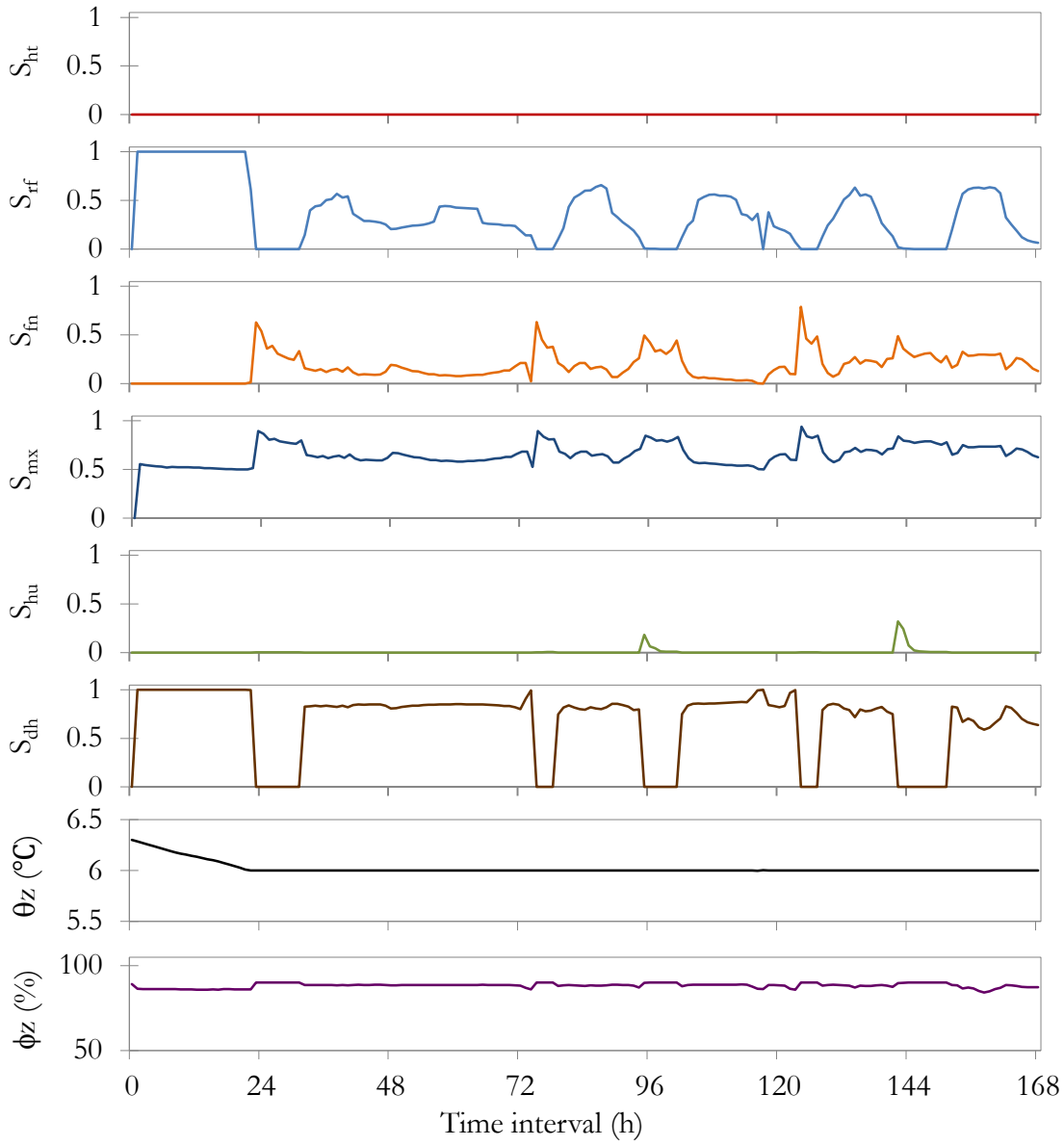

Figure 4.3: Optimal Zone 2 values of the decision variables for heating, refrigeration, fans, mixer, humidifier and dehumidifier, and resulting inside temperature and relative humidity, respectively, obtained from the storage facility model in multi-zone operation for Case 1 using RTP for a summer week.

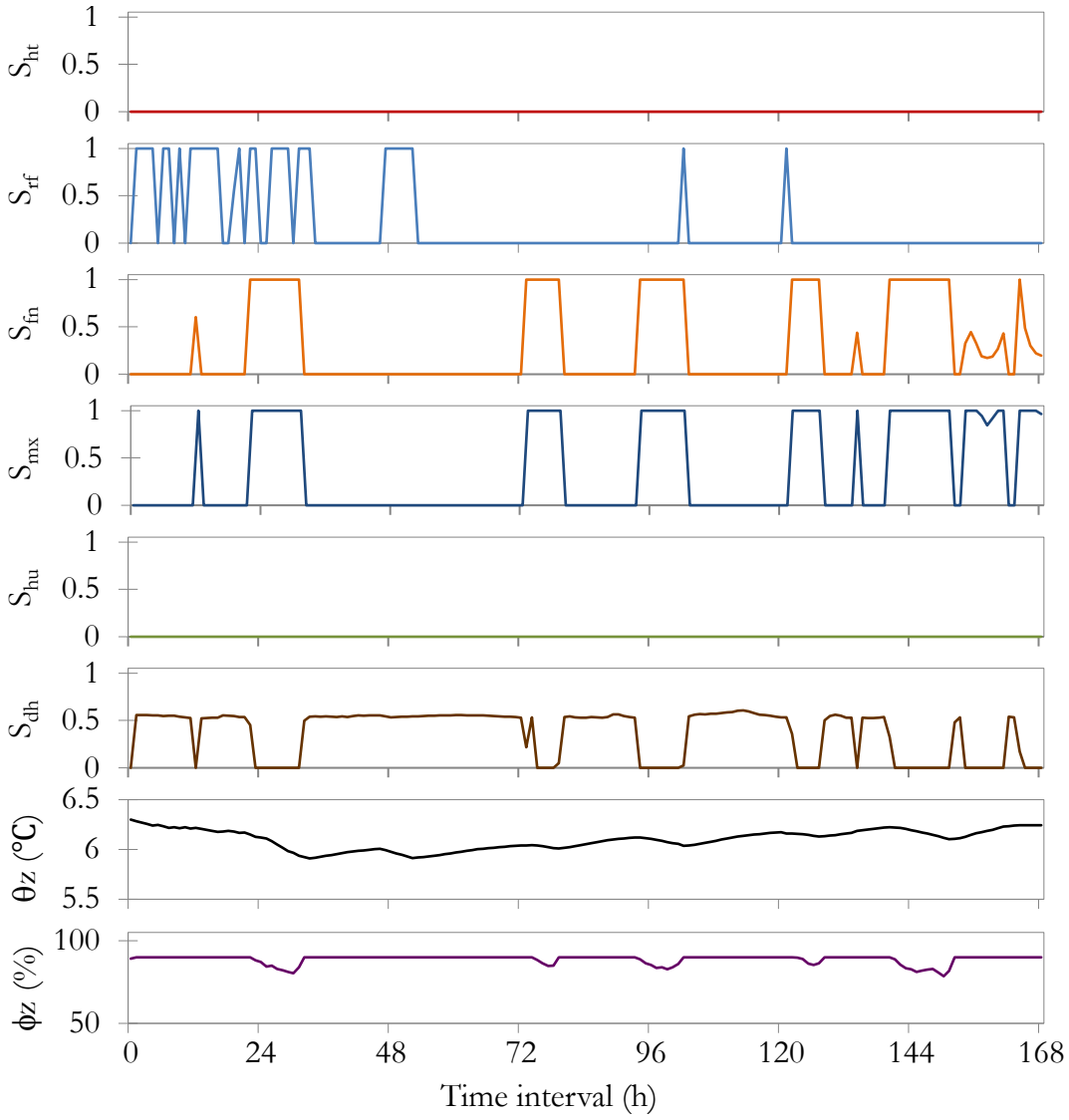

Figure 4.4: Optimal Zone 2 values of the decision variables for heating, refrigeration, fans, mixer, humidifier and dehumidifier, and resulting inside temperature and relative humidity, respectively, obtained from the storage facility model in multi-zone operation for Case 2 using RTP for a summer week.

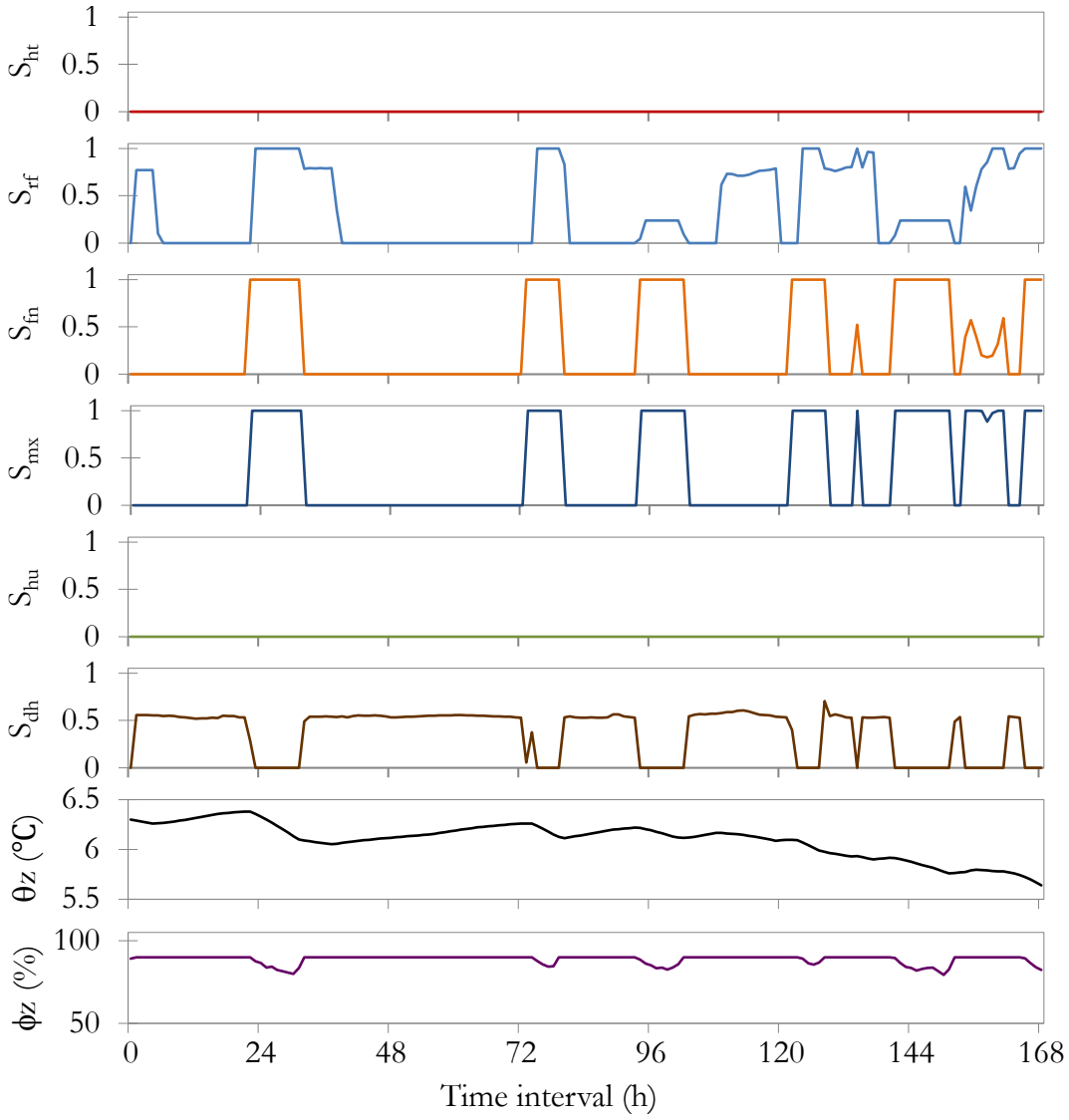

Figure 4.5: Optimal Zone 2 values of the decision variables for heating, refrigeration, fans, mixer, humidifier and dehumidifier, and resulting inside temperature and relative humidity, respectively, obtained from the storage facility model in multi-zone operation for Case 3 using RTP for a summer week.

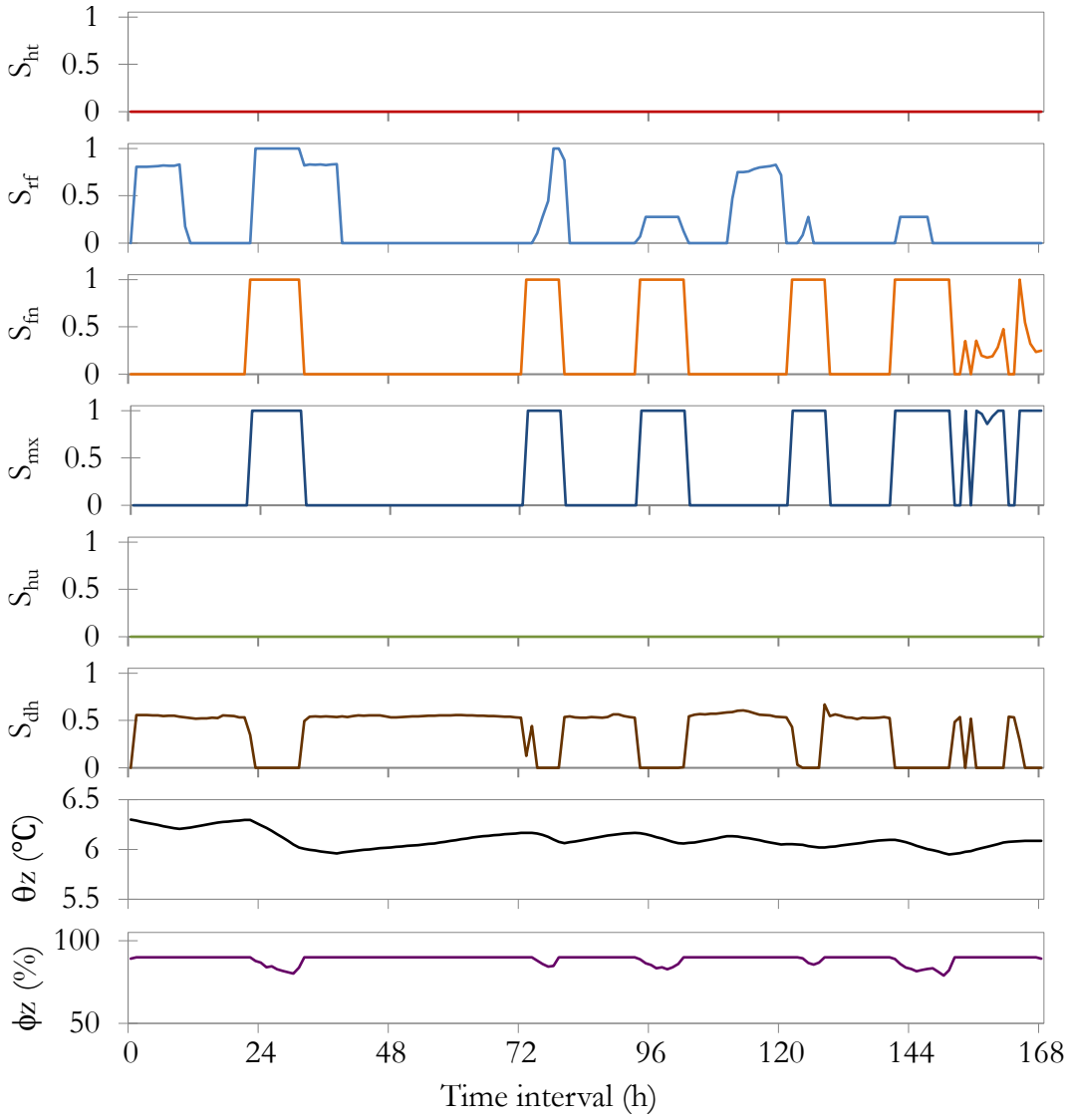

Figure 4.6: Optimal Zone 2 values of the decision variables for heating, refrigeration, fans, mixer, humidifier and dehumidifier, and resulting inside temperature and relative humidity, respectively, obtained from the storage facility model in multi-zone operation for Case 4 using RTP for a summer week.

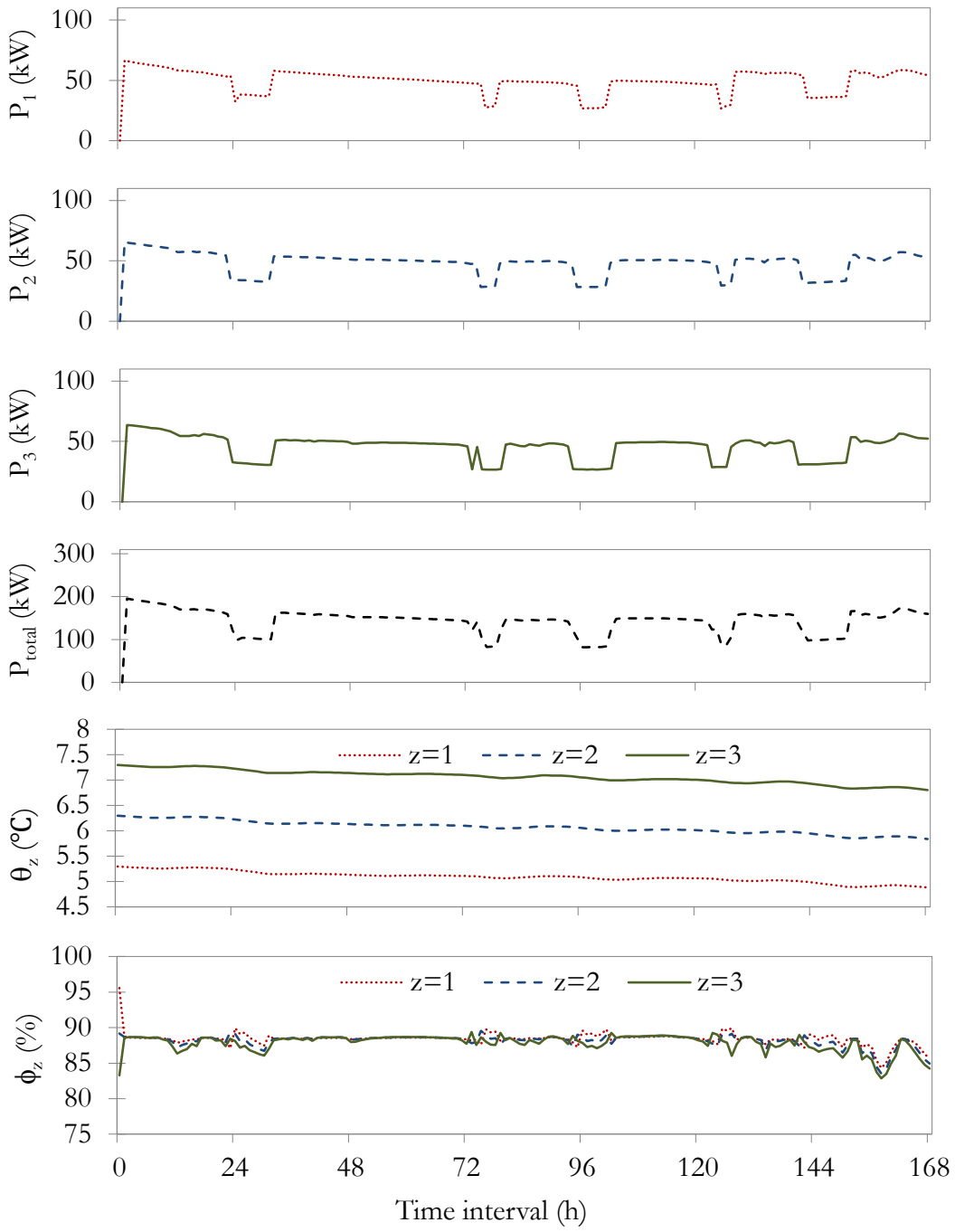

Figure 4.7: Power demand of each zone and corresponding inside temperatures and humidities obtained from the base case (Case 0) for multi-zone operation of the storage facility using RTP for a summer week.

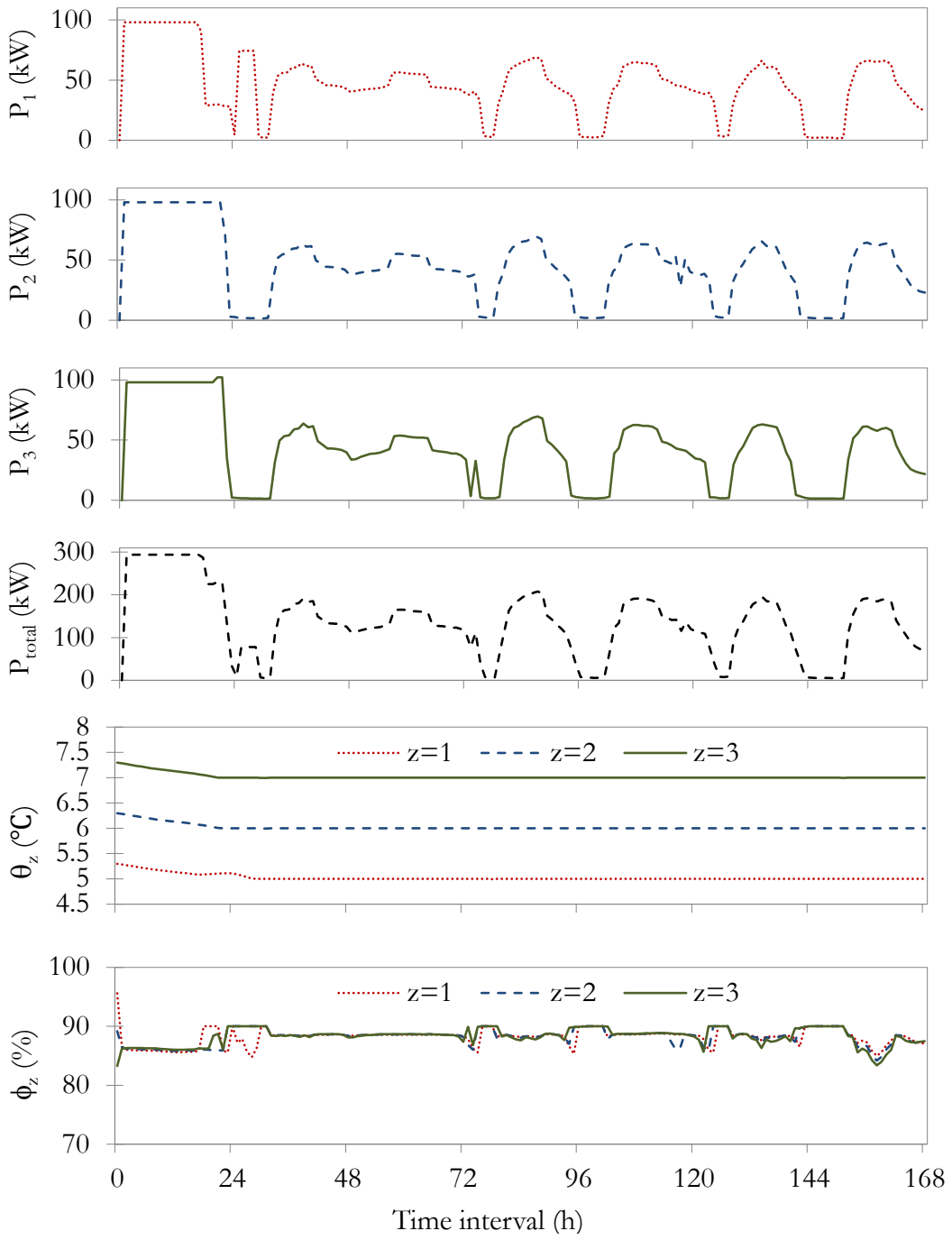

Figure 4.8: Power demand of each zone and corresponding inside temperatures and humidities obtained from Case 1 for multi-zone operation of the storage facility using RTP for a summer week.

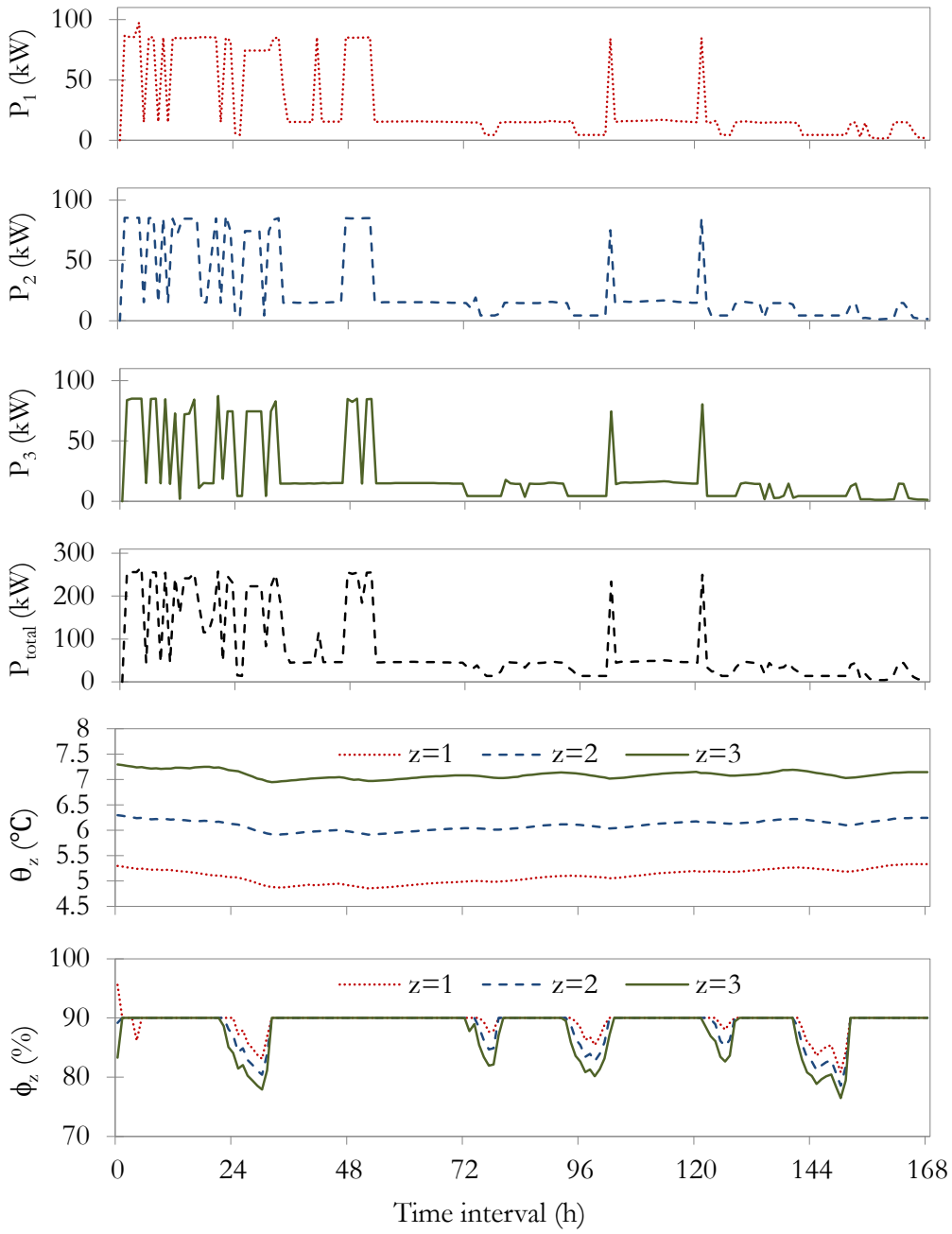

Figure 4.9: Power demand of each zone and corresponding inside temperatures and humidities obtained from Case 2 for multi-zone operation of the storage facility using RTP for a summer week.

reduced from 195.6 kW in Case 0 to 100 kW, yielding significant total cost reductions. By minimizing total costs (Case 4), the model allows temperature and relative humidity variations within the pre-defined limits, presented in Figure 4.11, while changing the operation of devices for each zones to reduce both energy costs and peak demand charges; thus, peak demand of the storage facility is reduced from 195.6 kW in Case 0 to 102.6 kW, yielding significant total cost reductions.

In Table 4.2, a comparison of energy costs, demand charges, and total costs is presented for multi-zone operation of the storage facility on a summer week for different pricing schemes. Observe that energy costs using FRP are higher than those obtained with TOU and RTP for all cases. In Case 2, the energy costs are significantly reduced for all three pricing schemes, whereas the demand charges increase as compared to the base case. In Case 3, the peak demand charges are the least among all cases, and energy costs are reduced compared to Case 0, although, total costs are higher than in Case 4. Energy costs and peak demand charges are reduced for all pricing schemes in Case 4, showing more than 40% reductions as compared to the base case.

4.4.4 Monte-Carlo Simulations

Expected Cost Savings

Monte-Carlo simulations are carried out to calculate the expected savings from the optimal operation of climate control systems of storage facilities. Outdoor weather conditions and the RTP are the uncertain parameters considered in these simulations. The expected average savings are calculated by performing multiple simulations over randomly generated data for a typical week in summer and winter. Actual data of outdoor temperature, humidity, and HOEP are used to perform these studies. Random values of RTP for each hour are generated using a uniform distribution with associated lower and upper limits for each hour obtained from actual HOEP data over each season. For outdoor temperature and humidity, random values are generated using normal distributions with mean values and standard deviations obtained from actual weather data for each hour over each season. Minimum, maximum and mean values of outdoor temperature, humidity and RTP used in these simulations are given in Appendix B.

Figure 4.12 and Figure 4.13, correspond to Case 0 and Case 4,respectively, show energy costs and demand chargers at each iteration and their mean values obtained from Monte-Carlo simulations in summer; notice that the Monte-Carlo simulations converge in about 100 iterations. Expected average energy costs and demand charges for Case 0 are $3017.3

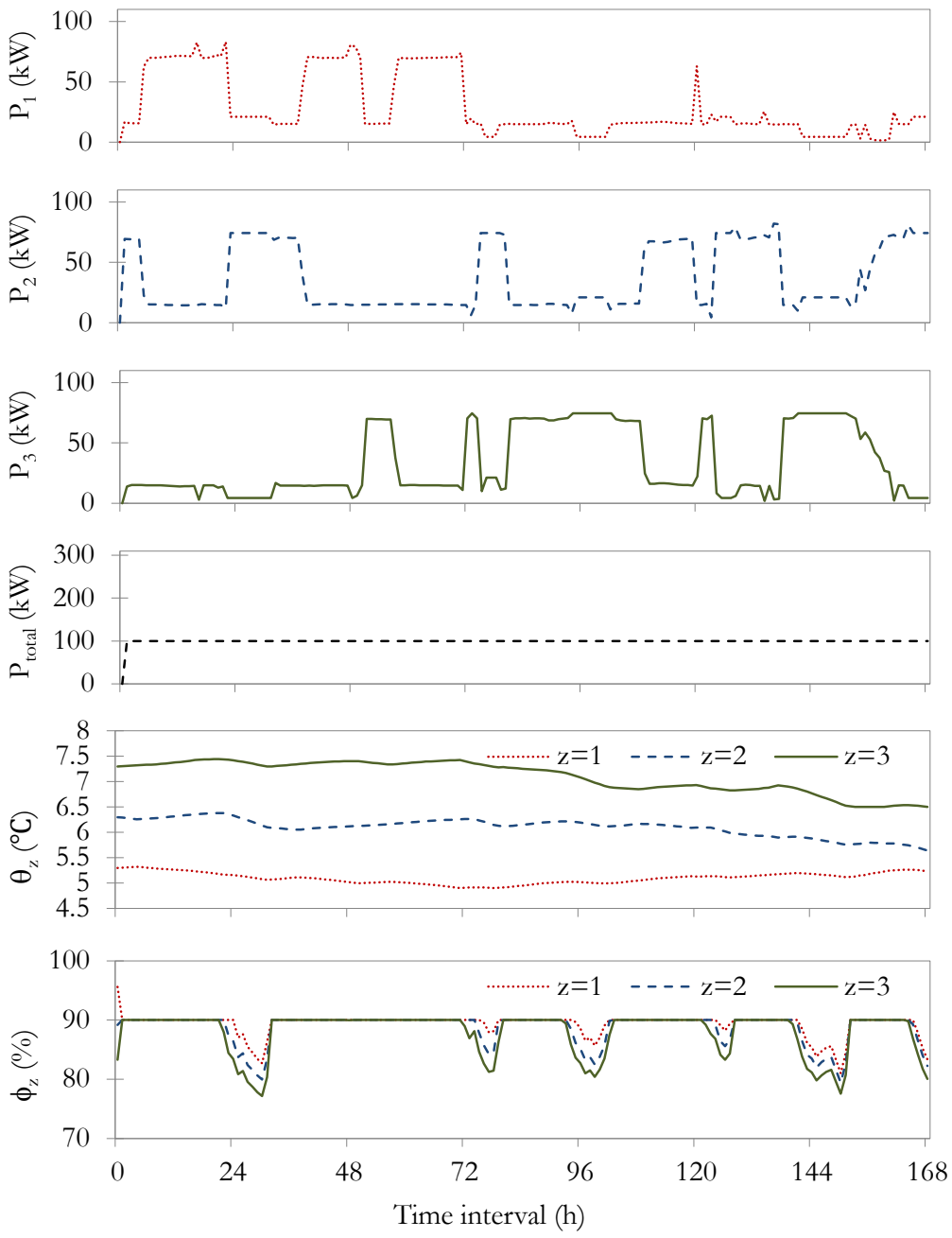

Figure 4.10: Power demand of each zone and corresponding inside temperatures and humidities obtained from Case 3 for multi-zone operation of the storage facility using RTP for a summer week.

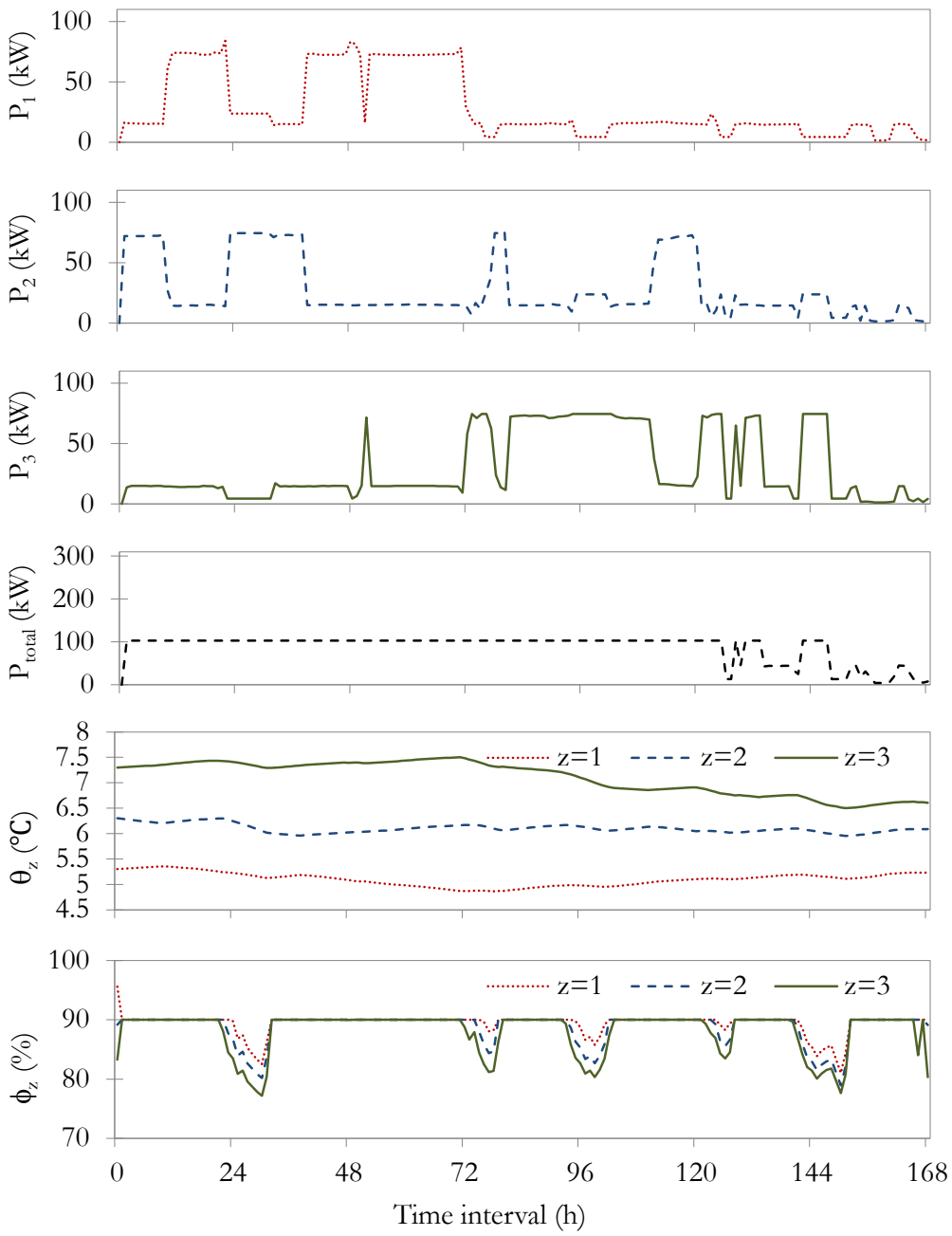

Figure 4.11: Power demand of each zone and corresponding inside temperatures and humidities obtained from Case 4 for multi-zone operation of the storage facility using RTP for a summer week.

Table 4.2: Case-wise comparison of energy costs and demand charges in multi-zone operation of the storage facility with different pricing schemes for a summer week.

Case	Pricing scheme	Energy (MWh)	Energy charges ($)	Peak demand (kW)	Demand charges ($)	Energy cost savings w.r.t Case 0 (%)	Demand charge savings w.r.t. Case 0 (%)
0	FRP	24.1387	1810.40	195.62	1564.97	-	-
	TOU	24.1387	1532.73	195.62	1564.97	-	-
	RTP	24.1387	847.532	195.62	1564.97	-	-
1	FRP	22.8464	1713.48	294.35	2354.76	5.4	-50.5
	TOU	22.8464	1551.04	294.35	2354.76	-1.2	-50.5
	RTP	22.8464	1676.13	294.34	2354.76	-97.8	-50.5
2	FRP	11.6778	875.84	256.23	2049.85	51.6	-31.0
	TOU	12.6935	702.90	256.23	2049.85	54.1	-31.0
	RTP	12.4151	379.01	268.16	2145.27	55.3	-37.1
3	FRP	16.8012	1260.09	100.01	800.06	30.4	48.9
	TOU	16.8012	1043.28	100.01	800.06	31.9	48.9
	RTP	16.8012	584.88	100.01	800.06	31.0	48.9
4	FRP	13.7318	1029.88	107.81	862.47	43.1	44.9
	TOU	14.2331	913.95	106.32	850.54	40.4	45.7
	RTP	14.7518	502.86	102.64	821.13	40.7	47.5

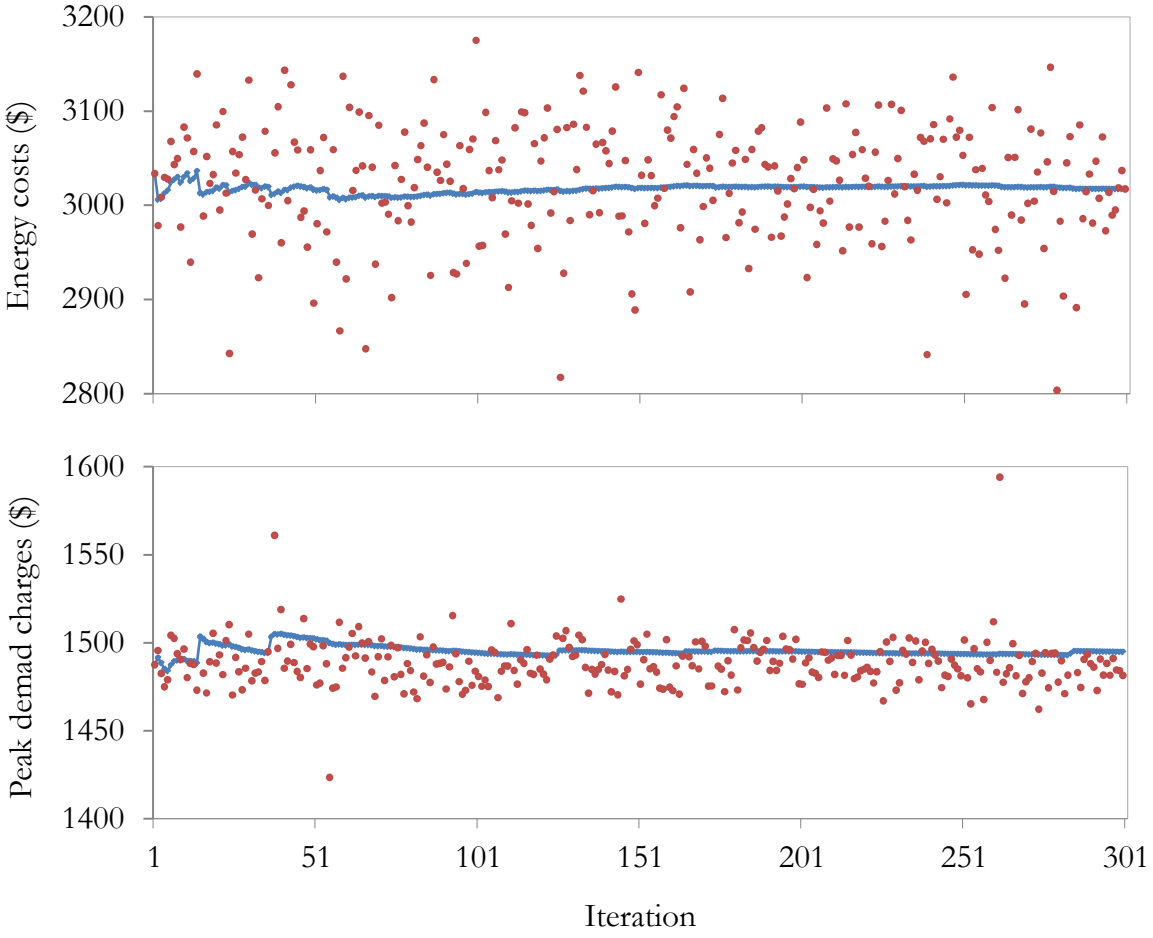

Figure 4.12: Energy costs and demand charges at each Monte-Carlo iteration, and corresponding expected mean values for Case 0 in a summer week for uncertainty in RTP and weather conditions.

and \$1494.8, respectively; while these values for Case 4 are \$2038.3 and \$1248.2, respectively. Therefore, expected total costs over a summer month (4 weeks) for Case 0 and Case 4 are \$13564 and \$9401, respectively, showing that even when considering large uncertainties in weather conditions and electricity prices (the largest actual observed values), the model yields significant costs savings (30% expected total cost savings).

Energy costs for summer months best fit a Burr probability density function (pdf) with k =9.513, shape = 55.942 and scale = 3170.5 parameters, and a Log-Logistic (3P) with shape = 46.136, scale = 1150.2 and location = 882.8 parameters in Case 0 and Case 4,

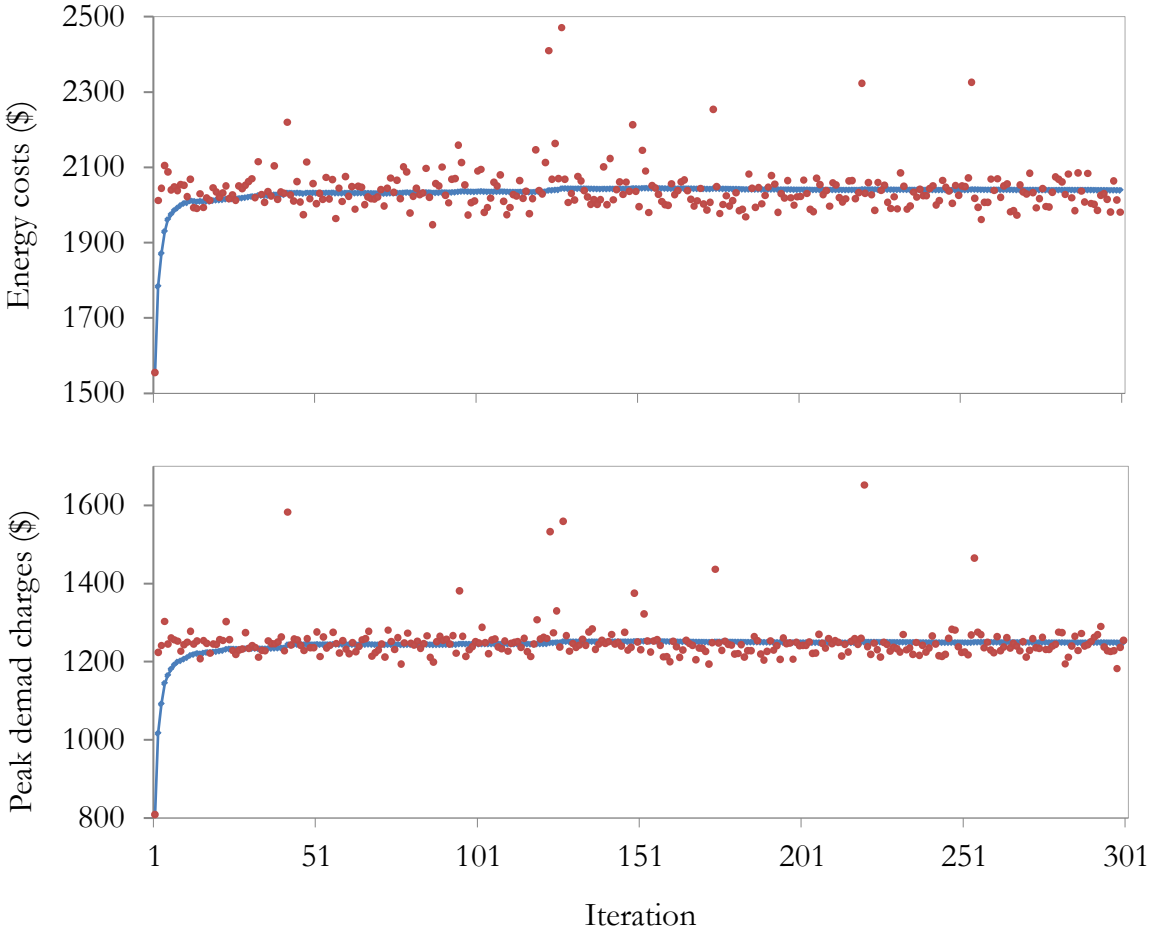

Figure 4.13: Energy costs and demand charges at each Monte-Carlo iteration and corresponding expected mean values for Case 4 in a summer week for uncertainty in RTP and weather conditions.

respectively. A Log-Logistic (3P) with shape = 8.514, scale = 72.03 and location = 1415.9 parameters, and a Cauchy with a scale = 12.376 and location = 1242.9 parameters, are the best fitting pdfs for summer months peak demand charges in Case 0 and Case 4, respectively. These pdfs are fairly narrow around the mean values indicating that significant savings can be expected most of the time, in spite of wide variations in electricity price and weather conditions.

Effects of Forecasts Errors

Monte-Carlo simulations are carried out to study the effect of electricity price and weather forecasts errors on optimal operation of climate control systems of storage facilities. Actual data of a week in summer 2010 in Ontario is used to carryout the simulations, where electricity price and weather condition forecast errors are modeled using an Error pdf with mean = HOEP at each hour and standard deviation = 16.2 $/MWh, and mean = actual temperature and humidity at each hour and standard deviation= 20% of the actual data, respectively. Thus, random values of electricity price, outdoor temperature and humidity are generated using these pdfs to carry out the simulations.

The results obtained from these Monte-Carlo simulations, which converge in 150 iterations, show expected average energy costs of $799 and $318.3 for Case 0 and Case 4, respectively,representing a 60% expected energy cost reduction. The expected average peak demand charges are $1357 and $918 for Case 0 and Case 4, respectively, showing a 32% peak demand charge reduction. These represent a 51% expected total costs reductions even in the presence of uncertainty in electricity price and weather forecasts. Observe that the *actual* energy costs and peak demand reductions, obtained using the observed prices and weather conditions for this summer week, are 40.7% and 47.5%, respectively, as shown in Table 4.2.

4.5 Real-Time Implementation

The proposed model for optimal operation of climate control systems of storage facilities is non-linear, and hence there is no guarantee that the optimal solution of this NLP problem can be obtained in a real-time application.Moreover, the hardware and software used for the purpose of pilot implementation in the EHMS project are single-board computers equipped with the freeware GLPK solver, which can only solve LP and MILP problems. Therefore, in this section a linearization method is proposed to convert the developed NLP problem into LP-relaxation subproblems that can be solved efficiently and are suitable for real-time implementation. The proposed method is based on an iterative B&B algorithm including RLT to generate the LP-relaxation subproblems.

4.5.1 LP–relaxation Subproblems

The RLT-relaxation discussed in Section 2.4.3 in Chapter 2, and the linearization of a exponential function using its Taylor series expansion around the point of interest is used

to generate the LP-relaxation subproblems. Thus, the saturated vapor pressure nonlinear equation used in the calculation of relative humidity is given in (**??**); this equation then can be linearized using Taylor series expansion around the mid-point of each zone's temperature range as follows:

$$P_{sat} = p_1 \left(-p_2 + p_3 e^{p_4 \frac{(\theta_z^{max} + \theta_z^{min})}{2}} \left(1 + p_4 \left(\theta_z(t) - \frac{(\theta_z^{max} + \theta_z^{min})}{2} \right) \right) \right) \tag{4.29}$$

Since the variation ranges of inside temperatures are narrow, this linearization provides enough accuracy for the purpose of the study performed in this thesis. By substituting (4.29) in the model equations, the developed NLP problem is transformed into a PP problem. Thus, the RLT discussed in Chapter 2 can be used to reduce the order of the PP problem to obtain LP-relaxation subproblems.

4.5.2 Iterative Algorithm

The iterative algorithm proposed to solve the developed model is presented in Figure 4.14, in which the original problem is first relaxed using RLT to obtain easier-to-solve, lower-bounding LP-relaxation subproblems. The subproblems solved at each iteration satisfy the same constraints as the LP-relaxation of the original problem with additionally tighter bounds on the relaxed variables. In each iteration, two sub-problems are formed using the best current solution to tighten the bounds of the relaxed variables, and the feasible subspace is divided into smaller subspaces. The strategy for selecting the subspace to be used at each iteration is based on the maximum relaxation error of the relaxed variables.

4.5.3 Numerical Results

Simulations are carried out to examine the effectiveness of the proposed solution procedure for real-time applications. Figure 4.15 to Figure 4.19 present the results obtained from solving the original NLP model using the IPOPT solver and the proposed LP-relaxation algorithm, solved with the CPLEX LP solver.

The optimal operational schedule of the devices obtained from the NLP model, and the proposed LP-relaxation model at the first and last iterations after converging to the optimal solution are depicted in Figure 4.15, Figure 4.16 and Figure 4.17, respectively. The proposed algorithm converged at the 474^{th} iteration to a solution with a maximum relaxation error less than 0.04. It was observed that 472 LP-relaxation subproblems were solved approximately in 100 seconds. Observe that the operational decisions obtained from

1. Initialize:
   (a) Load initial values of the upper and lower limits of the variables, $\underline{\mathbf{x}}_{\mathbf{0}}$ and $\overline{\mathbf{x}}_{\mathbf{0}}$.
   (b) Solve the LP-relaxation for the original problem with $\Omega_0 = [\underline{\mathbf{x}}_{\mathbf{0}}, \overline{\mathbf{x}}_{\mathbf{0}}]$.
   (c) Denote the obtained relaxation solution and the objective value as $\{\hat{\mathbf{x}}_0, LB_0\}$.
2. Iteration:
   (a) Find the maximum relaxation error among all the RLT variables, such as $|\hat{\mu}_{s,x} - \hat{s} \cdot \hat{x}|$.
   (b) If the maximum relaxation error is less than a specified value ϵ, stop and obtain $\{\hat{\mathbf{x}}_{k-1}, LB_{k-1}\}$.
   (c) In case the maximum relaxation error is $|\hat{\mu}_{s,x} - \hat{s} \cdot \hat{x}|$:
      i. If $\min\{\hat{s} - \underline{s}, \overline{s} - \hat{s}\} \cdot (\overline{s} - \underline{s}) \geq \min\{\hat{x} - \underline{x}, \overline{x} - \hat{x}\} \cdot (\overline{x} - \underline{x})$, then use Ω_{k-1} to form two new regions Ω_{k_1} and Ω_{k_2} by replacing $[\underline{s}, \overline{s}]$ with $[\underline{s}, \hat{s}]$ and $[\hat{s}, \overline{s}]$, respectively.
      ii. Else, use Ω_{k-1} to form two new regions Ω_{k_1} and Ω_{k_2} by replacing $[\underline{x}, \overline{x}]$ with $[\underline{x}, \hat{x}]$ and $[\hat{x}, \overline{x}]$, respectively.
      iii. Solve the LP-relaxation subproblem for Ω_{k_1} and Ω_{k_2}, and obtain $\{\hat{\mathbf{x}}_{k_1}, LB_{k_1}\}$ and $\{\hat{\mathbf{x}}_{k_2}, LB_{k_2}\}$.
   (d) If $LB_{k_1} \leq LB_{k_2}$, then let $\Omega_k = \Omega_{k1}$, $\hat{\mathbf{x}}_k = \hat{\mathbf{x}}_{k_1}$, and $LB_k = LB_{k_1}$.
   (e) Else if $LB_{k_2} < LB_{k_1}$, then let $\Omega_k = \Omega_{k2}$, $\hat{\mathbf{x}}_k = \hat{\mathbf{x}}_{k_2}$, and $LB_k = LB_{k_2}$.
   (f) Solve the LP-relaxation subproblem with Ω_k

Figure 4.14: The proposed iterative LP-relaxation algorithm.

the NLP model and the LP-relaxation at the last iteration are similar; also, the temperature and relative humidity results shown in Figure 4.19 and Figure 4.19 are practically the same.

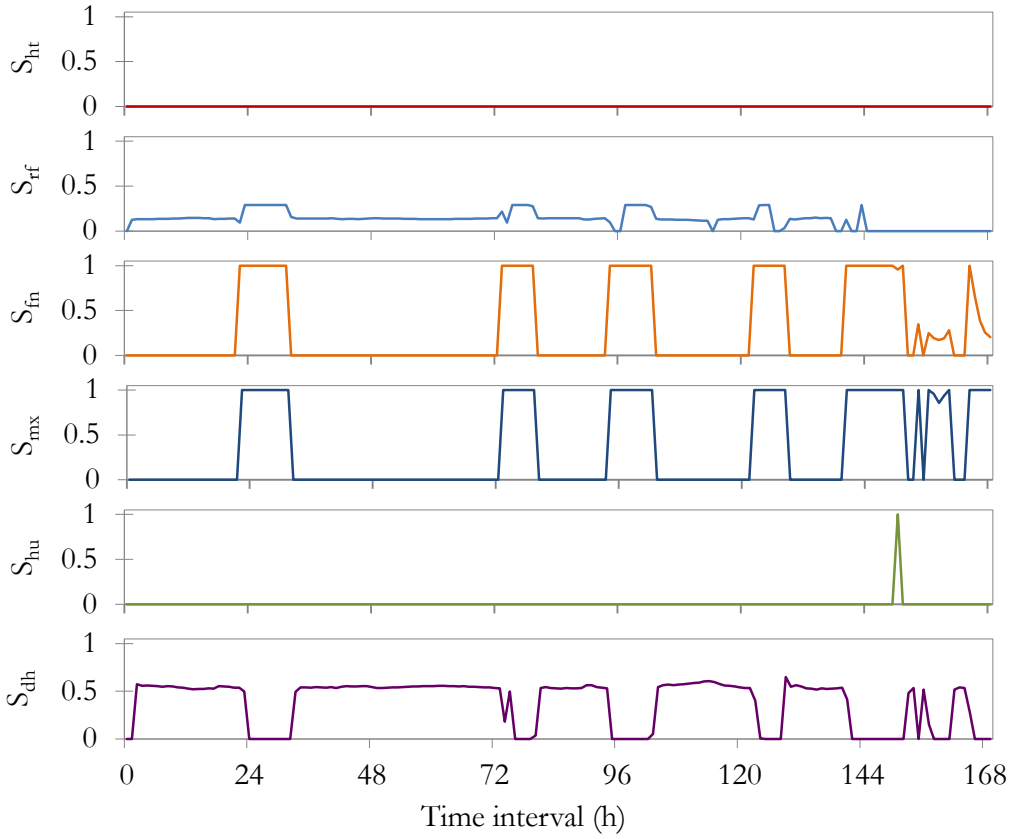

Figure 4.15: Optimal operational schedule of devices obtained from the NLP model.

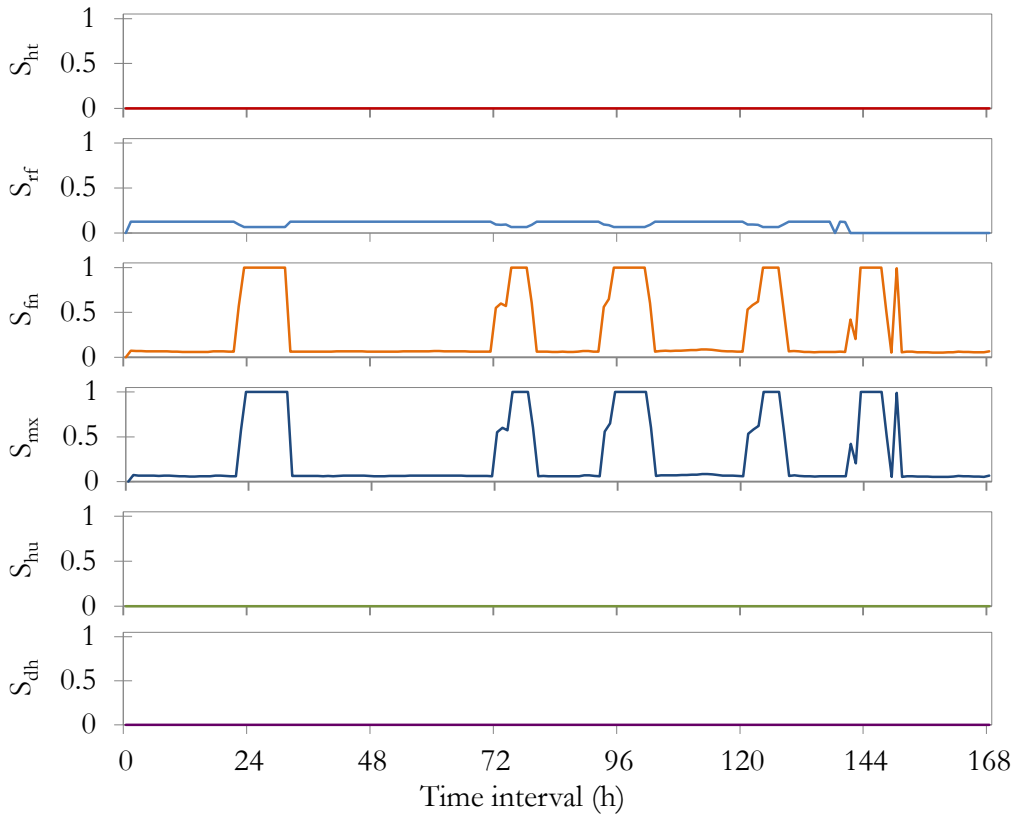

Figure 4.16: Optimal operational schedule of devices obtained from the LP relaxation model at first iteration.

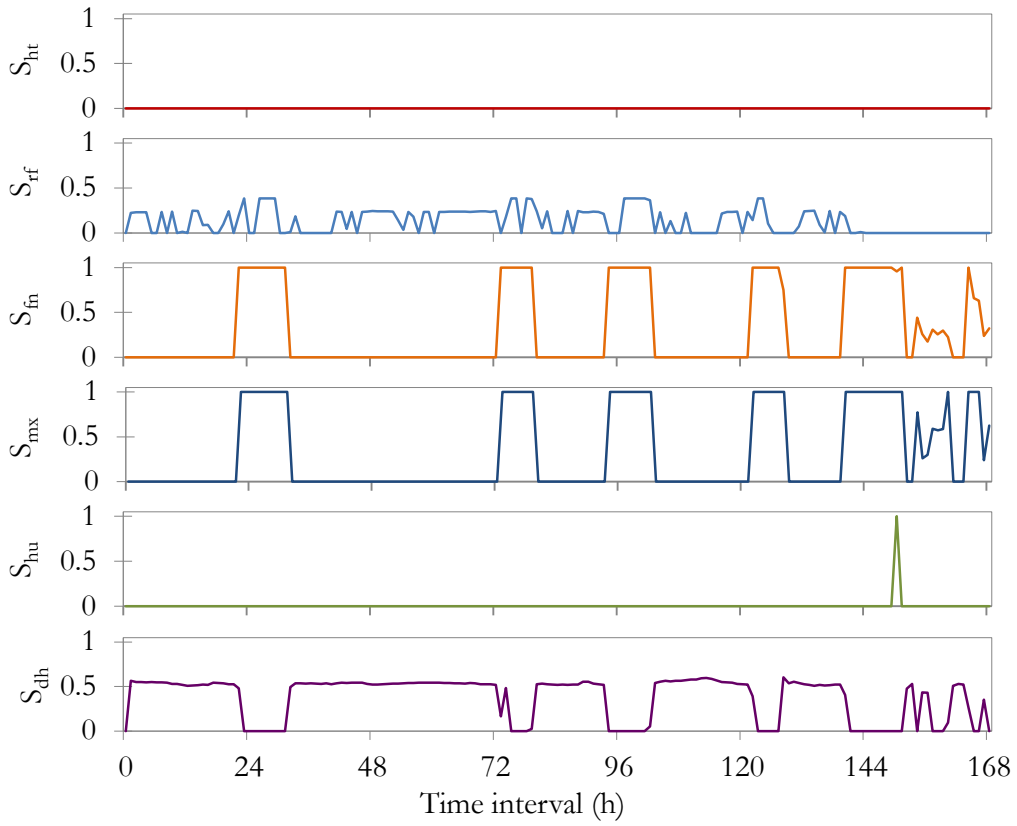

Figure 4.17: Optimal operational schedule of devices obtained from the LP relaxation model at the last iteration.

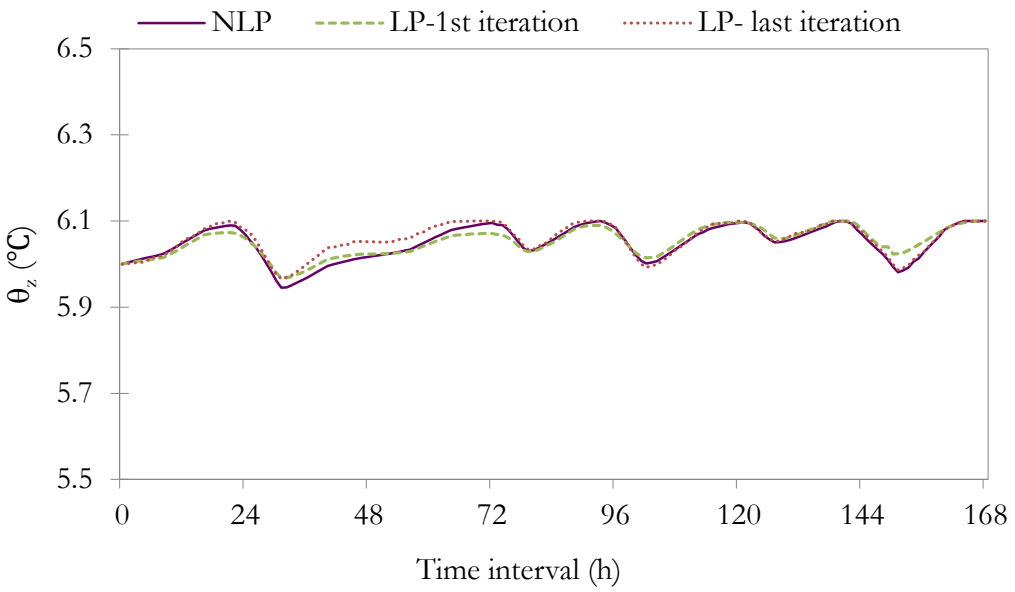

Figure 4.18: Comparison of inside temperatures obtained from the NLP model and the proposed iterative LP-relaxation algorithm.

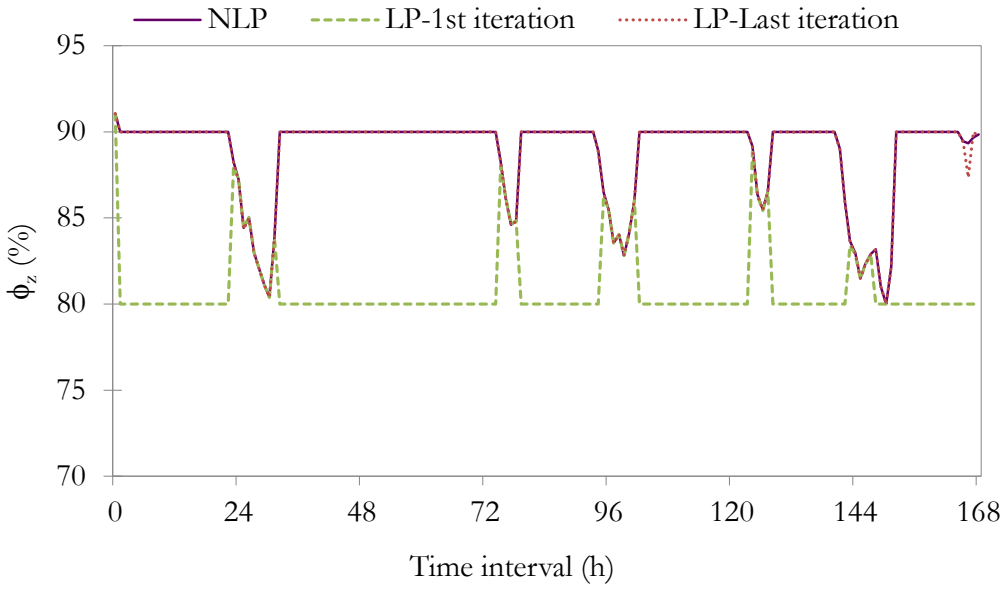

Figure 4.19: Comparison of relative humidities obtained from the NLP model and the proposed iterative LP-relaxation algorithm.

4.6 Summary

Mathematical models for optimal operation of climate control systems of storage facilities in the context of Smart Grid were proposed in this chapter. The developed models incorporate weather forecasts, electricity price information, and the end-user preferences to optimally operate existing climate control systems of produce storage facilities. These models are based on physical principles and previously published models for individual components of storage facilities, and consider important characteristics of these facilities such as inside temperature and humidity, which are kept within user-defined ranges, to schedule the operation of various devices to minimize total energy costs and demand charges. The presented simulation results for a realistic case study show the effectiveness of the proposed model to reduce total energy costs while maintaining required operational constraints.

Expected total cost savings in the presence of uncertainty in electricity price and weather inputs were calculated via Monte-Carlo simulations, showing that significant cost savings can be achieved using the proposed model even in the presence of large uncertainties in these inputs. The effects of forecast errors in electricity price and weather conditions on optimal operation of climate control systems were also studied via Monte-Carlo simulations, showing considerable total costs reductions in the presence of expected electricity price and weather forecast errors.

The developed model for optimal operation of climate control systems of storage facilities is non-linear, and hence it may not be appropriate for real-time applications. Therefore, a solution algorithm based on LP-relaxation of the original problem was proposed for real-time implementation purposes. The presented numerical results show that the developed model can be solved efficiently in real-time and is suitable for real-time applications.

Chapter 5

Optimal Operation of Agricultural Energy Hubs: Greenhouses

5.1 Introduction

This chapter presents mathematical optimization models of greenhouses to optimize the operation of their energy systems in the context of Smart Grids. In greenhouses, supplementary lighting, CO_2 production, and climate control systems consume considerable energy. Thus, a mathematical model of these systems appropriate for their optimal operation is developed that can be implemented as a supervisory control in existing greenhouse energy management systems, incorporating weather forecasts, electricity price information, and end-user preferences.

The objective of the proposed optimization model is to minimize total energy costs and demand charges while considering important parameters of greenhouses, i.e., inside temperature and humidity, CO_2 concentration, and lighting levels, which need to be kept within certain required ranges. Several case studies are conducted to examine the performance of the developed mathematical model for a realistic greenhouse, where parameters and device ratings are suitably chosen, and using realistic data inputs for outside temperatures, humidities, and solar irradiations. Monte-Carlo simulations are carried out to calculate the expected total cost savings for a summer month and a winter month using actual data, and to study the effects of uncertainty in electricity price and weather forecasts on optimal operation of the greenhouse. Finally, a robust optimization model is proposed to obtain operating schedules that account for errors in electricity price forecasts errors for the optimal operation of greenhouses.

The rest of this chapter is organized as follows: In Section 5.2 the proposed supervisory control strategy is described. This is followed in Section 5.3 by a description of the developed mathematical model of greenhouses, including definition of the model identifiers, objective functions, and constraints. The most relevant simulation case studies which demonstrate the effectiveness of the proposed mathematical model for optimal operation of greenhouses, including Monte-Carlo simulations, are presented and discussed in Section 5.4. In Section 5.5, a robust optimization model for optimal operation of greenhouses accounting for electricity price uncertainty is proposed, and some corresponding numerical results are presented. Finally, Section 5.6 summarizes the contents of this chapter.

5.2 Proposed Supervisory Operation Strategy

Energy systems of greenhouses are usually multi-carrier energy systems consisting of electricity, natural gas, and bio-fuels. As discussed in Section 2.3.3, most greenhouses manage their operation through ACSs which consist of central computers, sensors and data acquisition systems linked through communication channels. These ACSs coordinate and integrate the real-time control of greenhouse equipment and systems such as heaters, coolers, motors for window opening and closing, pumps and irrigation systems.

The goal in ACSs is to maintain the greenhouse climate within proper conditions to achieve the best plant growth. In this context, important parameters such as greenhouse temperature, relative humidity, lighting levels, and CO_2 concentrations are controlled by greenhouse climate control systems. Currently, common existing control algorithms in these systems work on logical On-Off and PID based controllers, and do not optimize the energy utilization in such multi-carrier agricultural facility. Therefore, a hierarchical supervisory framework is proposed and discussed next based on a mathematical model of greenhouses that uses internal and external information such as weather and energy price forecasts for optimal operation of greenhouses.

5.2.1 Hierarchical Operation Scheme

Nowadays, day-ahead electricity price forecasts and accurate weather forecasts for the next few days, updated every few hours, are available. In this thesis, these forecasts are used to design a hierarchical operation strategy to improve the operation of greenhouse climate control systems to reduce total energy costs and demand. The architecture of the proposed hierarchical scheme for the optimal operation of greenhouses is presented in

Figure 5.1. The existing feedback control systems remain at the lower hierarchical level, while at the higher level the proposed supervisory operation control generates set points for the feedback controllers, considering appropriate setting ranges and user preferences to optimize the operation of the climate control system.

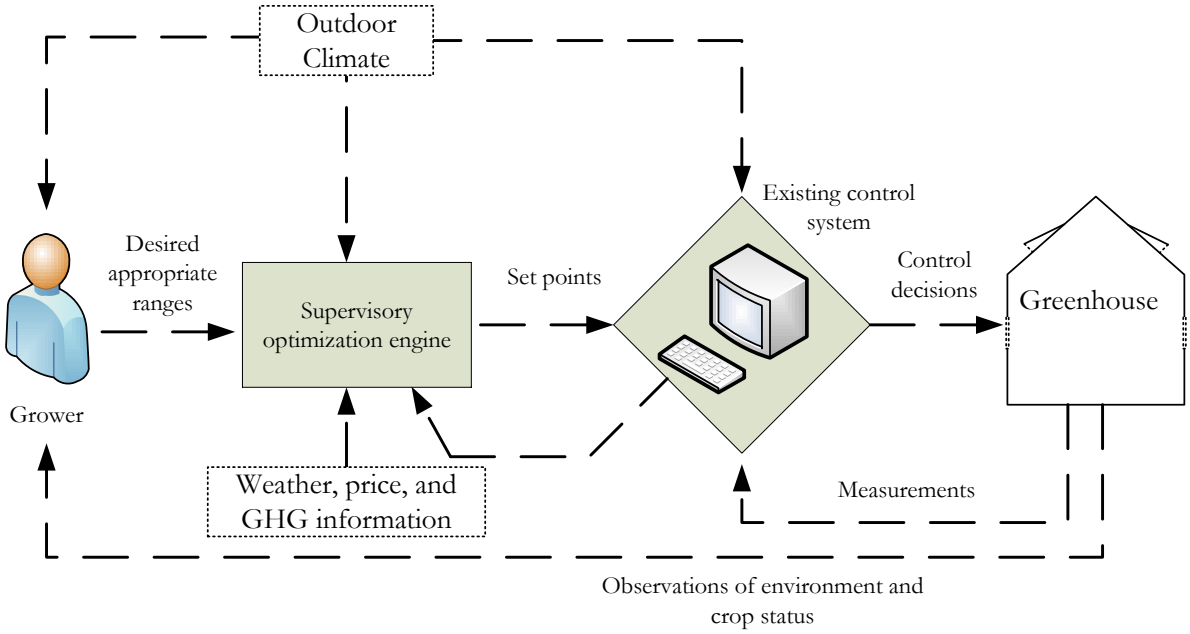

Figure 5.1: Greenhouse supervisory and existing controller architecture.

The proposed optimization model is at the supervisory level and its outputs are used as set points for the existing feedback control system, which perform the actual control actions such as turning on and off the devices. The supervisory control updates the outputs every hour, while the feedback controller continuously monitors the parameters under control and tracks the target set points in real time. The supervisory control also monitors the system, and in case of large discrepancies between the calculated and measured parameters, re-runs the model and updates the set points.

5.2.2 External Information

External information used in the proposed supervisory operation control (Figure 5.1) is weather forecasts such as average hourly outdoor temperature, humidity, wind speed, and

solar irradiations. Day-ahead forecasts of the wholesale electricity market prices and peak demand charges are also used to calculate the expected energy costs of greenhouses. This external information is assumed to be exogenous inputs to the proposed optimization model.

5.2.3 Scheduling Horizon

The scheduling horizon in the optimization model can vary from a few hours to days, with the selection depending on the type of the activities which take place within the greenhouse and the accuracy of weather and energy price forecasts. Without any loss of generality, daily scheduling horizon with time intervals of one hour are used in this thesis for optimal operation of greenhouses.

5.3 Mathematical Modeling of Greenhouses

In a typical greenhouse, the following categories of energy consuming components can be identified: supplementary lighting; climate controls of temperature, humidity, and CO_2 levels through heating and cooling systems; and natural and forced air ventilation and circulation. Each of these components has its own specific behaviour, operational constraints, and settings required to operate appropriately. The mathematical models that represent the components of the system considering their operational constraints are described next.

The model common sets, indices, parameters, and variables used in the mathematical optimization model of greenhouses are presented in Table 5.1.

Table 5.1: Description and definition of the greenhouse model indices, parameters, and variables.

Sets	**Description**
A	Set of devices; $A = \{cf, chl, chl_v, co_2, dh, fv, fog, hu, ht, ht_v, li, nv\}$
T	Set of indices in scheduling horizon; $T = \{1 \dots 24\}$

Continued on next page

Table 5.1 – continued from previous page

Indices	**Description**
i	Index of devices
l	Index of lighting system
t	Index of time interval
z	Index of zone
Subscripts	**Description**
a	Air
cf	Circulation fans
chl	Chiller
chl_p	Chilling pipe
chl_v	Valve of chilling pipe
co_2	CO_2 generator
dh	Dehumidifier
ev	Evaporation
fv	Forced ventilation
fog	Fogging system
gh	Greenhouse
ht	Heating system (boiler)
ht_p	Hearing pipe
ht_v	Heating system valve
li	Lighting
nv	Natural ventilation
out	Outdoor
p	Plants
$phot$	Photosynthesis
sl	Soil
sr	Solar radiation
w	Water

Continued on next page

Table 5.1 – continued from previous page

Subscripts	**Description**
wl	Wall
Variables	**Description**
$D_i(t)$	Binary variable denoting shut down of device i at time t: $D_i(t) = \begin{cases} 1 & \text{shutdown of device } i \text{ at time } t \\ 0 & \text{otherwise} \end{cases}$
Dmd	Peak demand variable (kW)
$\phi_z(t)$	Relative humidity of zone z at time t (%)
$\theta_z(t)$	Temperature of zone z at time t (°C)
$S_{i,z}(t)$	Operation state of device i of zone z at time t; $0 \leq S_{i,z}(t) \leq 1$
$w_z(t)$	Water content of air in zone z at time t (g_w/kg_a)
$\widehat{w}_z(t)$	Saturated vapour concentration in zone z at time t (g_w/kg_a)
$\mathcal{C}(t)$	CO_2 concentration in zone z at time t (g_{CO_2}/kg_a)
$\Psi_z(t)$	Lighting in zone z at time t (W/m^2)
$U_i(t)$	Binary variable denoting start up of device i at time t: $U_i(t) = \begin{cases} 1 & \text{startup of device } i \text{ at time } t \\ 0 & \text{otherwise} \end{cases}$
$\mu_{s,x}$	Axillary variable to represent $s \cdot x$
$\zeta(t) \geq 0$	Axillary variable used in the robust optimization model
$y(t) \geq 0$	Axillary variable used in the robust optimization model
$\beta \geq 0$	Axillary variable used in the robust optimization model
Parameters	**Description**
$A_{gh,z}$	Area of greenhouse in zone z (m^2)
$A_{wl,z}$	Area of greenhouse walls in zone z (m^2)
$A_{nv,z}$	Area of greenhouse ventilation window in zone z (m^2)
$A_{ht_p,z}$	Area of heating pipe in zone z (m^2)
$A_{chl_p,z}$	Area of cooling pipe in zone z (m^2)
C_a	Specific heat of air, 1.006 ($kJ/(kg\,K)$)

Continued on next page

Table 5.1 – continued from previous page

Parameters	Description
$C_{em}(t)$	Marginal cost of CO_2 at hour t (cents/kWh)
C_w	Specific heat of water, 4.1855 $(kJ/(kg\,K))$
C_z	Total heat capacity of zone z (kJ/K)
c_{re}	Respiration coefficient of crops in z $(g/(m^2\,h\,K))$
c_{phot}	Photosynthesis coefficient of crops in z (g/J)
$\mathcal{C}_{inj}^{max}$	Maximum carbon injected by CO_2 generator in zone z (g/m_{gh}^2)
$\mathcal{C}_z^{max}$	Maximum CO_2 concentration in zone z (g/m_{gh}^2)
$\mathcal{C}_z^{min}$	Minimum CO_2 concentration in zone z (g/m_{gh}^2)
C_p	Specific heat of the plants (woods and leaves) $(kJ/(kg\,K))$
c_{dc}	Demand charge (\$/kW)
$c_{ed}(t)$	Electricity price at time t (\$/kWh)
ε	Volumetric ratio of air to crops in the greenhouse (m_a^3/m_{gh}^3)
η_{chl}	Performance coefficient of the chilling system
η_{fog}	Fog to vapour conversion factor of the fogging system (no dim.)
η_{li}	Percentage of the lighting system power that is converted to heat (%)
η_{sr}	Light transmission factor of greenhouse cover (%)
et_i	Earliest operation time of device i (h)
Γ	Robustness degree used in robust optimization model
H_{gh}	Average hight of the greenhouse (m)
h_{ev}	Evaporation heat of water, 2270 (kJ/kg_w)
J	Objective function of the optimization model
λ	Percentage of wind speed which enters into the greenhouse (no dim.)
lt_i	Latest operation time of device i (h)
mdu	Minimum duration time for cloudy weather (h)
md_i	Minimum down time of device i (h)
mu_i	Minimum up time of device i (h)
$msot_i$	Maximum successive operation time of device i (h)

Continued on next page

Table 5.1 – continued from previous page

Parameters	Description
m_w	Molar mass of water, 18.0153×10^{-3} (kg/mol)
N_T	Total number of intervals in scheduling horizon T
p_1	Constant, 100 (no dim.)
p_2	Constant, 1.7001 (Pa)
p_3	Constant, 7.7835 (Pa)
p_4	Constant, 1/17.0789 (K^{-1})
p_5	Constant, 0.6228 (kg_w/kg_a)
p_6	Conversion factor from $(1/s)$ to $(1/h)$
p_7	Coefficients associated with the respiration rate of the crop
p_8	Coefficients associated with the respiration rate of the crop
P_a	Actual water vapour pressure (Pa)
P_{atm}	Atmospheric air pressure (Pa)
P_{sat}	Saturated water vapour pressure (Pa)
P_i	Rated power of device i (W)
P_{par}	Partial vapour pressure (Pa)
$q_z^i(t)$	Thermal effect of i on temperature in zone z (kJ/h)
Q_z	Volumetric air flow rate of ventilation fans in zone z $(m_a^3/(h\, m_{gh}^2))$
R_{wl}	Heat transfer coefficient of greenhouse walls $(kJ/(h\, K\, m^2))$
R_{sl}	Heat transfer coefficient of greenhouse soil $(kJ/(h\, K\, m^2))$
R_{pipe}	Heat transfer coefficient of pipes $(kJ/(h\, K\, m^2))$
R_{sr}	Heat transfer coefficient of greenhouse cover $(kJ/(h\, K\, m^2))$
$R_{pipe,sl}$	Heat transfer coefficient between pipes and soil $(kJ/(h\, K\, m^2))$
ρ_a	Density of air, 1.27 (kg/m^3)
ρ_w	Density of water, 1000 (kg/m^3)
ρ_p	Density of plants (kg/m^3)
R_g	Rate of CO_2 emissions from natural gas consumption (tonne/MWh)
rot_i	Required operation time of device i (h)

Continued on next page

Table 5.1 – continued from previous page

Parameters	Description
Ψ_z^{mdu}	Aggregated lighting over the minimum prove time in zone z (W/m^2)
$\Psi_z^{min_{mdu}}$	Minimum outdoor illumination to allow supplementary lighting to turn on in zone z (W/m^2)
$\Psi_z^{max_{aggr}}$	Maximum aggregated illumination in zone z (W/m^2)
$\Psi_z^{min_{aggr}}$	Minimum aggregated illumination in zone z (W/m^2)
$\Psi_{z,l}^{max}$	Maximum lighting provided by lighting system l in zone z (W/m^2)
$SR(t)$	Solar radiation at time t (W/m^2)
scc	Social cost of carbon dioxide emissions ($/tonne)
θ_{sl}	Soil temperature (°C)
θ_{out}^{min}	Minimum acceptable outdoor weather temperature to allow outdoor air ventilation (°C)
θ_z^{set}	Inside temperature set point in zone z (°C)
θ_z^{min}	Minimum inside temperature in zone z (°C)
θ_z^{max}	Maximum inside temperature in zone z (°C)
$\theta_z^{l_0}$	Lower limit of average temperature in zone z (°C)
$\theta_z^{u_0}$	Upper limit of average temperature in zone z (°C)
$\theta_{ht_p}^{min}$	Minimum hot water temperature (°C)
$\theta_{ht_p}^{max}$	Maximum hot temperature (°C)
$\theta_{chl_p}^{min}$	Minimum chilled water temperature (°C)
$\theta_{chl_p}^{max}$	Maximum chilled water temperature (°C)
τ	Length of time interval (h)
v_{wd}	Wind speed at time t (m/s)
$V_{gh,z}$	Volume of greenhouse zone z (m^3)
$V_{ht_p,z}$	Volume of water in heating pipes and tank in zone z (m^3)
$V_{chl_p,z}$	Volume of water in chilling pipes and tank in zone z (m^3)
$W_{evp}(z)$	Crop evaporation at each hour in zone z [146] $(g_w/(h\, m_{gh}^2))$
W_{fog}^{max}	Maximum water rate of fogging systems $(g_w/(m_{gh}^2 h))$

Continued on next page

Table 5.1 – continued from previous page

Parameters	Description
W_{dh}^{max}	Maximum rate of dehumidifier ($g_w/(m_{gh}^2\, h)$
$w_{out}(t)$	Absolute water content of outdoor air at time t (g_w/kg_a)

5.3.1 Objective Function

Minimization of the customer's energy costs, peak demand charges, total energy costs, and CO_2 emissions over the scheduling horizon are considered as possible objective functions for the proposed optimization model of greenhouses.

Minimization of temperature deviations

To track the temperature settings closely, one can either minimize the sum of squares of the temperature variations from given set points:

$$J_1 = \sum_{t \in T} \left(\theta_z(t) - \theta_z^{set}(t)\right)^2 \tag{5.1}$$

or minimize the sum of absolute values of the temperature deviations from given set points:

$$J_1 = \sum_{t \in T} |\theta_z(t) - \theta_z^{set}(t)| \tag{5.2}$$

The latter can be easily linearized either using piece-wise linearization or defining auxiliary variables and constraints. This objective could be utilized for plants that require a fixed temperature setting, since some temperature "drift" is allowed in existing climate control systems.

Minimization of energy costs

The following objective function corresponds to the minimization of the customer's energy costs over the scheduling horizon:

$$J_2 = \sum_{t \in T} \sum_{i \in A} \tau\, C_D(t)\, P_i\, S_i(t) \tag{5.3}$$

Minimization of peak demand charges

The following objective seeks to minimize the customers' demand charges, as follows:

$$J_3 = c_{dc} * Dmd \tag{5.4}$$

where Dmd is a non-negative variable used along with the following constraint to represent the peak demand during the scheduling horizon:

$$Dmd \geq \sum_{\substack{i \in A \\ i \notin \{co_2, dh, ht\}}} P_i \, S_i(t) \qquad \forall t \in T \tag{5.5}$$

Minimization of total energy costs

The objective function for minimization of total energy costs over the scheduling horizon can be represented as follows:

$$J_4 = J_2 + J_3 \tag{5.6}$$

Minimization of CO_2 emissions

The objective function is formulated using the hourly marginal cost of CO_2 as follows:

$$J_5 = \sum_{t \in T} \left[\sum_{\substack{i \in A \\ i \notin \{co_2, dh, ht\}}} C_{em}(t) \, P_i \, S_i(t) + \sum_{i \in \{ht, dh\}} scc \, R_g P_i S_i(t) \right] \tag{5.7}$$

The first term in this equation represents the carbon footprint of the greenhouse from the grid electricity usage, and the second term depicts CO_2 emissions from natural gas consumption within the greenhouse for heating and dehumidification. It is assumed that the CO_2 produced by the CO_2 generator is consumed within the greenhouse by the plants and is not released to outdoor air; therefore, the effect of CO_2 generator on emissions is not considered here.

5.3.2 Model Constraints

Heat transfer through walls and soil, solar radiation, and air ventilation are some examples of the ways that outdoor weather conditions can affect indoor climate. Also, the biological system within a greenhouse affects the indoor climate through evapotranspiration. Furthermore, inside humidity drives evaporation or condensation, and CO_2 concentration and lighting level affects plants photosynthesis and growth. Thus, the model need to represent the greenhouse temperature, humidity, CO_2 concentration, and lighting levels and maintain these variables within pre-defined ranges, while taking into account technical aspects of the associated systems' operation. Constraints representing these requirements within the proposed model are presented next.

Inside Humidity

Humidity inside a greenhouse needs to be controlled to provide a suitable environment for plant growth and to prevent fungal diseases. In the case of high humidity, which usually happens in winter nights, the plants stop transpiration, and condensation from the roof and plant leaves may cause fungal diseases. In the case of low humidity, which usually happens in hot dry weather conditions, the plants stop absorbing CO_2 and the photosynthesis process, resulting in slow plant growth. Therefore, controlling relative humidity in greenhouses should be modeled properly in the mathematical model.

Relative humidity of greenhouses is defined as [144]:

$$\phi = \frac{P_{par}}{P_{sat}} 100\% \tag{5.8}$$

where the saturated vapor pressure and the partial pressure can be approximated by:

$$P_{sat} = p_1 \left(-p_2 + p_3 e^{p_4 \theta}\right) \tag{5.9}$$

$$P_{par} = \frac{w P_{atm}}{p_5} \tag{5.10}$$

The saturated vapor pressure equation is linearized as follows, based on a Taylor series expansion:

$$P_{sat} = p_1 \left(-p_2 + p_3 e^{p_4 \frac{(\theta^l + \theta^u)}{2}} (1 + p_4 (\theta - \frac{(\theta^l + \theta^u)}{2}) \right) \tag{5.11}$$

To model the humidity inside the greenhouses, the water content of air inside the greenhouse needs to be modeled; this can be represented by the following constraint based on the mass balance principle:

$$\begin{aligned} w_z(t) =& w_z(t-1) + \frac{\tau}{\rho_a V_z} [W_{evp,z} A_z \\ &+ Q_z \rho_a A_z S_{fv,z}(t) \left(w_{out}(t) - w_z(t)\right) \\ &+ v_w(t) \lambda_z \rho_a A_z S_{nv,z}(t) (w_{out}(t) - w_z(t)) \\ &+ S_{fog,z}(t) W^{max}_{fog,z} A_z \\ &- S_{dh,z}(t) W^{max}_{dh,z} A_z] \qquad \forall t \in T \end{aligned} \tag{5.12}$$

This equation states that the water content of the greenhouse air at time t is a function of its water content at time $t-1$; moisture ventilated by the forced and natural air ventilation system; and the operation of the fogging and dehumidification systems.

Using (5.8) and substituting associated terms from (5.10) and (5.11), the following constraints guaranties that the relative humidity of inside air is kept within the desired limits:

$$w_z(t) \leq \phi^{max}_z \frac{P_{par} p_5}{P_{atm}} \qquad \forall t \in T \tag{5.13a}$$

$$w_z(t) \geq \phi^{min}_z \frac{P_{par} p_5}{P_{atm}} \qquad \forall t \in T \tag{5.13b}$$

Inside Temperature

Thermal dynamics of the greenhouse are modeled using the following equations:

$$\begin{aligned} \theta_z(t) =& \theta_z(t-1) + \frac{\tau}{C_z} \left[q^{sr}_z(t) + q^{ht_p}_z(t) - q^{chl_p}_z(t) - q^{wl}_z(t) - q^{nv}_z(t) \right. \\ &\left. - q^{fv}_z(t) - q^{sl}_z(t) + q^{li}_z(t) + q^{co_2}_z(t) + q^{dh}_z(t) - q^{ev}_z(t)\right] \end{aligned} \tag{5.14}$$

This constraint states that the temperature of the greenhouse space at time t is a function of its temperature at time $t-1$; absorbed heat from sunshine; heat transfer through heating and chilling pipes; heat loss through walls, soil, air leakage and ventilation; heat produced by the lighting, CO_2 generation and dehumidification systems; and evaporation heats of the fogging system.

The thermal effect of each component in this equation can be calculated from the following equations:

- The solar radiation heat that enters into the greenhouse through the cover considering its heat transmission factor:

$$q_z^{sr}(t) = 3.6 \times R_{sr} SR(t) A_{gh,z} \tag{5.15}$$

- The heat injected to the greenhouse through hot water pipes as a function of its thermal conductance, temperature difference between the pipe and greenhouse, and operation of hot water valve:

$$q_z^{ht_p}(t) = R_{pipe} A_{ht_p,z} S_{ht_v,z}(t) \left(\theta_{ht_p}(t) - \theta_z(t)\right) \tag{5.16}$$

- The injected cold into the greenhouse through chilled water pipes as a function of its thermal conductance, temperature difference between the pipe and greenhouse, and operation of chilled water valve:

$$q_z^{chl_p}(t) = R_{pipe} A_{chl_p,z} S_{chl_v,z}(t) \left(\theta_{chl_p}(t) - \theta_z(t)\right) \tag{5.17}$$

- The heat loss through greenhouse walls:

$$q_z^{wl}(t) = R_{wl} A_{wl,z} \left(\theta_{out}(t) - \theta_z(t)\right) \tag{5.18}$$

- The thermal effect of natural air ventilation as a function of wind speed, area of natural ventilation window, opening degree of the window, and temperature difference between outdoor and indoor air:

$$q_z^{nv}(t) = 3600 \times \rho_a c_a v_w \lambda_z A_{nv,z} S_{nv,z}(t) \left(\theta_{out}(t) - \theta_z(t)\right) \tag{5.19}$$

- The thermal effect of forced air ventilation as a function of operation of fans, their volumetric air flow rate, and temperature difference between outdoor and indoor air:

$$q_z^{fv}(t) = \rho_a Q_z c_a S_{fv,z}(t) \left(\theta_{out}(t) - \theta_z(t)\right) \tag{5.20}$$

- The heat loss through greenhouse soil:

$$q_z^{sl}(t) = R_{sl} A_{gh,z} \left(\theta_z(t) - \theta_{sl}(t)\right) \tag{5.21}$$

- The thermal effect of operation of the lighting systems within the greenhouse:

$$q_z^{li}(t) = 3.6 \sum_{l=1}^{L} P_{li,l}^{max} \eta_{li} S_{li,z,l} \tag{5.22}$$

- The heat generated by operation of CO_2 generator:

$$q_z^{co_2}(t) = 3.6 \times P_{co_2}^{max} \eta_{co_2} S_{co_2,z} \tag{5.23}$$

- The heat generated by operation of dehumidifier:

$$q_z^{dh}(t) = 3.6 \times P_{dh}^{max} \eta_{dh} S_{dh,z} \tag{5.24}$$

- The cooling effect of evaporation of water drops injected into the greenhouse by the fogging system:

$$q_z^{ev}(t) = h_{evp} \eta_{fog} S_{fog,z}(t) W_{fog,z}^{max} A_{gh,z} \tag{5.25}$$

Temperatures of hot and chilled water inside pipes in (5.16) and (5.17) are calculated as follows:

$$\begin{aligned} \theta_{ht_p,z}(t) =& \theta_{ht_p,z}(t-1) \\ &+ \frac{\tau}{c_w \rho_w V_{ht_p,z}} [3.6 \times P_{ht}^{max} S_{ht,z}(t) \\ &- R_{pipe} A_{ht_p,z} S_{ht_p,z}(t) \left(\theta_{ht_p}(t) - \theta_z(t)\right) \\ &- R_{sl} A_{ht_p,z} \left(\theta_{ht_p}(t) - \theta_{sl}(t)\right)] \qquad \forall t \in T \end{aligned} \tag{5.26}$$

$$\begin{aligned} \theta_{chl_p,z}(t) =& \theta_{chl_p,z}(t-1) \\ &+ \frac{\tau}{c_w \rho_w V_{chl_p,z}} [3.6 \times P_{chl}^{max} S_{chl,z}(t) \\ &- R_{pipe} A_{chl_p,z} S_{chl_v,z}(t) \left(\theta_{chl_p}(t) - \theta_z(t)\right) \\ &- R_{sl} A_{chl_p,z} \left(\theta_{chl_p}(t) - \theta_{sl}(t)\right)] \qquad \forall t \in T \end{aligned} \tag{5.27}$$

These constraints state that the average temperature inside the pipes at time t is a function of: its temperature at time $t-1$; absorbed heat (cold) from operation of heating (chilling) system; heat transfer through pipes to the greenhouse space; and heat loss through soil.

The calculated inside temperature of the greenhouses must be kept within a range specified by minimum and maximum limits, and average inside temperature over the scheduling horizon must be within a tighter pre-defined temperature range. These requirements are represented in the model using the following constraints:

$$\theta_z^l \leq \theta_z(t) \leq \theta_z^u \qquad \forall t \in T \tag{5.28a}$$

$$\theta_z^{l_0} \leq \sum_{t \in T} \theta_z(t)/N_T \leq \theta_z^{u_0} \tag{5.28b}$$

Inside CO_2 Level

Plants need sunlight and CO_2 for photosynthesis. When there is sunlight, plants consume CO_2 inside the greenhouse and thus CO_2 concentration drops. Thus, to keep a high level of photosynthesis and plant growth, it is essential to supply CO_2 into the greenhouse and maintain CO_2 concentration within a desired range. While outdoor CO_2 concentration is around 300 ppm, greenhouses typically provide 1000 ppm to 1300 ppm CO_2 concentration by operating CO_2 generators. CO_2 concentration within the greenhouse is modeled as follows, based on the mass balance principle:

$$\begin{aligned}\mathcal{C}_z(t) = \mathcal{C}_z(t-1) + \frac{\tau}{\rho_a V_{gh,z}} \big[&\mathcal{C}^{max}_{inj,z} S_{co_2,z}(t) A_{gh,z} \\ &+ p_6 v_w \lambda_z A_{nv,z} S_{nv,z}(t) \left(\mathcal{C}_{out}(t) - \mathcal{C}_z(t)\right) \\ &+ \xi_z S_{fv,z}(t) \left(\mathcal{C}_{out}(t) - \mathcal{C}_z(t)\right) \\ &+ c_{res,z} A_{gh,z} \left(p_7 + p_8 \theta_z(t)\right) \\ &- p_6 c_{phot,z} SR(t) \eta_{sr} A_{gh,z}\big] \qquad \forall t \in T \end{aligned} \tag{5.29}$$

This constraint states that CO_2 balance within the greenhouse is determined by the CO_2 supply, the plants consumption of CO_2 and the air exchange by ventilation.

Concentration of CO_2 inside the greenhouses must be kept within a range specified by minimum and maximum values, which is represented in the model by the following constraint:

$$\mathcal{C}^{min}_z \leq \mathcal{C}_z(t) \leq \mathcal{C}^{max}_z \qquad \forall t \in T \tag{5.30}$$

Lighting

Supplemental lighting for greenhouses is required to increase photosynthesis and plats growth especially in areas that receive few hours average daily sunshine. High Intensity Discharge (HID) lamps such as metal halide and high pressure sodium lamps are commonly used for the purpose of supplying artificial lighting in greenhouses. Operational requirements of these supplementary lighting systems in the proposed model are formulated and explained next.

Total lighting at each time interval is calculated as a summation of sunshine lighting

and supplementary lighting systems installed in each zone, thus:

$$\Psi_z(t) = \tau \left(SR(t)\eta_{sr} + \sum_{l=1}^{L} S_{li,z,l}(t)\Psi_{z,l}^{max} \right) \tag{5.31}$$

Since HID lamps are not designed for cyclical On/Off operation, minimum up time and minimum down time requirements of these lighting systems are modeled here by the following constraints:

$$U_{li,z,l}(t) \geq S_{li,z,l}(t) - S_{li,z,l}(t-1) \tag{5.32a}$$

$$\sum_{k=t-mu_{li}+1}^{t} U_{li,z,l}(t) \leq S_{li,z,l}(t) \tag{5.32b}$$

$$\sum_{k=t-md_{li}+1}^{t} U_{li,z,l}(t) \leq 1 - S_{li,z,l}(t) \tag{5.32c}$$

Minimum and maximum aggregated lighting requirements of the plants in greenhouse are formulated in the model as follows:

$$\sum_{t=et_{li}}^{lt_{li}} \sum_{l=1}^{L} \Psi_{z,l}(t)\tau \leq \Psi_z^{max_{Aggr}} \tag{5.33a}$$

$$\sum_{t=et_{li}}^{lt_{li}} \sum_{l=1}^{L} \Psi_{z,l}(t)\tau \geq \Psi_z^{min_{Aggr}} \tag{5.33b}$$

Plants use the provided lighting more efficiently if a lower amount of lighting is provided over a longer time period than a high amount over a short period. Thus, it is common practice in greenhouses to lower intensity of supplementary light and increase its duration as long as it does not conflict with the photo-period requirements of the plant. Therefore, the following constraint enforces a maximum successive On time of the lighting system to represent this requirement in the proposed model:

$$\sum_{k=t}^{t+msot_{li}} S_{li,z,l}(t) \leq msot_{li} \tag{5.33c}$$

It is more efficient to provide supplementary lighting before dawn or after dust; however, it is common to turn on artificial lighting whenever sunlight levels drops below a set point

(cloudy weather condition) for more than a pre-defined period during the day. These operational constraints of the lighting system are modeled in the proposed optimization model using the minimum duration and the minimum lighting of cloudy weather as follows:

$$(1 - S_{li,z,l}(t)) \left(\sum_{k=t-mdu}^{t} SR(t)\tau - \Phi_z^{mdu} \right) \geq 0 \tag{5.34a}$$

$$S_{li,z,l}(t) \left(\Psi_z^{min_{mdu}} - SR(t) \right) \geq 0 \tag{5.34b}$$

Air Circulation

Air circulation is needed in greenhouses to maintain a uniform temperature and CO_2 concentration throughout the greenhouse. Without operation of circulation fans, cool air stays around the plants and warm air rises to the top of the greenhouse. Usually, a number of fans are used to develop a circular air flow within the greenhouse. The circulation fans should operate for at least a user-defined required operation time (rot_{cf}); this can be modeled as follows:

$$\sum_{k=1}^{NT} S_{cf,z}(t) \geq rot_{cf} \tag{5.35}$$

The circulation fans should also operate whenever the CO_2 generation unit is On to distribute CO_2 uniformly:

$$S_{cf,z}(t) \geq S_{co_2,z}(t) - LPN\,(1 - S_{co_2,z}(t)) \tag{5.36}$$

Other Devices' Operational Constraints

Forced ventilation in a greenhouse uses fans and inlet louvers to replace inside greenhouse air with outside air. Usually, these fans are sized such that can exchange the total volume of the air in the greenhouse each minute. When inside humidity and temperature is high and outdoor condition is appropriate, greenhouse controllers utilize these fans to decrease inside temperature and humidity. As previously mentioned, the operation of the ventilation fans are controlled in the proposed model based on their effects on greenhouse temperature, humidity, and CO_2 concentration. Additionally, when the outdoor temperature is less than a pre-specified value θ_{out}^{min}, forced ventilation and natural ventilation should not operate and circulate very cold air into the greenhouse; these requirements are modeled here as follows:

$$\left(\theta_{out}(t) - \theta_{out}^{min}\right) S_{fv,z}(t) \geq 0 \qquad \forall t \in T \tag{5.37}$$

$$\left(\theta_{out}(t) - \theta_{out}^{min}\right) S_{nv,z}(t) \geq 0 \qquad \forall t \in T \tag{5.38}$$

Fogging and dehumidification systems should not operate simultaneously. This is represented in the proposed model by the following complementarity constraint:

$$0 \leq S_{fog,z}(t) \perp S_{dh,z}(t) \geq 0 \qquad \forall t \in T \tag{5.39}$$

Also, the following complementarity constraint enforces that valves of the heating and chilling pipes do not open simultaneously to inject heat and clod into the greenhouse at the same time:

$$0 \leq S_{chl_v,z}(t) \perp S_{ht_v,z}(t) \geq 0 \qquad \forall t \in T \tag{5.40}$$

Notice that the heating system (boiler) and the cooling system (chiller) might operate simultaneously to take advantage of storing heat and clod during low electricity prices.

5.3.3 Exact Linear Equivalent of Bi-linear Terms

The developed model for optimal operation of greenhouse is an MINLP problem because of the bi-linear terms in the model. However, these terms can be linearized to obtain an MILP problem which is more suitable for real-time applications. Thus, assume S is a binary variable and x is a continuous variable bounded by $\underline{x} \leq x \leq \overline{x}$; hence a new variable $\mu_{S,x}$ can be defined to obtain the exact equivalent of $S \cdot x$ such that $\mu_{S,x} = S \cdot x$ using the following constraints:

$$\mu_{S,x} >= x - (1 - S) \cdot \overline{x} \tag{5.41a}$$

$$\mu_{S,x} <= x \tag{5.41b}$$

$$S \cdot \underline{x} <= \mu_{S,x} \tag{5.41c}$$

$$\mu_{S,x} <= S \cdot \overline{x} \tag{5.41d}$$

Therefore, all the bi-linear terms in the developed model are replaced with the associate $\mu_{S,x} = S \cdot x$ variables and constraints, resulting in an MILP mathematical optimization model (or Mixed Integer Quadratic Programming (MIQP) problem if (5.1) is used) for optimal operation of greenhouses.

5.4 Numerical Results of Greenhouse Model

Several case studies have been conducted to examine the performance of the developed mathematical model for optimal operation of greenhouses, of which the most relevant ones are presented in this section. In these case studies, the mathematical model is run for a typical greenhouse, where parameters and device ratings are suitably chosen and realistic data inputs for outside temperatures, humidity, wind speed, solar irradiation, electricity price and demand charges are used (All these data are provided in Appendix C). RTP and demand charges for electricity costs, FRP for natural gas, and a typical kWh equivalent of bio-fuels costs in Ontario-Canada are used to calculate total energy costs. AMPL [127], a modeling language for mathematical programming, is used to implement the developed mathematical models of the greenhouse, and CPLEX [128], a popular solver for LP, MILP and MIQP problems, is used to solve these models.

5.4.1 Simulation Scenarios

The following four case studies are considered to examine the various operation paradigms of greenhouses using the developed model here:

- Case 0: The optimization model is solved to minimize a constant value, finding a feasible solution for the model, while all constraints on operation of the devices, inside temperature, humidity, and CO_2 concentration are met. The solution obtained in this case is one of the many possible solutions that represent actual operation of a greenhouse, and is considered here to be a realistic "base case" to establish a reference for comparison purposes.
- Case 1: The objective is to minimize total costs of energy consumption while all the constraints are the same as the base case.
- Case 2: The objective is to minimize electricity demand charges while all the constraints are the same as the base case.
- Case 3: The objective is to minimize total energy costs including energy consumption and demand charges while all the constraints are the same as the base case.

Optimal operational decisions and resulting trajectories generated by the proposed model for optimal operation of the greenhouse on a summer day are presented in Figure 5.2 to Figure 5.9. In these figures, decision variables for all devices and the resulting inside

temperatures, relative humidities, and CO_2 concentrations are presented. Observe that the model operates the heater, dehumidifier, chiller, CO_2 generator, natural ventilation, and circulation fans to maintain greenhouse climate conditions within pre-defined ranges. Figure 5.2 and Figure 5.3 depict the obtained solution for the base case, and Figure 5.4 and Figure 5.5 depict the optimal solution obtained from minimizing energy costs, where the model reduces costs by operating the devices during lower energy price periods. The optimal solution obtained from minimizing peak demand charges and total costs, i.e., energy and demand charges, are presented in Figure 5.6 to Figure 5.9, respectively. In these cases, while the inside temperature, relative humidity, and CO_2 concentrations vary within the pre-defined ranges, the model reduces total costs by operating the devices during lower energy price periods and by lowering the peak demand of the greenhouse. Similar results were found for a winter day.

The resulting electric power demands of the greenhouse for each case are shown in Figure 5.10. It is observed that peak demand of the greenhouse in Case 2 and Case 3 peak demand is reduced to 106 kW, resulting in significant total costs reductions as compared to Case 0 and Case 1, where the peak demand is 206 kW. For a winter day, the peak demand can not be significantly reduced due to the need to operate the supplementary lighting system, as shown in Figure 5.11. Notice as well that the heating system needs to be operated in these case.

A comparison of energy costs and demand charges for optimal operation of the greenhouse in all cases for the summer and winter days considered are presented in Table 5.2 and Table 5.3, respectively. In Case 1, the energy costs are reduced significantly as compared to Case 0 and are the least among all cases, while the demand charges remain the same as the base case for both summer and winter days. In Case 2, the demand charges of the greenhouse is reduced significantly for the summer day, whereas this reduction is not considerable for the winter day as the supplementary lighting system has to be operated on the winter day, which results in larger electricity demand for the greenhouse,. In Case 3, energy costs and demand charges are reduced as compared to the base case for both winter and summer days. In general, the proposed model for optimal operation of greenhouses significantly reduces energy costs and demand charges for a summer day, and achieves considerable energy costs reductions for a winter day.

5.4.2 Monte-Carlo Simulations

The expected total cost savings over a billing period (one month) for summer and winter are calculated via Monte-Carlo simulations. Thus, randomly generated inputs from actual data

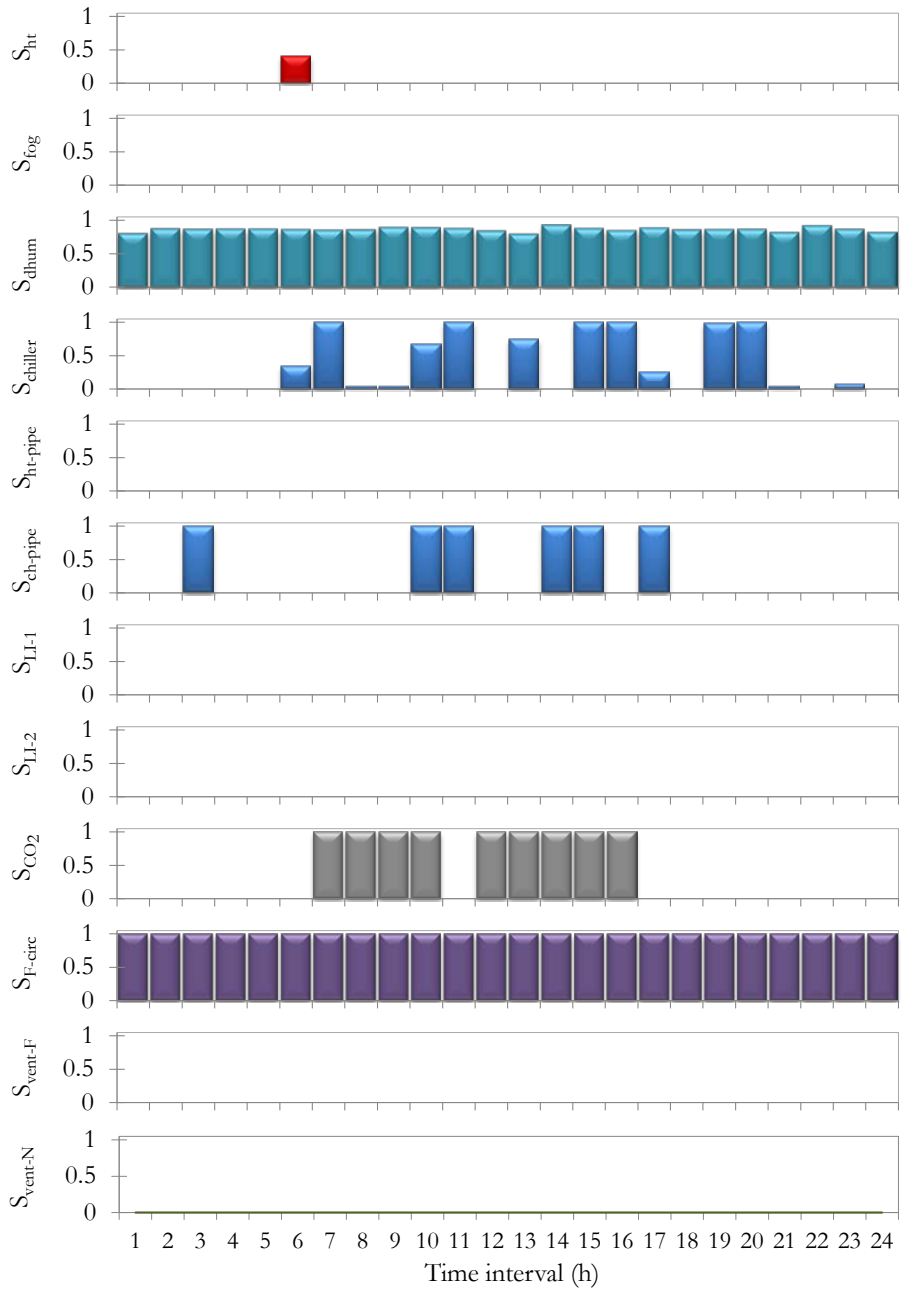

Figure 5.2: Values of the decision variables for heating, fogging, dehumidification, chiller, heating system valve, chilling system valve, lighting, CO_2 generator, circulation fans, and forced and natural ventilation fans, respectively, obtained from the greenhouse model for the base case (Case 0) using RTP for a summer day.

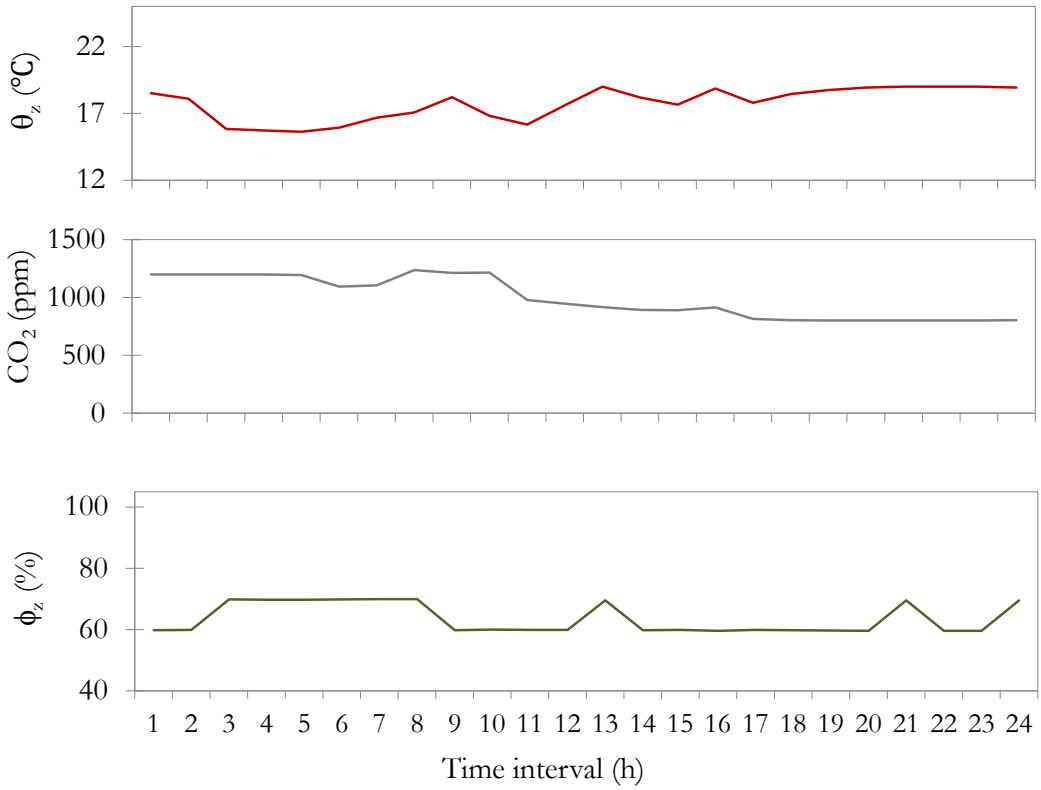

Figure 5.3: Inside temperature, CO_2 level and relative humidity, respectively, obtained from the greenhouse model for the base case (Case 0) using RTP for a summer day.

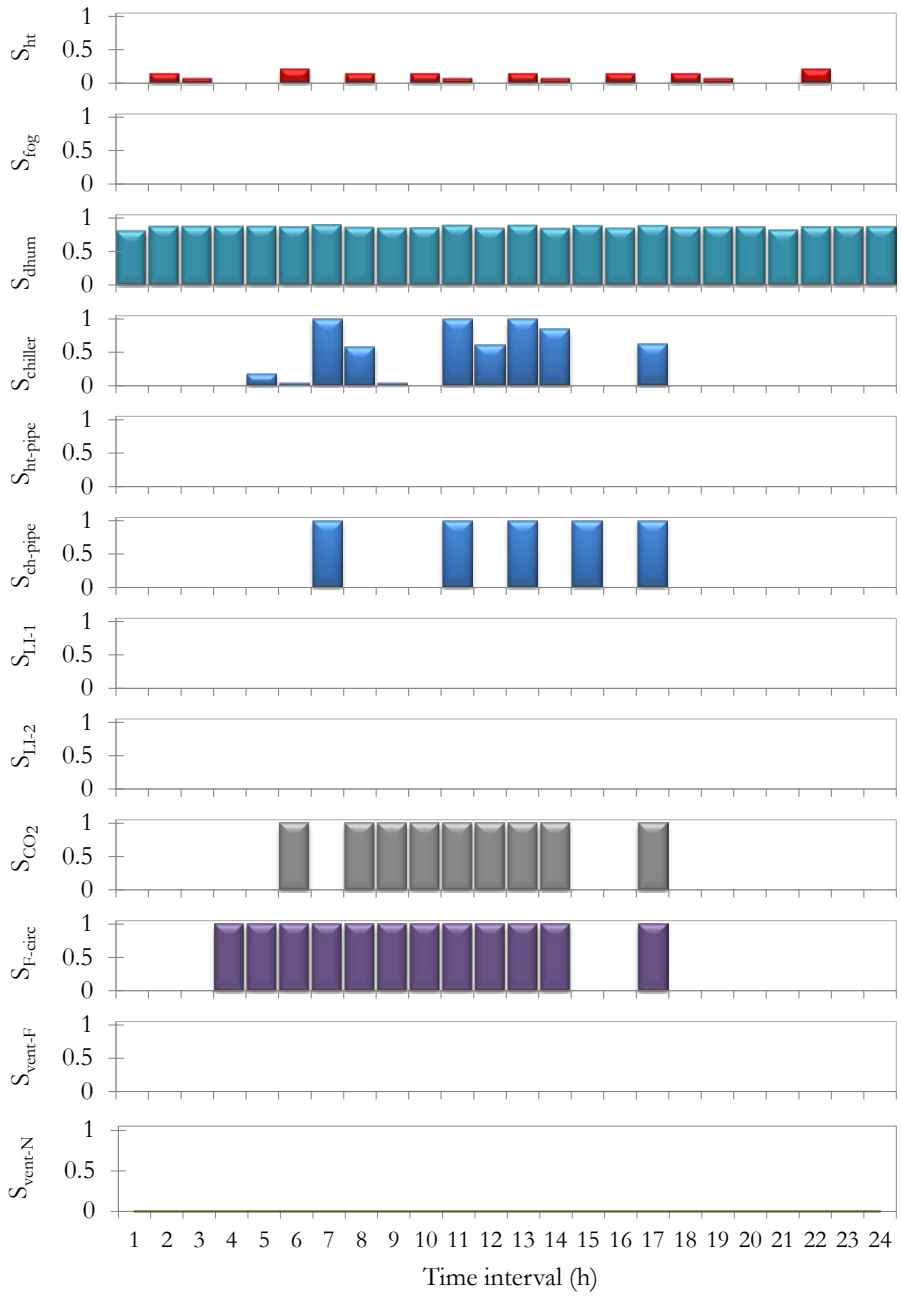

Figure 5.4: Optimal values of the decision variables for heating, fogging, dehumidification, chiller, heating system valve, chilling system valve, lighting, CO_2 generator, circulation fans, and forced and natural ventilation fans, respectively, obtained from the greenhouse model for Case 1 using RTP for a summer day.

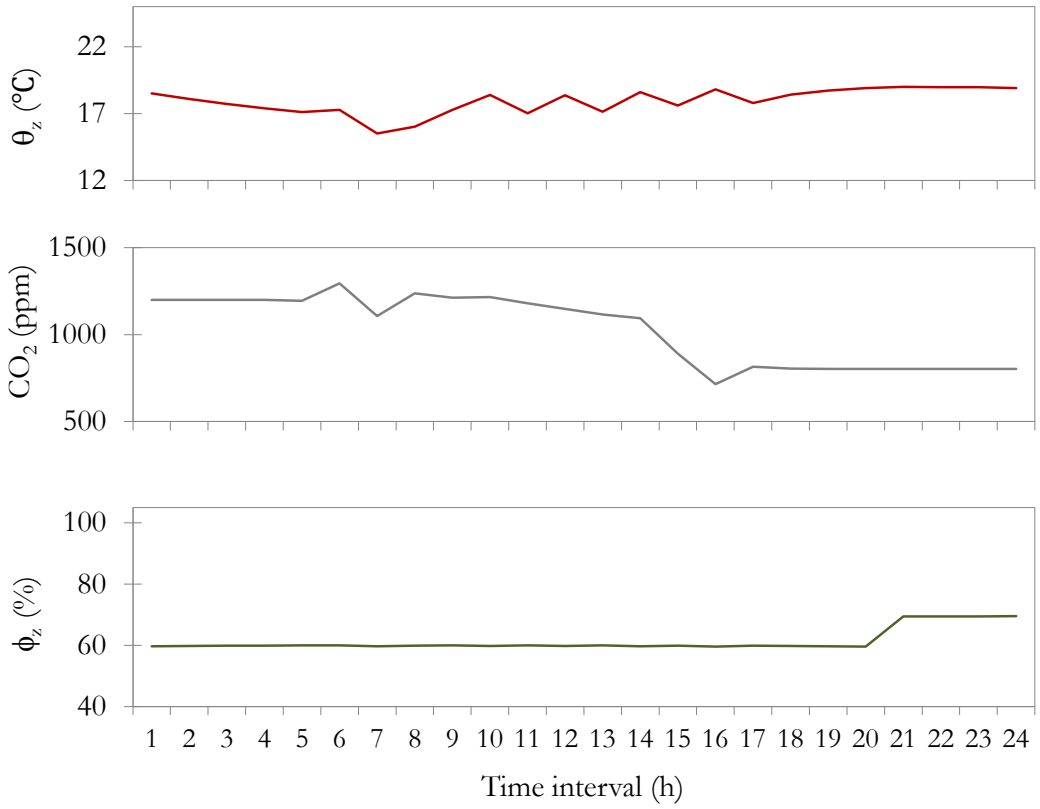

Figure 5.5: Inside temperature, CO_2 level and relative humidity, respectively, obtained from the greenhouse model for Case 1 using RTP for a summer day.

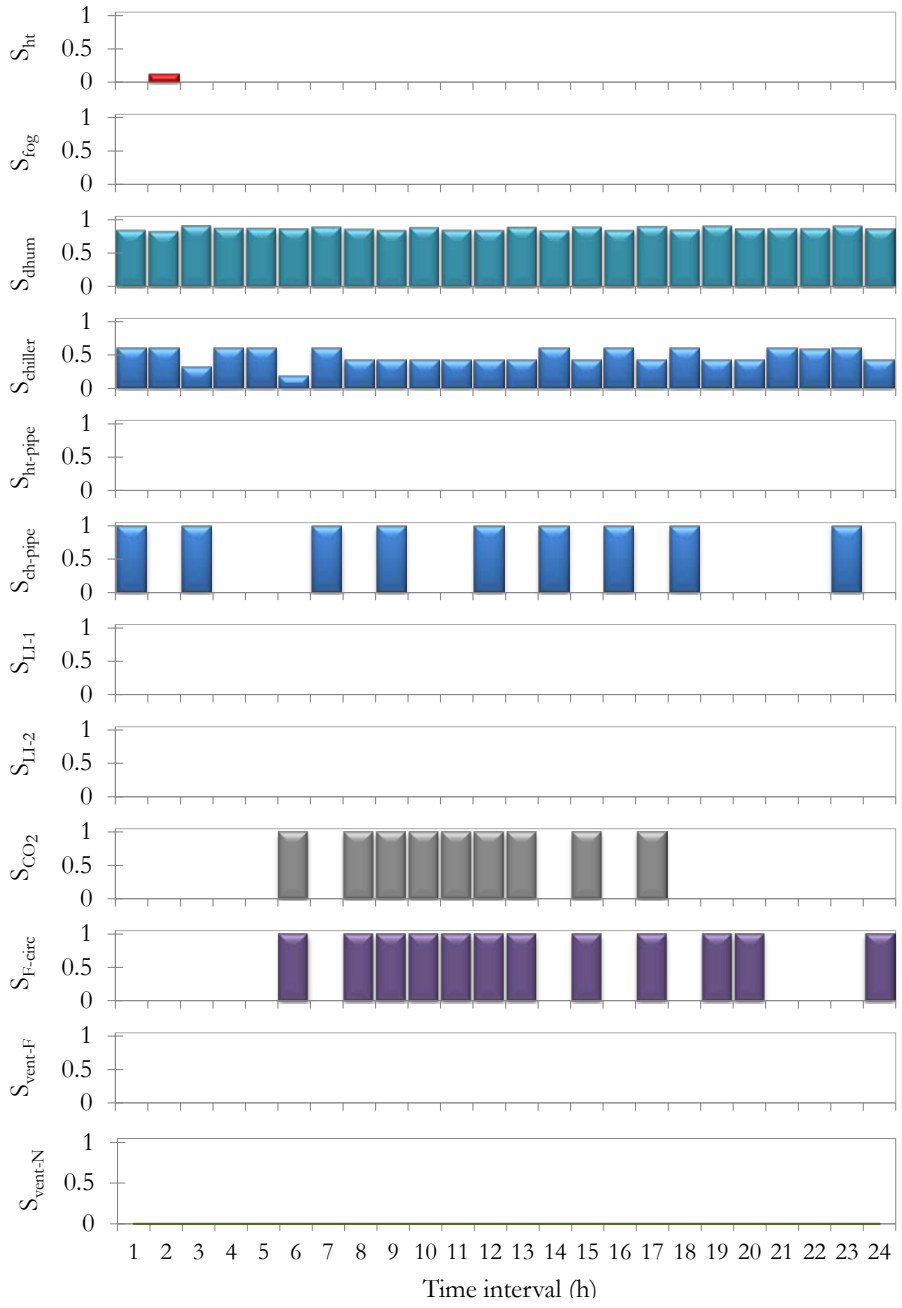

Figure 5.6: Optimal values of the decision variables for heating, fogging, dehumidification, chiller, heating system valve, chilling system valve, lighting, CO_2 generator, circulation fans, and forced and natural ventilation fans, respectively, obtained from the greenhouse model for Case 2 using RTP for a summer day.

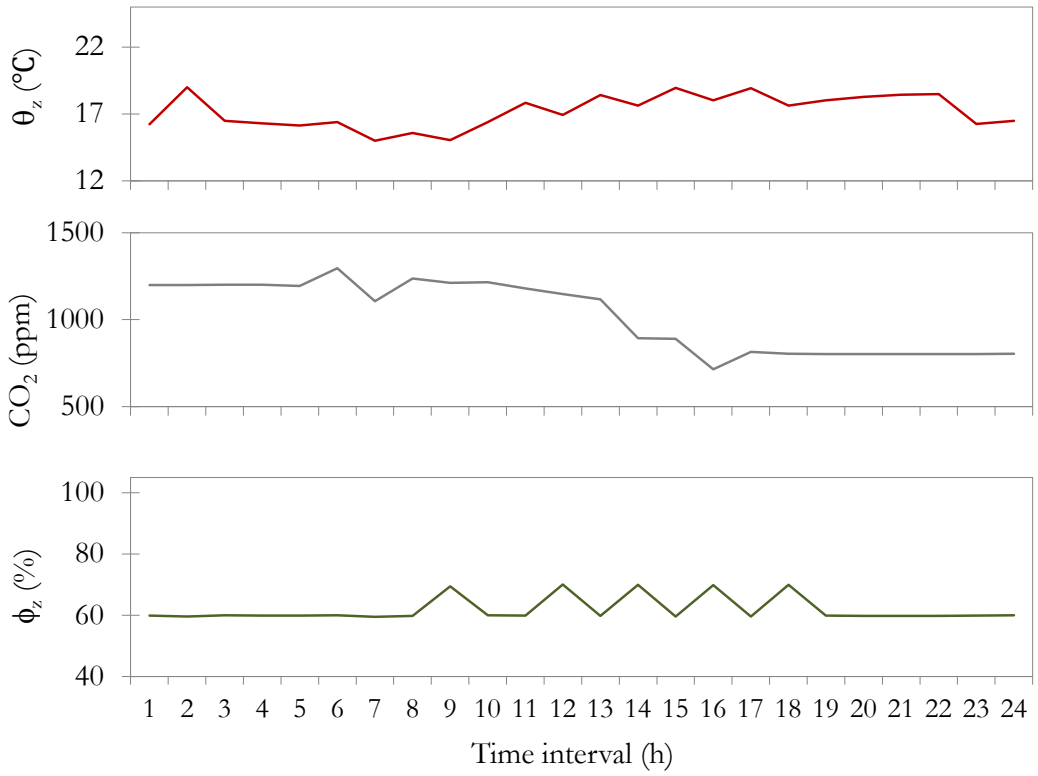

Figure 5.7: Inside temperature, CO_2 level and relative humidity, respectively, obtained from the greenhouse model for Case 2 using RTP for a summer day.

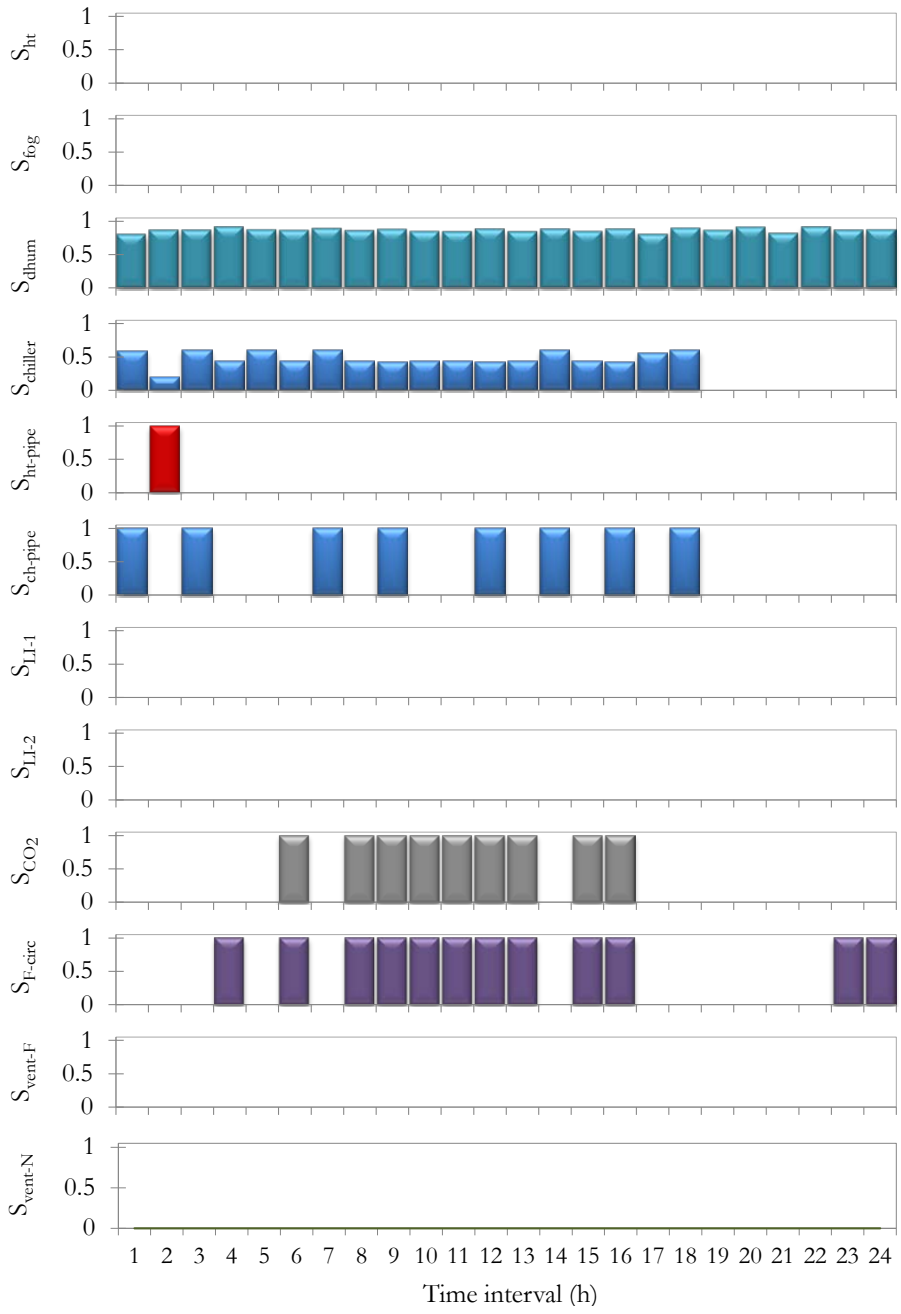

Figure 5.8: Optimal values of the decision variables for heating, fogging, dehumidification, chiller, heating system valve, chilling system valve, lighting, CO_2 generator, circulation fans, and forced and natural ventilation fans, respectively, obtained from the greenhouse model for Case 3 using RTP for a summer day.

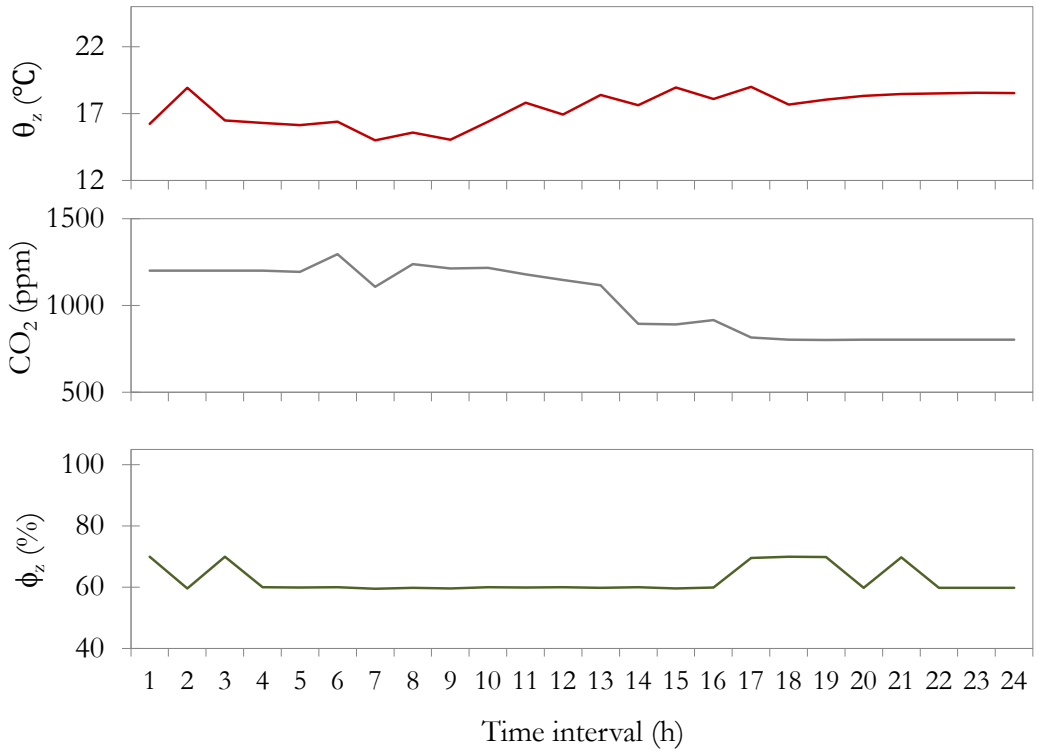

Figure 5.9: Inside temperature, CO_2 level and relative humidity, respectively, obtained from the greenhouse model for Case 3 using RTP for a summer day.

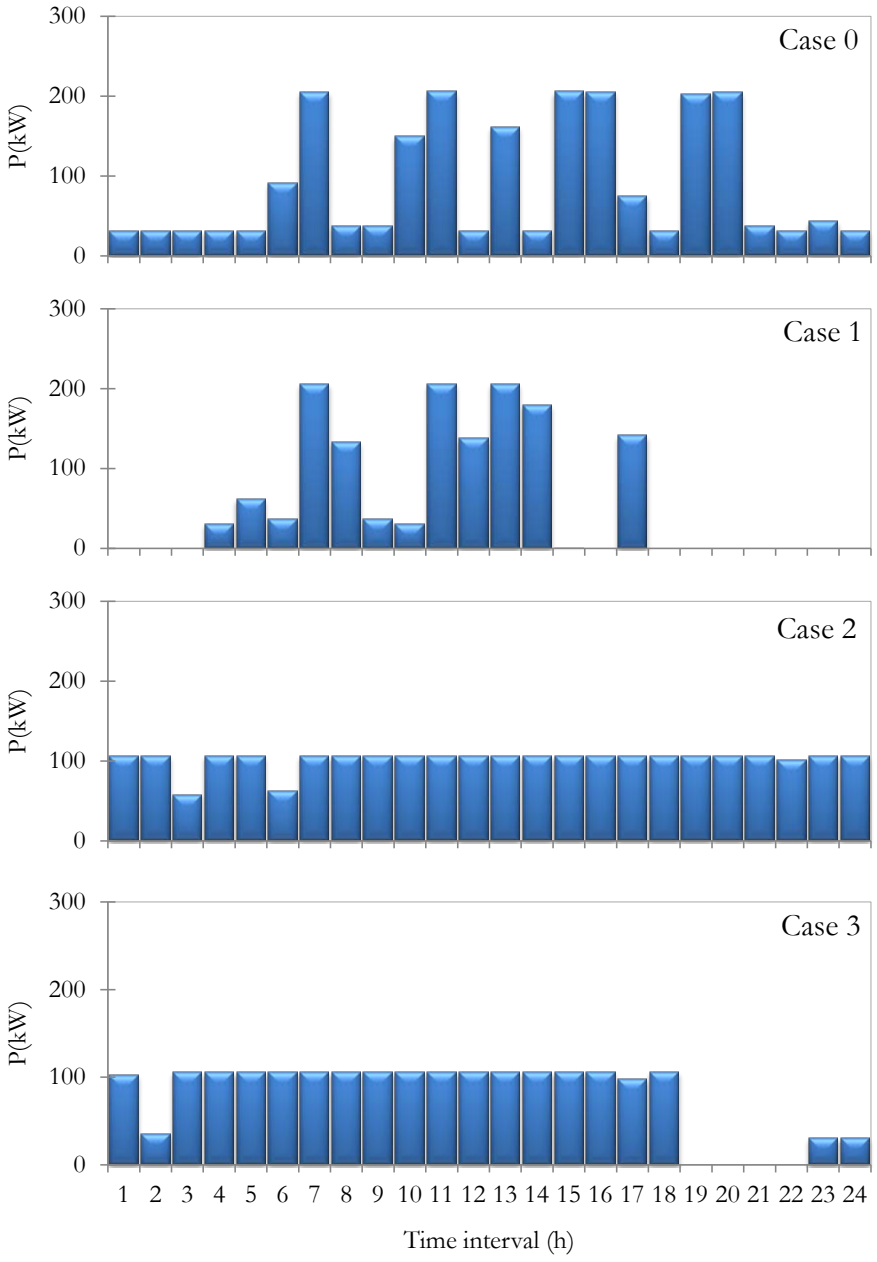

Figure 5.10: Electric power demand of the greenhouse for all cases on a summer day.

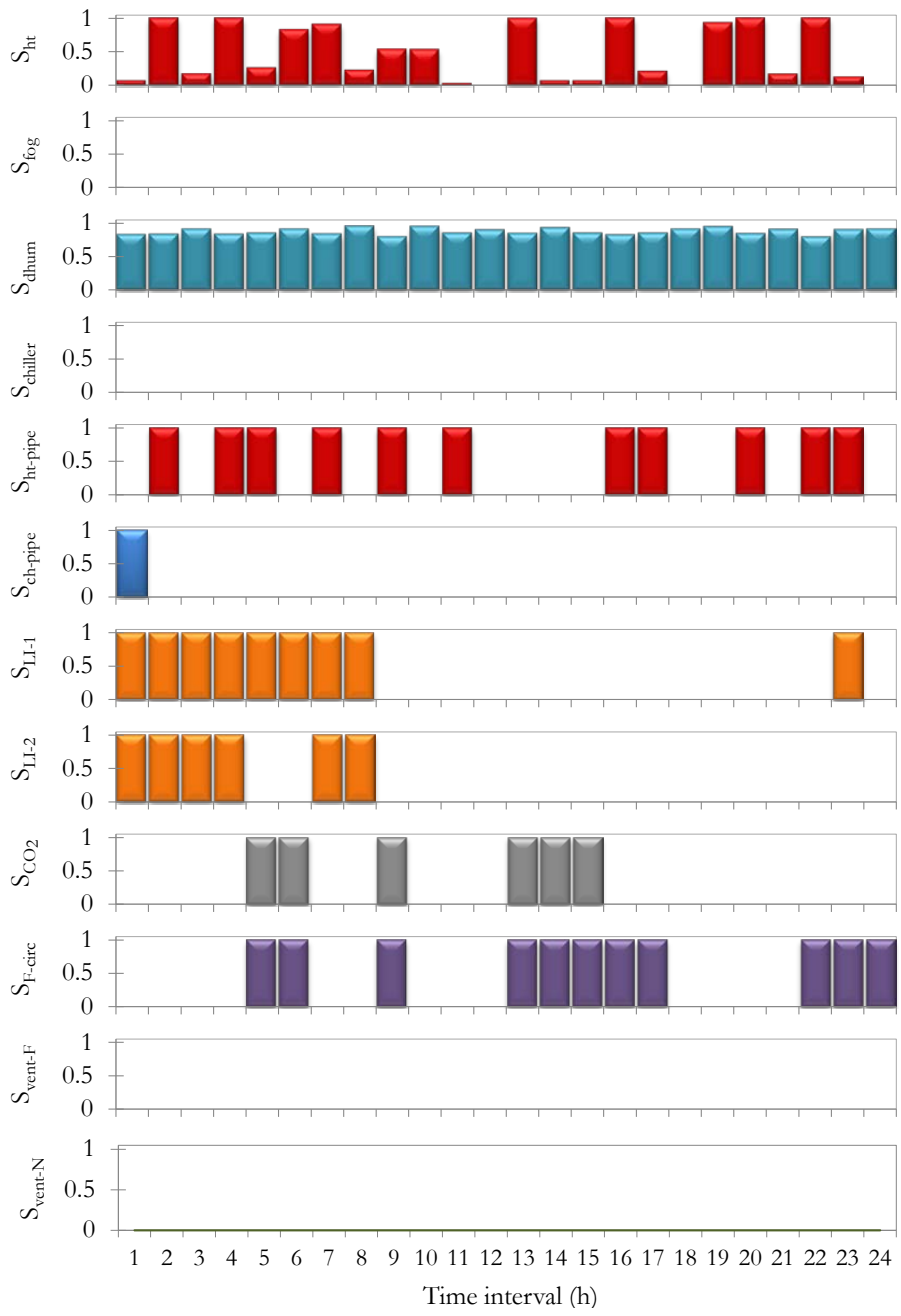

Figure 5.11: Optimal values of the decision variables for heating, fogging, dehumidification, chiller, heating system valve, chilling system valve, lighting, CO_2 generator, circulation fans, and forced and natural ventilation fans, respectively, obtained from the greenhouse model for Case 3 using RTP for a winter day.

Table 5.2: Case-wise comparison of greenhouse energy charges (using RTP) and demand charges for a summer day.

Item	Energy (kWh)	Peak demand (kW)	Energy costs ($)	Demand charges ($)	Energy costs savings w.r.t Case 0 (%)	Demand charges savings w.r.t Case 0 (%)
Case 0	6029.47	206.00	161.47	1648.00	0.00	0.0
Case 1	7535.11	206.00	108.34	1648.00	32.90	0.0
Case 2	5737.65	106.00	157.50	848.01	2.46	48.5
Case 3	4933.54	106.02	135.69	848.16	15.97	48.5

Table 5.3: Case-wise comparison of greenhouse energy charges (using RTP) and demand charges for a winter day.

Item	Energy (kWh)	Peak demand (kW)	Energy charges ($)	Demand charges ($)	Energy costs savings w.r.t Case 0 (%)	Demand charges savings w.r.t Case 0 (%)
Case 0	54169.50	4031.00	1167.39	28217.00	0.00	0.0
Case 1	55638.43	4031.00	948.21	28217.00	18.77	0.0
Case 2	54959.19	4000.00	1135.06	28000.00	2.77	0.8
Case 3	55133.69	4000.50	949.39	28003.50	18.67	0.8

of outdoor temperature, humidity, wind speed, and HOEP variations are used to perform multiple simulations. Random values of RTP, temperature and humidity for each hour are generated using a normal distribution with associated mean and standard deviations for each hour of a day obtained from actual data for each season. For wind speed, random values are generated using a Weibull distribution with the scale and shape parameters obtained from actual hourly data for each each season. Random solar irradiation inputs are generated using uniform distribution with reasonable minimum and maximum values for each hour a day for each season. The input data used in these Monte-Carlo simulations are given in Appendix C.

Energy costs and peak demand charges at each iteration and their expected mean values obtained from the Monte-Carlo simulations for a summer day in Case 0 and Case 3 are shown in Figure 5.12 and Figure 5.13, respectively. Observe that the Monte-Carlo simulations converge in 150 iterations. Expected average energy costs and peak demand charges in Case 0 are \$269.8 and \$8721.3, respectively, while these values for Case 3 are \$159.6 and \$5258.4, respectively. Therefore, expected total costs, which are assumed to be 30 times the expected daily energy costs plus the expected peak demand charges, are \$16816.8 and \$10046.4 over a summer month for Case 0 and Case 3, respectively. Therefore, even when considering large variations in weather and energy price data, the model yields a significant total cost reduction of 40% for summer months.

Monte-Carlo simulation results for a winter day, depicted in Figure 5.14 and Figure 5.15, show that the model results in more than 19% and 2% reductions in expected energy costs and demand charges, respectively. These reductions yield a 13% expected total cost savings for winter months even when considering large variations (the largest observed actual variations) in weather and energy price data.

5.5 Robust Optimization Model of Greenhouses

In this section, a Robust Mixed Integer Linear Programming (RMILP) problem is formulated based on the developed model for optimal operation of greenhouses and the robust optimization method discussed in Section 2.4.4. This RMILP model considers uncertainty in electricity price forecasts in optimal operation of greenhouses, but instead of using price variations as in the case of Monte-Carlo simulations, price confidence intervals are considered at each time interval to reflect the data uncertainty. The generated optimal decisions are robust within the upper and lower bounds of the confidence intervals.

The developed model for optimal operation of greenhouse has the general MILP form

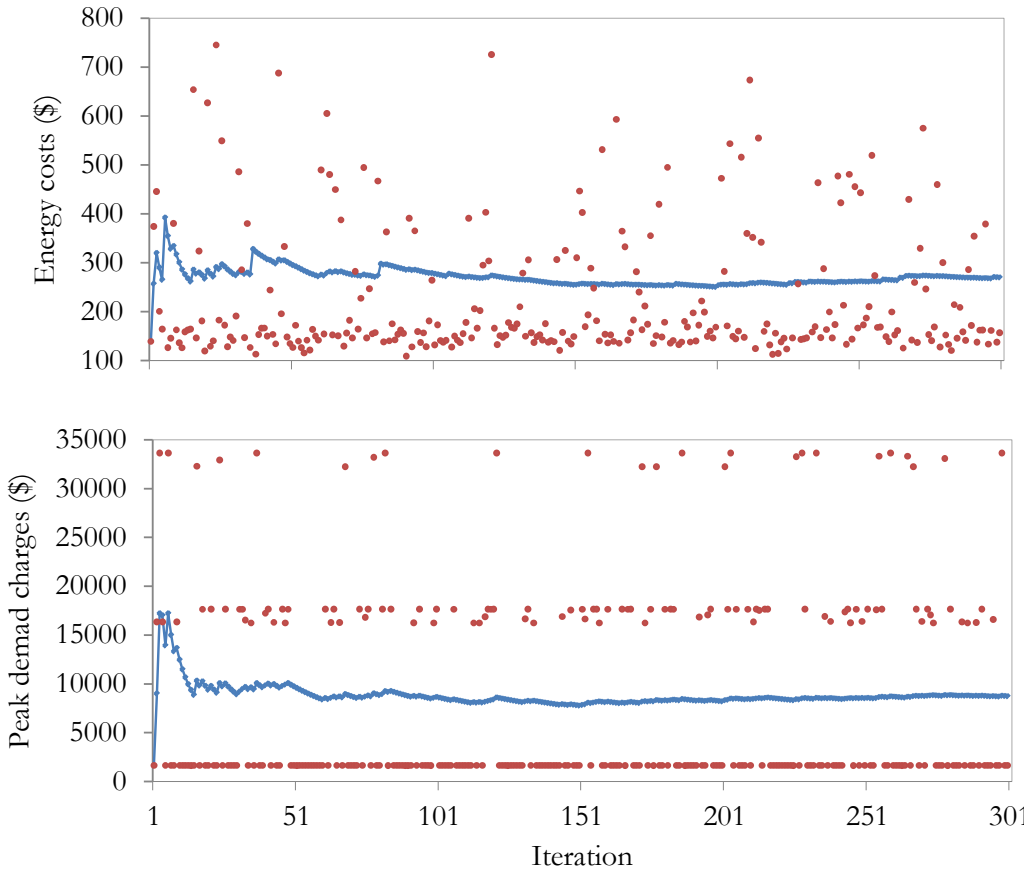

Figure 5.12: Energy costs and peak demand charges at each iteration and their mean results from Monte-Carlo simulations for Case 0 in a summer day.

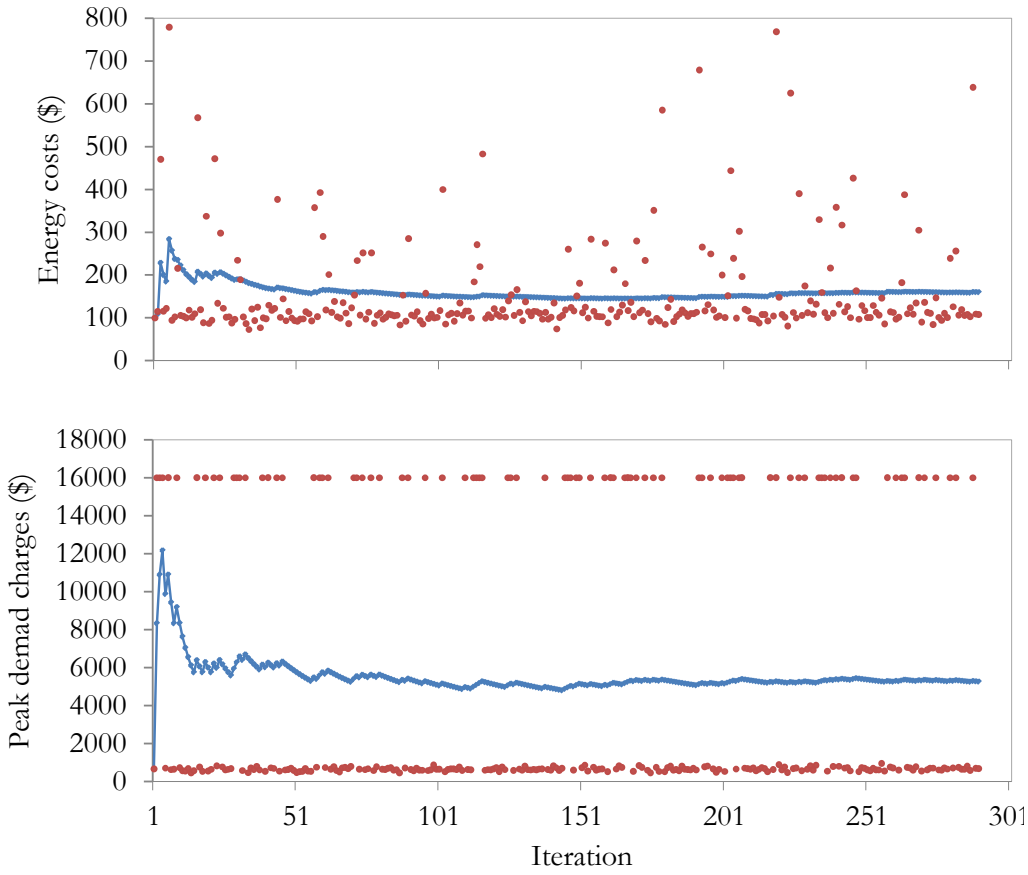

Figure 5.13: Energy costs and peak demand charges at each iteration and their mean results from Monte-Carlo simulations for Case 3 in a summer day.

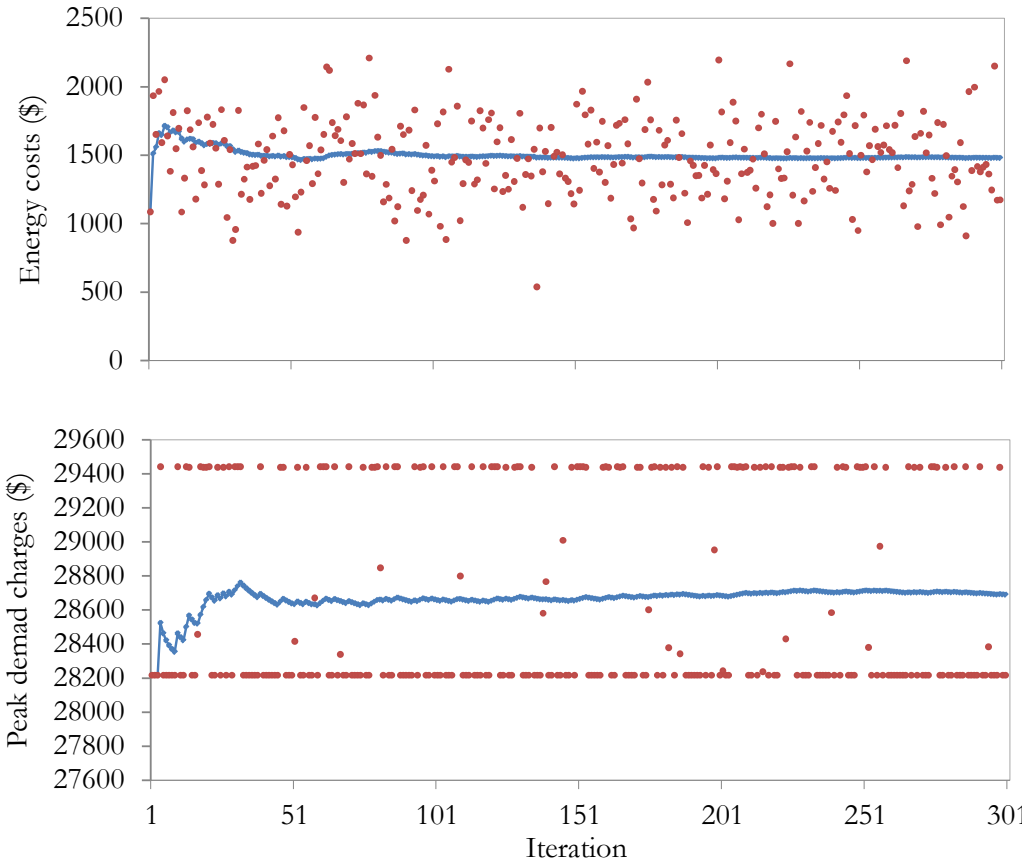

Figure 5.14: Energy cost and peak demand charges at each iteration and their mean results from Monte-Carlo simulations for Case 0 in a winter day.

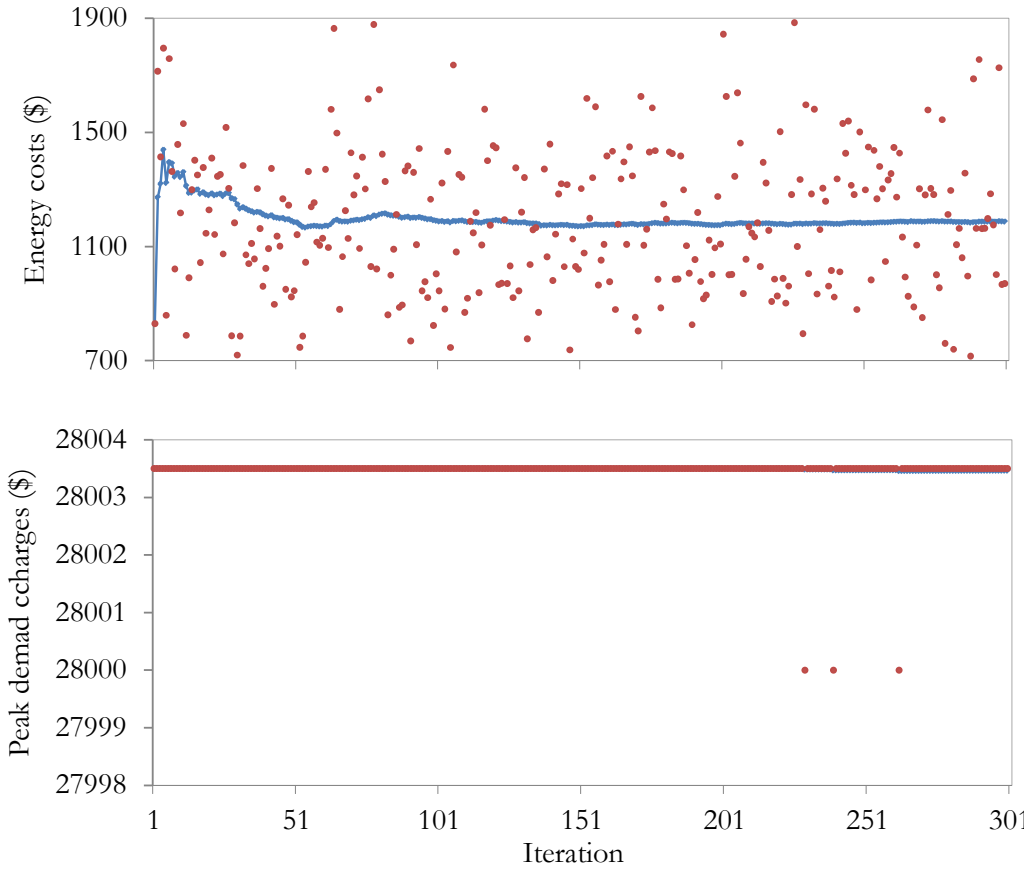

Figure 5.15: Energy costs and peak demand charges at each iteration and their mean results from Monte-Carlo simulations for Case 3 in a winter day.

shown in (2.6), which can be transformed into the RMILP model (2.8) by assuming uncertainties in the electricity price. In this model, if $\Gamma_0 = 0$, it completely ignores the influence of the price uncertainty, while if $\Gamma_0 = 24$, all possible price deviations for the next 24 intervals are considered, which results in the most conservative solution.

The proposed RMILP formulation is implemented using AMPL [127] and solved with CPLEX [128] to carry out simulations. In these simulations, it is assumed that the electricity price forecasts may have up to 25% errors, (i.e., the maximum price at each hour could be 25% more than its actual value), and the model is run for different robustness degrees from $\Gamma_0 = 0$ (i.e., ignoring all price uncertainties and assuming that the forecasted prices are the same as the observed ones) to $\Gamma_0 = 24$ (i.e., considering all possible price deviations for the next 24 hours which results in the most conservative solution).

The summary comparisons of the RMILP simulation results are presented in Table 5.4 and Table 5.5 for summer and winter days, respectively. The results of the base case (Case 0) obtained from the MILP model are presented in the first row in these tables, and the robust results for minimization of total costs with different robustness degrees are compared with respect to Case 0. Notice that the energy costs savings are reduced by increasing the "budget of robustness". Observe also that energy costs reductions with respect to Case 0 for the summer day in the most optimistic and the worst cases are 25.36% and 16.07%, respectively. Similarly, for the winter day, energy costs reductions with respect to Case 0 are between 18.67% for the most optimistic case ($\Gamma_0 = 0$) and 7.63% for the worst case ($\Gamma_0 = 24$).

Notice that robust optimization simulation results agree with the Monte-Carlo simulation results. Monte-Carlo simulation results show savings of 40% and 19% in the expected energy costs for summer and winter days, respectively, showing that considerable cost reductions can be achieved using the proposed model even in the presence of large uncertainties in the electricity price.

5.6 Summary

Novel mathematical models for optimal operation of greenhouses in the context of Smart Grids were presented. Thus, mathematical models of supplementary lighting, CO_2 generation, air circulation and ventilation, and heating and cooling systems were formulated to optimally operate existing control systems in greenhouses. The developed models are based on physical principles and previously published models for individual components of these systems, and incorporate weather forecasts, electricity price information, and the

Table 5.4: Comparison of energy charges for various robustness degrees using RMILP model for a summer day.

Case	Energy consumption (kWh)	Energy costs ($)	Energy costs reduction w.r.t Case 0 in MILP model (%)
min. CTE (Case 0)	6029.47	181.80	0.00
min. Total costs (Γ=0)	4933.54	135.69	25.36
min. Total costs (Γ=5)	4933.54	143.18	21.24
min. Total costs (Γ=10)	4934.04	147.57	18.83
min. Total costs (Γ=15)	4934.04	150.94	16.98
min. Total costs (Γ=20)	4934.39	152.58	16.07

Table 5.5: Comparison of energy charges for various robustness degrees using RMILP model for a winter day.

Case	Energy consumption (kWh)	Energy costs ($)	Energy costs reduction w.r.t Case 0 in MILP model (%)
min. CTE (Case 0)	54169.50	1167.40	0.00
min. Total costs (Γ=0)	55133.70	949.40	18.67
min. Total costs (Γ=5)	54725.80	1038.20	11.07
min. Total costs (Γ=10)	55050.10	1076.30	7.80
min. Total costs (Γ=15)	52227.00	1077.60	7.69
min. Total costs (Γ=20)	54797.70	1078.30	7.63

end-user preferences to minimize total energy costs and peak demand charges while considering important parameters of greenhouses climate control. The presented simulation results show the effectiveness of the proposed model to reduce total energy costs while maintaining required operational constraints of a greenhouse. Expected total cost savings were calculated via Monte-Carlo simulations using actual data variation ranges, showing 40% and 13% expected total cost reductions for summer and winter months, respectively. Finally, a robust optimization model was developed to consider the effect of uncertainty in electricity price forecasts on optimal operation of greenhouses, with the simulations results showing that significant cost savings can be achieved using the proposed model even in the presence of large forecast errors.

Chapter 6

Conclusions

6.1 Summary

The research conducted in this thesis concentrates on the optimal operation of energy hubs in the context of Smart Grids. The motivation of the research was presented in Chapter 1, followed by identifying the main research objectives based on a literature review on the relevant research areas. In the next chapters, mathematical optimization models of energy hubs that can readily be integrated into automated decision making technologies such as HAS and EMSs were proposed. The proposed mathematical models can be solved efficiently in real time, and thus facilitates the integration of various energy hubs into Smart Grids.

The main contents and conclusions of this thesis can be summarized as follows:

- In Chapter 2, the background topics relevant to the research on optimal operation of energy hubs in the context of Smart Grids were reviewed. Thus, DSM and DR programs, and their objectives, strategies, and approaches were presented, followed by a discussion on the state-of-the-art in EMSs in residential, commercial, and agricultural sectors. A brief review of the relevant mathematical programming methods and tools for development of mathematical optimization models were also presented. Finally, information on energy pricing and estimation of CO_2 emission values are discussed.

- Chapter 3 presented and discussed a novel mathematical model of residential energy hubs which can be readily integrated into HAS, HEM, and EMSs to increase

their functionality and improve their effectiveness, thus facilitating the integration of residential customers into Smart Grids. Mathematical models were formulated for major household devices in a typical house, i.e., fridge, freezer, dishwasher, washer and dryer, stove, water heater, hot tub, pool pumps, lighting, heating and air conditioning, solar PV panels, and energy generation/storage.The developed mathematical models result in an MILP optimization problem for the optimal operation scheduling of residential energy hubs, whose objective is to minimize demand, total costs of energy, emissions and peak demand over the scheduling horizon while considering end-user preferences and comfort levels. The developed model incorporates electricity and gas energy carriers, prioritize customers' preferences, and takes into account human comfort factors and CO_2 emissions.

The applications of the proposed models to a real household in Ontario, Canada, considering a number of simulation case studies were presented, showing that savings of up to 20% on energy costs and 50% on peak demand can be achieved, while maintaining the household owner's desired comfort levels. The results of the various realistic simulations demonstrated that by choosing appropriate objective functions, the proposed mathematical model has the capability of generating optimal operational schedules of devices to minimize total energy costs, energy consumption and emissions, while taking into account the end-user preferences and comfort. The developed mathematical models have been implemented and tested on a single board computer, demonstrating that these models can be solved efficiently in real-time applications to optimally control all major residential energy loads, storage and production components, while ensuring total energy costs and emissions reductions for customers taking into account their preferences and comfort levels.

- Chapter 4 presented and discussed a novel mathematical model of produce storage facilities to optimize the operation of their energy systems in the context of Smart Grids. The developed mathematical model, appropriate for optimal operation of the climate control systems of storage facilities, could be implemented as a supervisory control in existing climate controllers. The proposed model is based on approximate physical models of produce storage facilities and climate condition predictions, and incorporates weather forecasts, electricity price information, and end-user preferences to optimally operate existing climate controllers. The objective is to minimize total energy costs and demand charges while considering important parameters of storage facilities, i.e., inside temperature and humidity should be kept within acceptable ranges. The presented simulation results for a realistic case study showed the effectiveness of the proposed model to reduce total energy costs while maintaining required operational constraints.

Effects of uncertainty in electricity price and weather inputs on optimal operation of the storage facilities were studied via Monte-Carlo simulations. Thus, expected average total cost savings for a summer month was calculated using actual electricity price and weather data variations, showing that significant cost savings could be achieved using the proposed model even in the presence of large variations in these inputs. Effects of forecast errors in electricity price and weather conditions on optimal operation of climate control systems were also studied via Monte-Carlo simulations, showing that the proposed model could yield considerable total costs reductions even in the presence of electricity price and weather forecast errors.

Finally, a solution algorithm was proposed for real-time implementation purposes of the developed NLP model, based on an iterative B&B approach, relaxed sub-problems obtained from Taylor series expansion of the nonlinear terms, and RLT.

- Chapter 5 presented and discussed a novel mathematical optimization model of greenhouses to optimize the operation of their energy systems in the context of Smart Grids. The proposed supervisory operation strategy and the mathematical model could be implemented as a supervisory control in existing greenhouse management systems. Mathematical models of heating, cooling, natural and forced air ventilations, supplementary lighting, CO_2 generation, and humidity control systems were developed. Based on these models, an MILP optimization problem was formulated to minimize total energy costs and demand charges of greenhouses while considering important parameters and acceptable ranges for inside temperature and humidity, CO_2 concentration, and lighting levels. The proposed model incorporates electricity, gas and bio-fuel energy carriers, considers weather and electricity price forecasts, and takes into account the end-user preferences to optimally operate existing control systems in greenhouses.

  Several realistic case studies were simulated to examine the performance of the model for a greenhouse energy hub, suitably choosing parameters, device ratings, and realistic data inputs for outside temperatures, humidities, and solar irradiations. The presented simulation results showed the effectiveness of the proposed model to reduce total energy costs, while maintaining required operational constraints. Monte-Carlo simulations were carried out to calculate the expected total cost savings for a summer and winter month using actual data, showing 40% and 13% expected average total cost savings in summer and winter months, respectively.

  Finally, based on the developed MILP model of greenhouse, a robust optimization model considering uncertainties in electricity price forecasts was proposed and some simulation results were presented. In this RMILP problem, instead of using accurate

price predictions, price confidence intervals are considered at each hour to reflect data uncertainty. The presented simulation results showed the effectiveness of the proposed model to reduce total energy costs even in the presence of electricity price forecast errors; for example, in the presence up to of 25% electricity price forecast errors, the results showed more than 16% and 7.6% reductions in energy costs for a summer and winter day, respectively.

6.2 Contributions

The main contributions of the research presented in this thesis are as follows:

1. Novel mathematical models for scheduling and optimal operation of the following components of residential energy hubs are formulated: fridge, freezer, dishwasher, washer and dryer, stove, water heater, hot tub, pool pumps, lighting, heating and air-conditioning systems, solar PV panels, and energy storage/generation devices.

2. A multi-period, multi-carrier, MILP optimization model of residential energy hubs is proposed so that it can be integrated into automated decision making technologies such as HASs and EMSs in the context of Smart Grids. The developed mathematical model includes electricity and natural gas, and incorporates the mathematical models of the energy system components, weather and energy price information, and CO_2 emissions profiles of the grid to optimize customers' total energy costs, demand, CO_2 emissions and comfort levels. The proposed optimization model can be solved efficiently for real-time applications, and by considering different objective functions such as minimization of demand, total cost of electricity and gas, emissions and peak load over the scheduling horizon, the model facilitates the integration of residential customers into Smart Grids.

3. A realistic and novel mathematical optimization model of produce storage facilities in the commercial sector is formulated to optimize the operation of their energy systems in the context of Smart Grids. The developed model can be implemented as a supervisory control in existing climate controllers, while incorporating weather forecasts, electricity price information, and end-user preferences to optimally operate existing climate control systems of multiple produce storage facilities in a single site. The proposed model minimizes customer's total energy costs and demand charges while considering important parameters of storage facilities.

4. A solution algorithm based on an iterative B&B approach, which relies on relaxed linearized subproblems of the developed NLP model, is proposed for real-time implementation of the proposed model for optimal operation of storage facilities. Using the proposed algorithm, the developed model for optimal operation of storage facilities can be implemented in real-time applications, and thus facilitates the integration of these commercial customers into Smart Grids.

5. A novel MILP model for optimal operation of greenhouses in the agricultural sector which can be implemented as a supervisory control in existing greenhouse management systems is proposed and developed. The proposed optimization model incorporates weather forecasts, electricity price information, operational constraints of devices, and end-user preferences to reduce total energy costs and CO_2 emissions, considering humidity, temperature, lighting levels, and CO_2 concentration characteristics of the greenhouse, and keeping these important parameters within acceptable ranges. The proposed mathematical model is appropriate for real-time applications, and facilitates the integration of greenhouses into Smart Grids by optimally operating these energy hubs.

6. A robust optimization approach is applied to formulate an RMILP model of the proposed model for optimal operation of greenhouses to consider the uncertainty in electricity price forecasts on optimal operation of these energy hubs.

The main contents and contributions of Chapter 3 have been published as a US Provisional Patent application, and submitted as two IEEE journal papers for publication [147, 148, 149]. The proposed models and corresponding results presented in this thesis have been submitted as IP disclosures for patenting, licensing, and publication purposes [150, 151, 152]. Energent Inc. has indicated their desire to exclusively license the IP of this research and negotiations are currently under way.

6.3 Future Work

Based on the research presented in this thesis, the following some ideas and directions for further research are suggested:

1. Based on the results of the upcoming implementation and monitoring phases of the residential energy hubs, some adjustments of the mathematical models may be necessary. However, based on the implementation work, validation tests and simulations

so far, it is not expected to have any significant technical hurdles for the integration of the proposed models in some existing and future EMSs.

2. The activity level index proposed in this thesis is based on a simple average energy consumption in residential energy hubs. More sophisticated statistical approaches can be investigated to achieve a better representation of the activity level index of householders.

3. In addition to the various customers considered in this research, optimal operation of other types of energy hubs in commercial, agricultural, and industrial sectors, such as supermarkets, ice rinks, schools, and hospitals could be investigated.

4. The focus of the research presented in this these was on developing mathematical models for optimal operation of micro hubs from the end-user prospective; however, significant benefits may be achieved from both customers and the utility's point of view if the operation of a number of these "micro hubs" can be coordinated together. Therefore, development of mathematical models for optimal operation of "macro hubs", which would incorporate the micro hubs and system level information, need to be studied. This would result in a "multi-level" optimization problem to optimize the operation of the energy hubs from both the customers' and the utility's point of view.

5. The proposed mathematical models for optimal operation of storage facilities and greenhouses are based on physical principles and previously published models for individual components of these systems, and have been developed to be implemented in pilot locations to investigate the accuracy of these models, monitor their performance, and apply necessary adjustments in real-world applications.

APPENDICES

Appendix A

Input Data for Residential Sector Case Studies

The external inputs and data and assumed parameter settings of the devices used in the residential energy hub simulation case studies, presented in Chapter 3, are given in this appendix.

A.1 Price Data

TOU, RTP and FRP tariffs for electricity, and FRP scheme for natural gas are used to calculate the total energy costs. Figure A.1 presents the energy pricing data used in the simulations. In Ontario the Hourly Ontario Electricity Price (HOEP) is the RTP that applies to large customers [4]; hence, this is the price used in this chapter for the study of residential customers.

A.2 Emissions Profile

Ontario's CO_2 emissions profile is considered for a summer weekday using the forecasting method described in Chapter 2. Using the actual demand profile of July 14, 2009, the Ontario's forecasted power generation from coal- and gas-fired power plants and corresponding emissions profile, correspondingly depicted in Figure A.2 and Figure A.3, are obtained and used in the case studies presented in this thesis [135].

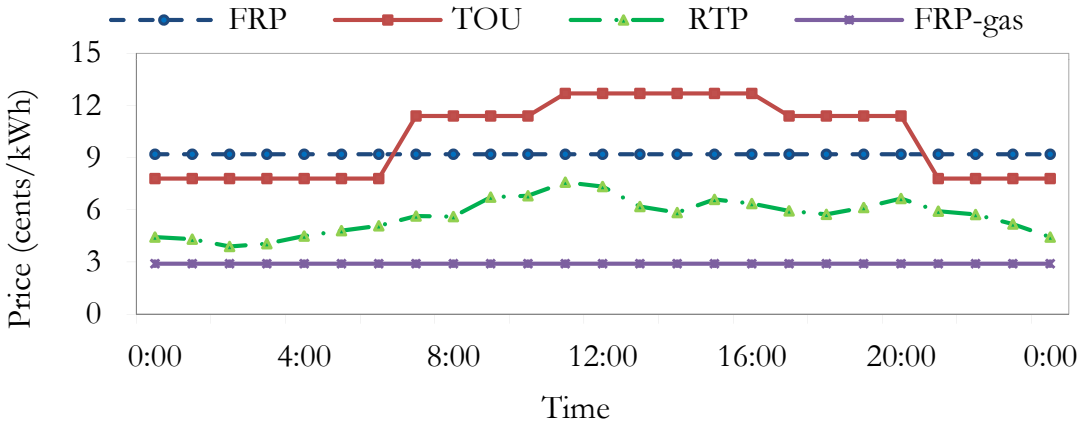

Figure A.1: TOU, RTP and FRP tariffs inputs for the residential energy hub simulations.

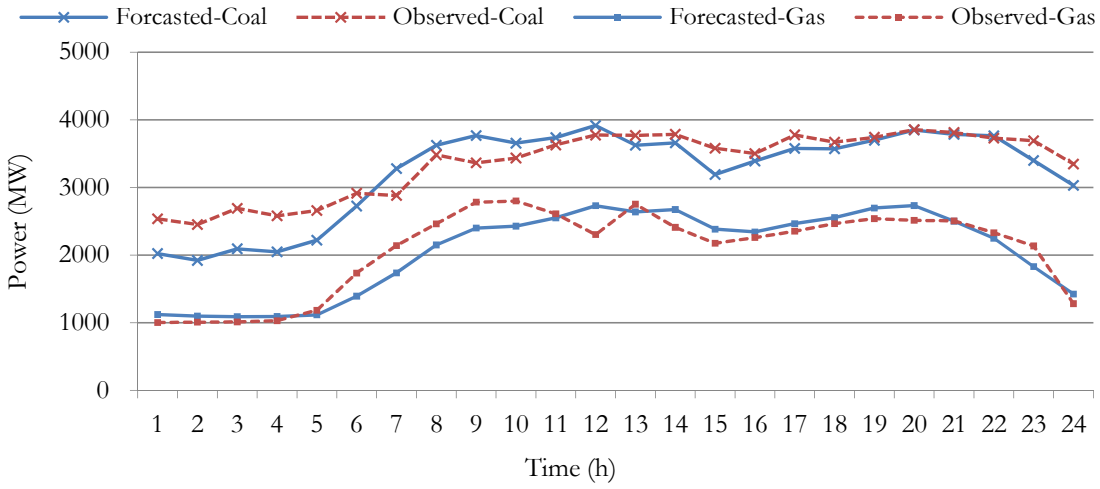

Figure A.2: Forecasted power generation from coal- and gas-fired power plants in Ontario for a summer day.

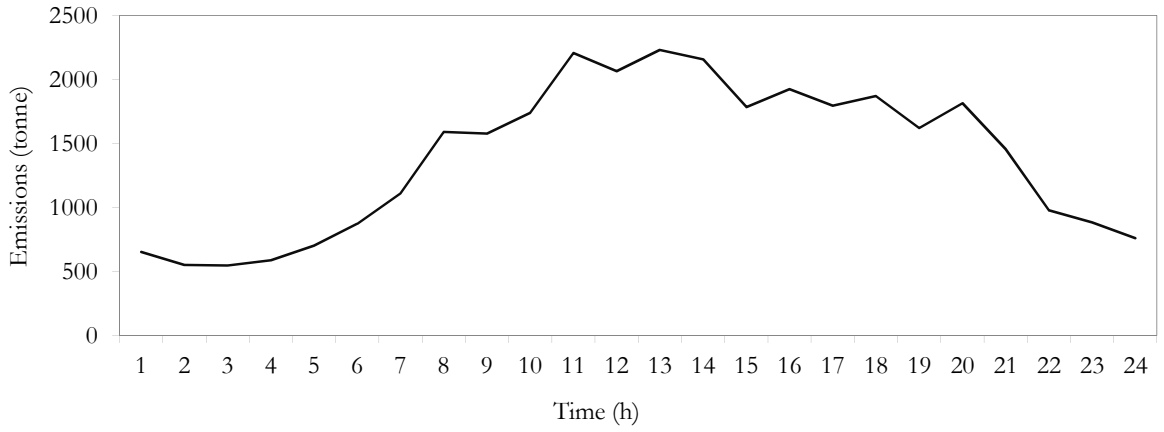

Figure A.3: Ontario's emissions profile for a summer day.

A.3 Ambient Air Temperature

The outside ambient air temperatures for a specific summer (July) and a winter (January) day considered for the case studies in this chapter are shown in Figure A.4.

A.3.1 Illumination Level

The data of incoming short wave radiations in W/m^2 used here is taken from the University of Waterloo Weather Station [6]. It is assumed that each illumination level inside a zone is equal to 200 lx, with a 150 W demand. The outside illumination level information required by the model for residential lighting is assumed to be in per unit as discussed in section 3.3.2; therefore, normalized data is used as shown in Figure A.5.

A.4 Solar PV Panel

A 3 kW solar PV roof top panel with battery storage system is assumed for the ESD model, with minimum and maximum storage levels of the battery being 6 kWh and 30 kWh, respectively. Energy is exported to the grid at 80.2 cents/kWh, which is the contract price set by the Ontario Power Authority (OPA) for residential participants in the Micro-FIT program. Typical power generation levels from a solar PV panel for summer and winter days are shown in Figure A.6.

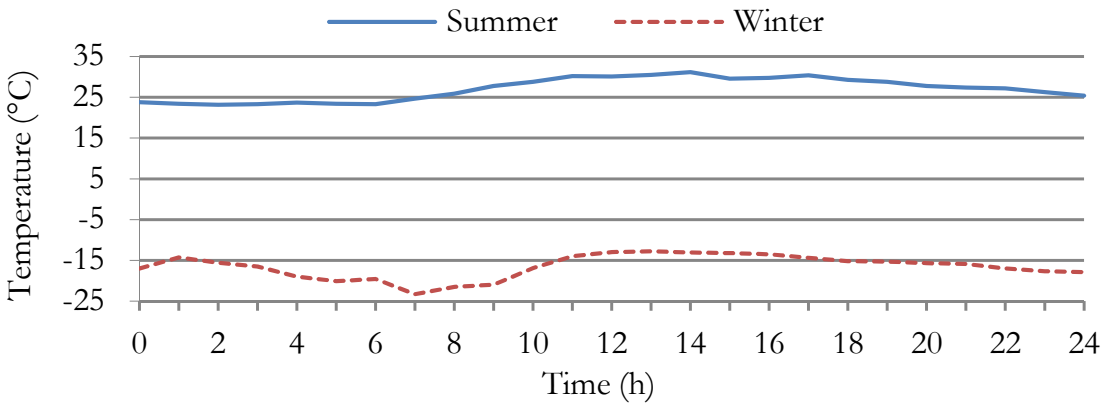

Figure A.4: Ambient air temperatures for summer and winter simulations.

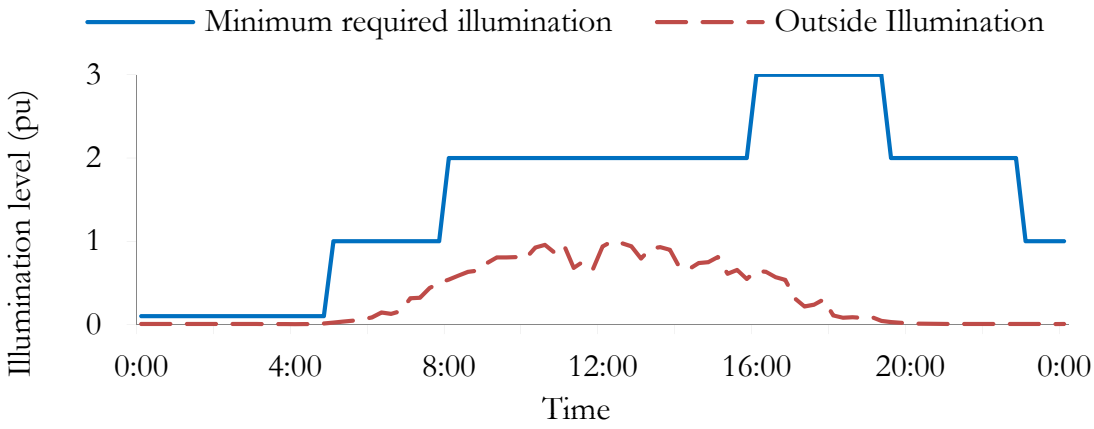

Figure A.5: Outside and minimum required illumination level.

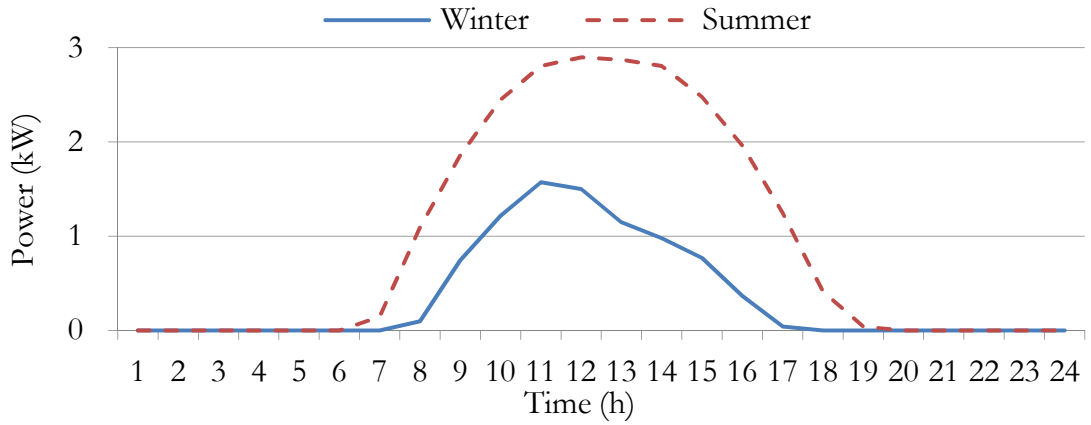

Figure A.6: Typical power generation levels from a solar PV panel for summer and winter days.

A.5 Activity Level

Figure A.7 shows the Activity Level over a day for a single detached house used in this chapter for simulations. This is similar to hourly variations of energy consumption of the household on a summer day.

A.6 Hourly Hot Water Usage (HWU)

The methods proposed in [141] and [143] are used to predict the hourly hot water use in a house to carryout case studies. The HWU(t) obtained for the household is shown in Figure A.8.

A.7 Other Inputs

The model parameters and other data used in the simulation case studies of the residential energy hub are presented in Table A.1.

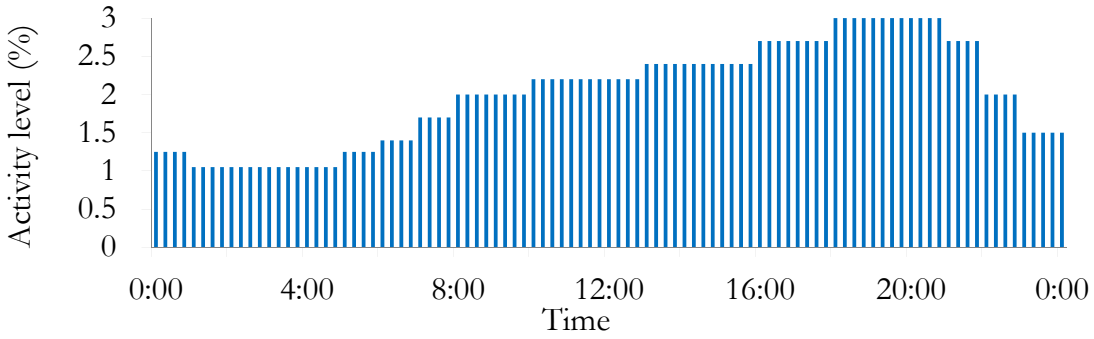

Figure A.7: Activity Level over a day for a single detached house.

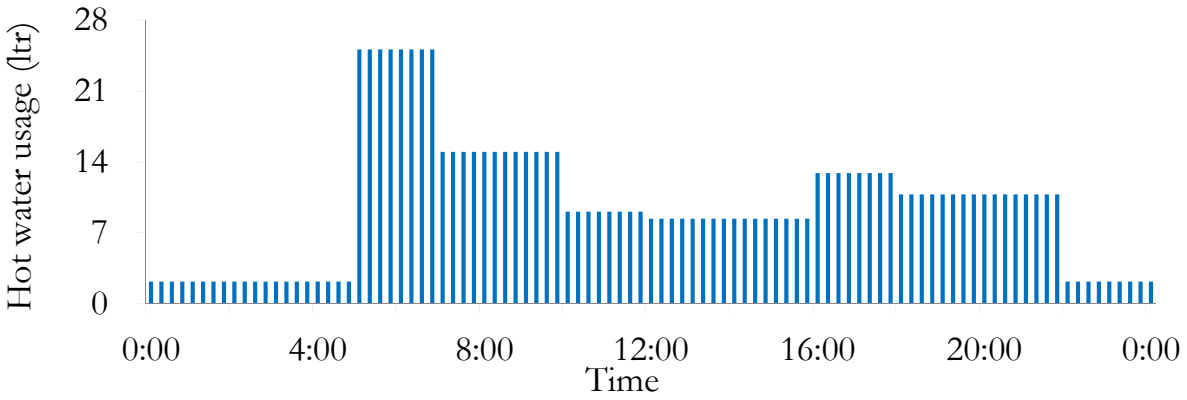

Figure A.8: Estimated average hourly hot water usage profile in a household.

Table A.1: Parameter settings in the residential energy hub simulations.

Device	Parameter	Sample Value	Parameter	Sample Value
Fridge	P_{fr}	600 W	θ_{fr}^{low}	2 °C
	et_{fr}	1	γ_{fr}	0.14
	lt_{fr}	96	α_{fr}	2.75
	θ_{FR}^{up}	8 °C	β_{fr}	0.605
AC/Heating	P_{AC}	2200 W	lt_{ac}	96
	θ_{in}^{up}	23 °C	ρ_{ac}	0.0075
	θ_{in}^{low}	17 °C	α_{ac}	0.33
	et_{ac}	1	β_{ac}	0.044
	P_{ht}	1150 W	γ_{ht}	0.0075
Water heater	HR_{ht}	0.534	α_{ht}	0.67
	P_{wh}	600 W	θ_{wh}^{up}	58 °C
	HR_{WH}	0.297	θ_{wh}^{low}	48 °C
	et_{wh}	1	α_{wh}	4.44
	lt_{wh}	96	θ_{wh}^{up}	58 °C
	γ_{wh}	0.05	*tanksz*	185
	Hr	38	*therm*	55
	β_{wh}	0.068	*wtmp*	8
			atmp	-10
Stove	P_{stv}	1500 W	rot_{stv}	12
	et_{stv}	65	mut_{stv}	4
	lt_{stv}	88	$msot_{stv}$	12
Pool Pump	P_{pmp}	750 W	lt_{pmp}	96
	et_{pmp}	29	rot_{pmp}	40
Energy Storage Device	dch_{esd}	3	chd_{esd}	--
	ESL_{esd}^{min}	6 kWh	ESL_{esd}^{max}	30 kWh
	et_{esd}	1	lt_{esd}	96
PV solar array	P_{pv}	--	ESL_{pv}^{max}	30 kWh
	chd_{pv}	3 kW	et_{pv}	1
	ESL_{pv}^{min}	6 kWh	lt_{pv}	96
Lighting	P_{ilz}	150 W	et_{il}	1
			lt_{il}	96
Dishwasher	P_{dw}	700 W	mut_{dw}	8
	et_{dw}	65	mdt_{dw}	4
	lt_{dw}	92	$msot_{dw}$	8
Washer	P_{wr}	450 W	mut_{wr}	8
	et_{wr}	64	mdt_{wr}	4
	lt_{wr}	92	$msot_{wr}$	8
Dryer	P_{dry}	1100 W	mut_{dry}	8
	et_{dry}	64	mdt_{dry}	4
	lt_{dry}	92	$\Delta_{wr,dry}$	12

Appendix B

Input Data for Commercial Sector Case Studies

The external inputs and data and assumed parameter settings of the devices used in the commercial energy hub simulation case studies, presented in Chapter 4, are given in this appendix. Figure B.1 to Figure B.6 show actual values of outdoor temperature, relative humidity and electricity prices used for summer and winter simulations in Chapter 4. Minimum, maximum and mean values of outdoor temperature, relative humidity and RTP used in summer and winter Monte-Carlo simulations in Chapter 4 are depicted in Figure B.7 to Figure B.12, respectively.

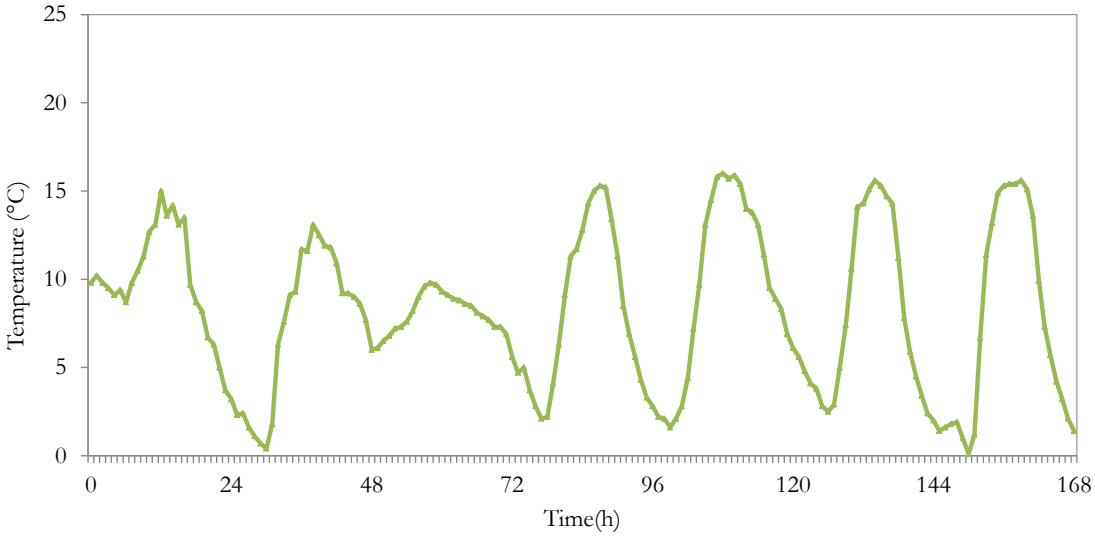

Figure B.1: Actual outdoor temperature during 14^{th} – 20^{th} September 2010, used for summer case studies.

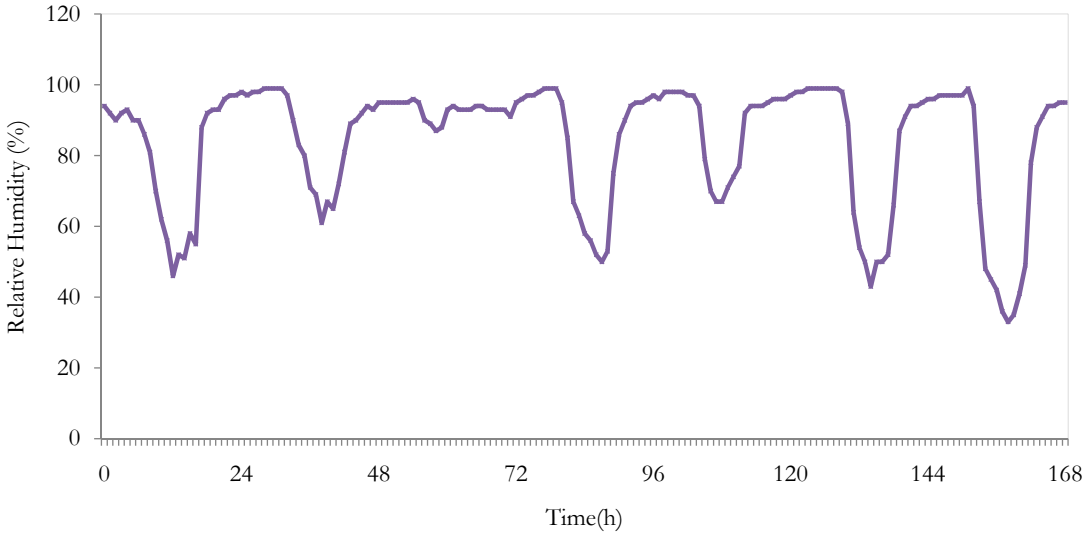

Figure B.2: Actual outdoor relative humidity during 14^{th} – 20^{th} September 2010, used for summer case studies.

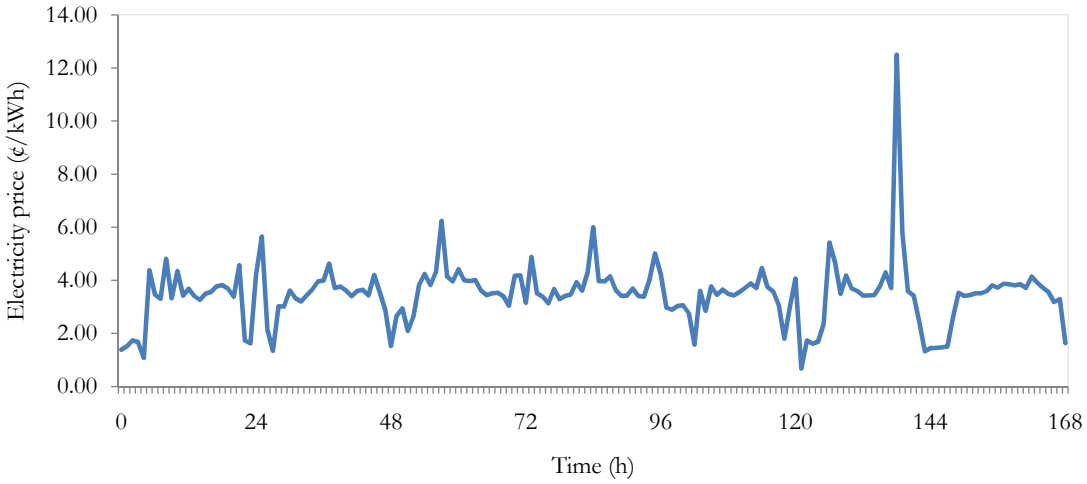

Figure B.3: Actual HOEP (RTP) during 14^{th} – 20^{th} September 2010, used for summer case studies.

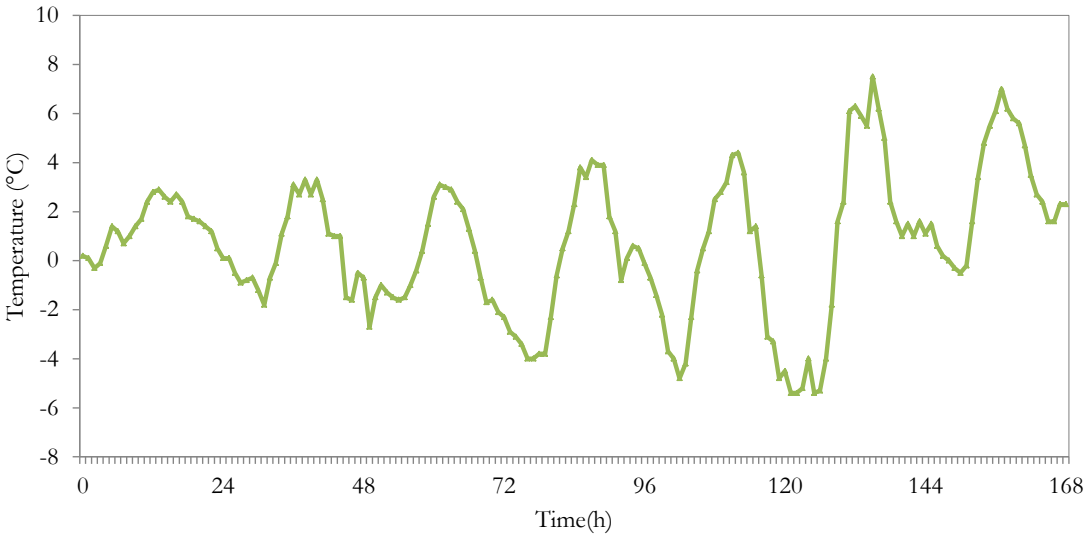

Figure B.4: Actual outdoor temperature during 1^{st} to 7^{th} March 2010, used for winter case studies.

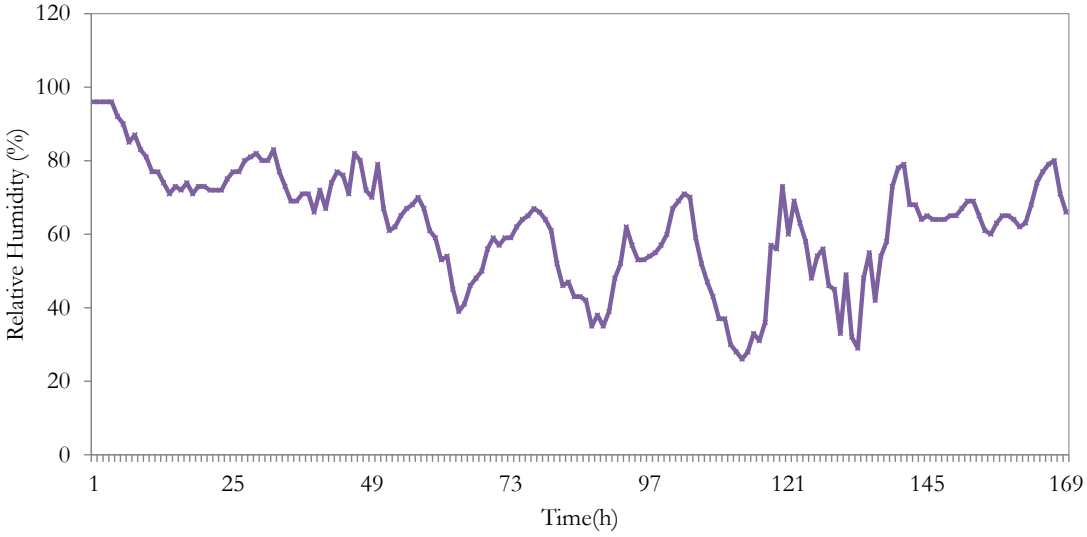

Figure B.5: Actual outdoor relative humidity during 1^{st} to 7^{th} March 2010, used for winter case studies.

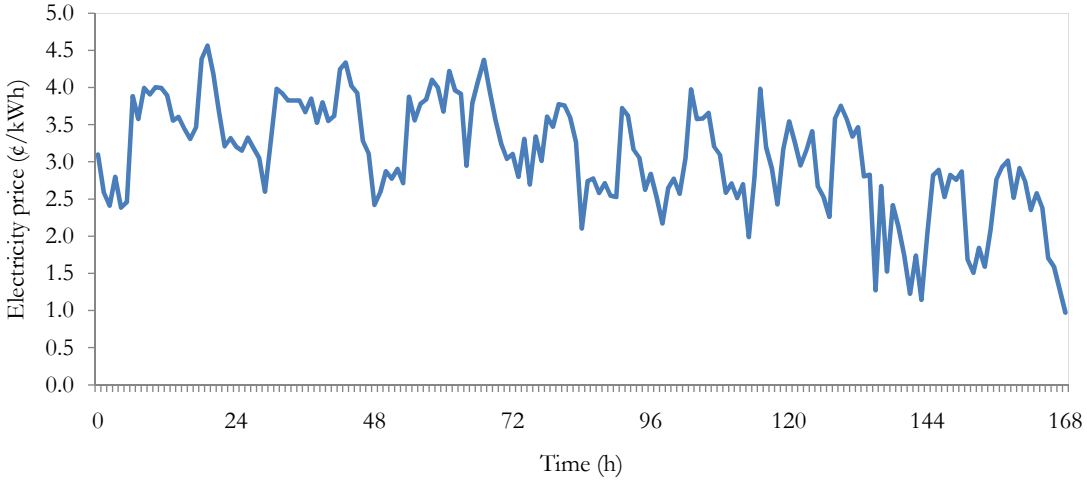

Figure B.6: Actual HOEP (RTP) during 1^{st} to 7^{th} March 2010, used for winter case studies.

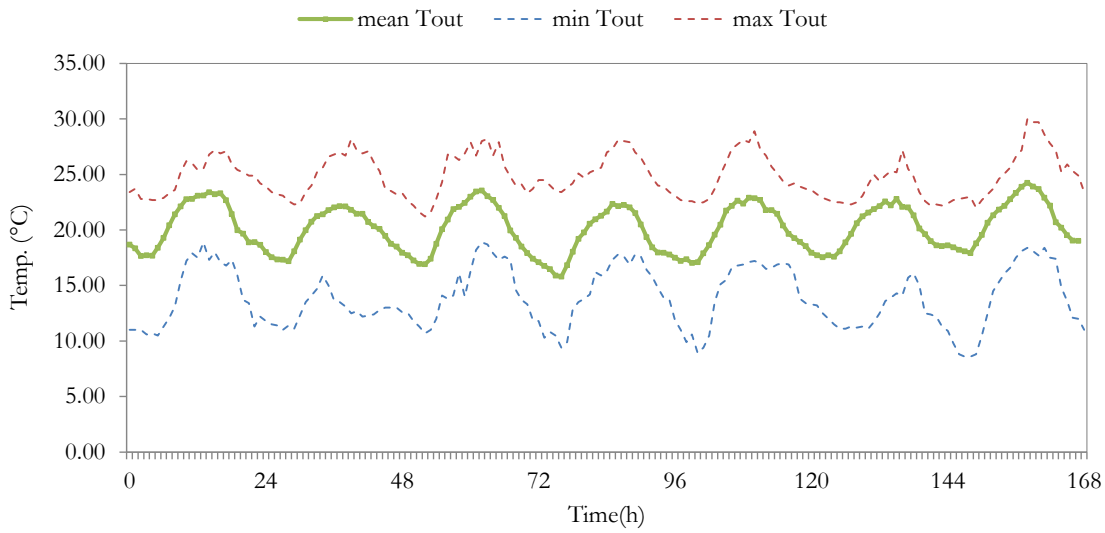

Figure B.7: Actual minimum, maximum, and mean values of outdoor temperature in summer 2010, used in the Monte-Carlo simulations.

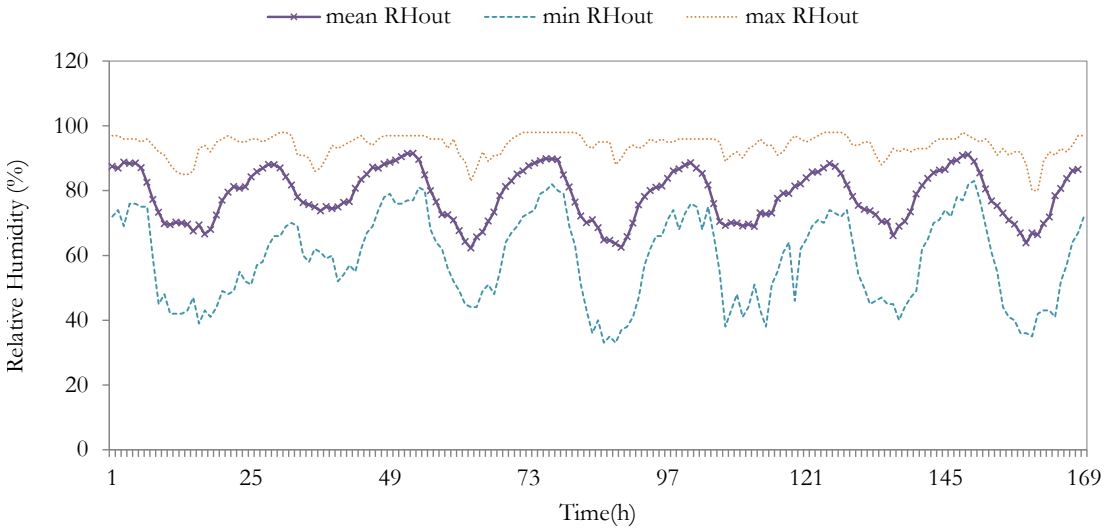

Figure B.8: Actual minimum, maximum, and mean values of outdoor humidity in summer 2010, used in the Monte-Carlo simulations.

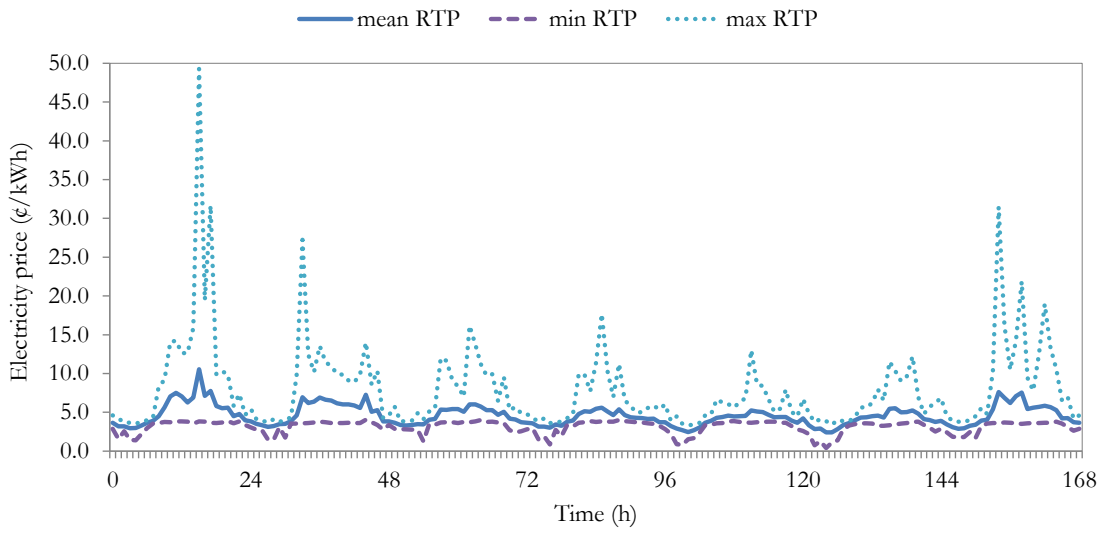

Figure B.9: Actual minimum, maximum, and mean values of HOEP prices (RTP) in summer 2010, used in the Monte-Carlo simulations.

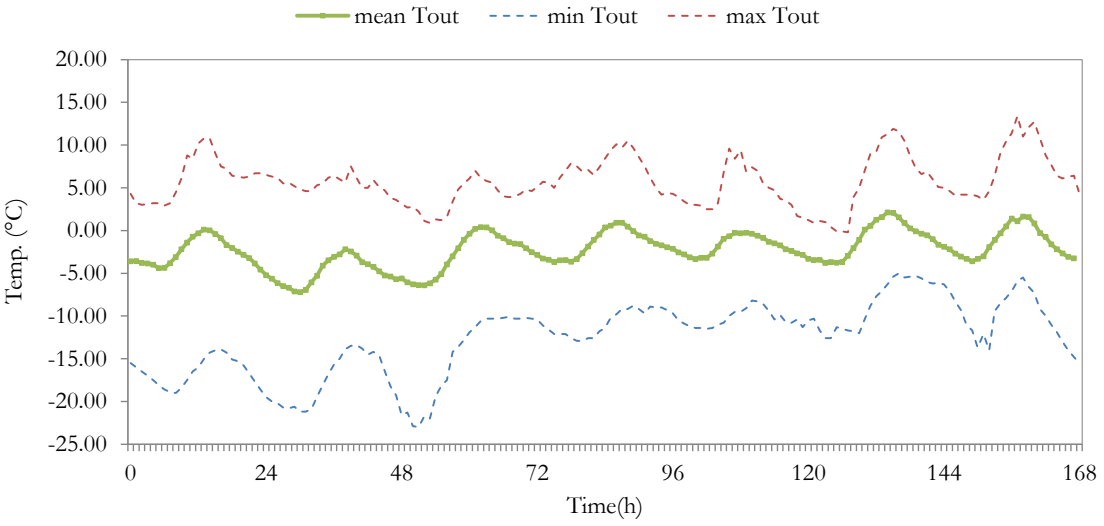

Figure B.10: Actual minimum, maximum, and mean values of outdoor temperature in winter 2010, used in the Monte-Carlo simulations.

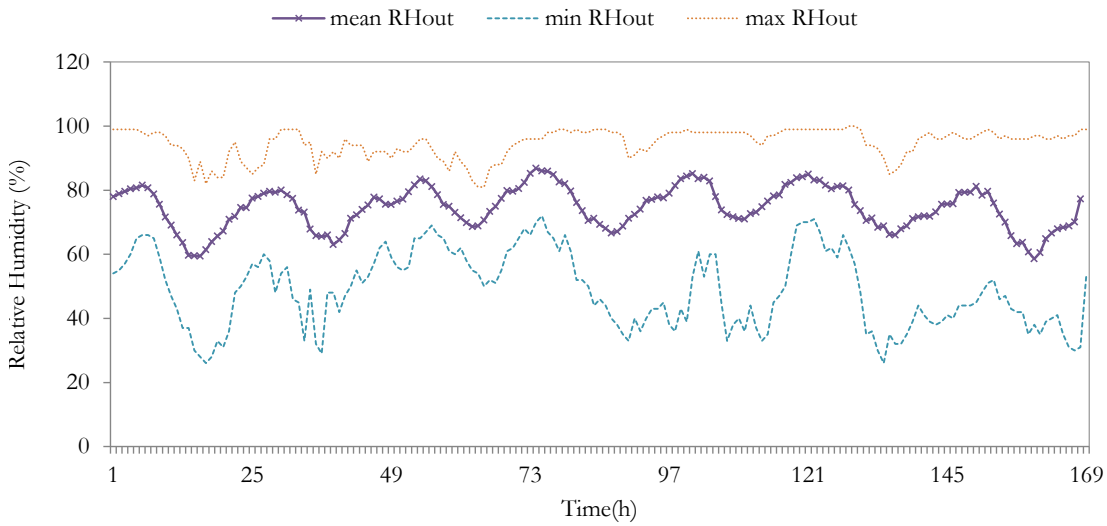

Figure B.11: Actual minimum, maximum, and mean values of outdoor humidity in winter 2010, used in the Monte-Carlo simulations.

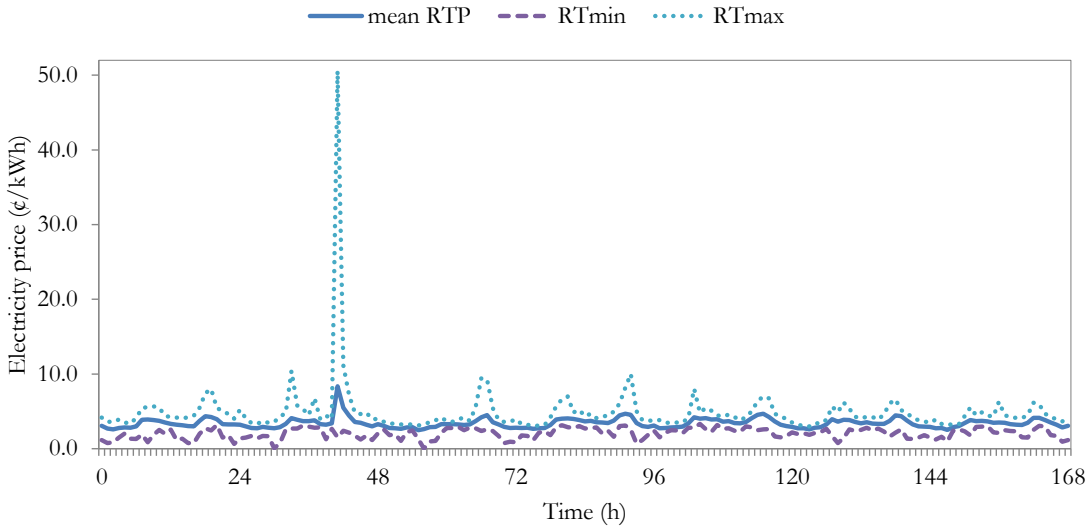

Figure B.12: Actual minimum, maximum, and mean values of HOEP prices (RTP) in winter 2010, used in the Monte-Carlo simulations.

Table B.1: Parameter settings in the storage facilities model simulations.

Parameter	**Sample value**	**Parameter**	**Sample value**
A_{sp}	50 (m^2_{pr}/m^3_b)	p_3	7.7835 (Pa)
c_{dc}	8 (\$)	p_4	0.058549 (K^{-1})
c_a	1.006 ($kJ/(kg$ °C))	p_5	0.6228 (kg_w/kg_a)
c_p	3.6 ($kJ/(kg$ °C))	Q^{leak}	290 (m^3/h)
ϕ_1^{min}	70 (%)	Q^{max}	29000 (m^3/h)
ϕ_2^{min}	70 (%)	R	8.314472 ($J/(mol\,K)$)
ϕ_3^{min}	70 (%)	ρ_a	1.27 (kg/m^3)
ϕ_1^{max}	90 (%)	ρ_b	670 (kg/m^3)
ϕ_2^{max}	90 (%)	ρ_p	1020 (kg/m^3)
ϕ_3^{max}	90 (%)	τ	1 (h)
h_{ev}	2270 (kJ/kg_w)	θ_{out}^{min}	-3 (°C)
h_{re}	19.5 $\times 10^{-3}$ ($kJ/(kg_{pr}h)$)	θ_1^{max}	5.5 (°C)
k_{ev}	0.14 ($kg_a/(m^2_{pr}\,h)$)	θ_2^{max}	6.5 (°C)
m_w	18.0153e-3 (kg/mol)	θ_3^{max}	7.5 (°C)
$M_{pr,1}$	1666000 (kg)	θ_1^{min}	4.5 (°C)
$M_{pr,2}$	1666000 (kg)	θ_2^{min}	5.5 (°C)
$M_{pr,3}$	1666000 (kg)	θ_3^{max}	6.5 (°C)
N_T	169	UA_1	3836 ($kJ/(h$ °C)
P_{fan}	3700 (W)	UA_2	3836 ($kJ/(h$ °C)
P_{rf}	70000 (W)	UA_3	3836 ($kJ/(h$ °C)
P_{ht}	20000 (W)	V_1	5184 (m^3)
p_{mx}	750 (W)	V_2	5184 (m^3)
P_{hu}	750 (W)	V_3	5184 (m^3)
P_{dh}	27700 (W)	V_a	0.34 (no dim.)
P_{atm}	0.965e5 (Pa)	V_p	0.66 (no dim.)
p_1	100 (no dim.)	w_h^{max}	3.5 (kg_w/h)
p_2	1.7001 (Pa)	w_{dh}^{max}	19.5 (kg_w/h)
		z	1 ,2 ,3

Appendix C

Input Data for Agricultural Sector Case Studies

The external inputs and data and assumed parameter settings of the devices used in the agricultural energy hub simulation case studies, presented in Chapter 5, are given in this appendix.

Input data for outdoor temperature, relative humidity and RTP, and their minimum, maximum and mean values used in summer and winter case studies presented in Chapter 5 are obtained from the first 24 hours of corresponding data presented in Appendix B. Additionally, Figure C.1 to Figure C.3 show solar irradiations and wind speeds used in summer and winter case studies in Monte-Carlo simulations in Chapter 5.

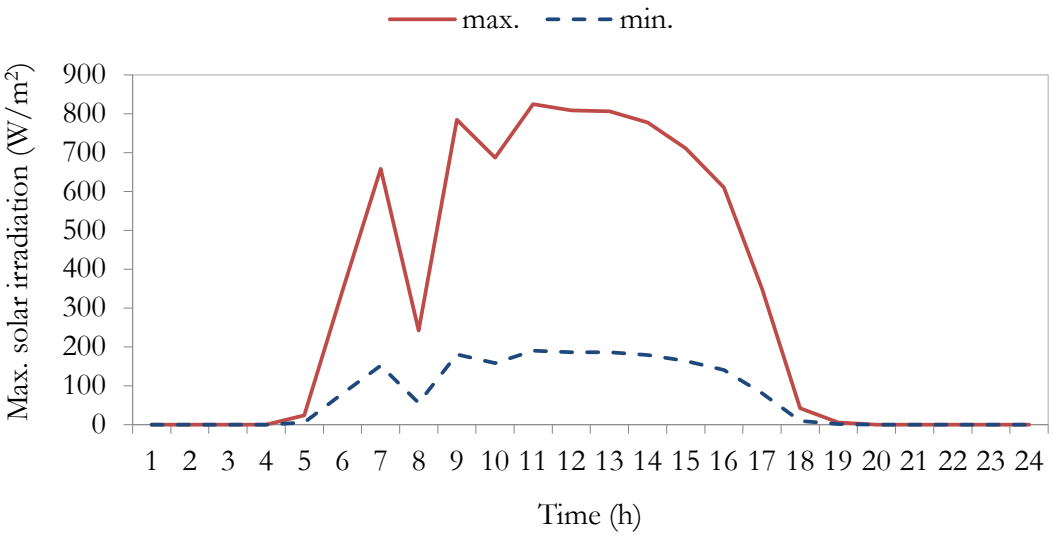

Figure C.1: Minimum and maximum solar irradiations used in summer Monte-Carlo simulations.

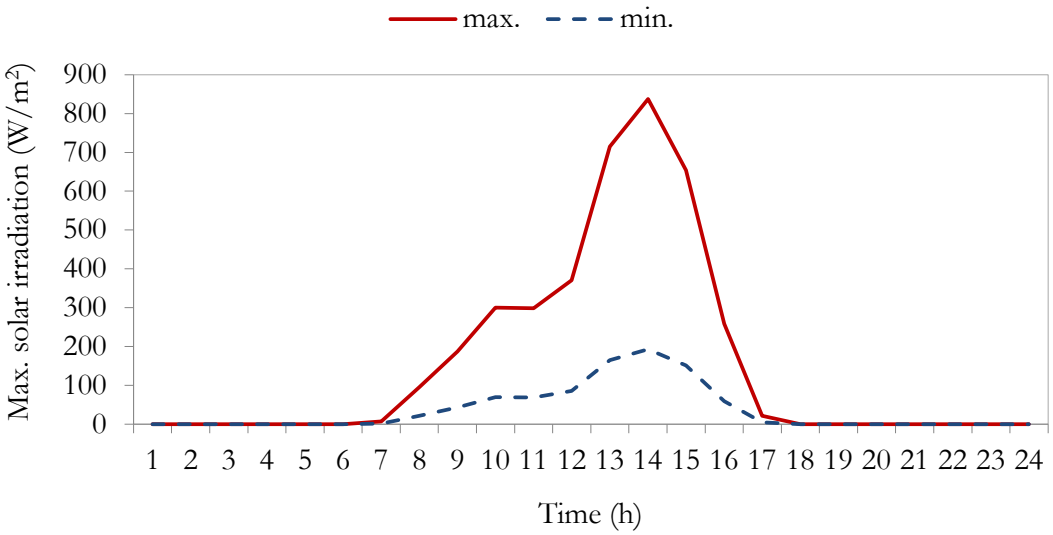

Figure C.2: Minimum and maximum solar irradiations used in winter Monte-Carlo simulations.

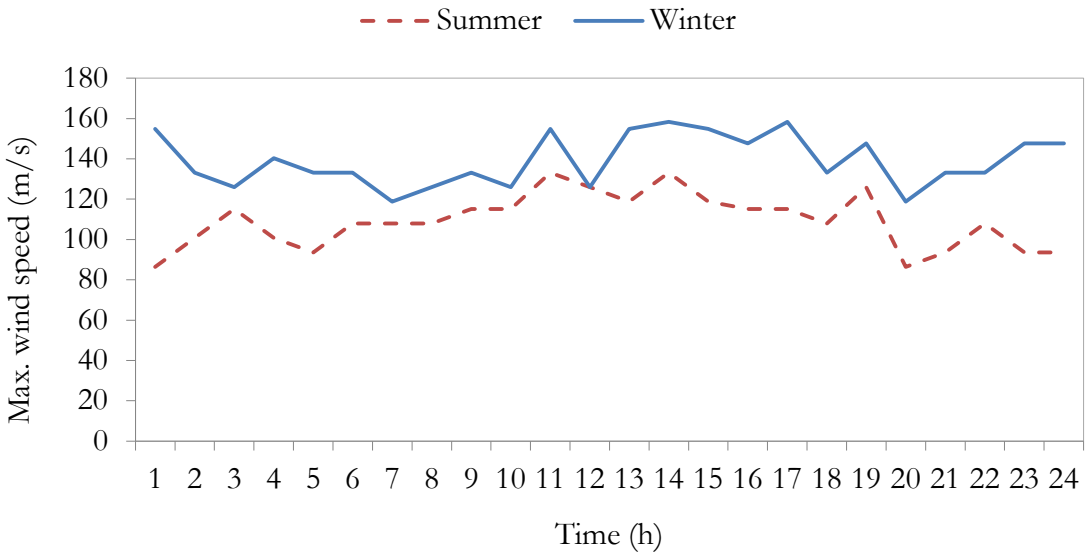

Figure C.3: Maximum wind speed used in summer and winter Monte-Carlo simulations.

Table C.1: Parameter settings in the greenhouse model simulations.

Parameter	**Sample value**	**Parameter**	**Sample value**
$A_{gh,z}$	20000 (m^2)	R_{wl}	180 $(kJ/(h\,K\,m^2))$
$A_{wl,z}$	22400 (m^2)	R_{sl}	20.7 $(kJ/(h\,K\,m^2))$
$A_{nv,z}$	450 (m^2)	R_{pipe}	1200 $(kJ/(h\,K\,m^2))$
$A_{ht_p,z}$	1625 (m^2)	R_{sr}	0.7
$A_{chl_p,z}$	1625 (m^2)	$R_{pipe,sl}$	3.6 $(kJ/(h\,K\,m^2))$
C_a	1.006 $(kJ/(kg\,K))$	P_{fog}	16 (kW)
C_w	4.1855 $(kJ/(kg\,K))$	P_{ht}	2 (MW)
c_{re}	1.224e-3 $(g/(m^2\,h\,K))$	$P_{li,1}$	2 (MW)
c_{phot}	46.03e-8 (g/J)	$P_{li,2}$	2 (MW)
$\mathcal{C}_{inj}^{max}$	0.8 (g/m_{gh}^2)	P_{nv}	500 (W)
$\mathcal{C}_{z}^{max}$	0.7 (g/m_{gh}^2)	Q_z	18.3 $(m_a^3/(h\,m_{gh}^2))$
$\mathcal{C}_{z}^{min}$	1.3 (g/m_{gh}^2)	ρ_a	1.27 (kg/m^3)
C_p	3 $(kJ/(kg\,K))$	ρ_w	1000 (kg/m^3)
c_{dc}	8 (\$/kW)	ρ_p	1010.2 (kg/m^3)
ε	0.85 (m_a^3/m_{gh}^3)	R_g	0.5148 (tonne/MWh)
η_{chl}	1	rot_{cf}	12 (h)
η_{fog}	0.05	Ψ_z^{mdu}	200 (W/m^2)
η_{li}	0.3	$\Psi_z^{min_{mdu}}$	200 (W/m^2)
η_{sr}	0.9	$\Psi_z^{max_{aggr}}$	10000 (W/m^2)
H_{gh}	4 (m)	$\Psi_z^{min_{aggr}}$	4000(W/m^2)
h_{ev}	2270 (kJ/kg_w)	$\Psi_{z,1}^{max}$	100 (W/m^2)
λ	0.0075 (no dim.)	$\Psi_{z,2}^{max}$	100 (W/m^2)
mdu	1 (h)	scc	100 (\$/tonne)
md_{li}	2 (h)	θ_{sl}	8 (°C)
mu_{li}	2 (h)	θ_{out}^{min}	-3 (°C)
$msot_{li}$	8 (h)	θ_z^{set}	17 (°C)
m_w	18.0153×10^{-3} (kg/mol)	θ_z^{min}	15(°C)
N_T	24	θ_z^{max}	19 (°C)
p_1	100 (no dim.)	$\theta_z^{l_0}$	16 (°C)
p_2	1.7001 (Pa)	$\theta_z^{u_0}$	18 (°C)
p_3	7.7835 (Pa)	$\theta_{ht_p}^{min}$	60 (°C)
p_4	1/17.0789 (K^{-1})	$\theta_{ht_p}^{max}$	95 (°C)
p_5	0.6228 (kg_w/kg_a)	$\theta_{chl_p}^{min}$	4 (°C)
p_6	3600 (no dim.)	$\theta_{chl_p}^{max}$	10 (°C)
p_7	-0.27 (°C)	τ	1 (h)
p_8	0.05 (no dim.)	$V_{gh,z}$	80000 (m^3)
P_{atm}	0.65e5 (Pa)	$V_{ht_p,z}$	100 (m^3)
P_{cf}	30.5 (kW)	$V_{chl_p,z}$	50 (m^3)
P_{chl}	175 (kW)	$W_{evp}(z)$	125.8 $(g_w/(h\,m_{gh}^2))$
P_{co_2}	200 (kW)	W_{fog}^{max}	9.6 $(g_w/(m_{gh}^2 h))$
P_{dh}	60 (kW)	W_{dh}^{max}	145 $(g_w/(m_{gh}^2\,h)$
P_{fv}	14 (kW)	ξ_z	366000 (h^{-1})

References

[1] "Emissions of greenhouse gases in the united states 2006," U.S. Department of Energy: Energy Information Administration, Tech. Rep. DOE/EIA-0573, Nov. 2007. [Online]. Available: ftp://ftp.eia.doe.gov/pub/oiaf/1605/cdrom/pdf/ggrpt/057306.pdf

[2] A. Ipakchi, "Smart grid of the future with large scale DR/DER penetration," in *Proc. IEEE PES Power Systems Conference and Exposition*, 2009.

[3] F. Rahimi and A. Ipakchi, "Demand response as a market resource under the smart grid paradigm," *IEEE Transactions on Smart Grid*, vol. 1, no. 1, pp. 82 –88, 2010.

[4] C. C. A. Rajan, "Demand side management using expert system," in *Proc. Conference on Convergent Technologies for Asia-Pacific Region*, vol. 1, 2003, pp. 440–444.

[5] D. Chattopadhyay, R. Banerjee, and J. Parikh, "Integrating demand side options in electric utility planning: a multi-objective approach," *IEEE Transactions on Power Systems*, vol. 10, no. 2, pp. 657–663, May 1995.

[6] F. Rahimi and A. Ipakchi, "Overview of demand response under the smart grid and market paradigms," in *Innovative Smart Grid Technologies (ISGT)*, 2010, pp. 1–7.

[7] L. Perez-Lombard, J. Ortiz, and C. Pout, "A review on buildings energy consumption information," *Energy and Buildings*, vol. 40, no. 3, pp. 394–398, 2008.

[8] "Annual energy review 2009," U.S. Department of Energy: Energy Information Administration, Tech. Rep. DOE/EIA-0384, August 2010. [Online]. Available: http://www.eia.gov/aer

[9] D. G. Hart, "Using ami to realize the smart grid," in *IEEE PES General Meeting–Conversion and Delivery of Electrical Energy in the 21st Century*, 2008, pp. 1–2.

[10] A. Faruqui and S. S. George, "The value of dynamic pricing in mass markets," *The Electricity Journal*, vol. 15, no. 6, pp. 45–55, 7 2002.

[11] A. Moholkar, P. Klinkhachorn, and A. Feliachi, "Effects of dynamic pricing on residential electricity bill," in *Proc. IEEE PES Power Systems Conference and Exposition*, vol. 2, 2004, pp. 1030–1035.

[12] H. Allcott, "Rethinking real time electricity pricing," MIT Center for Energy and Environmental Policy Research, Tech. Rep. MIT-CEEPR-2009-015, Oct. 2009. [Online]. Available: http://hdl.handle.net/1721.1/51713

[13] A. Stokke, G. Doorman, and T. Ericson, "An analysis of a demand charge electricity grid tariff in the residential sector," *Energy Efficiency*, vol. 3, pp. 267–282, 2010. [Online]. Available: http://dx.doi.org/10.1007/s12053-009-9071-9

[14] H. Saele and O. S. Grande, "Demand response from household customers: Experiences from a pilot study in norway," *IEEE Transactions on Smart Grid*, vol. 2, no. 1, pp. 90–97, 2011.

[15] C. M. Chu and T. L. Jong, "A novel direct air-conditioning load control method," *IEEE Transactions on Power Systems*, vol. 23, no. 3, pp. 1356–1363, Aug. 2008.

[16] D.-C. Wei and N. Chen, "Air conditioner direct load control by multi-pass dynamic programming," *IEEE Transactions on Power Systems*, vol. 10, no. 1, pp. 307–313, Feb. 1995.

[17] S. El-Ferik, S. A. Hussain, and F. M. Al-Sunni, "Identification of physically based models of residential air-conditioners for direct load control management," in *Proc. 5th Asian IEEE Control Conference*, vol. 3, 2004, pp. 2079–2087.

[18] A. Molina, A. Gabaldon, J. A. Fuentes, and C. Alvarez, "Implementation and assessment of physically based electrical load models: application to direct load control residential programmes," *IEE Proceedings on Generation, Transmission and Distribution*, vol. 150, no. 1, pp. 61–66, Jan. 2003.

[19] N. E. Ryan, J. T. Powers, S. D. Braithwait, and B. A. Smith, "Generalizing direct load control program analysis: implementation of the duty cycle approach," *IEEE Transactions on Power Systems*, vol. 4, no. 1, pp. 293–299, Feb. 1989.

[20] C. N. Kurucz, D. Brandt, and S. Sim, "A linear programming model for reducing system peak through customer load control programs," *IEEE Transactions on Power Systems*, vol. 11, no. 4, pp. 1817–1824, Nov. 1996.

[21] S. Koch, M. Zima, and G. Andersson, "Local load management: Coordination of a diverse set of thermostat-controlled appliances," in *Smart Energy Strategies 2008 – Meeting the Climate Change Challenge*, Sept. Zurich, Switzerland, 2008. [Online]. Available: http://www.eeh.ee.ethz.ch/uploads/tx_ethpublications/Koch_Zima_Andersson_LLM_SES08.pdf

[22] J. C. Laurent, G. Desaulniers, R. Malhame, and F. Soumis, "A column generation method for optimal load management via control of electric water heaters," *IEEE Transactions on Power Systems*, vol. 10, no. 3, pp. 1389–1400, Aug. 1995.

[23] H. Jorge, C. H. Antunes, and A. G. Martins, "A multiple objective decision support model for the selection of remote load control strategies," *IEEE Transactions on Power Systems*, vol. 15, no. 2, pp. 865–872, May 2000.

[24] R. P. Hamalainen and J. Mantysaari, "Dynamic multi-objective heating optimization," *European Journal of Operational Research*, vol. 142, no. 1, pp. 1–15, 2002.

[25] K. Bhattacharyya and M. L. Crow, "A fuzzy logic based approach to direct load control," *IEEE Transactions on Power Systems*, vol. 11, no. 2, pp. 708–714, May 1996.

[26] H. Sane and M. Guay, "Minmax dynamic optimization over a finite-time horizon for building demand control," in *Proc. American Control Conference*, 2008, pp. 1469–1474.

[27] M. A. A. Pedrasa, T. D. Spooner, and I. F. MacGill, "Coordinated scheduling of residential distributed energy resources to optimize smart home energy services," *IEEE Transactions on Smart Grid*, vol. 1, no. 2, pp. 134–143, 2010.

[28] A. Mohsenian-Rad, V. W. S. Wong, J. Jatskevich, R. Schober, and A. Leon-Garcia, "Autonomous demand-side management based on game-theoretic energy consumption scheduling for the future smart grid," *IEEE Transactions on Smart Grid*, vol. 1, no. 3, pp. 320–331, 2010.

[29] A. Mohsenian-Rad and A. Leon-Garcia, "Optimal residential load control with price prediction in real-time electricity pricing environments," *IEEE Transactions on Smart Grid*, vol. 1, no. 2, pp. 120–133, 2010.

[30] A. Esser, A. Kamper, M. Franke, D. Most, and O. Rentz, "Scheduling of electrical household appliances with price signals," *Proceedings of the*

Operations Research, vol. 2006, pp. 253–258. [Online]. Available: http://www.springerlink.com/content/l714q911m13466m6/

[31] "Demand responsive electrical appliance manager." [Online]. Available: http://dr.berkeley.edu/dream/

[32] G. Diana and P. Govender, "Demand side management: a case study of a tertiary institution," in *Proc. International Conference on Electric Utility Deregulation and Restructuring and Power Technologies*, 2000, pp. 419–424.

[33] P. Kadar, "Understanding customer behaviour," in *Proc. IEEE PES Transmission and Distribution Conference and Exposition: Latin America*, 2008, pp. 1–4.

[34] H. Hagras, I. Packharn, Y. Vanderstockt, N. McNulty, A. Vadher, and F. Doctor, "An intelligent agent based approach for energy management in commercial buildings," in *IEEE International Conference on Fuzzy Systems*, 2008, pp. 156–162.

[35] K. Fong, V. Hanby, and T. Chow, "HVAC system optimization for energy management by evolutionary programming," *Energy and Buildings*, vol. 38, no. 3, pp. 220–231, 2006.

[36] W. Huang, M. Zaheeruddin, and S. Cho, "Dynamic simulation of energy management control functions for HVAC systems in buildings," *Energy conversion and management*, vol. 47, no. 7-8, pp. 926–943, 2006.

[37] K. Fong, V. Hanby, and T. Chow, "System optimization for HVAC energy management using the robust evolutionary algorithm," *Applied Thermal Engineering*, vol. 29, no. 11-12, pp. 2327–2334, 2009.

[38] S. Wang and Z. Ma, "Supervisory and optimal control of building HVAC systems: A review," *HVAC&R Research*, vol. 14, no. 1, pp. 3–32, 2008.

[39] D. S. Naidu and C. G. Rieger, "Advanced control strategies for heating, ventilation, air-conditioning, and refrigeration systems – an overview: Part I: hard control," *HVAC&R Research*, vol. 17, no. 1, pp. 2–21, 2011.

[40] J. Xu, P. Luh, W. Blankson, R. Jerdonek, and K. Shaikh, "An optimization-based approach for facility energy management with uncertainties," *HVAC&R Research*, vol. 11, no. 2, pp. 215–237, 2005.

[41] L. Lukasse, J. de Kramer-Cuppen, and A. van der Voort, "A physical model to predict climate dynamics in ventilated bulk-storage of agricultural produce," *Journal of Refrigeration*, vol. 30, no. 1, pp. 195–204, 2007.

[42] K. Gottschalk, "Mathematical modelling of the thermal behaviour of stored potatoes & developing of fuzzy control algorithms to optimise the climate in storehouses," in *Proc. ISHS Acta Horticulturae 406*, 1994, pp. 331–340.

[43] Y. Xu and D. Burfoot, "Predicting condensation in bulks of foodstuffs," *Journal of Food Engineering*, vol. 40, no. 1-2, pp. 121–127, 1999.

[44] K. Keesman, D. Peters, and L. Lukasse, "Optimal climate control of a storage facility using local weather forecasts," *Control Engineering Practice*, vol. 11, no. 5, pp. 505–516, 2003.

[45] S. van Mourik, H. Zwart, and K. Keesman, "Switching control for post-harvest food storage," 2007, pp. 189–194.

[46] L. Lukasse, J. van Maldegem, E. Dierkes, A. van der Voort, J. de Kramer-Cuppen, and G. van der Kolk, "Optimal control of indoor climate in agricultural storage facilities for potatoes and onions," *Control Engineering Practice*, vol. 17, no. 9, pp. 1044–1052, 2009.

[47] G. Verdijck, "Product quality control," Ph.D. dissertation, University of Eindhoven, 2003.

[48] T. Morimoto, J. Suzuki, and Y. Hashimoto, "Optimization of a fuzzy controller for fruit storage using neural networks and genetic algorithms," *Engineering Applications of Artificial Intelligence*, vol. 10, no. 5, pp. 453–461, 1997.

[49] K. Gottschalk, L. Nagy, and I. Farkas, "Improved climate control for potato stores by fuzzy controllers," *Computers and Electronics in Agriculture*, vol. 40, no. 1-3, pp. 127–140, 2003.

[50] K. Refsgaard, N. Halberg, and E. S. Kristensen, "Energy utilization in crop and dairy production in organic and conventional livestock production systems," *Agricultural Systems*, vol. 57, no. 4, pp. 599–630, 1998.

[51] T. Horndahl, "Energy use in farm buildings," Swedish University of Agricultural Sciences, Tech. Rep. 2008:8, Nov. 2008. [Online]. Available: http://pub-epsilon.slu.se/396/01/Eng-rapport145-v1.pdf

[52] E. Brown and R. N. Elliott, "On-farm energy use characterizations," American Council for an Energy-Efficient Economy, Tech. Rep. IE052, March 2005.

[53] M. Meul, F. Nevens, D. Reheul, and G. Hofman, "Energy use efficiency of specialised dairy, arable and pig farms in flanders," *Agriculture, Ecosystems & Environment*, vol. 119, no. 1-2, pp. 135–144, 2 2007.

[54] J. A. Bailey, R. Gordon, D. Burton, and E. K. Yiridoe, "Energy conservation on nova scotia farms: Baseline energy data," *Energy*, vol. 33, no. 7, pp. 1144–1154, July 2008.

[55] E. Brown, R. N. Elliott, and S. Nadel, "Energy efficiency programs in agriculture: Design, success, and lessons learned," American Council for an Energy-Efficient Economy, Tech. Rep. IE051, Jan. 2005.

[56] G. van Straten, E. van Henten, L. van Willigenburg, and R. van Ooteghem, *Optimal control of greenhouse cultivation*. New York, USA: CRC Press, 2010.

[57] G. D. Pasgianos, K. G. Arvanitis, P. Polycarpou, and N. Sigrimis, "A nonlinear feedback technique for greenhouse environmental control," *Computers and Electronics in Agriculture*, vol. 40, no. 1-3, pp. 153–177, 10 2003.

[58] A. Pawlowski, J. L. Guzman, F. Rodrguez, M. Berenguel, J. Snchez, and S. Dormido, "Simulation of greenhouse climate monitoring and control with wireless sensor network and event-based control," *Sensors*, vol. 9, no. 1, pp. 232–252, 2009.

[59] C. J. Taylor, P. C. Young, A. Chotai, A. R. McLeod, and A. R. Glasock, "Modelling and proportional-integral-plus control design for free air carbon dioxide enrichment systems," *Journal of Agricultural Engineering Research*, vol. 75, no. 4, pp. 365–374, 4 2000.

[60] E. V. Henten and J. Bontsema, "Time-scale decomposition of an optimal control problem in greenhouse climate management," *Control Engineering Practice*, vol. 17, no. 1, pp. 88–96, 2009.

[61] H. Pohlheim and A. Heisner, "Optimal control of greenhouse climate using genetic algorithms," in *Proc. International Conference on Genetic Algorithms*, vol. 96, 1996, p. 112119.

[62] X. Luan, P. Shi, and F. Liu, "Robust adaptive control for greenhouse climate using neural networks," *International Journal of Robust and Nonlinear Control*, vol. 21, no. 7, pp. 815–826, 2011.

[63] N. Bennis, J. Duplaix, G. Ena, M. Haloua, and H. Youlal, "Greenhouse climate modelling and robust control," *Computers and Electronics in Agriculture*, vol. 61, no. 2, pp. 96–107, 2008.

[64] R. Salazar, I. Lopez, and A. Rojano, "A neural network model to control greenhouse environment," in *Sixth Mexican International Conference on Artificial Intelligence (MICAI 2007)*, 2007, pp. 311–318.

[65] R. Linker, I. Seginer, and P. Gutman, "Optimal CO_2 control in a greenhouse modeled with neural networks," *Computers and Electronics in Agriculture*, vol. 19, no. 3, pp. 289–310, 1998.

[66] D. Kolokotsa, G. Saridakis, K. Dalamagkidis, S. Dolianitis, and I. Kaliakatsos, "Development of an intelligent indoor environment and energy management system for greenhouses," *Energy Conversion and Management*, vol. 51, no. 1, pp. 155–168, Jan. 2010.

[67] R. Castaneda-Miranda and E. Ventura-Ramos, "Fuzzy greenhouse climate control system based on a field programmable gate array," *Biosystems engineering*, vol. 94, no. 2, pp. 165–177, 2006.

[68] F. Lafont and J. F. Balmat, "Optimized fuzzy control of a greenhouse," *Fuzzy Sets and Systems*, vol. 128, no. 1, pp. 47–59, 2002.

[69] P. Salgado and J. B. Cunha, "Greenhouse climate hierarchical fuzzy modelling," *Control Engineering Practice*, vol. 13, no. 5, pp. 613–628, 5 2005.

[70] M. E. Ghoumari, H. J. Tantau, and J. Serrano, "Non-linear constrained mpc: Real-time implementation of greenhouse air temperature control," *Computers and Electronics in Agriculture*, vol. 49, no. 3, pp. 345–356, 2005.

[71] J. P. Coelho, P. B. de Moura Oliveira, and J. B. Cunha, "Greenhouse air temperature predictive control using the particle swarm optimisation algorithm," *Computers and Electronics in Agriculture*, vol. 49, no. 3, pp. 330–344, 12 2005.

[72] Q. Zou, J. Ji, S. Zhang, M. Shi, and Y. Luo, "Model predictive control based on particle swarm optimization of greenhouse climate for saving energy consumption," in *IEEE World Automation Congress*, 2010, pp. 123–128.

[73] M. Berenguel, F. Rodriguez, J. Guzman, D. Lacasa, and J. Prez-Parra, "Greenhouse diurnal temperature control with natural ventilation based on empirical models," in *ISHS Acta Horticulture 719*, 2006, pp. 57–64.

[74] X. Blasco, M. Martnez, J. Herrero, C. Ramos, and J. Sanchis, "Model-based predictive control of greenhouse climate for reducing energy and water consumption," *Computers and Electronics in Agriculture*, vol. 55, no. 1, pp. 49–70, 2007.

[75] E. Fitz-Rodrguez, C. Kubota, G. A. Giacomelli, M. E. Tignor, S. B. Wilson, and M. McMahon, "Dynamic modeling and simulation of greenhouse environments under several scenarios: A web-based application," *Computers and Electronics in Agriculture*, vol. 70, no. 1, pp. 105–116, 2010.

[76] N. Sigrimis, K. Arvanitis, and G. Pasgianos, "Synergism of high and low level systems for the efficient management of greenhouses," *Computers and Electronics in Agriculture*, vol. 29, no. 1-2, pp. 21–39, 2000.

[77] F. Rodriguez, J. Guzmn, M. Berenguel, and M. Arahal, "Adaptive hierarchical control of greenhouse crop production," *International Journal of Adaptive Control and Signal Processing*, vol. 22, no. 2, pp. 180–197, 2008.

[78] K. Ferentinos, L. Albright, and D. Ramani, "Optimal light integral and carbon dioxide concentration combinations for lettuce in ventilated greenhouses," *Journal of Agricultural Engineering Research*, vol. 77, no. 3, pp. 309–315, 2000.

[79] M. Amin and B. F. Wollenberg, "Toward a smart grid: power delivery for the 21st century," *IEEE Power and Energy Magazine*, vol. 3, no. 5, pp. 34–41, 2005.

[80] H. Farhangi, "The path of the smart grid," *IEEE Power and Energy Magazine*, vol. 8, no. 1, pp. 18–28, 2010.

[81] "The smart grid: an introduction." [Online]. Available: http://www.oe.energy.gov/DocumentsandMedia/DOE_SG_Book_Single_Pages.pdf

[82] A. Schneider, "The smart grid in review." [Online]. Available: http://www.kema.com/consulting_services/cross_sector/INC/Automation_Insight/December_2008/Smart_Grid_Review.asp

[83] A. Ipakchi and F. Albuyeh, "Grid of the future," *IEEE Power Energy Magazine*, vol. 7, no. 2, pp. 52–62, 2009.

[84] M. Geidl and G. Andersson, "Optimal power flow of multiple energy carriers," *IEEE Transactions on Power Systems*, vol. 22, no. 1, pp. 145–155, Feb. 2007.

[85] M. Geidl, G. Koeppel, P. Favre-Perrod, B. Klockl, G. Andersson, and K. Frohlich, "Energy hubs for the future," *IEEE Power and Energy Magazine*, vol. 5, no. 1, pp. 24–30, Jan.-Feb. 2007.

[86] M. Schulze, L. Friedrich, and M. Gautschi, "Modeling and optimization of renewables: applying the energy hub approach," in *Proc. IEEE International Conference on Sustainable Energy Technologies*, 2008, pp. 83–88.

[87] P. Favre-Perrod, M. Geidl, B. Klockl, and G. Koeppel, "A vision of future energy networks," in *IEEE Inaugural Conference and Exposition in Africa,*. IEEE, 2005, pp. 13–17.

[88] "Energy hub management system," May 2011. [Online]. Available: http://www.energyhub.uwaterloo.ca/

[89] F. Boshell and O. P. Veloza, "Review of developed demand side management programs including different concepts and their results," in *Proc. IEEE/PES Transmission and Distribution Conference and Exposition: Latin America*, 2008, pp. 1–7.

[90] "Assessment of demand response and advanced metering: Staff report," U.S. Department of Energy: Federal Energy Regulatory Commission, Tech. Rep., Sep. 2007. [Online]. Available: http://www.ferc.gov/legal/staff-reports/09-07-demand-response.pdf

[91] M. H. Albadi and E. F. El-Saadany, "A summary of demand response in electricity markets," *Electric Power Systems Research*, vol. 78, no. 11, pp. 1989–1996, 11 2008.

[92] D. S. Kirschen, G. Strbac, P. Cumperayot, and D. de Paiva Mendes, "Factoring the elasticity of demand in electricity prices," *IEEE Transactions on Power Systems*, vol. 15, no. 2, pp. 612–617, 2000.

[93] F. Rahimi and A. Ipakchi, "Overview of demand response under the smart grid and market paradigms," in *Innovative Smart Grid Technologies (ISGT)*, 2010, pp. 1–7.

[94] D. S. Kirschen, "Demand-side view of electricity markets," *IEEE Transactions on Power Systems*, vol. 18, no. 2, pp. 520–527, 2003.

[95] K. Spees and L. B. Lave, "Demand response and electricity market efficiency," *The Electricity Journal*, vol. 20, no. 3, pp. 69–85, 4 2007.

[96] M. Albadi and E. El-Saadany, "Demand response in electricity markets: An overview," in *Proc. IEEE PES General Meeting*, 2007, pp. 1 –5.

[97] A. T. D. Almeida and A. H. Rosenfeld, "Demand-side management and electricity end-use efficiency," in *NATO Science Series, Series E: Applied Sciences*, vol. 149, 1988.

[98] A. S. Chuang and C. W. Gellings, "Demand-side integration in a restructured electric power industry," *CIGRE General Session, Paris*, August 24-29 2008.

[99] A. Baitch, A. Chuang, G. Mauri, and C. Schwaegerl, "International perspectives on demand-side integration," in *Proc. International Conference on Electricity Distribution*, 2007.

[100] K. Johnson, "The fundamental of linking demand side management strategies with program implementation tactics," *Market Development Group*. [Online]. Available: https://www.utilityexchange.org/docs/white_paper_program_implementation.pdf

[101] J. Eto, "The past, present, and future of U.S. utility demand side management programs," LBNL, University of California, Berkeley, Tech. Rep. 39931, Dec. 1996. [Online]. Available: http://eetd.lbl.gov/ea/EMP/reports/39931.pdf

[102] S. Talukdar and C. W. Gellings, *Load Management*. IEEE, 1987.

[103] "Primer on demand side management: A report prepared for the world bank," Charles River Associates, Tech. Rep. No. D06090, Feb. 2005. [Online]. Available: http://siteresources.worldbank.org/INTENERGY/Resources/PrimeronDemand-SideManagement.pdf

[104] M. H. Didden and W. D. Dhaeseleer, "Demand side management in a competitive european market: Who should be responsible for its implementation?" *Energy Policy*, vol. 31, no. 13, pp. 1307–1314, 2003.

[105] R. M. Delgado, "Demand-side management alternatives," *Proceedings of the IEEE*, vol. 73, no. 10, pp. 1471–1488, 1985.

[106] C. H. Lien, Y. W. Bai, and M. B. Lin, "Remote-controllable power outlet system for home power management," *IEEE Transactions on Consumer Electronics*, vol. 53, no. 4, pp. 1634–1641, 2008.

[107] J. Han, H. Lee, and K. R. Park, "Remote-controllable and energy-saving room architecture based on zigbee communication," *IEEE Transactions on Consumer Electronics*, vol. 55, no. 1, pp. 264–268, 2009.

[108] G. Song, F. Ding, W. Zhang, and A. Song, "A wireless power outlet system for smart homes," *IEEE Transactions on Consumer Electronics*, vol. 54, no. 4, pp. 1688–1691, 2008.

[109] Y. W. Bai and C. H. Hung, "Remote power on/off control and current measurement for home electric outlets based on a low-power embedded board and zigbee communication," in *IEEE International Symposium on Consumer Electronics*. IEEE, 2008, pp. 1–4.

[110] D. M. Han and J. H. Lim, "Smart home energy management system using ieee 802.15. 4 and zigbee," *IEEE Transactions on Consumer Electronics*, vol. 56, no. 3, pp. 1403–1410, 2010.

[111] R. Torbensen, "Ohas: Open home automation system," in *IEEE International Symposium on Consumer Electronics*, 2008, pp. 1–4.

[112] A. Alheraish, "Design and implementation of home automation system," *IEEE Transactions on Consumer Electronics*, vol. 50, no. 4, pp. 1087–1092, 2004.

[113] G. Patricio and L. Gomes, "Smart house monitoring and actuating system development using automatic code generation," in *IEEE International Conference on Industrial Informatics*, 2009, pp. 256–261.

[114] K. Gill, S.-H. Yang, F. Yao, and X. Lu, "A zigbee-based home automation system," *IEEE Transactions on Consumer Electronics*, vol. 55, no. 2, pp. 422–430, 2009.

[115] W. Kastner, G. Neugschwandtner, S. Soucek, and H. M. Newmann, "Communication systems for building automation and control," *Proceedings of the IEEE*, vol. 93, no. 6, pp. 1178–1203, 2005.

[116] D. Dietrich, D. Bruckner, G. Zucker, and P. Palensky, "Communication and computation in buildings: A short introduction and overview," *IEEE Transactions on Industrial Electronics*, vol. 57, no. 11, pp. 3577–3584, 2010.

[117] K. J. Keesman and T. Doeswijk, "Uncertainty analysis of weather controlled systems," in *Coping with Uncertainty*. Springer, 2010, vol. 633, pp. 247–258.

[118] C. Stanghellini and W. T. m. van Meurs, "Environmental control of greenhouse crop transpiration," *Journal of Agricultural Engineering Research*, vol. 51, pp. 297–311, 4 1992.

[119] J. M. Aaslyng, J. B. Lund, N. Ehler, and E. Rosenqvist, "Intelligrow: a greenhouse component-based climate control system," *Environmental Modelling & Software*, vol. 18, no. 7, pp. 657–666, 9 2003.

[120] R. Morais, M. A. Fernandes, S. G. Matos, C. Serdio, P. J. S. G. Ferreira, and M. J. C. S. Reis, "A zigbee multi-powered wireless acquisition device for remote sensing applications in precision viticulture," *Computers and Electronics in Agriculture*, vol. 62, no. 2, pp. 94–106, 7 2008.

[121] G. Soto-Zaraza, A. Romero-Archuleta, A. Mercado-Luna, M. Toledano-Ayala, E. Rico-Garca, R. Pniche-Vera, and G. Herrera-Ruiz, "Trends in automated systems development for greenhouse horticulture," *International Journal of Agricultural Research*, vol. 6, no. 1, pp. 1–9, 2011.

[122] S. S. Rao, *Engineering Optimization: Theory and Practice*. New York: John Wiley & Sons, Inc., 1996.

[123] H. Sherali and C. Tuncbilek, "A global optimization algorithm for polynomial programming problems using a reformulation-linearization technique," *Global Optimization*, vol. 2, no. 1, pp. 101–112, 1992.

[124] H. Sherali and W. Adams, *A reformulation-linearization technique for solving discrete and continuous nonconvex problems*. Kluwer Academic Publishers, 1999.

[125] D. Bertsimas and M. Sim, "The price of robustness," *Operations Research*, pp. 35–53, 2004.

[126] ——, "Robust discrete optimization and network flows," *Mathematical Programming*, vol. 98, no. 1, pp. 49–71, 2003.

[127] R. Fourer, D. M. Gay, and B. W. Kernighan, *AMPL: A Modeling Language for Mathematical Programming*. Thomson/Brooks/Cole, 2003.

[128] *ILOG CPLEX 11.0 Users Manual*. ILOG SA, Gentilly, France, 2008.

[129] A. Wachter and L. Biegler, "On the implementation of an interior-point filter line-search algorithm for large-scale nonlinear programming," *Mathematical Programming*, vol. 106, no. 1, pp. 25–57, 2006.

[130] "Electricity prices in Ontario." [Online]. Available: http://www.oeb.gov.on.ca/OEB/For+Consumers/Understanding+Your+Bill+Rates+and+Prices/Electricity+Prices+in+Ontario

[131] "A guide to electricity charges - market participants." [Online]. Available: http://www.ieso.ca/imoweb/role/wholesaleCharges.asp

[132] "A guide to electricity charges for business." [Online]. Available: http://www.ieso.ca/imoweb/siteshared/electricity_charges.asp

[133] "U.S. Department of Energy: Energy Information Administration – natural gas," 2010. [Online]. Available: http://www.eia.doe.gov/naturalgas/

[134] "National Energy Board – energy pricing information for canadian consumers," 2010. [Online]. Available: http://www.neb-one.gc.ca/clf-nsi/rnrgynfmtn/prcng/prcng-eng.html

[135] S. A. Hashmi, "Evaluation and improvement of the residential energy hub management system," Master's thesis, University of Waterloo, Sept. 2010.

[136] "eGrid," U. S. Environmental Protection Agency, Tech. Rep., Apr. 2007. [Online]. Available: http://epa.gov/cleanenergy/documents/egridzips/eGRID2006V2_1_Summary-_Tables.pdf

[137] "Natural gas 1998: Issues and trends," U.S. Department of Energy: Energy Information Administration, Tech. Rep., Apr. 1999. [Online]. Available: http://www.eia.doe.gov/oil_gas/natural_gas/analysis_publications/natural_gas_1998_issues_and_trends/it98.html

[138] N. Stern and G. Treasury, *The economics of climate change: The Stern review*. Cambridge University Press, 2007.

[139] J. V. Paatero and P. D. Lund, "A model for generating household electricity load profiles," *International Journal of Energy Research*, vol. 30, no. 5, pp. 273–290, 2006.

[140] M. Räsänen, J. Ruusunen, and R. P. Hämäläinen, "Object-oriented modeling software for electric load analysis and simulation," *Simulation*, vol. 66, no. 5, pp. 275–288, May 1996.

[141] H. Hassen, "Implementation of energy hub management system for residential sector," Master's thesis, University of Waterloo, April 2010.

[142] J. Lutz, X. Liu, J. McMahon, C. Dunham, L. Shown, and Q. McCure, "Modeling patterns of hot water use in households," Lawrence Berkeley National Laboratory Berkeley, California, Tech. Rep. LBL-37805 Rev., Nov. 1996.

[143] "Hourly water heating calculations," Pacific Gas and Electric Company, Tech. Rep., 2002. [Online]. Available: http://www.energy.ca.gov/title24/2005standards/archive/documents/2002-05-30_workshop/2002-05-17_WTR_HEAT_CALCS.PDF

[144] T. G. Doeswijk, "Reducing prediction uncertainty of weather controlled systems," Ph.D. dissertation, Wageningen University, 2007.

[145] J. Landry, "Computer software for the control of potato storage environment," Ph.D. dissertation, McGill University, 1994.

[146] R. G. Allen, L. S. Pereira, D. Raes, and M. Smith, "Crop evapotranspiration–guidelines for computing crop water requirements," *FAO Irrigation and Drainage Paper*, 1998. [Online]. Available: http://www.fao.org/docrep/X0490E/X0490E00.htm

[147] M. Chehreghani Bozchalui, H. Hassen, S. A. Hashmi, C. A. Canizares, K. Bhattacharya, and G. D. Ellis, "System, computer program, and method for providing an energy hub," *US Provisional Patent*, no. 61470098, March 2011.

[148] M. Chehreghani Bozchalui, H. Hassen, S. A. Hashmi, C. A. Canizares, and K. Bhattacharya, "Optimal operation of residential energy hubs in smart grids—Part I: The concept and mathematical modeling," *Submitted to IEEE Transactions on Smart Grid*, March 2011.

[149] M. Chehreghani Bozchalui, S. A. Hashmi, H. Hassen, C. A. Canizares, and K. Bhattacharya, "Optimal operation of residential energy hubs in smart grids—Part II: Simulations and implementation aspects," *Submitted to IEEE Transactions on Smart Grid*, March 2011.

[150] M. Chehreghani Bozchalui, H. Hassen, S. A. Hashmi, C. A. Canizares, and K. Bhattacharya, "Mathematical models for optimal operation of residential energy hubs," *Technology IP Disclosure, University of Waterloo*, pp. 1–72, August 2010.

[151] M. Chehreghani Bozchalui, C. A. Canizares, and K. Bhattacharya, "Optimal operation of climate control systems of produce storage facilities in smart grids," *Technology IP Disclosure, University of Waterloo*, March 2011.

[152] ——, "Optimal operation of climate control systems of greenhouses in smart grids," *Technology IP Disclosure, University of Waterloo*, June 2011.